Fundamentals of Power Reactors

Module One
Science & Engineering Fundamentals

Copyright Notice

Basis of Nuclear Structure and Fission

Training Objectives

The participant will be able to describe or understand:

1   the atomic and nuclear structure,
2   the basic vocabulary of nuclear energy: typical length scales, mass and energy units, etc.,
3   the atomic and nuclear phenomena,
4   the fission and energy release processes,
5   the types of radiation,
6   the concept of neutron spectrum,
7   the conecpt of cross section
8   the concept of irradiation

# Basis of Nuclear Structure and Fission

Table of Contents

December 1995

1 Introduction

The nuclear energy is a powerful energy source related to the strength and stability of the atomic nucleus. It may be available in two different ways, either by fusion of light elements or by fission of heavy nuclei.

The process called nucleosynthesis is taking place in stars and uses the fusion reaction to create heavy weight atomic nuclei. In this process, the fusion reaction brings together protons, neutrons and energy. They become bound by strong interactions in the nucleus. It is unlikely that the fusion reaction will be used in an industrial process of energy production in the near future. The major problem is that a tremendous amount of energy (of the order of magnitude of the temperature in stars, 100 millions degrees) is required to initiate the fusion reaction. Below is a list of various fusion reactions with their energy balance:

$$_1^2D + {}_1^2D \ \rightarrow \ _2^3He(0.82MeV) + {}_0^1n(2.45MeV) + 3.27Mev$$

$$_1^2D + {}_1^2D \ \rightarrow \ _1^3T(1.01MeV) + {}_1^1p(3.02MeV) + 4.03Mev$$

$$_1^2D + {}_1^3T \ \rightarrow \ _2^4He(3.56MeV) + {}_0^1n(14.03MeV) + 17.59Mev$$

$$_1^3T + {}_1^3T \ \rightarrow \ _2^4He \ + 2{}_0^1n + 17.59Mev$$
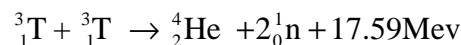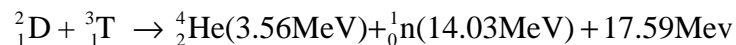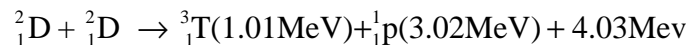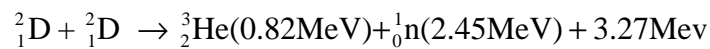
To date, the only macroscopic application of the fusion reaction is the H bomb (the third of the above equations). Figure 1.1 below illustrates the fusion reaction between deuterium and tritium.

Fig. 1.1:
Fusion reaction between deuterium and tritium
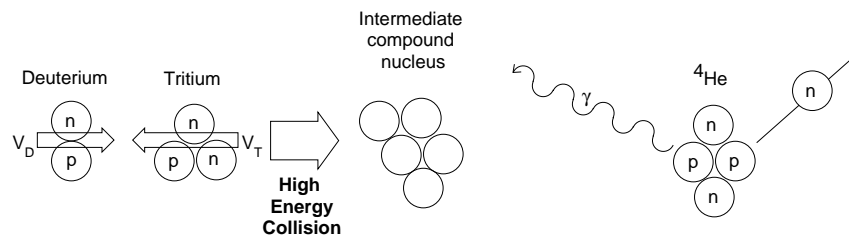
In comparison, the fission reaction is "easier" to produce; it is the source of energy in a nuclear reactor: neutron-induced fission of uranium and plutonium nuclei. As it is the process of interest for nuclear energy production, it will be treated in greater details in this lesson. The fission reaction can liberate part of the binding energy by breaking the nuclear structure. According to the concept of equivalence of mass and energy established by Einstein, the amount of energy ΔE released is given by the following equation:

$$\Delta E = \Delta m \ c^2$$

where c is the speed of light and Δm is the mass defect. The determination of

nuclear masses has shown that the mass of a heavy nucleus is higher than the sum of the individual masses of its constituent nucleons. It is called the mass defect.

Figure 1.2 below illustrates the neutron-induced fission reaction of uranium.

Fig. 1.2:

Uranium fission reaction
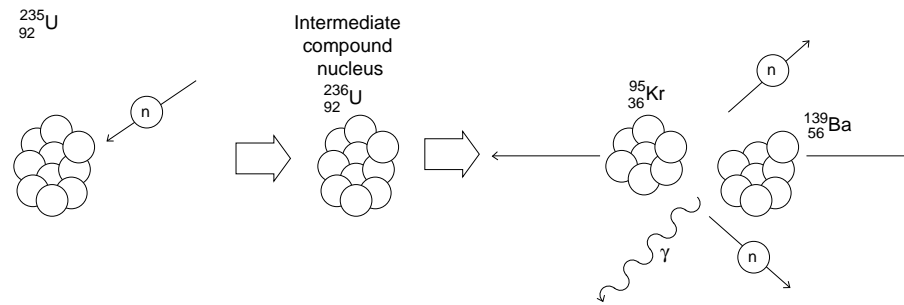
Reactor physics is the study of the fission chain reaction and its dependence on the materials in the reactor core and their geometrical configuration. The reactor physicist area of interest is in core neutronics: the distribution in space, time and energy of the neutron population. Reactor physics shares methods and results with thermohydraulics, safety, fuel management and operation.

Fig. 1.3:

Relations between reactor physics and other disciplines
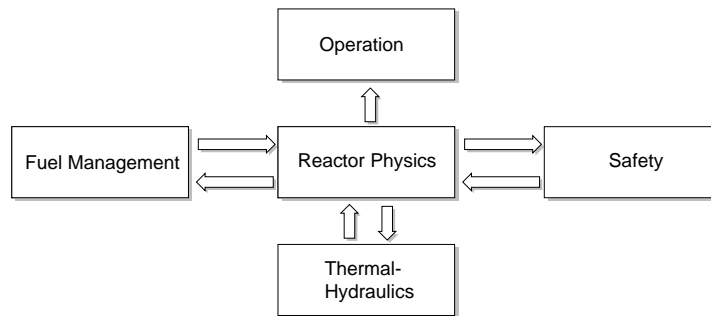
2 Basics of Nuclear Physics

2.1 Structure of the atom and nucleus

2.1.1 Nuclear structure

An atom of a chemical element consists of a small, positively charged, massive nucleus surrounded by a large, negatively charged, light electron cloud. The radius of the atom is of the order of 10^{-8} cm (≈ 1Å (ångström)), whereas the radius of the nucleus is of the order of only 10^{-13}-10^{-12} cm (about 10 thousands times smaller). In spite of this, more than 99.9% of the mass (and therefore of the energy) of the atom resides in the nucleus.

The nucleus consists of positively charged protons and uncharged neutrons. Protons and neutrons are collectively called nucleons. The mass of a proton is about 1836 times, while that of a neutron is about 1838 times, the mass of an electron.

The number of protons in the nucleus - denoted by Z - (or, equivalently, the number of electrons in the neutral atom) is called the atomic number and determines the chemical element. For instance, Z = 1 (one proton) corresponds to hydrogen, Z = 8 corresponds to oxygen, Z = 92 corresponds to uranium. The number of neutrons in the nucleus is denoted by N. The total number of nucleons in the nucleus is the mass number, $A \equiv Z+N$. A given combination of a specific Z and a specific N is a specific "nuclide", X. Thus any two of Z, N and A are sufficient to specify the nuclide, and it is represented by the symbol X. Figure 2.1 shows the atomic structure of various nuclides.

2.1.2 Isotopes

The atomic number determines the chemical nature of an element because the chemical properties depend on the (orbital) electrons surrounding the nucleus, and their number must be equal to the number of protons, since the atom as a whole is electrically neutral. Consequently, atoms with nuclei containing the same number of protons, i.e., with the same atomic number, but with different mass numbers, are identical chemically, although they frequently exhibit marked differences in their nuclear characteristics. Such species, having the same atomic numbers but different mass numbers, are called isotopes. For instance, uranium has several isotopes, but two of them, ^{238}U and ^{235}U (with 146 and 143 neutrons respectively) make up almost 100% of the naturally occurring uranium. The relative isotopic abundance of ^{238}U to ^{235}U in natural uranium is 99.28% to 0.72%. In the CANDU reactor, it is the natural UO_2 that is used whereas enriched fuel (natural uranium enriched in ^{235}U) is used in LWR (Light Water Reactors). Hydrogen has three possible isotopes: ^{1}H (the most abundant, with no neutrons in the nucleus), ^{2}H or deuterium (heavy hydrogen), with one neutron, and ^{3}H or tritium, with two neutrons. This is illustrated in figure 2.1.

Fig. 2.1:
Nuclear structure of H, D, T, U-235 and U-238
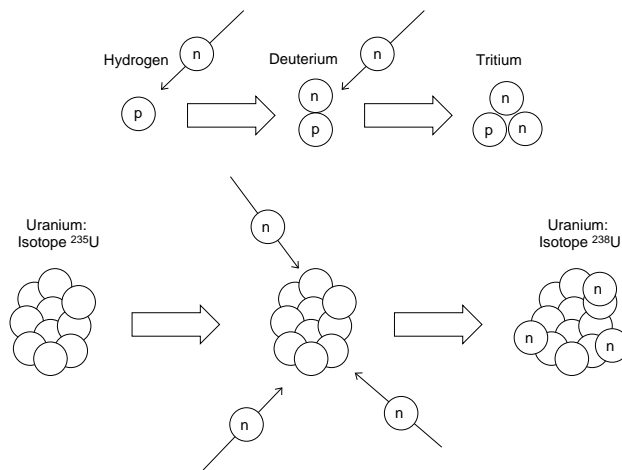
2.1.3 Nuclear stability

Even though an element can have several isotopes, not every combination of Z and N is possible. For light elements (small values of Z), the most probable value for N is Z (e.g. ^{12}C, Z=N=6, or ^{16}O, Z=N=8).

Two forces are competing in the nucleus: the fist one is the coulombian repulsion which is mainly proportional to the number of protons, and the second one is the strong nuclear attraction between nucleons. As the atomic number increases, the size of the nucleus increases and exceeds steadily the characteristic length of strong nuclear force. Therefore, for heavy elements, an excess of neutrons is needed to "glue" the nucleus and also to overcome the electric repulsion between protons; the most probable value of N increases steadily beyond Z. Figure 2.2 shows that in a Z-N plot, the naturally occurring stable nuclides occupy a band which starts along the diagonal line N=Z but steadily moves higher above it.

Fig. 2.2:
Numbers of neutrons and protons in stable nuclei
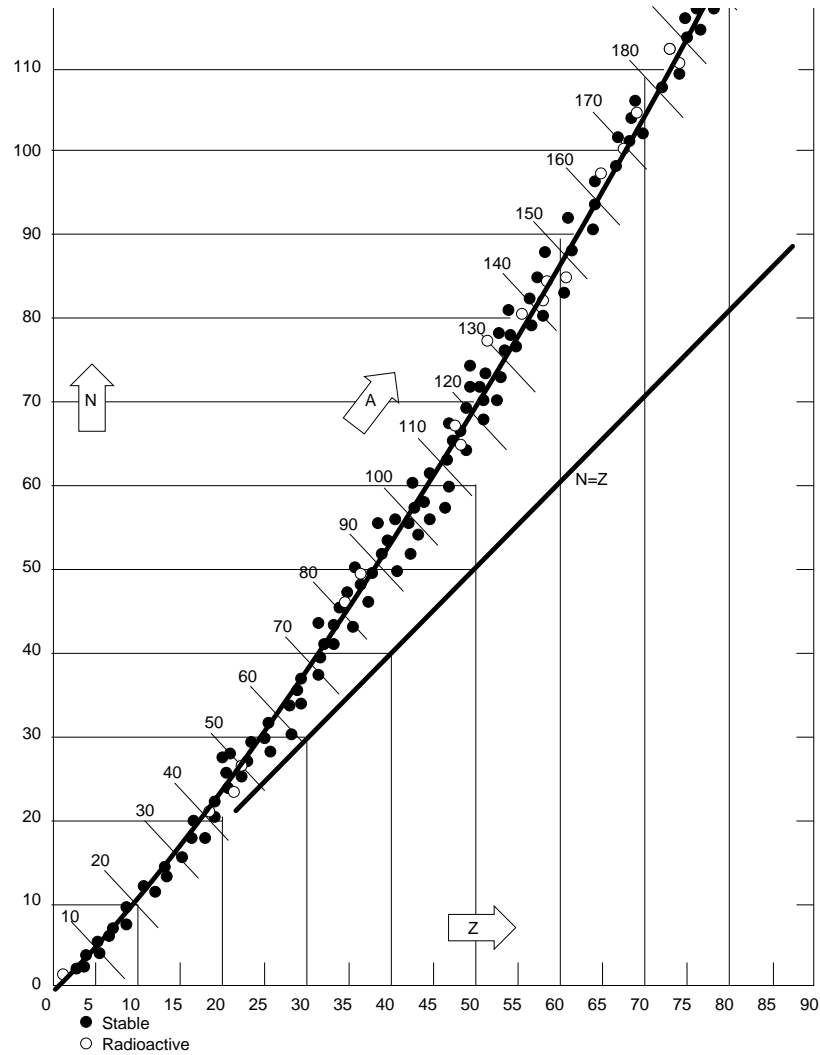
This explains why the fission of a heavy nuclide is accompanied by the emission of neutrons. Most of the neutrons are emitted instantaneously. Yet, most of the fission products are unstable. Their composition is outside the stability range plotted in figure 2.2. They are radioactive. The ratio N/Z is greater than 1.5 for radioactive isotopes of uranium. To seek for stability, the fission products undergo successive negative charged Beta particle decays. A neutron is replaced in the nucleus by a proton with the emission of an electron (n → p + e); so that the neutron/proton ratio decreases. The resulting nucleus will be more stable (longer decay period), although not necessarily stable.

2.2 Binding energy and excited states of the nucleus

2.2.1 Energy and mass units

A standard unit of energy (or work) in physics is the Joule (J), equal to the work performed by a 1 Newton force acting over a 1 metre distance:

$1 J = 1 N.m$

In atomic physics a much smaller unit of energy is needed, due to the extremely microscopic size of the phenomena (Avogadro's number, the number of molecules in a mole of substance, is $6.02 \bullet 10^{23}$). For this purpose, the unit of electron-volt (eV) has been defined. It is the kinetic energy gained by an electron accelerated through an electric potential of 1 volt. From the value of the electron charge ($1.6 \bullet 10^{-19}$ Coulomb), and the fact that 1 Coulomb.Volt = 1 J, the following relationship emerges:

$1 eV = 1.6 \bullet 10^{-19} J$

It is obvious that the eV is a very small unit of energy indeed, but it is a useful and natural one to employ when discussing atomic and molecular (i.e., chemical) phenomena.

When discussing nuclear phenomena, on the other hand, the larger unit of a million electron volts (MeV) is more appropriate:

$1 MeV = 10^6 eV$

Note that in view of Einstein's relation between rest mass and energy,

$E = mc^2,$

eV and MeV can also effectively be used as units of mass. In these units, the (rest) mass of the electron is

$m_e = 0.511$ eV [more correctly $m_e c^2 = 0.511$ eV]

while the rest mass of the neutron is approximately

$m_n = 940$ MeV

2.2.2 Binding energy of the nucleus

When protons and neutrons "come together" to form a nucleus, some of the total mass of the nucleons is transformed into energy and escapes. As a consequence (and as a result of the Law of Conservation of Energy), the mass of the nucleus is less than the total mass of the "free" nucleons. If m_p and m_n represent the masses of the proton and neutron respectively and M is the mass of the resulting nucleus, then

$M \text{ (nuclide Z, N)} < Z . m_p + N . m_n$

The difference is called the mass defect Δ:

$M \text{ (nuclide Z, N)} = Z . m_p + N . m_n - \Delta$

or

$Mc^2 \text{ (nuclide Z, N)} = Z m_p c^2 + N m_n c^2 - B$

The binding energy B is the energy which would have to be supplied, to break apart the nucleus into its constituent nucleons. Figure 2.3 gives the binding energy per nucleon plotted as a function of the mass number. It shows that the binding energy per nucleon B is relatively low for nuclei of small mass number but increases, with increasing mass number, to a maximum of about 8 Mev in the mass region of roughly 50 to 75; subsequently B decreases steadily. Nuclides with the largest B, i.e., the largest binding energy, are the most stable. It can be seen from figure 2.3 that the most stable nuclides are those of mass number equal to about 60 (e.g. Fe, Ni, Co).

Fig. 2.3:
Binding energy per nucleon versus mass number
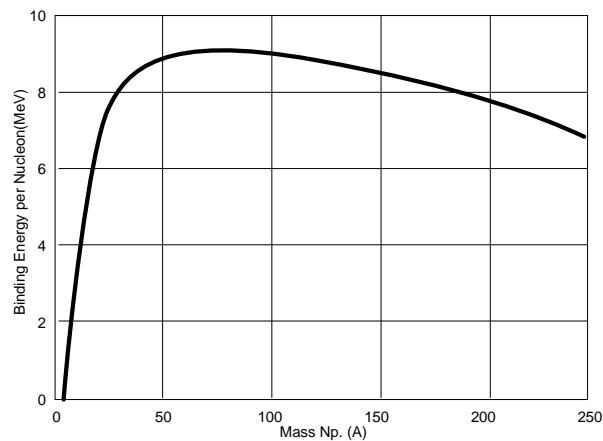
Figure 2.3 indicates also that the binding energy per nucleon will increase if (a) light nuclides (those with small mass number A) can be made to fuse (join) into bigger ones, or (b) heavy nuclides (those with large mass number A) can be made to break up (fission) into smaller ones. When the binding energy increases, the mass defect Δ increases. In a nuclear reaction such as those described, the missing mass appears as energy (in the form of radiation and/or kinetic energy of particles) which can in principle be recovered in the degraded form of heat. This is the basis of the "energy producing" processes of fusion and fission, corresponding to (a) and (b) above respectively.

2.2.3 Comparison of chemical and nuclear energies
Whereas binding energies of nucleons in nuclei are measured in MeV, the binding energies of electrons in atoms and molecules are measured in eV or tens or hundreds of eV. This is a difference of 4 to 6 orders of magnitude from the nuclear binding energy.

This is why nuclear processes or nuclear reactions release so much more energy than chemical reactions, which involve interactions of the electron clouds of atoms and molecules. For example, the energy generated in the fission of a kilogram of uranium is approximately 20,000 times that generated by burning a kilogram of hydrocarbons.

2.2.4 Excited state of the nucleus

The nuclear binding energy corresponds to the lowest-energy state (ground state) of nuclei. However, nuclei can also be in higher-energy, "excited", states. These states are unstable, and nuclei in excited states tend to "drop" to their ground state with a release of energy (or matter). Correspondingly, a nucleus in the ground state can absorb energy and be moved "up" to an excited state.

Figure 2.4 illustrates this for radioactive phenomena. In radioactive gamma (γ) decay, the nucleus in the excited state (E_i) goes down to a lower state of energy by emitting a photon. The "excited" nucleus can reach its fundamental state (ground state E_o) directly or after having gone through successive lower states of energy.

Fig. 2.4:
Transition between ground and excited state
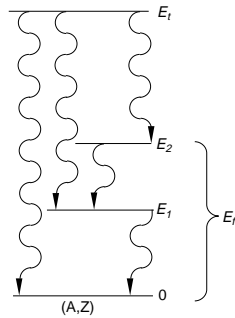
2.3 Radioactivity

The nucleus stability is maintained by the number of neutrons which can compensate the electric repulsive forces between protons. However, there is a limit to the excess of neutrons over protons which a nucleus can contain and still remain stable. Consequently, the elements of atomic number larger than 83 have no stable isotopes; although elements 84 (polonium) through 92 (uranium) exist in nature, they are unstable and exhibit the phenomenon of radioactivity.

Radioactive nuclides undergo spontaneous change at a definite rate which varies with the nature of the nuclide. The unstable nucleus emits a characteristic particle (or radiation) and is thereby transformed into a different nucleus which may (or may not) be radioactive.

In the context of nuclear reactions, several types of radiation are distinguished. The main ones are:

December 1995

Alpha (α) radiation:
A nucleus $_Z^A X$ which undergoes an α decay will transform into a daughter

nucleus $_{Z-2}^{A-4} Y$ and a nucleus $_2^4 He$ called α particle.

$$_Z^A X \rightarrow {}_{Z-2}^{A-4} Y + \alpha \left({}_2^4 He \right)$$
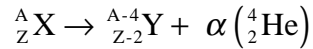
Alpha particles are positively charged and are stopped by a sheet of paper. They are considered heavy particles.

The emission of an α particle is a process which depends on strong nuclear interactions acting between nucleons. The process is usually fast. The decaying nucleus emits a positively charged α particle which has to escape the coulumbian barrier of the atomic cloud of electrons. This overcomes the α emission process and explains the discrete nature of its emission spectrum.

Beta (β) radiation:
A β decay is characterized by the emission of (negatively charged) free electrons
    neutron $\rightarrow$ proton + electron (β particle) + anti-neutrino

These can pass through 1 cm of water or human tissue. A neutron is unstable and has a decay period of about 12 minutes.

The β radiation is a process which depends on weak nuclear interactions. The process is usually slow; a β transition of about one MeV has a decay period of a few minutes. The emission spectrum of β transition is continuous because the resulting energy is continuously distributed between the electron and anti-neutrino kinetic energies.

Gamma (γ) radiation:
This is an electromagnetic radiation. Gamma rays are high-energy photons or (hard) X-rays. These can pass right through the human body, but are almost completely absorbed by 1 m of concrete. Materials such as lead or concrete are often used for shielding against gamma rays.

The γ radiation is a process which depends on electromagnetic interactions. The process is usually faster than β transition: a dipolar γ emission of about one MeV has a period of 10^{-15} s. The γ emission spectrum is discrete due to the distribution of discrete energy levels of the excited nucleus states (see Figure 2.4).

Neutrons:
High-kinetic-energy neutrons are very penetrating. An effective shielding material against neutrons is water or low atomic number material (wood).

In order to illustrate the various emission processes, figure 2.5 gives the example of the uranium chain. The "double box" indicates a fissile nuclide. The non-fissile nuclides or nuclides that are fissionable only by high kinetic energy (fast) neutrons are framed in a single box. The others have a short period and are of interest as they transform into other nuclides. The neutron-induced reaction is symbolized by a double arrow, whereas single arrows represent radiations. For each arrow the particle or ray emitted is indicated, as well as the decay period. Starting with ^{238}U, it can be seen that the nuclide can suffer two transformations. It can transform into ^{239}U by emitting a γ radiation. This nuclide will become, after a very short decay period of 23.5 min and the emission of a β particle, ^{239}Np, which will suffer the same type of transformation to form ^{239}Pu. The alternate transformation is characterized by the expulsion of 2 neutrons followed by one β decay, a radiative capture (see Section 3. 2), and a second β decay to form ^{238}Pu. A neutron-induced reaction may transfer this nuclide into ^{239}Pu with the emission of 2 neutrons.

Fig. 2.5:
Uranium chain

December 1995
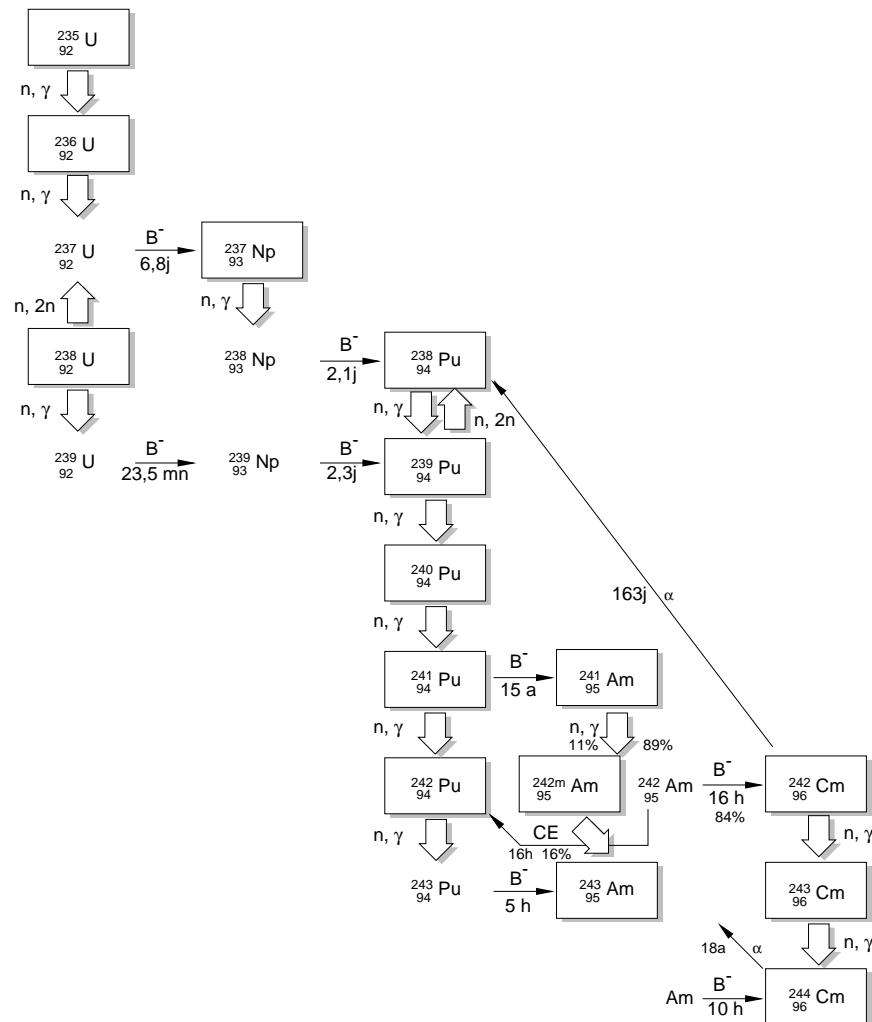
Table 1 summarizes the characteristics and hazards associated to the four different types of radiations. Radiation can affect a human body in two different ways: at distance (external radiation) or by contact or absorption (contamination).

Table 2.1

Type of radiation	Particles or rays emitted	Penetrating ability	External irradiation hazard	Contamination hazard
Alpha (α)	2 protons + 2 neutrons	low	null	very high
Beta (β)	electrons	medium	low	high
Gamma (γ)	high energy photons	high	"medium"	"medium"
Neutron	neutrons	medium-high	high	high

3 Fundamentals of Reactor Physics

3.1 Fast and thermal neutrons

3.1.1 Fast neutrons
Fast neutrons are neutrons which possess high kinetic energy, in the million electron volt range.

Consider a neutron with a kinetic energy of 1 MeV:

$$\frac{1}{2}m_n v^2 = 1 \text{ MeV}$$

As already mentioned, the rest mass of a neutron is approximately equal to 940 MeV,

$$m_n c^2 = 940 \text{ MeV}$$

therefore:

$$v^2 = \frac{2}{940}c^2$$

Since $c \approx 300{,}000$ km/s, we find that the 1 MeV neutron has a velocity $v \approx 13{,}800$ km/s. Such a neutron is called a fast neutron.

The lower bound of energies for "fast" neutrons is not precisely defined. Sometimes fast neutrons may mean all neutrons with energy above the thermal energy range (see next section). The plot of energy range of fast neutrons is given in figure 3.1.

Fig. 3.1:

Fast neutron energy spectrum
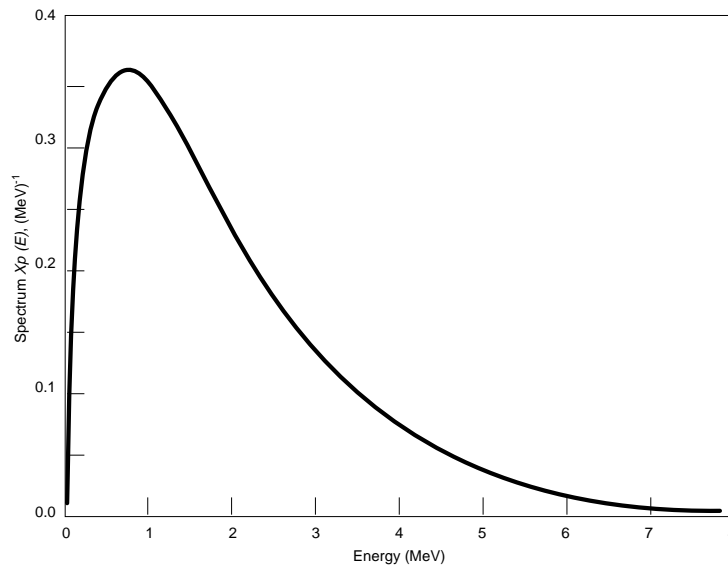
3.1.2 Thermal Neutrons

When a neutron population is in thermal equilibrium with the surrounding material, it is said to be made up of thermal neutrons. A true thermal-neutron population has a Maxwellian distribution of energy; see Figure 3.2.

Fig. 3.2:

Maxwellian energy spectrum of thermal neutrons
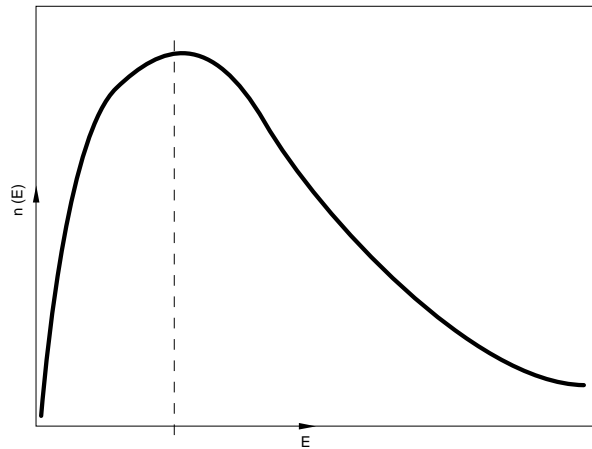
When the ambient temperature is 20°C (i.e., room temperature), the most probable neutron velocity in the distribution corresponds to an energy of 0.025 eV. Denoting this velocity by v_o, we can write:

$$\frac{1}{2}m_n v_o^2 = 0.025 \text{ eV}$$

From equations (3.2) and (3.4) we obtain

$$v_o = 2200 \text{ m/s,}$$

a convenient reference value. It is clear that thermal neutrons are slow neutrons, relative to the fast neutrons of the previous section.

The definition of the thermal-neutron energy range is somewhat arbitrary, but is often taken to include neutron energies up to 0.625 eV.

3.2 Neutron-nucleus reactions

As neutrons diffuse through the materials of the reactor core, they may enter into a number of reactions with nuclei of various elements. The neutron-nuclei reactions fall mainly into three general categories, namely, scattering, capture and fission. As a general rule, the first step in such interactions is that the nucleus absorbs the neutron to form a compound nucleus in an excited state of high internal energy.

In scattering reactions, the compound nucleus rapidly expels a neutron with a lower kinetic energy than the absorbed neutron, the excess energy remaining on the residual nucleus. If this additional energy is in the form of internal energy, so that the nucleus is an excited state, the phenomenon is referred to as inelastic scattering. On the other hand, if the extra energy which the nucleus has acquired is solely kinetic in nature, a form of elastic scattering has occurred. The term "scattering" is used to describe these reactions because the direction of motion of the neutron after the interaction with a nucleus is generally different from that prior to the interaction.

If, instead of expelling a neutron, the excited compound nucleus formed by the absorption of a neutron emits its excess energy in the form of gamma radiation, the process is referred as radiative capture. This process, represented by the symbol (n, γ), is very common and occurs more readily with slow than with fast neutrons. The absorption of the neutron by the nucleus can also result in a β decay. In this process, one neutron in the nucleus changes to a proton with emission of a β ray (electron) and a neutrino.

Fission only occurs if the original nucleus is fissionable (see section 4). When fission occurs, the excited compound nucleus formed after absorption of a neutron breaks up into two or three lighter nuclei, called fission products.

3.3 Concept of nuclear cross section

3.3.1 Macroscopic and microscopic cross sections
In reactor physics, the rates at which various reactions occur are prime quantities of interest. In particular, it is important to know the rates of reactions that neutrons undergo as they travel in the reactor core. The number of reactions of a particular type i (e.g. scattering, absorption, fission, etc.) which a neutron undergoes per unit distance of travel is called the macroscopic cross section for the reaction i, and is denoted Σ_i. It has units of inverse length (e.g. cm^{-1}).

From the definition of Σ_i, the total number of reactions i that a neutron is expected to undergo in a projected path length s of travel is given by $\Sigma_i.s$. The total number of reactions of a group of neutrons will also be $\Sigma_i.s$ if s is the total cumulative projected path length of all the neutrons.

The nuclear cross sections for scattering (Σ_s), absorption (Σ_a), fission (Σ_f), etc., depend on the material in which the neutron is travelling and are typically functions of the energy of the neutron.

The total cross section Σ_{tot}, which measures the total number of all types of reaction per unit distance, is
$$\Sigma_{tot} = \Sigma_s + \Sigma_a$$

(Note that the fission cross section is included in the absorption cross section)

The macroscopic cross section Σ of a material can be related to the microscopic cross section s, the effective area presented to the neutron by one nucleus of the material.

Fig. 3.3:
Concept of cross section

Thin slab of material

σ = area presented to neutron by nucleus

I - dI

Incident beam of radiation   I

dx

$$-dI = I\,(N\sigma)\,dx$$
$$I = Ioe^{-N\sigma x}$$
$$\Sigma = N\sigma$$
$$\lambda = 1/\Sigma$$
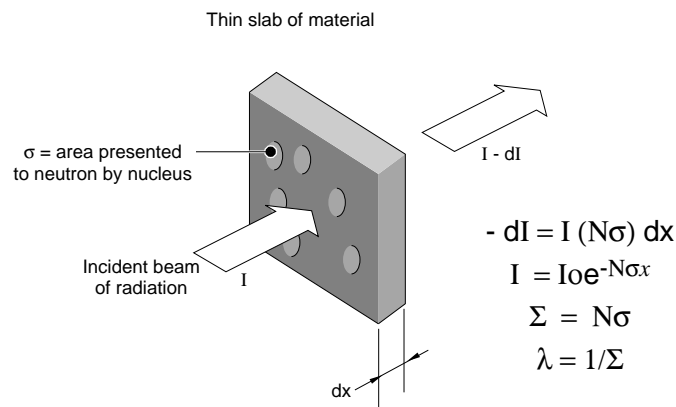
Imagine a monoenergetic beam of neutrons of velocity v, all moving in the same direction, impinging upon a slice of unit area and thickness Δx of the material (see Figure 3.3). If the beam intensity in the slice Δx is $I(x)$ n cm^{-2}, the total path length of neutrons in a unit area of beam in the slice Δx is
$$s = I(x).\Delta x$$

The number of reactions of type i that these neutrons undergo in the slice of material is, by the definition of Σ_i,
$$\text{Number of reactions of type i} = \Sigma_i.s = \Sigma_i\, I(x).\Delta x$$

On the other hand, the number of reactions can also be calculated as follows. Suppose the atomic density in the material is N atoms cm^{-3}. The number of nuclei of material in the slice (of unit area) is thus $N.\Delta x$. If each nucleus presents a microscopic cross section σ_i to the incoming neutrons for reactions of type i, the total area presented to the neutrons for the reaction i is $N.\Delta x\ \sigma_i$, and the total number of reactions is given by

Number of reactions of type i = $I(x).N.\Delta x.\sigma_i$

Comparison of equations (3.8) and (3.9) shows that

$\Sigma_i = N\sigma_i$

The microscopic cross section σ_i is expressed in cm^2 or in barns,
where 1 barn = $10^{-24}\ cm^2$.
(Note: If several different types of nuclei are present in the material, then a number of partial products $N\sigma_i$ for the various nuclide types must be added together to obtain Σ_i.)

In equation (3.10) N can be derived from the density of the material and the atomic weight of the element, whereas σ_i depends on the type of nucleus and on the neutron energy. The value of σ_i is obtained by experiment.

3.3.2 Beam intensity

As neutrons in the beam undergo reactions, the beam intensity is reduced. In the slice Δx of Figure 3.3, the number of reactions of all types can be derived from equation (3.8), using the total cross section Σ_{tot}. The beam attenuation in the slice is thus

$\Delta I = -\Sigma_{tot}.I(x).\Delta x$

In differential form, this equation is

$\dfrac{dI}{dx} = -\Sigma_{tot}.I(x)$

the solution of which is

$I(x) = I_o\ e^{-\Sigma_{tot}\ x}$

The beam intensity attenuates exponentially with distance within the material.

3.3.3 Mean free path

The mean free path of a neutron in the material is the average distance travelled by the neutron before it undergoes a reaction. Using equation (3.10) for the number of reactions in a slice $\Delta(x)$, the mean free path, denoted λ can be calculated as follows:

$$\lambda = \frac{\int_0^\infty x.\Sigma_{tot}.I(x)dx}{\int_0^\infty \Sigma_{tot}.I(x)dx}$$

$$= \frac{\int_0^\infty x.I(x)dx}{\int_0^\infty I(x)dx}$$

and using equation (3.13),

$$\lambda = \frac{\int_0^\infty xI_o e^{-\Sigma_{tot}x}dx}{\int_0^\infty I_o e^{-\Sigma_{tot}x}dx}$$

which yields

$$\lambda = \frac{1}{\Sigma_{tot}}$$

That is, the mean free path is the reciprocal of the total macroscopic cross section.

3.4 Rates of neutron reactions

3.4.1 Reactions rates

Consider a neutron beam in which n is the neutron density (see figure 3.4), i.e., the number of neutrons per cm^3; if v is the neutron velocity (considering they all travel at the same speed), then nv is the number of neutrons falling on 1 cm^2 of target material per second. Since σ (cm^2) is the effective area per single nucleus for a given reaction or reactions (section 3.3.2) then Σ is the effective area (cm^{-1}) of all the nuclei per cm^3 target. Hence, the product Σnv gives the number of interactions (between neutron and nuclei) per cm^3 of target material per second. Since each nuclear interaction involves one neutron,

reaction rate (monoenergetic neutrons)
= $\Sigma(v)$ nv (neutrons/cm^3 s)

Fig. 3.4:
Concept of reaction rate and neutron flux
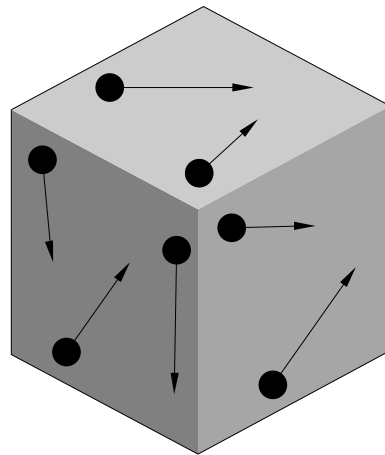
Each point represents a neutron in the unit volume. The lengths of the arrow is equal to the velocity of the neutron. The flux is the sum of all arrow lenths

3.4.2 Neutron flux

Equation (3.17b) can be written in a slightly different form by introducing the neutron flux instead of the neutron density. The neutron flux is defined as the product of the neutron density and the velocity, i.e.,

$\emptyset(v) = nv$,   (for monoenergetic neutrons)

so that it is expressed in units of neutrons per cm^2 per second. It is equal to the total distance (sum of all the path lengths) travelled in one second by all the neutrons present in one cm^3.

When there is a distribution of velocities v, the total flux is obtained by integrating over velocity:

$\emptyset = \int n(v) \, v.dv$

If the interest is in neutrons of a particular velocity or range of velocities, then specific fluxes such as thermal-neutron flux, "fast-neutron" flux, etc, can be calculated.

The reaction rate can also be expressed as a function of the neutron flux:

reaction rate (monoenergetic neutrons)
$= \Sigma(v) \, \emptyset(v)$ (neutrons/cm^3 s)

Here again, if there is a distribution of neutron velocities, the reaction rate can be integrated over the distribution, i.e.,

reaction rate over all neutrons
$= \int \Sigma(v) \, \emptyset(v) \, dv$

In a real reactor, the values of neutron population and neutron flux are a function of location in the core. Because the neutron flux is an essential ingredient in the computation of reactor rates, the determination of the spatial distribution of the

neutron flux in the core is an important part of reactor physics. The value of the neutron flux at a given point in the core will depend on the distribution of nuclear properties (cross sections) throughout the core, and on the position of the point in relation to the central part of the core and to the external surface of the reactor. The neutron flux drops to zero at, or just beyond, the radial and axial boundaries of the core (see figure 3.5). The behaviour of the flux in the core and its rate of decline towards the boundaries must, for realistic situations, be calculated by means of (large) computer codes.

Fig. 3.5:
Typical CANDU neutron flux distribution
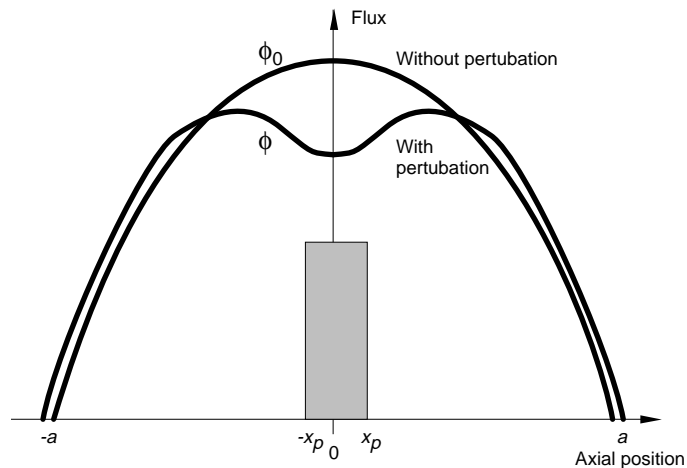
3.4.3 Concept of the neutron current

When the neutron flux is not spatially uniform (see figure 3.5), there is at any point a net leakage of neutrons from regions of high flux to regions of low flux. The net movement of neutrons at any point can be expressed in terms of the neutron current, denoted by the vector quantity $\vec{j}$. Just as the neutron flux depends on the position in the reactor, so does the neutron current. In diffusion theory, it can be shown that the neutron current is proportional to the gradient of the flux:

$$\vec{j} = -D\nabla\phi$$

where the proportionality constant D is called the diffusion coefficient. D is a function of the properties of the medium, and also depends on the neutron energy. It is related to the total cross section Σ_S by

$$D = \frac{1}{3\Sigma_S}$$

3.5 Concept of irradiation

The irradiation of a material, denoted ω, is a measure of the time spent by the material in a given neutron flux. Mathematically, it is defined as the product of the neutron flux and time:

$$\omega = \text{ø}.t$$

The units of irradiation are neutrons/cm^2, or more conveniently, neutrons per thousand barns (neutrons per kilobarn n/kb).

3.6 Fuel burnup

Fuel burnup is the (cumulative) quantity of fission energy produced per mass of nuclear fuel during the latter's residence time in the core. The two most commonly used units for fuel burnup are Megawatt-hours per kilogram of uranium, i.e., MWh/kg(U), and Megawatt-days per tonne of uranium, i.e., MW.d/t(U). The energy considered here is the energy released as a result of fissions.

Fuel burnup is an important economic quantity, and is essentially the inverse of the specific fuel consumption in the reactor (measured e.g. in t(U) per Full Power Days of operation).

4 Fission

4.1 Mechanism of nuclear fission

Fission is the splitting of an atomic nucleus. Generally, a nucleus does not break up spontaneously for the same reason a drop of liquid does not split in two spontaneously (see Figure 4.1). Before the rupture of the drop, a certain amount of energy is required to initiate the deformation. The liquid-drop model is often used to explain the fission mechanism.

Fig. 4.1:
Liquid-drop model of fission

A   B   C   D   E
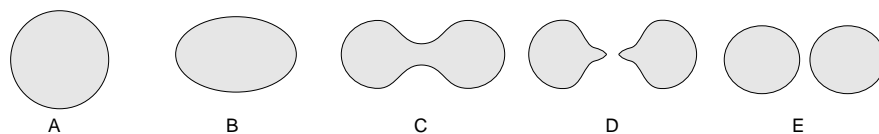
Spontaneous fission may occur naturally for some uranium nuclei; however, the time involved is usually longer than the radioactive α decay. The type of fission which is of practical interest in a nuclear reactor is that induced by collision between a neutron and a fissionable nucleus.

Only three nuclides, having sufficient stability to permit storage for a long time, namely, uranium-233, uranium-235, and plutonium-239 are fissionable by neutrons of all energies, for thermal values (or less) to millions of eV. Uranium-235 is the only one that is found in nature, the other two are produced artificially (see Figure 2.5). Several other species are known to be capable of undergoing fission by neutrons of all energies, but they are highly radioactive and decay so rapidly that they have no practical value for the release of nuclear energy. In addition to those, there are nuclides that require fast neutrons to cause fission; among these, thorium-232 and uranium-238 can be mentioned. Since fission of thorium-232 and uranium-238 is possible with sufficiently fast neutrons, they are known as fissionable nuclides. In distinction, uranium-233, uranium-235, and plutonium-239, which will undergo fission with neutrons of any energy, are referred to as fissile nuclides.

Fission may occur in a certain fraction of collisions between a neutron and a fissionable nucleus. This is shown in Figure 4.2. The nucleus breaks up into two large fission fragments, which are themselves nuclei of other elements, e.g., cesium, iodine, xenon, krypton, and many others. These elements are the fission products of the reaction. There also emerge from each fission a number of neutrons (usually two or three), gamma and beta radiation, and neutrinos.

Fig. 4.2:
Schematic fission chain reaction
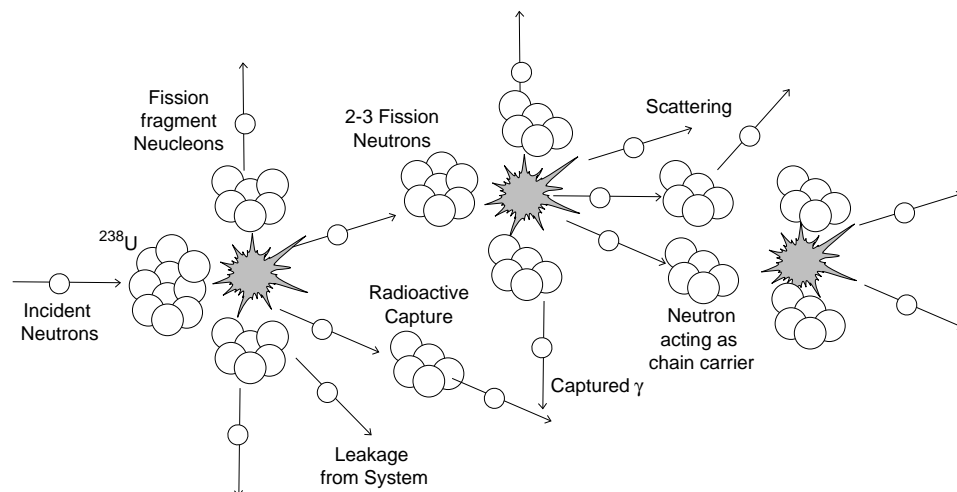
The importance of fission, from the standpoint of the utilization of nuclear energy, lies in two facts. First, the process is associated with the release of a large amount of energy per unit mass of nuclear fuel (Section 4.2) and, second, the fission reaction, which is initiated by neutrons, is accompanied by the liberation of neutrons. It is the combination of these two circumstances that makes possible the design of a nuclear reactor in which a self-sustaining fission chain reaction occurs with the continuous release of energy.

Once the fission reaction has been started in a few nuclei by means of an external or internal source of neutrons, it can be maintained in other nuclei by the neutrons produced in the reaction. It should be noted that it is only with the fissile nuclides mentioned above that a self-sustaining chain reaction is possible. Uranium-238 cannot support a fission chain because the fission probability is small even for neutrons with energies in excess of the threshold of 1 MeV, and inelastic scattering soon reduces the energies of many neutrons below the threshold value. Table 4.1 gives the average number of neutrons emerging from the thermal-neutron-induced fission of various fissile nuclides.

Table 4.1:

Average number of neutrons per fission

Isotope	ν
^{233}U	2.49
235U	2.43
^{239}Pu	2.87
^{241}Pu	2.97

Most of the fission neutrons emerge instantaneously from the reaction. However, a small fraction (~0.5%) of the neutrons are produced by the decay of the fission products or their daughters, and are thus "delayed". The delay corresponds to the decay time constant of the specific delayed-neutron precursor; these time constants range from a fraction of a second to minutes. In spite of their relatively small numbers, delayed neutrons play a crucial role in reactor regulation since they ensure the control of the sustained chain reaction (this will be explained in lesson 3).

4.2 Energy release in fission

Fission is accompanied by a large release of energy, about 200 MeV per fission. In a conventional chemical reaction, the energies involved are several orders of magnitude smaller and are measured in eV (about 4 eV for the oxidation of an atom of carbon-12).

The major proportion, over 80 %, of the energy of fission appears as kinetic energy of the fission fragments, and this immediately manifests itself as heat. Part of the remaining 20 % or so is liberated in the form of instantaneous gamma rays from excited fission fragments and as kinetic energy of the fission neutrons.

The rest is released gradually as energy carried by the beta particles and gamma rays emitted by the radioactive fission products as they decay over a period of time. This decay energy ultimately appears in the form of heat as the radiation interact with and are absorbed by matter. About 7% of the total heat generated in the reactor is obtained from the decay of radioactive fission products. This "decay heat" does not disappear immediately when the reactor is shut down. In fact, large quantities of heat are generated, and must be safely removed, for weeks and months after reactor shutdown. The distribution of the fission energy for uranium-235 is given in table 4.2.

Table 4.2:
Distribution of energy release from ^{235}U fission

Form	Energy Per Fission (Mev)
1. K.E. Of Fission Products	167.0
2. K.E. Of Fission Neutrons	4.8
3. Prompt γ	7.2
4. γ From Fission Products	6.1
5. β From Fission Products	7.4
6. Neutrinos	10.4
Total Fission Energy	**202.9**

The 10 MeV energy of the neutrinos accompanying the beta radioactivity is not available for power production; all the neutrinos escape carrying their energy.

4.3 Neutron-energy considerations

Both the energy of the neutrons emerging from fission and the energy of the neutrons causing fission have to be considered in a fission reaction. The kinetic energy of neutrons emitted in fission (called fission neutrons) follows a distribution or spectrum of the type shown in Figure 3.1. The most probable energy of a fission neutron is 1 MeV.

As mentioned in Section 4.1, neutrons of any energy can induce fission in ^{235}U, ^{239}Pu , and ^{233}U. Thus all neutrons emerging from fission have the potential to continue the chain reaction in these nuclei. However, the cross section for fission is not constant with neutron energy, but is instead much larger for thermal neutrons than for neutrons in the MeV range (see Figure 3.1). In thermal reactors, there is a forced accumulation of neutrons around an energy of about 0.025 eV, and it can be seen from Figure 4.3 that the fission cross section is high at this energy. Therefore, thermal neutrons induce more likely fission reaction than fast neutrons which need to be "thermalised" or slowed down.

Fig. 4.3:
Fission cross section versus neutron energy
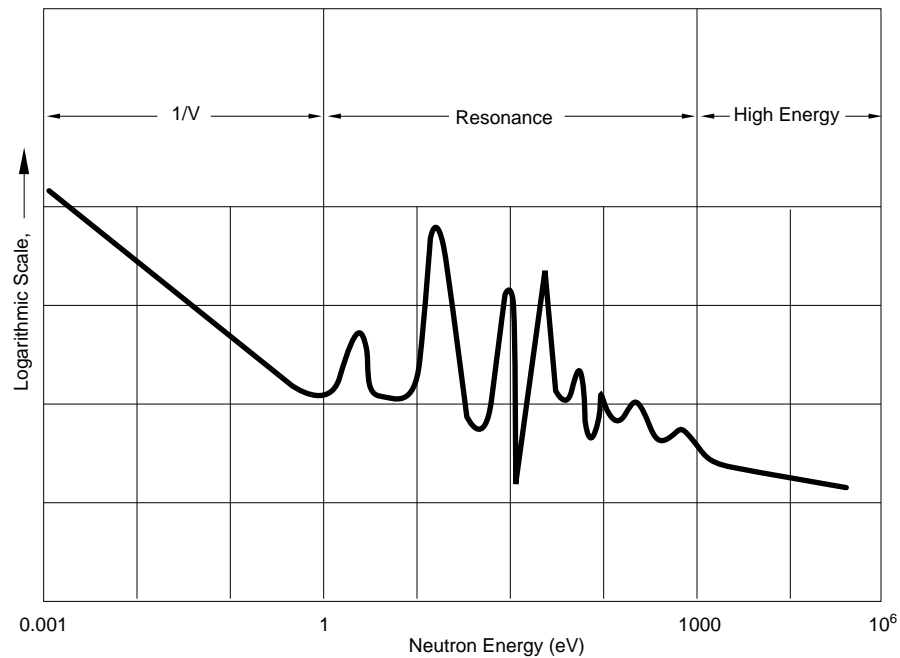
It can be seen from Figure 4.3, that the variation of the absorption cross section with neutron energy is characterized by three regions (however, each nuclide exhibits a specific curve). There is, first, a low-energy region where the cross section decreases steadily with increasing neutron energy. Cross-sections obey the 1/v law, where v is the neutron velocity. Following the 1/v region for slow neutrons the element under consideration exhibits a resonance region, for neutron of roughly 0.1 to 1000 eV energy. This region is characterized by the occurrence of peaks where the absorption cross section rises fairly sharply to high values for certain neutron energies. After the resonance region, the nuclear cross section decreases steadily with increasing neutron energy. The fast-neutron region starts at energies in excess of about 10 keV.

As mentioned in Section 4.1, ^{238}U is not a suitable nuclear fuel on its own; however, fast-neutron fission in ^{238}U makes a small contribution to the overall fission rate in a reactor.

4.4 Thermal reactors

In order to take advantage of the large fission cross section at low neutron energies, a material is placed in the reactor core to slow the fission neutrons down to thermal energies. This material is the moderator.

Reactors which rely on thermal neutrons are called thermal reactors. All current commercial reactors are of this type. Depending on circumstances, the fuel in a

thermal power reactor may range from natural uranium, with 0.7% of uranium-235, to material enriched up to 4% in the fissile isotope. Some reactors rely on fast neutrons (fast reactors) have been designed and built, but these are mostly prototypes and are not operating in large numbers.

Concepts of Reactivity and Criticality

Training Objectives

The participant will be able to describe or understand:

1   the neutron economy and sustained chain reaction,
2   the typical nuclear lattice of a CANDU reactor,
3   the various mechanisms of production, absorption and leakage of neutrons,
4   the neutron multiplication factors k_∞ and k_{eff},
5   the concept of reactivity,
6   the concept of criticality,
7   the four factor formula for the multiplication factor.

Concepts of Reactivity and Criticality

Table of Contents

1 Introduction

The major challenge in the nuclear energy production is to sustain and control the nuclear fission. The chain reaction is sustained by balancing the production and loss of neutrons. Therefore, the general form of the neutron balance equation is :

$$\begin{bmatrix} Net\ rate\ of\ gain\ of \\ neutrons \end{bmatrix} = \begin{bmatrix} Rate\ of\ production\ of \\ neutrons\ by\ fission \end{bmatrix} - \begin{bmatrix} Rate\ of\ loss\ of\ neutrons \\ by \\ leakage\ and\ absorption \end{bmatrix}$$

The chain reaction has a multiplicative nature: that each fission event induced by a single neutron can produce two or three neutrons. Therefore, the neutron population has the potential to grow exponentially in an uncontrolled chain reaction.

When the balance between production and loss is reached in a nuclear reactor, the number of neutrons produced equals the number of neutrons lost for a given time interval. The overall neutron population within the reactor is then maintained, and both the neutron flux and the resulting neutronic power are held constant. The steady-state neutron balance equation is :
    Production = absorption + leakage

In a critical system, the rate of production of neutrons by fission just balances the rate of loss in various ways, and thus the above equation is the most general form of the critical equation for a reactor.

The control of the neutronic power production in a reactor is achieved by varying what is called the "reactivity" of the reactor core. Adding or subtracting reactivity contributions by the action of specially designed "reactivity devices" enables to increase or decrease the neutron population. The balance between the sources and the sinks of neutrons is moved accordingly toward the sources or the sinks. Figure 1.1 illustrates the effect of the insertion of a control rod along the axis of a cylindrical thermal reactor on the neutron flux. The absorption of neutrons by the control rod induces a decrease of the flux in the centre of the core. Considering the case of multiple rods inserted near the centre, the overall effect would be a flattened flux distribution in the centre.

Fig. 1.1 :
Flux distribution in a reactor core with and without a central control rod
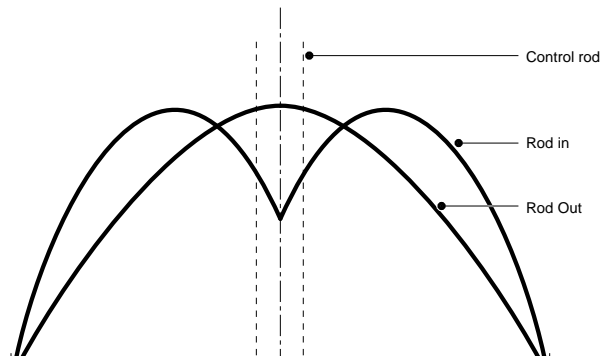
Reactor physics should also perfectly encompass the nuclear kinetics including the overall time table of the combined nuclear processes. The control of the chain reaction depends on the rate of the exponential variation of the neutron population. The reactor is more easily controlled if this rate is slow compared to the time scale of the control interventions. Let say for the moment, that the chain reaction can be controlled in a thermal reactor because the time response depends more on "delayed" neutrons emitted after the slow decay of precursors rather than fast (high kinetic energy) neutrons alone coming directly from immediate fissions.

When a fast neutron is born during a fission process the time after which this neutron can produce another fission is extremely short (fraction of a second). On the other hand a fission creates two or three elements and some of them decay through the emission of a "delayed" neutron. This neutron is emitted a few seconds after the original fission. It is with that population of neutrons that the reactor can be controlled.

2 The Nuclear Lattice

The physical configuration of fuel, moderator, and other materials in the reactor core follows a repetitive geometrical pattern. This array is called the nuclear lattice, and its smallest unit is called the lattice cell.

There are two reasons to arrange the various materials in a reactor core into a lattice: a technological reason and a physical reason. The first one is natural. The fuel needs to be cooled in order to evacuate the energy produced. Therefore, there is a need to increase the heat exchange area between the fuel and the coolant to extract the thermal power. The neutronic considerations are not as simple. The lattice configuration may have opposite effects depending, for one thing, on the type of nuclear reactor under consideration (thermal neutrons

reactor or fast neutrons reactor). The physical shape and the size of the reactor as well as the various materials present in the core (relative proportions and physical configuration) determine the possible neutron fates in the reactor core (see Section 3). The lattice (or heterogeneous structure) is the configuration adopted in thermal reactors.

Fig. 2.1:
Nuclear lattice of a typical CANDU reactor
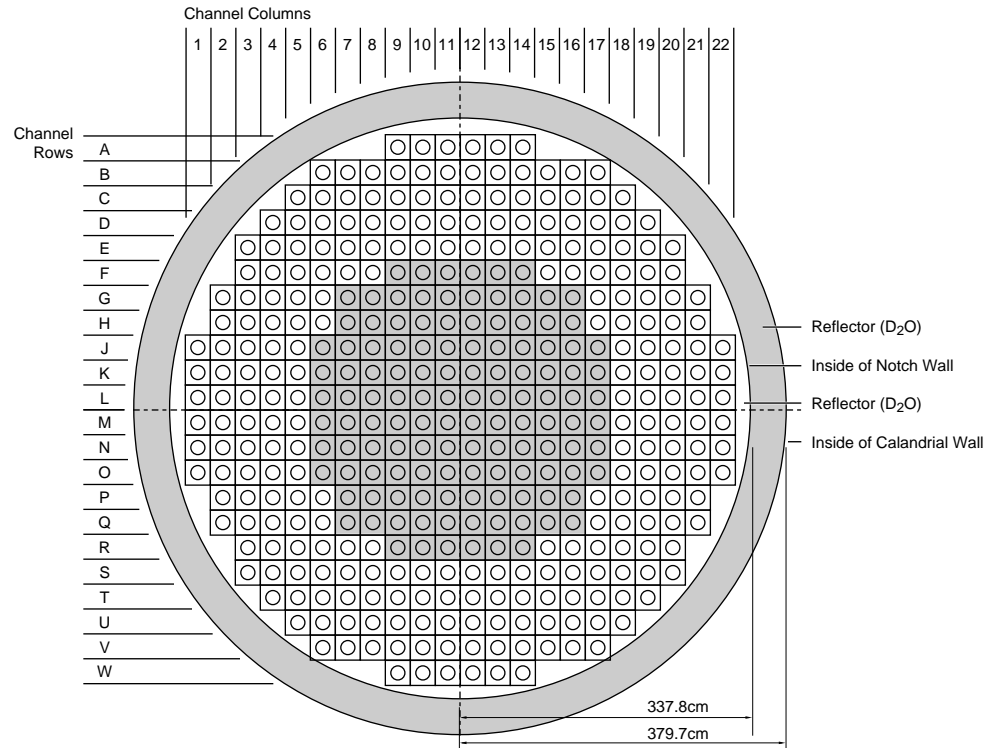
In a CANDU reactor the fuel is arranged on a square lattice (Figure 2.1). A two-dimensional section of the CANDU lattice cell is shown in Figure 2.2. It consists of fuel pins and coolant, surrounded by a pressure tube, a gas annulus, a calandria tube, and a volume of moderator. The width of the cell is equal to a lattice pitch, the distance between fuel channels; this pitch is 28.575 cm in the CANDU reactor. In the third direction, the dimension of the cell is the length of a fuel bundle, viz 49.53 cm. The cross section and the longitudinal view of a fuel bundle are shown in Figure 2.3.

Fig. 2.2:
A lattice cell of a CANDU 600

Lattice Cell Boundary
(Containing D_2O moderator)

Calandria Tube

Annulus (Gas Gap)

Pressure Tube
(Containing D_2O coolant)

Fuel Bundle
(Fuel element made of
UO_2 in a Zircaloy tube)
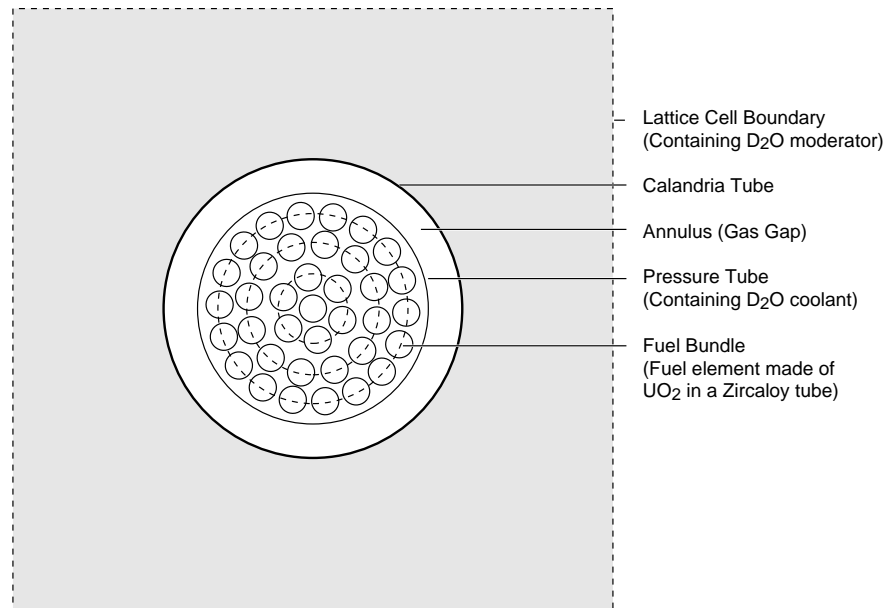
Some materials inside the reactor core are not shown in the basic lattice cell of Figure 2.2, because they do not appear in every cell of the reactor. An example of this are control rods or other regulating-system or instrumentation devices, inserted at only certain core positions. These devices are not usually considered part of the basic cell, but their effect must be appropriately taken into account.

Fig. 2.3:
End plate and CANDU 600 type fuel bundle

Outside Ring

Middle Ring

Inner Ring

End Plate

Fuel Rod
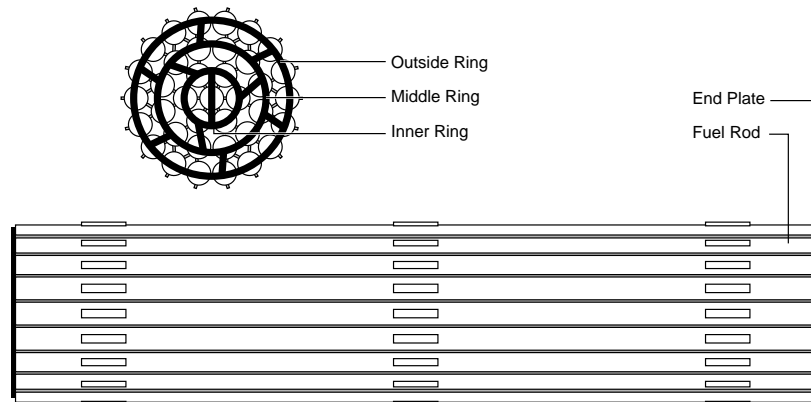
Note that, if the unit cell is repeated infinitely in all three directions, it yields the infinite nuclear lattice, a useful idealized concept. Leakage from an infinite lattice is necessarily zero, since there is no bounding surface.

3 The Various Fates of Neutrons

Since neutrons are the mediators of the chain reaction, the latter will best be sustained when neutrons are conserved and "managed" in such a manner as to promote further fissions. This is what is meant by neutron economy. As a consequence, it is important to understand the various processes in which neutrons can be lost. These processes belong to two broad categories: leakage and absorption. The various possibilities described below are summarized graphically in Figure 3.1.

When a neutron is born in fission, it can, firstly, simply escape from the reactor, i.e., leak out from the system.

If it does not escape, it starts to diffuse through the reactor core and can, first, be absorbed as a fast neutron in various core materials. In most such absorptions the neutron will be lost, the most probable process being a radiative capture (n, γ). Even though the neutron is lost, its energy could be recovered. In a small number of fast-neutron absorptions in ^{238}U, fission occurs, making a positive contribution to the chain reaction and to neutron economy.

The other fate which can befall a fast neutron is to be slowed down. This occurs mostly in collisions with moderator nuclei, whose intended function is precisely to slow neutrons down to thermal energies. As a neutron slows down through multiple collisions, it can, however, still be lost through leakage or absorption. One particularly "hazardous" energy interval, ranging from approximately 100 keV to 1 eV, contains numerous "resonances" in which various fuel nuclei, in particular ^{238}U, have a high cross section for capturing the neutron.

If the neutron survives slowing down through the resonance region without being captured, and becomes a thermal neutron, it can leak out from the system as a thermal neutron, or it can be absorbed in the various core materials. If it is absorbed in a non-fuel material ("parasitic" absorption), it is lost. If absorbed in fuel, the thermal neutron will, in a certain fraction of such absorptions, induce fission and thus produce a new generation of neutrons to keep the chain reaction going.

December 1995

Fig. 3.1:

Neutrons fates
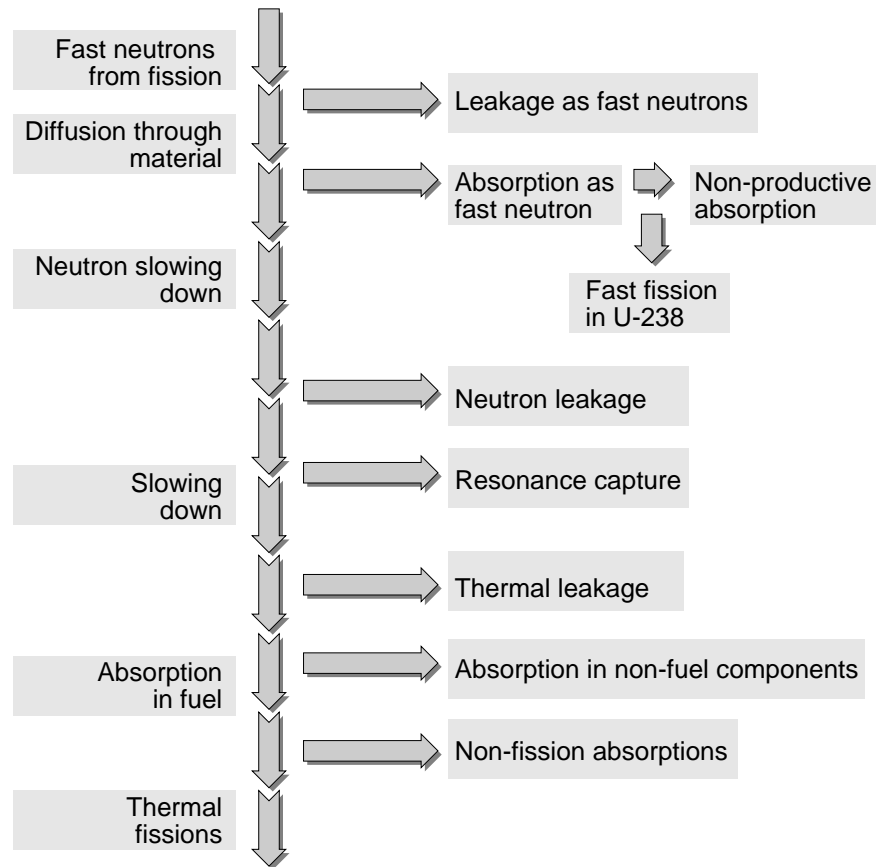
Non-fission absorptions in ^{238}U eventually produce ^{239}Pu through the formation of U-239 and its subsequent double beta decay:

$$^{238}_{92}\text{U} + ^{1}_{0}\text{n} \rightarrow ^{239}_{92}\text{U} \rightarrow ^{239}_{93}\text{Np} + \beta - \rightarrow ^{239}_{94}\text{Pu} + \beta - + \beta -$$
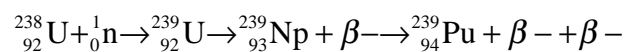
The intermediate ^{239}U has a half-life of 23.5 minutes, and ^{239}Np has a half-life of 2.35 days.

The above process effectively creates a new source of fissions, since Pu-239 is fissile. For this reason, ^{238}U is called a fertile nuclear material. Through additional neutron absorptions, ^{239}Pu also gives rise to some ^{240}Pu and fissile $^{241}_{94}$Pu :

$$^{239}_{94}\text{Pu} + ^{1}_{0}\text{n} \rightarrow ^{240}_{94}\text{Pu} + ^{1}_{0}\text{n} \rightarrow ^{241}_{94}\text{Pu}$$
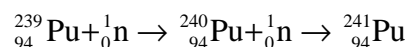
Once formed, ^{239}Pu and ^{241}Pu contribute to the chain reaction in much the same way as ^{235}U, whose depletion they partially offset.

Whether the chain reaction is self-sustaining, and to what degree, depends on the relative number of neutrons from one generation which succeed in "giving

birth" to a new generation. The following sections discuss various aspects of this question.

4 Multiplication Factors, Reactivity and Criticality

4.1 The multiplication factors k_∞ and k_{eff}

A nuclear reactor is designed to achieve the very delicate balance between fission reaction, neutrons capture and neutrons leakage. This requirement can be expressed in a mathematical form. Since the neutrons play the central role in maintaining the fission chain reaction, our attention will be focussed on them. A given neutron will be "born" in a fission event and will then usually scatter about the reactor until it meets its eventual "death" in either an absorption reaction or by leaking out of the reactor. Certain numbers of these neutrons will be absorbed by fissile or fissionable nuclei and induce further fission, thereby leading to the birth of new fission neutrons, that is, to a new generation of fission neutrons. If it is possible to measure the number of neutrons in two successive fission neutron generations, then, the ratio of these numbers can be defined. This ratio is called the multiplication factor k and characterizes the chain reaction:

$$k = \frac{\text{Number of neutrons in one generation}}{\text{Number of neutrons in preceding generation}}$$

The multiplication factor for a infinite nuclear lattice is labelled k_∞. In an infinitely large system, there is no loss of neutrons by leakage and it is only by absorption (in fuel, moderator, etc...), that neutrons would be removed. Therefore, k_∞ can also be defined as:

$$k_\infty = \frac{\text{Number of neutrons in one generation}}{\text{Number of neutrons absorbed in the preceding generation}}$$

For a real, finite reactor, the analogous quantity is called the effective multiplication factor and is labelled k_{eff}. In this case, the multiplication factor accounts for leakage effects.

4.2 Concept of reactivity

A quantity closely related to the multiplication constant is the reactivity, denoted by the symbol ρ and defined as:

$$\rho = \frac{k-1}{k}$$

The reactivity measures the deviation of core multiplication from its critical value k = 1.

One unit of reactivity (or of changes or differences in reactivity) is the milli-k, where

1 milli-k = 0.001

For example, when

  k = 1, ρ = 0
  k = 1.002, $\rho \cong$ 0.002 = 2 milli-k
  k = 0.995, $\rho \cong$ -0.005 = -5 milli-k

The unit milli-k is abbreviated to mk.

Two other units of reactivity based on the same definition are also used, the pcm and the dollar.

  1 pcm = 10^{-5}
  1 dollar = β_{eff} (effective delayed neutrons fraction)

4.3 Concept of criticality

4.3.1 Definition of criticality

If k_{eff} is greater than 1 (ρ > 0), a greater number of neutrons are born in every successive generation, i.e., the chain reaction in the reactor is more than self-sustained. The neutron population and the power level increase with time. The reactor is said to be supercritical.

If k_{eff} is exactly equal to 1 (ρ = 0), the chain reaction is self-sustained and the reactor is said to be critical. The neutron population and power level are in a steady-state condition. In this condition there is an exact balance between neutron production and neutron losses.

If k_{eff} is less than 1 (ρ < 0), the chain reaction is not self-sustained. The reactor is said to be subcritical. In this case, the neutron population and the power level decrease with time.

These various possibilities are summarized in Figure 4.1. k_{eff} = 1 (reactivity = 0) means that the reactor is critical, but it does not mean that the reactor is necessarily at full power. The reactor can be critical at any power level: full power, very low power, power greater than normal. In a critical reactor the power level is steady. On the other hand, departure from criticality signifies that the power level is changing: increasing when the reactor is supercritical, decreasing when it is subcritical. As a corollary, "going critical" does not mean "at full power". During startup, the reactor goes critical at a very small fraction ($\sim \leq 10^{-6}$) of full power.

Fig. 4.1:

Multiplication factor, reactivity and criticality

$$k \left(\rho = \frac{k-1}{k} \right) \begin{cases} > 1 \ (\rho > 0) \text{ Supercritical} \\ = 1 \ (\rho = 0) \text{ Critical} \\ < 1 \ (\rho < 0) \text{ Subcritical} \end{cases}$$

4.3.2 Departure from criticality and criticality control

Most of the time it is desired to maintain the reactor at steady full power. Then it must be kept critical. When it is desired to increase or decrease power, the reactor must be made supercritical or subcritical for some length of time until the desired power is reached, after which criticality must be regained. This refers to the control of criticality. To shut the reactor down, subcriticality must be achieved and maintained. What must be avoided are situations where the reactor is uncontrollably supercritical for too long, since a divergent power "excursion" may lead to overheating of the fuel and other core components.

Thus, for effective reactor control, it is important that there be means of changing and controlling the reactivity of the system. According to the definition of the multiplication factor, the multiplication may be adjusted by changing production, absorption and/or leakage. Typical procedures may concentrate on one aspect but may end up changing all three to some extent. In order to control a nuclear reactor, provisions must be made to accommodate power-level changes and to compensate for fuel depletion and related effects.

Active neutron-balance control in reactors operate on one or more of the three following terms:
- production:
  - adjust the amount of fissile material in the core region;
  - adjust the effectiveness of the moderator.
- absorption:
  - use solid, moveable absorbers (control rods);
  - dissolve absorbing material in the coolant (soluble poisons);
  - employ solid, fixed absorbers (burnable poisons) which "burn out" gradually with neutron reactions over the lifetime of the reactor fuel.
- leakage:
  - change system dimensions and density and/or modify the effectiveness of neutron reflection.

Most power reactors designs rely on one or more of the neutron-absorption procedures. However, in the CANDU reactor, the neutron-production control is exercised by on-line refuelling. The various reactivity devices available for regulation and shutdown in a standard CANDU 600 are listed in Table 4.1, which also shows the reactivity range of the devices.

Table 4.1:

CANDU 600 reactivity devices and maximum rates

Devices	Function	Total Reactivity worth (mk)	Maximum Reactivity insertion rate (mk/s)
14 Liquid Zone Controllers	Control	7.1	± 0.14
21 Mechanical **Adjusters**	Control	15.3	± 0.09
4 Mechanical Control Absorbers	Control	10.8	± 0.075 driving - 3.5 dropping
Moderator poison	Control	—	-0.0125 extracting
28 Shutoff Rods	Safety	80	- 50.
6 Poison Injection Nozzles	Safety	> 300	- 50.

Neutron-balance control is also important in fuel cycle operations outside nuclear reactor cores. Here, it is most desirable to maintain all fissionable materials in the subcritical state. Basic nuclear criticality safety for this case depends on geometric controls applied to the neutron balance in one or more of the following ways:
- production:
    - limit fissile mass and concentration
- absorption:
    - use fixed or soluble neutron poisons
- leakage:
    - employ high leakage, "favourable" geometry equipment and containers
    - limit neutron reflection
    - separate equipment and, or storage containers to limit neutronic interaction

5 Leakage and Critical Mass

5.1 Non-leakage probability

The difference between the infinite and effective multiplication factors is related to the leakage from the reactor, since neutrons which leak out from the finite

reactor cannot participate in the chain reaction. From the definition of these two factors previously given, it is seen that:

$$\frac{k_{eff}}{k_{\infty}} = \frac{\text{Neutrons absorbed}}{\text{Neutrons absorbed} + \text{neutrons leaking out}} = P$$

The fraction defining P is thus a measure of the probability that neutrons will not leak out the finite system, but will remain until absorbed. Hence, it is possible to write:

$$k_{eff} = k_{\infty}P$$

where P is called the non-leakage probability of the system. The problem of deriving the condition for criticality, i.e., $k_{eff} = 1$, thus fall into two parts. The first is the evaluation of the infinite multiplication factor which is a function of the material, e.g., fuel, moderator, coolant, structure, etc., of the reactor. The second involves the determination of the non-leakage probability, which is dependent on the materials but also largely on the geometry, i.e., size and shape, of the system. The non-leakage probability increases with size, for a reactor of given composition, and approaches unity for a system of infinite size, i.e., when k_{∞} and k_{eff} are identical. As a general rule, the smaller the volume-to-boundary surface ratio of a reactor, the larger the leakage, and the smaller P (and therefore k_{eff}) is.

Since the non-leakage probability P is less than unity more generally for a finite system as neutron leakage may occur, k_{∞} has to be greater than 1 in order to achieve a critical chain reaction in the real reactor.

5.2 Critical mass

As mentioned in Section 5.1 and as it appears from equation 5.2, two parameters are involved in the determination of a critical system: the non-leakage probability P and the infinite multiplication factor k_{∞}. Therefore, a finite reactor may be constructed starting with a cell from a supercritical infinite lattice ($k_{\infty} > 1$) and gradually increasing the size of the reactor by adding more an more of this type of cells. As the size increases, the non-leakage probability will increase (i.e., leakage will decrease), and there will be one value of P, for the given k_{∞}, for which k_{eff} will be equal to 1. In other words, there is a minimum size of the system which enables a self-sustained chain reaction; this minimum size is the critical size, also called the critical mass.

The critical size depends firstly on the supercriticality of the infinite lattice (k_{∞}), and secondly on the shape of reactor core fuel configuration, as it affects the non-leakage probability P. If the material proportions in the basic cell make the infinite lattice subcritical (i.e., if $k_{\infty} < 1$), then no size of reactor can be critical.

To illustrate the importance of the reactor shape on the neutrons leakage,

consider the eighteen fuel bundles arrangement shown in Figure 5.1(a). Supposing that this configuration corresponds to the critical mass, then, the same eighteen bundles arranged in a single tube (Figure 5.1(b)) would not be critical as the leakage would be far too great.

Fig. 5.1:
Illustration of the importance of the core shape
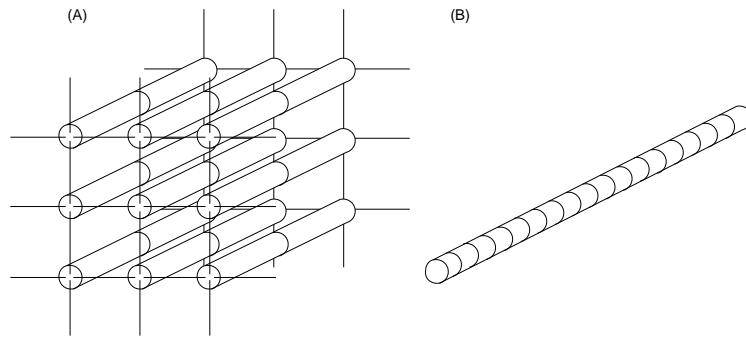
The shape which gives the highest volume over surface ratio will give the smallest neutron leakage; therefore, the reactor core should be spherical. But, such a reactor would be difficult and expensive to build. Therefore the next best shape used for "industrial" reactor cores is a cylinder in which the height is approximately equal to the diameter. In a LWR, the core is a vertical cylinder whereas in a CANDU it is horizontal.

5.3 Neutron reflector

Neutron leakage from a reactor can be diminished by surrounding the fuelled region of the core by a "reflector" which function is to reflect straying neutrons back towards the fuel. As a result more neutrons are available for fission (increase of neutron economy) and the given fuel-moderator system can become critical when the dimensions are appreciably less than required for a bare reactor. The use of a reflector, thus, results in a decrease of the critical mass.

The material used as a reflector must have good neutron scattering properties to reflect back neutrons. For a thermal reactor, light water, heavy water or graphite are usually used for this purpose. It is also desirable that the reflector does not absorb too many neutrons (low absorption cross-section). These requirements also apply to the moderator; for this reason the material used for the moderator and the reflector are usually the same. For the CANDU, it is heavy water (D_2O). The typical geometry of a CANDU reflector is shown in Figure 2.1 of section 2.

There are several interests in using a reflector. The first one, as mentioned previously, is to have more neutrons available for fission. But also, as it is illustrated in Figure 5.2, there is a better utilization of fuel in the outer region as the neutron flux is higher at the edge of the core due to reflection. It can be noted from this figure, that the ratio of average flux to maximum flux is increased. The

hump in the curve is due to the fact that fast neutrons escape into the reflector where they are thermalized and they are not as likely to be absorbed there as they are in the core.

Fig. 5.2:
Effect of a reflector on the thermal-neutron flux distribution
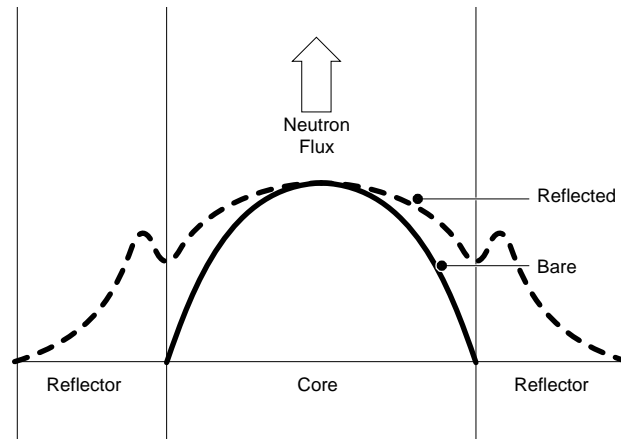
Approximate thermal-neutron flux distribution in bare and reflected reactors

Note also that in practice the size of a reactor must be chosen somewhat larger than the critical mass determined from the above considerations. The reasons for this are that provision must be made, firstly, for rods and other absorbers not accounted for in the basic cell, and, secondly, for loss of reactivity of the core with irradiation. This effect is being minimized if a constant, or near-constant, refuelling is carried out, as in a CANDU reactor, or if sufficient reactivity is stored in the core at the beginning of the cycle as in a LWR.

6 The Four-Factor Formula

Returning to the definition of the infinite multiplication constant and to the various processes involving neutrons, as seen in Section 4.1, a useful equation called the four-factor formula can be developed. This can be achieved by making use of the neutron cycle shown in Figure 6.1.

Fig. 6.1:
Neutron cycle in the infinite lattice
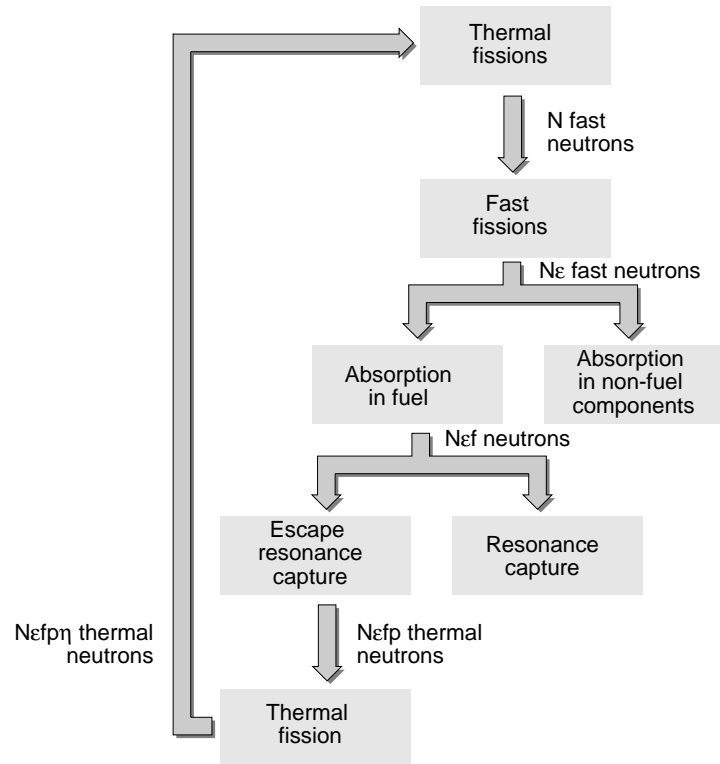
Consider an infinite lattice, suppose we start with N fast neutrons born from thermal fissions in a given fission generation and follow the above mentioned neutron cycle.

Before these fast neutrons have slowed down some will be captured by, and cause fission of, uranium-235 and uranium-238. At neutron energies greater than about 1 MeV, most of the fast neutron fissions in the fuel will be of uranium-238 because of its greater concentration. Since more than one neutron is produced in each fast-neutron fission, there will be an increase of the neutron population by a factor ε. The quantity ε is called the fast-fission factor; it is defined as:

$$\varepsilon = \frac{\text{Total number of fission neutrons (from both fast and thermal neutrons)}}{\text{Number of fission neutrons from thermal fission}}$$

It typically has the value of about 1.02 to 1.03. Consequently, this results in $N\varepsilon$ fast neutrons slowing down past the fission threshold of uranium. Figure 6.2 illustrates the neutron moderation cycle in a reactor in terms of neutron energy levels.

Fig. 6.2:
Neutron generation in a thermal reactor
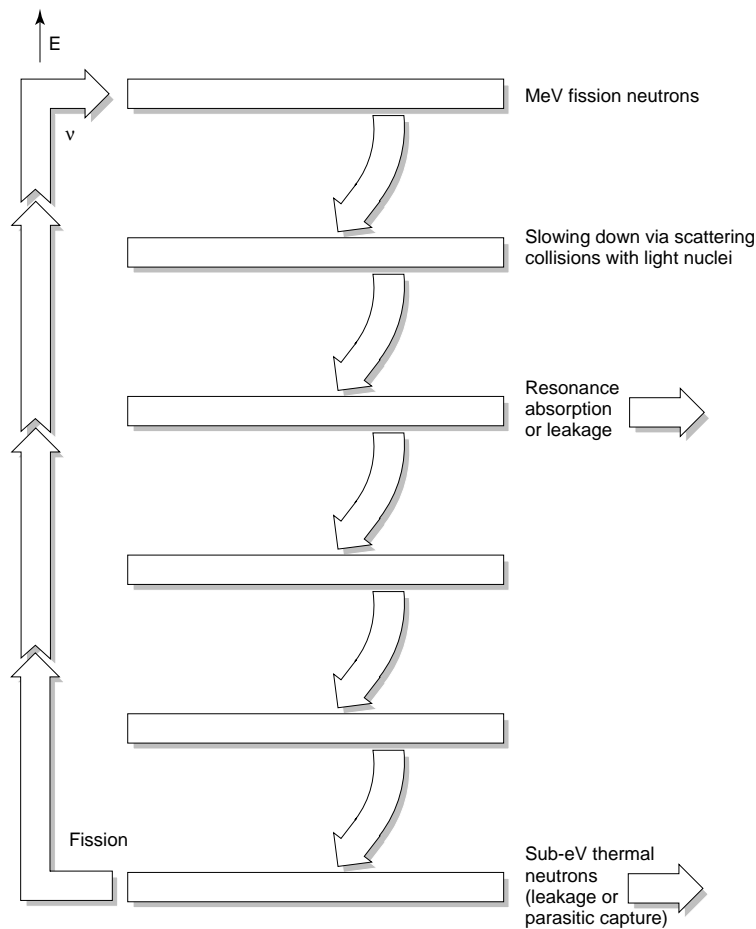
In the course of further slowing down, some of the neutrons are captured in nonfission processes, and the fraction escaping resonance capture in the fuel is p, called the resonance escape probability and defined as:

$$p = \frac{\text{Fission neutrons which escape resonance capture}}{\text{Total fission neutrons}}$$

It typically has a value of about 0.91. Thus Nεp neutrons survive to become thermal neutrons.

When the neutrons have become thermalized, they will diffuse for a time in the infinite system until they are ultimately absorbed by fuel, by moderator or by such impurities, often referred as "poisons", as may be present. Of the thermal neutrons, a fraction f, called the thermal utilization factor, will be absorbed in fuel; the value of f is thus represented by:

$$f = \frac{\text{Thermal neutrons absorbed in fuel}}{\text{Total thermal neutrons absorbed}}$$

It typically has a value of about 0.94. As a result, Nϵpf thermal neutrons are absorbed in fuel.

A certain fraction of thermal neutron absorption result in fissions. Each thermal fission emits η neutrons. Therefore, the number of fast neutrons in the next generation is Nϵpfη. The quantity η is called the thermal reproduction factor and is defined as:

η = number of neutrons emitted per thermal neutron absorption in fuel

The quantity η must be distinguished from the quantity ν which is defined as the number of neutrons liberated for every neutron absorbed in a fission reaction. However, η is related to ν by the following relationship:

$$\eta = \upsilon \times \frac{\text{Neutrons absorbed in fission reaction}}{\text{Total number of neutrons absorbed in fuel}}$$

An alternative way of expressing the relationship is by using the microscopic cross sections σ_f and σ_a:

$$\eta = \nu \times \frac{\sigma_f}{\sigma_a}$$

where σ_f is the fission cross section and σ_a is the total absorption cross section for the nuclide. The quantity η is different for different fissile nuclides, and has a complicated dependence on the incident neutron energy; see Figure 6.3.

Fig. 6.3:
η *versus neutron energy*
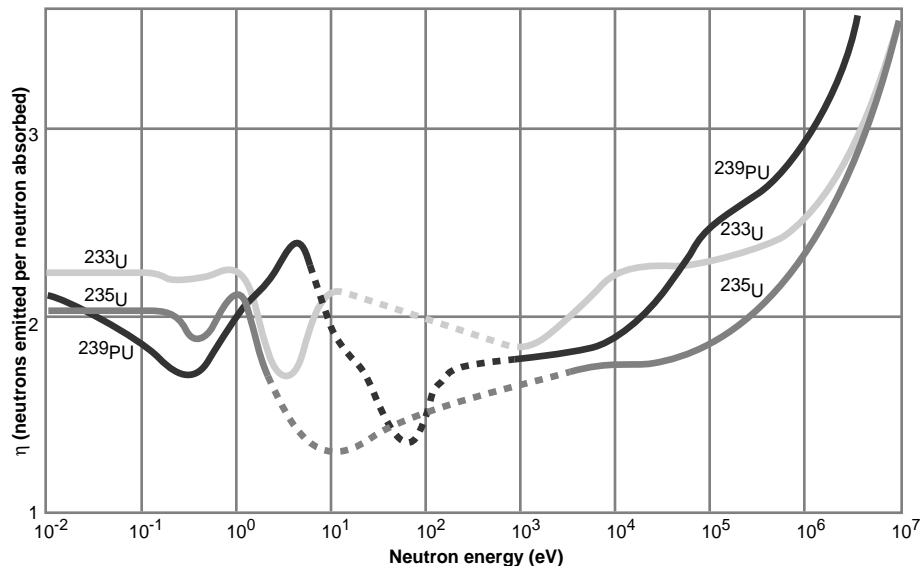
By the definition of the infinite multiplication constant, we can write:

$$k_\infty = \frac{N \, \epsilon \, p \, f \, \eta}{N}$$

$$k_\infty = \epsilon \, p \, f \, \eta$$

which is the four-factor formula.
For the finite reactor, we can write

$$k_{eff} = \varepsilon \, p \, f \, \eta \, P$$

where P is the non-leakage probability. The simplified approach of two energy groups (fast or more correctly above thermal energies, and thermal) can be used to express the overall non-leakage probability as

$$P = P_f \, P_t$$

where P_f and P_t are respectively the fast and thermal non-leakage probabilities.

The four factors ε, p, f, and η are a function of the isotopic composition of the fuel and the other materials in the nuclear lattice. It is clear from Figure 6.3 that η, in particular, will depend in a complex way on the precise spectrum (energy distribution) of neutrons interacting with the fuel. The non-leakage factors depend on the size and shape of the reactor, as discussed in the previous section.

For illustration, the values of the four factors for a typical fresh-natural-uranium CANDU 600 lattice (at full power) are:

ε = 1.0261
p = 0.9072
f = 0.9374
η = 1.2424

This gives

k_∞ = 1.0841

The infinite fresh lattice is thus substantially supercritical. The non-leakage factors in the CANDU 600 are typically

P_f = 0.988
P_t = 0.981

which gives

k_{eff} = 1.0841 x 0.988 x 0.981
= 1.051

From this it would seem that the finite reactor is also supercritical. However k_{eff} is, in practice, reduced to exactly unity, i.e., the reactor is rendered critical, by the effect of in-core reactivity devices (zone controllers, adjusters, moderator boron poison, . . .) whose effect were excluded above.

7 Physical Factors Affecting Reactivity

As mentioned earlier, the materials of the lattice cell, and their geometrical configuration, affect the lattice reactivity. A few examples are listed here.

• The type of moderator affects reactivity through the manner in which it slows neutrons down (i.e., the neutron energy spectrum it produces), and through the fraction of neutrons it absorbs.

• The size of lattice pitch affects reactivity, as it determines the amount of moderator in a unit cell. In general there is a value of lattice pitch which

maximizes reactivity (see Figure 7.1); a much smaller lattice pitch results in insufficient neutron thermalization, whereas a larger lattice pitch results in too much neutron absorption in the moderator. In practice the "optimum" lattice pitch may be somewhat different from the value which maximizes reactivity as other practical, or control oriented, considerations may influence the final design.

Fig. 7.1:
Variation of reactivity with lattice pitch in a CANDU reactor
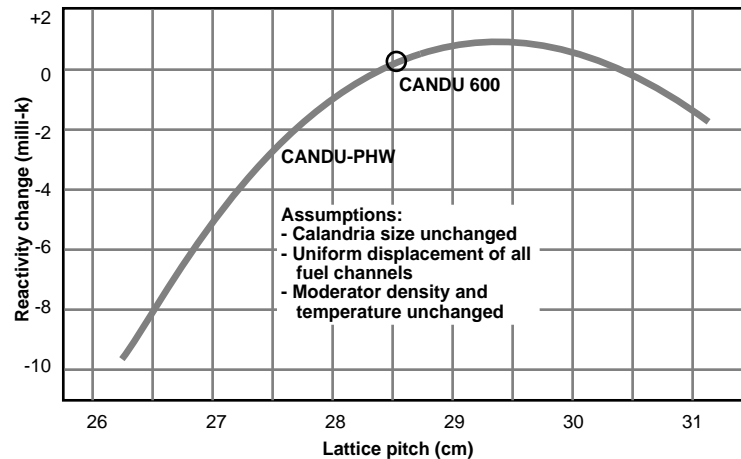
- The ratio of fuel to non-fuel material directly affects the thermal utilization factor f. For instance, a thicker pressure or calandria tube increases the parasitic absorption and decreases f. The material of the tube is also very important in increasing f. Alloys of zirconium, which have a very low neutron absorption cross section, are desirable.

  Similarly, the thickness and material of the fuel sheath affect the thermal utilization factor.

- The fuel temperature affects the resonance escape probability p. At a higher fuel temperature, there is an energy broadening of the resonances (the "Doppler" effect), and neutrons have a lower probability of escaping resonance capture. Thus reactivity decreases as the fuel temperature increases.

- The surface/volume ratio of the fuel (see Figure 7.2) affects reactivity through the amount of resonance absorption, i.e., through p. The resonance capture cross section is so large that most resonance absorptions take place at the surface of the fuel. Fuel nuclei in the interior of the fuel are "shielded" by nuclei at the surface and contribute little to resonance capture. Thus the surface of fuel "visible" to neutrons entering the fuel cluster from the moderator determines the fraction of these neutrons which suffer resonance capture. The number of fuel pins and their precise geometrical configuration

also affect the level of resonance capture of neutrons originating from within the fuel cluster itself.

Fig. 7.2:

Basic data for CANDU fuel bundles

Reactor	**N.P.D.**	**N.P.D. & Douglas Pt.**	
Number of Rods/Bundles	7	19	19
Rod Diameter mm	25.4	15.25	15.22

Reactor	**Pickering**	**Bruce & 600MW**
Number of Rods/Bundles	28	37
Rod Diameter mm	15.19	13.08
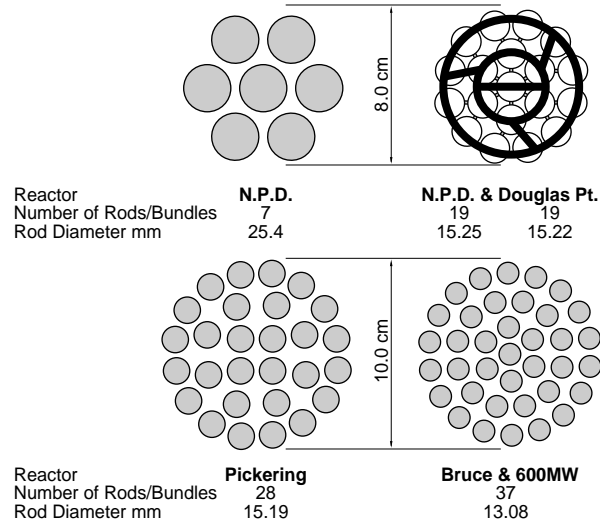
- The amount and temperature of coolant inside the fuel cluster affect the spectrum of neutrons therein, and therefore the fast-fission factor ε

- The isotopic composition of the fuel has a major effect on reactivity. As fuel is irradiated, ^{235}U is depleted and plutonium isotopes and fission products are created. This is a very important effect and will be discussed in detail in the next section.

- Certain fission products, most importantly ^{135}Xe, have a very large neutron absorption cross section, and therefore a significant effect on reactivity.

8 Variation of Four Factors and k_∞ with Irradiation

The composition of the fuel will change quite significantly during its life in the reactor. When the fuel in the reactor is still fresh, there is zero irradiation. As the reactor generates power, the fuel (as well as all core materials) is subjected to neutron irradiation.

With increasing irradiation, there are changes in composition which occur in the fuel. Two factors have a negative effect on the chain reaction and reduce the lattice reactivity. The uranium-235 content (0.72 atom % in natural uranium) gradually depletes as more and more fissions take place, and fission products are formed and accumulate, increasing neutron absorption.

However, with irradiation some fissile ^{239}Pu and ^{241}Pu are formed. These isotopes contribute in a positive way to sustain the chain reaction, and therefore increase the reactivity. The variation of reactivity with irradiation is shown in Figure 8.1 for the different nuclides present in the reactor core.

Fig. 8.1:

Plot of reactivity versus irradiation
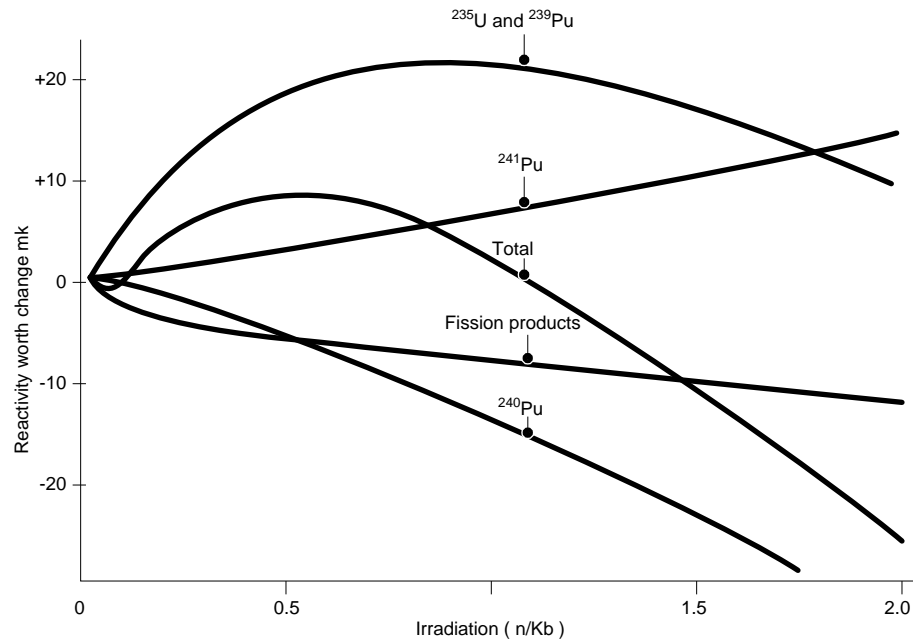
Initially the burnup of uranium-235 and its replacement by a smaller number of plutonium-239 nuclei leads to an increase of the total reactivity due to a higher fission cross section of ^{239}Pu. At higher irradiation, uranium-235 is still removed (see Figure 8.2) but the build up of ^{239}Pu becomes less rapid as it approaches its equilibrium level when the production of ^{239}P will equal the removal due to absorption. Consequently, at high irradiation the overall reduction in the number of fissile nuclei causes a reduction in reactivity. The build up of plutonium-240 produces a large negative reactivity contribution due to significant neutron absorption. This is partially offset by the build-up of fissile ^{241}Pu.

Fig. 8.2:
Isotopic composition versus irradiation
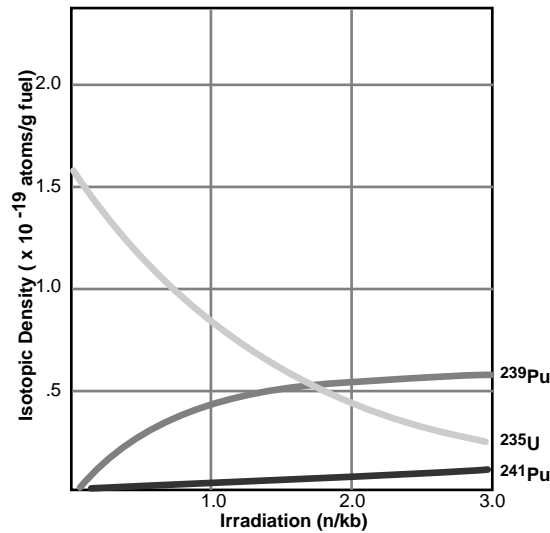
The above effects can be examined quantitatively through the variation with irradiation of the different quantities in the four-factor formula. This is shown graphically in Figure 8.3 for the standard CANDU lattice.

Fig. 8.3:
Variation of four-factor parameters, k_{eff} and k_{∞} with irradiation
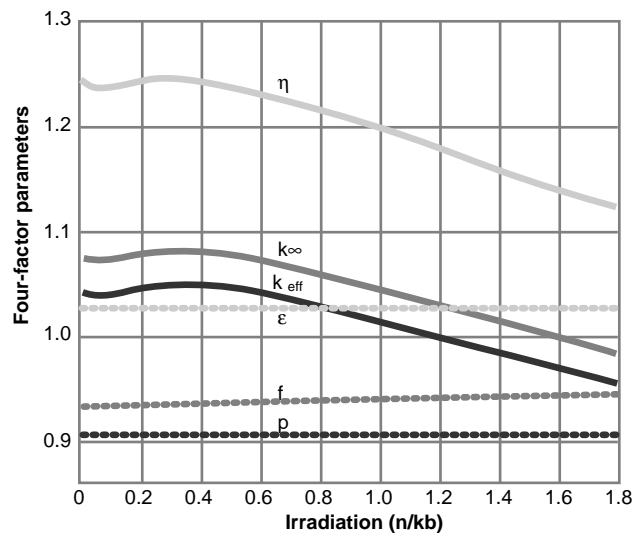
Neither the fast fission factor E nor the resonance escape probability p show any significant variation and can be assumed constant with irradiation. This is due to the fact that most fast fission and resonance capture take place in ^{238}U which constitutes about 99% of the fuel whether it is fresh or irradiated.

The only basic quantity which changes significantly with irradiation is η, the thermal reproduction factor (neutron yield per thermal neutron absorption in

fuel). Therefore, the variation of the lattice reactivity with irradiation (Figure 8.4) is essentially determined by that of η. This variation can be understood in the following way. Starting from fresh fuel, the production of fissile plutonium at first outbalances the depletion of ^{235}U and the formation of fission products. Thus there is a net increase in lattice reactivity up to an irradiation of about 0.4 n/kb. The increase of reactivity reflects in an increase of the quantity η because, and referring to the definition of η (equation 6.1), the fission cross section of plutonium is higher (see Table 4.1 of Lesson 1, ν for different nuclides). The maximum in reactivity is called the plutonium peak. Past the plutonium peak, the build up of fission products and therefore net absorption without fission in the fuel, and the increasing ^{235}U depletion result in a monotonic decrease in reactivity.

The size of the plutonium peak depends on the initial fraction of ^{235}U. For instance, the plutonium peak would be much higher in a depleted-fuel lattice, as seen in Figure 8.4 for fuel with an initial ^{235}U fraction of 0.52%. This is because plutonium production is relatively more significant in depleted fuel. In contrast, LWR enriched-uranium fuel shows no plutonium peak.

Fig. 8.4:
Reactivity versus irradiation for natural and depleted fuel
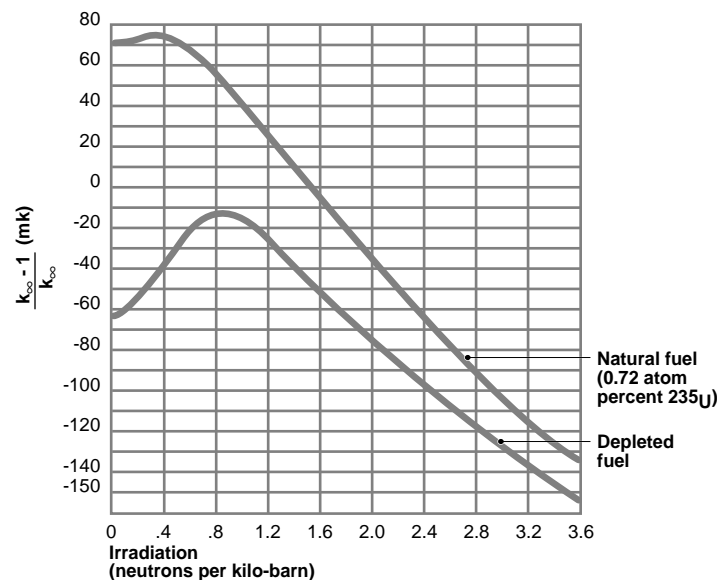
The determination of the four factors is important because, each factor corresponds to a specific nuclear aspect and can be treated separately from the other factors. This has to be kept in mind when studying the reactor calculation methods. However, the four-factor formula applies to the different nuclear technologies, to fast reactors as well as thermal reactors. The multiplication factor is also of great importance in the theoretical treatment of the time-dependent behaviour (kinetics) of a reactor.

Neutron thermalisation and Reactor kinetics

Training Objectives

The participant will be able to describe or understand:

1   the neutron thermalisation;
2   the moderator;
3   prompt kinetics and reactor period;
4   the delayed neutron and point kinetics equations;
5   simple solutions of the point kinetics equations;
6   examples of power transients in a reactor: prompt jump, stable period, prompt drop, reactor trip;
7   the principal factors affecting reactivity during reactor operation;
8   reactivity devices requirements: reactor control, protection and operational safety.

Neutron thermalisation and Reactor kinetics

Table of Contents

1 Introduction

One of the key concepts which helps to understand the reactor kinetics is the distinction between fast and thermal neutrons. This difference is in fact inherent to the design of a thermal nuclear reactor.

The main difference between fast and thermal neutrons is their respective energy range. We have seen that they feature different energy distributions. These distributions can be characterized by Maxwellian distributions centred on 0.025 eV for the thermal group neutrons and on 1-2 MeV for the fast neutrons (see lesson I, figures 3.1 and 3.2). The overall neutron energy spectrum is divided in these two groups because of the corresponding fission processes: fast fission and thermal fission which are taking place in a sustained chain reaction.

If we recall the illustration of the neutron life cycle (lesson II, figure 3.1) we observe that in a sustained chain reaction, most of the neutrons produced in the cycle are coming from thermal fissions. Since most of the neutrons obtained by fission are fast neutrons, they have to be slowed down in order to induce thermal fission and maintain the chain reaction. The thermal nuclear reactor uses this principle.

Figure 1.1 gives the figures of the various neutron fates in the case of the equilibrium core of the CANDU 600 thermal reactor. The figure shows that 94.4% of the overall neutron production comes from thermal fission. The remaining 5.6% comes from fast fission. All neutrons born by fission are fast. A small percentage of 0.6% will rapidly escape and fast absorption will immediately occur for 3.2%. As they are slowed down, 8.9% of the neutrons will disappear by resonance absorption mainly in the ^{238}U isotope. The thermalisation process continues for the remaining 87.3%. During the process, 2.3% will leak and 85% will become available for thermal absorption. After the slowing down, 6.3% of the overall neutron population is thermally absorbed in non fuel core components leaving 78.7% for thermal absorption in the fuel to maintain the neutron production by fission. The neutron life cycle is complete and the chain reaction is sustained.

Fig. 1.1 :
Neutron balance in the CANDU 600 equilibrium core.

```
┌──────────────────────────────────────────────────┐
│ Production                                         │
│ 56.5 neutrons from ²³⁸U fast fission               │
│ 491.9 neutrons from ²³⁵U thermal fission           │
│ 438.4 neutrons from ²³⁹Pu thermal fission          │
│ 13.2 neutrons from ²⁴¹Pu thermal fission           │
│ Total = 1000 neutrons                              │
└──────────────────────────────────────────────────┘
```

Production
56.5 neutrons from ^{238}U fast fission
491.9 neutrons from ^{235}U thermal fission
438.4 neutrons from ^{239}Pu thermal fission
13.2 neutrons from ^{241}Pu thermal fission
Total = 1000 neutrons

Fast leakage
6.0 neutrons

Fast absorption in fuel
31.7 neutrons

Slowing down

Resonance absorption in ^{238}U
89.4 neutrons

Thermal leakage
23.0 neutrons

Thermal absorption
849.9 neutrons

Thermal absorption in non fuel core components
14.4 neutrons in moderator
0.3 neutrons in coolant
19.0 neutrons in P T
8.5 neutrons in C T
6.2 neutrons in sheath
15.0 neutrons in adjusters, zone controllers and parasitic absorbers
Total = 63 neutrons

Thermal absorption in fuel
242.3 neutrons in ^{235}U
238.2 neutrons in ^{238}U
228.1 neutrons in ^{239}Pu
15.6 neutrons in ^{240}Pu
6.2 neutrons in ^{241}Pu
0.1 neutrons in ^{242}Pu
0.6 neutrons in Np
7.7 neutrons in "Sm"
25.2 neutrons in Xe
2.6 neutrons in "Rh"
19.9 neutrons in PFP
Total = 786.5 neutrons

Notes:
Fast group denotes 10 MeV > E > 100 keV
Resonance group denotes 100 keV > E > 10 eV
Thermal group denotes sum of Thermal group
E < 0.625 eV and Epithermal group 10 eV > E > 0.625 eV

2 Neutron Thermalisation

Neutron thermalisation is the process of slowing down fast neutrons to thermal energy and it occurs as the neutrons diffuse through the reactor core material without being lost. The successive collisions and momentum exchanges decrease the neutron kinetic energy which is transferred to the nuclei of the reactor core material. As the process continues, the neutron energy and the corresponding neutron temperature decrease to a certain point where the neutron gas is considered in thermal equilibrium with the core material. In term of its energy E, a given neutron stays in the fast group for an initial energy as high as 10 MeV and decreasing down to about 100 keV. At about 100 keV the neutron is still considered as a fast neutron which enters the resonance group where the

resonance absorption becomes more probable and may occur down to 10 eV. The general definition of the thermal group denotes the sum of the strictly defined thermal group corresponding to a neutron energy less than 0.625 eV and the epithermal group with a neutron energy in the range between 0.625 eV and 10 eV or just below the maximum of resonance absorption cross-section.

The moderator is a reactor core material chosen specifically for its ability to thermalise neutrons in as few collisions as possible. As a result of less collisions, the average loss of neutron energy per collision is higher, and the likelihood that the neutron will escape much of the resonance energy range during slowing down is enhanced (see Figure 2.1). The larger the loss of energy per collision, the lesser the number of collisions with a neutron energy exactly in the resonance range. Due to momentum conservation, the kinetic energy decrement will be higher during elastic scattering if the mass of the target nucleus is comparable to the neutron rest mass. Therefore, the moderator which contains the target nuclei for the neutron thermalisation process should consist of light atoms.

Fig. 2.1:
Effect of moderator on neutron energy during the slowing-down process
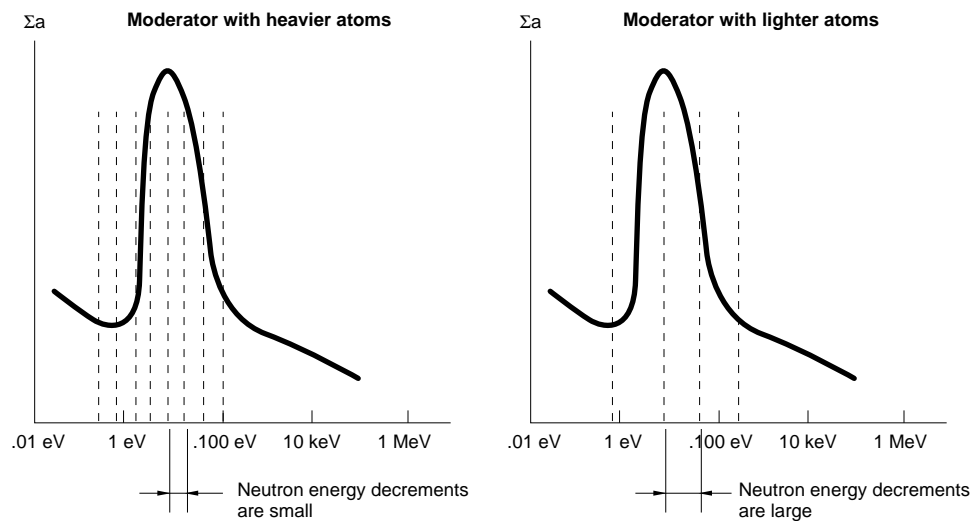
The best candidate for moderator is the lightest nucleus: hydrogen (proton). Other good candidates are light nuclei composed of few protons and neutrons (see Table 2.1): deuterium (D), beryllium (Be) and carbon (C). The usual forms in which H, D and C are provided are ordinary water (H_2O), heavy water (D_2O) and graphite. It should be noted from Table 2.1 that heavier atoms constitute poor moderators due to the higher number of collisions required to thermalize a fast 2 MeV neutron.

Table 2.1:

Number of collisions to thermalize a fast 2 MeV neutron.

Material	Number of Collisions
$_{1}^{1}\text{H}$ (gas at STP)	18
H_2O	20
$_{1}^{2}\text{H}$ (gas at STP)	25
D_2O	36
$_{2}^{4}\text{He}$ (gas at STP)	43
$_{3}^{7}\text{Li}$	67
$_{1}^{9}\text{Be}$	83
BeO	105
$_{6}^{12}\text{C}$	115
$_{92}^{238}\text{U}$	2172

However, the moderator atomic mass is not the only criterion since the moderator should thermalize without absorbing neutrons too readily. Based on the elastic scattering process, one can define a mean log energy decrement ξ over the resonance energy range:

$$\xi = \frac{1}{N} \text{Ln} \frac{E_i}{E_f}$$

where E_f and E_i are respectively the final and initial energies, N the number of collisions required to thermalize.

The moderating ratio M.R. measures the efficiency of a moderator and it is defined as the ratio of the slowing-down power of the material $\xi\Sigma_s$ to its neutron absorption cross section:

$$\text{M.R.} = \xi \frac{\Sigma_s}{\Sigma_a}$$

where Σ_s and Σ_a are respectively the elastic scattering cross-section and the absorption cross-section.

Taking into account the absorption cross-section, hydrogen is not the best moderator, because it has a relatively high neutron absorption cross section (see Table 2.2). Heavy water (D_2O), one of the best moderators, is chosen for CANDU reactor technology and it allows the use of natural uranium (see the typical CANDU lattice cell: Lesson II, figure 2.2). The moderating ratio of heavy water varies strongly with its purity indicated in Table 2.2 as the mass ratio D_2O / ($D_2O + H_2O$). Therefore, the utilisation of heavy water as moderator requires the monitoring of its isotopic purity.

Table 2.2:

*Moderating ratio for different moderators*

Moderator	ξ Mean Log Decrement	Σ_s Elastic Scat. Cross-Section (cm^{-1})	Σ_a Absorption Cross-Section (cm^{-1})	M.R. Moderating Ratio
H_2O	0.927	1.47	22x10^{-3}	60
^9_4Be	0.206	0.74	1.17x10^{-3}	130
$^{12}_6C$ (reactor grade)	0.158	0.38	0.38x10^{-3}	160
BeO	0.174	0.69	0.68x10^{-3}	180
D_2O (99.0% pure)	0.510	0.35	2.53x10^{-4}	712
D_2O (99.75% pure)	0.510	0.35	0.88x10^{-4}	2047
D_2O (100% pure)	0.510	0.35	0.33x10^{-4}	5500

A final remark on reactor physics and the consequence of using heavy water as the moderator concerns the production of photoneutrons as a neutron source in the reactor. In fact photoneutrons are produced in reactors with heavy water used as the moderator or heat transport fluids. When photons with energies greater than 2.2 MeV are absorbed by a deuterium nuclei ($^2H_1$ noted also as D):

$$\gamma + {}^2_1D \;\rightarrow\; {}^1_1H + {}^0_1n + \gamma'.$$
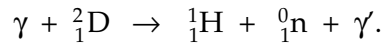
In the nominal configuration, the reactor has a steady inventory of fission products whose γ decay photons have E > 2.2 MeV. After shutdown, the photoneutron source is still active due to decaying fission products. This source is even larger than the spontaneous fission and helps to start up the reactor after a shutdown.

Neutron distribution ollowing fission

Time (seconds)
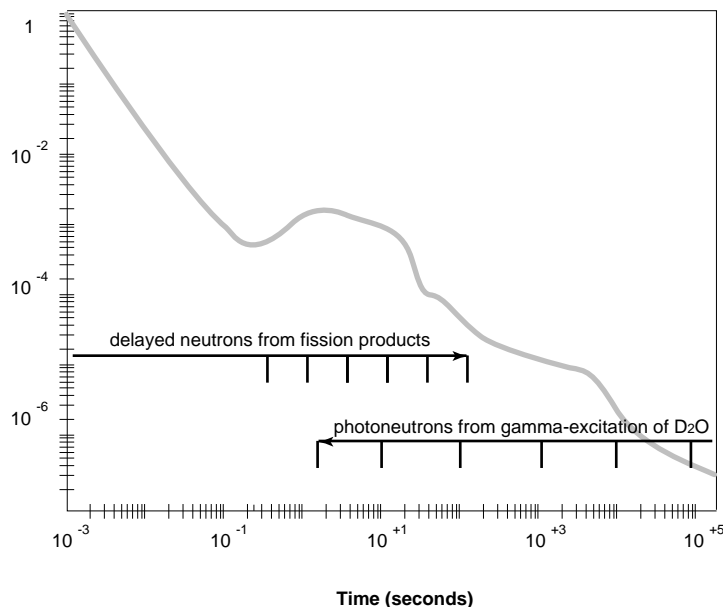
3 Reactor Kinetics

3.1 Neutron power and neutron flux

The first goal of reactor kinetics is to predict the changes in reactor power with time. Since we are interested in what is happening in the reactor core, we will study how neutron power changes with time. As an introduction to this discussion, it must be recognized that neutron density n, neutron flux ø, and neutron power P are all related by physical or design constants such that they are proportional. Their relationships are:

$$P = \kappa \, V \, \Sigma_f \, \phi$$
$$\phi = n \, v$$

where:

κ:	energy release per fission;
V:	reactor volume;
Σ_f:	macroscopic fission cross-section;
ϕ:	neutron flux;
n:	neutron density;
v:	average neutron velocity.

3.2 Prompt kinetics and reactor period

In lesson II, we have explained that reactor power will stay constant providing that $k_{eff} = 1$ (the reactor is critical). Any departure from criticality means that the neutron densities of successive neutron generations are varying. The change of the neutron density in one generation is related to k_{eff} by the following:

$$\frac{n + \Delta n}{n} = k_{eff}$$

or

$$\frac{\Delta n}{n} = k_{eff} - 1$$

where Δn is the increment in neutron population from one generation to the next. The time over which this increment is realized is the average time interval between successive neutron generations, denoted Λ

Using, therefore, $\Delta t = \Lambda$, we see from equation (3.2) that

$$\frac{1}{n} \frac{\Delta n}{\Delta t} = \frac{k_{eff} - 1}{\Lambda}$$

which can be rewritten at the limit $\Delta t \to 0$ in the differential form:

$$\frac{dn}{dt} = n \frac{k_{eff} - 1}{\Lambda} = \frac{k_{eff} \, n}{\Lambda} \frac{k_{eff} - 1}{k_{eff}} \approx \frac{n}{\Lambda} \rho$$

where we introduce the reactivity $\rho = (k_{eff} - 1) / k_{eff}$ and we use the approximation $\Lambda / k_{eff} \approx \Lambda$ since k_{eff} is close to one.

The neutron power variation in time P(t) is proportional to n(t) and comes from the exponential solution for n(t) of the differential equation 3.3:

$$n\left(t\right) = n_0 \; e^{\frac{\rho t}{\Lambda}} \qquad P\left(t\right) = P_0 \; e^{\frac{\rho t}{\Lambda}}$$

The solution indicates that under a perturbation of reactivity ρ, the neutron population grows exponentially with time and diverges for as long as the perturbation lasts.

For a reactor with only prompt neutrons generation, the reactor period is calculated as the time for a factor e variation: $\tau = \Lambda / \rho$. As a numerical example, suppose that the reactor is supercritical, i.e. $k_{eff} = 1.0005 \Rightarrow \rho = + 0.5$ mk . If there were no delayed neutrons, Λ would be the time interval Λ_p between prompt neutron generations, which can be conveniently considered as comprised of a slowing-down time t_s and a neutron-diffusion time t_d:

$$\Lambda_p \; = \; t_s + t_d$$

In CANDU $t_s \approx 10^{-7}$ s while $t_d \approx 10^{-3}$ s, thus

$$\Lambda_p \; \approx \; t_d \; \approx \; 10^{-3} \, s \; = \; 1 \, ms$$

Considering a reactor supercritical by 0.5 milli-k in the numerical example:

$$\tau_p \; = \; \Lambda_p \, / \rho \; = \; 0.001 \, / \, 0.0005 \; s \; = \; 2 \, s$$

This means that with the reactor only slightly supercritical ($k_{eff} = 1.0005$), power is increasing by a factor of e (272%) every 2 s. If the departure from criticality is 10 times higher, $\rho = 5$ milli-k, the characteristic time will be 10 times smaller: $\tau_p \; = \; \Lambda_p \, / \rho \; = \; 0.001 \, / \, 0.005 \; = \; 0.2$ s. This is a very steep rate of power increase, which would render reactor control very difficult.

From the prompt neutron point of view, the chain reaction is a multiplicative process which can lead to uncontrolled exponential divergence. The prompt kinetics can be illustrated by a simple discrete process. A multiplication factor α can be defined as the ratio of the prompt neutron density of one generation to the density of the preceding generation:

$$\alpha \; = \; N_{n+1} \, / \, N_n \; = \; k \; \approx \; (1 + \rho)$$

according to the discrete multiplicative chain process of figure 3.1.

Fig. 3.1:

Chain process illustration for prompt kinetics

$$\text{Pr}\,ompt\;\;Multiplication$$

$$Chain\,Process\,line\;\;\frac{PROMPT}{N_n \to x\,\alpha \to N_{n+1}}\;\;\frac{N_n}{Input\,of}\;\to x\,2 \to \frac{N_{n+1}}{Output\,of}$$
$$the\,process\qquad the\,process$$

The process is iterative going from one generation to the next one. If we go back to the first generation unperturbed neutron density N_0, the resulting density after n+1 generations is expressed as

$$N_{n+1} = \alpha^{n+1}\,N_0$$

which is divergent for $\alpha > 1$ as n goes to infinity.

The prompt kinetics, without considering the mitigating effect of delayed neutrons, poses safety concerns due to too small reactor characteristic periods which may become almost negligible for large insertions of positive reactivity in the reactor core. A safe reactor control would not be possible if the neutron population would consist only of prompt neutrons.

In a thermal reactor, the variation of neutron population is not dominated by the prompt neutrons but instead by the decay process of the precursors and by the emission of delayed neutrons. This allows longer characteristic time which enables the appropriate regulation of the neutron population in the reactor core within safe procedures.

3.3 Delayed neutrons: simplified approach

Because some of the fission neutrons are delayed, the time Λ_p between generations is increased over the value 1 ms given in the previous section.

There are many delayed-neutron precursors, each with its own decay time constant. If there are g precursors, and the ith precursor has a lifetime l_i and yields a fraction β_i of all fission neutrons, then a very simplified treatment suggests that the average time between generations is

$$l_d = \left(1 - \beta\right) l_p + \sum_{i=1}^{g} \beta_i\, l_i$$

where $l_p = \Lambda_p$ is the prompt-neutron lifetime (≈ 0.001 s) and β is the sum of the delayed-neutron fractions.

Although the β_i are small (total $\beta \approx 0.0065$), some l_i are of the order of seconds, so that the effective value of l_d in equation (3.6) turns out to be ≈ 0.1 s.

Thus, in the case of the 5 milli-k supercritical reactor, a characteristic time T can be estimated as

$$T = \frac{l_d}{\rho} \approx \frac{0.1 \text{ s}}{0.005} = 20 \text{ s}$$

therefore, in l s the power increases approximately by a factor of $e^{0.05} \approx 1.05$.

Because of delayed neutrons, the rate of power changes in transients is slowed down considerably. Delayed neutrons therefore play a very important role in making reactor control manageable. Due to the presence of the delayed neutrons, we will show that a power transient can become convergent under the condition $\rho < \beta$ instead of being divergent as shown for the prompt kinetics.

The delayed kinetics can be illustrated by a simple discrete process. A multiplication factor α can be defined as the ratio of the prompt neutron density Np of a given generation to the neutron density N of the preceding generation:

$$\alpha_n = Np_{n+1} / N_n = [1 + (\rho_n - \beta)]$$

according to the discrete multiplicative chain and line queuing of figure 3.2.

Fig. 3.2:
Chain process and line queuing illustration for delayed kinetics.
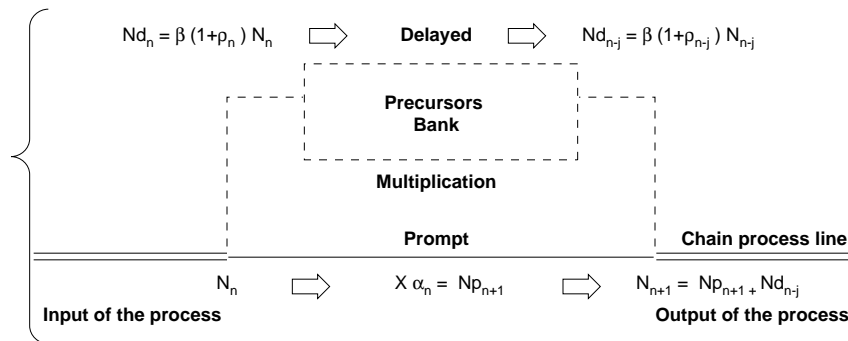
The chain process is iterative going from one generation to the next. If we go back to the first generation unperturbed neutron density N_0, the resulting overall density after the fist few generations can be expressed as the sum of delayed and prompt fractions. Using the approximation $\beta (1 + \rho) \approx \beta$ (for $\rho << 1$) this leads to:

$$N_1 = \alpha N_0 + \beta N_0$$

$$N_2 = \alpha N_1 + \beta N_0 = \alpha^2 N_0 + \alpha \beta N_0 + \beta N_0$$

$$N_3 = \alpha N_2 + \beta N_0 = \alpha^3 N_0 + \alpha^2 \beta N_0 + \alpha \beta N_0 + \beta N_0$$

$$N_{n+1} / N_0 = \alpha^{n+1} + \beta (\alpha^n + \alpha^{n-1} + ... + \alpha + 1)$$

$$N_{n+1} / N_0 \rightarrow \beta / (1 - \alpha) \qquad \text{if} \quad \alpha < 1. \qquad\qquad 3.7$$

After n+1 iterations the series in parenthesis is recognized as the well-known geometric progression and it has a convergent sum for $\alpha < 1$ as n goes to infinity.

The condition $\alpha = [1 + (\rho - \beta)] < 1$ is equivalent to $\rho < \beta$. The series then converges to a value which is usually referred to as the prompt jump:

$$\text{PROMPT JUMP} \equiv \beta / (1 - \alpha) = \beta / (\beta - \rho).$$

In the real reactor the prompt generation time is about 10^{-3} s and the prompt jump is achieved in less than a second (thousand of generations). Some examples of the line queuing analogy are given in the Figure 3.3.

In the case where $\rho > \beta$ the series is divergent. The reactor is then said super-prompt-critical and exponential divergence becomes possible. Power transient will be dominated by the prompt neutron kinetics.

Fig. 3.3:

Line queuing analogy of the multiplicative process of the chain reaction.

Even though we create 105 precursors we get only 100 delayed neutrons from the precursor bank since it contains precursors produced earlier.

This chain proceeds as follows:
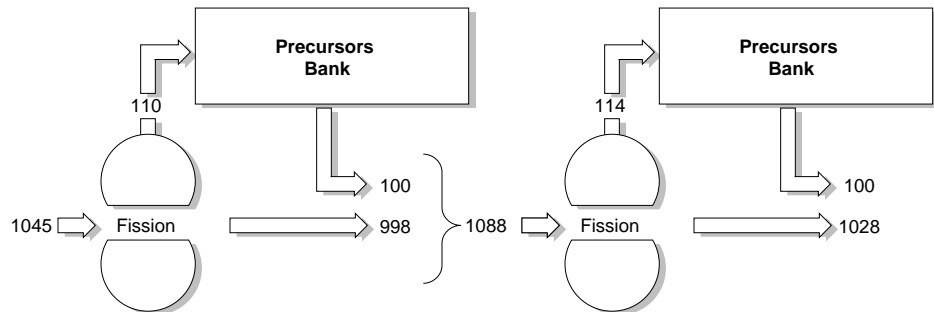
If we assume that the output of the precurors bank does not change for a second, we have time for one thousand prompt generatrions in which time the series will converge to:
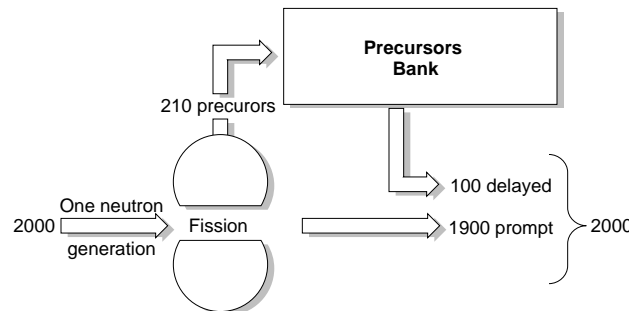
In safety analysis, the effects of delayed neutrons must be taken into account when analyzing rapid power transients. An accurate analysis requires a more sophisticated numerical treatment than the simplified treatment given above. The next section will deal with a more appropriate treatment of the delayed neutron effect on reactor kinetics.

3.4 Delayed neutrons and point kinetics equations

Considering a fraction β of delayed neutrons, the neutron balance equation 3.2 has to be modified in order to take into account the distinction between the production of prompt and delayed neutrons. This leads to the following form:

$$\frac{dn}{dt} = \frac{k_{eff}\, n}{\Lambda}(1 - \beta) + \lambda C - \frac{n}{\Lambda}$$

where the first term on the right hand side is the production of prompt neutrons in the present generation. The second term is the production of delayed neutrons in the present generation and the third term represents the total number of neutrons in the preceding generation. The sum of all three terms on the right hand side gives the instantaneous variation of the neutron density n. Also:

β: fraction of delayed neutrons. Typical value is 0.0065;

C: delayed neutron precursors concentration;

λ: precursors decay constant. Typical average for all precursors is $0.1\ s^{-1}$.

The presence of the precursors concentration in equation (3.9) indicates that another equation expressing the balance between the production of the precursors and their decay after the time constant λ is also needed to give a complete basic description of the reactor kinetics.

The usual formulation of the point kinetics equations include two differential equations, one for the neutron density n(t) and the other for precursors concentration C(t). Grouping the factors of the neutron density in equation (3.9) and using the definition of the reactivity ρ = (k_{eff} - 1) / k_{eff} lead to the following expression:

$$\frac{dn}{dt} = \frac{k_{eff}\, n}{\Lambda}(\rho - \beta) + \lambda C$$

The second equation for precursors concentration is given by:

$$\frac{dC}{dt} = \frac{k_{eff}\, n}{\Lambda}\beta - \lambda C$$

where the first term of the right hand side is the production rate and the second term is the decay rate of the precursors.

Depending on the values of ρ, the reactivity associated with a given reactor transient, and of β, the fraction of delayed neutrons, we can classify the different reactor states and the related consequences as follows:

1) if ρ < β the divergence of the prompt kinetics is avoided. When k_{eff} > 1 the reactor is SUPER-CRITICAL but the reactivity insertion can be less than the fraction of delayed neutron production. The power variation is then dominated by delayed neutrons. The neutronic power increases during the transient and converges to the prompt jump value.

2) if $\rho = \beta$, the chain reaction is becoming less dependent on the delayed neutrons, hence power is changing more rapidly. The reactor state is then called PROMPT-CRITICAL. The nuclear reactor may become unstable since any small positive fluctuation of reactivity can be amplified and may result in a divergent power excursion (see 3).

3) if $\rho > \beta$, the reactor state is called SUPER-PROMPT-CRITICAL. The neutronic power is increasing without having to "wait" for the delayed neutrons. This shortens the reactor response time. The power diverges according to the prompt kinetics behaviour since the prompt neutrons dominate the neutron imbalance.

4 Power Transients and Reactivity Variations

4.1 Simple solution of point kinetic equations

The solution of the kinetics point equations is easily found assuming the following hypotheses:

1) $\rho < \beta$,
2) a step variation of ρ occurs at $t = 0$, and
3) the neutron density n(t) was constant prior to the insertion of reactivity.

The neutronic power P(t) can be expressed using two terms P_1 and P_2 which are proportional to the solution n(t) of the point kinetic equations:

$$P(t) = P_1(t) + P_2(t)$$

where:

$$P_1(t) = P_0 \frac{\beta}{(\beta - \rho)} e^{+\frac{\lambda \rho}{(\beta - \rho)} t}$$

$$P_2(t) = - P_0 \frac{\rho}{(\beta - \rho)} e^{-\frac{\beta - \rho}{\Lambda} t}$$

The first term has the dominant behaviour in time. It is a slowly increasing exponential featuring a positive reactor period: $\tau = (\beta - \rho) / \lambda \rho$
(≈ 120 s for $\rho = 0.5$ mk). The amplitude P_0 is multiplied by the a factor $\beta / (\beta - \rho)$ already defined as the prompt jump. The prompt jump factor is greater than one if the reactivity is positive.

The second term is a negative decreasing exponential which dies away rapidly with a time constant: $\tau_- = \Lambda /(\beta - \rho)$ (≈ 0.17 s for $\rho = 0.5$ mk). This term can be neglected after a long period of time.

In the more general case without the simple assumptions of constant perturbation applied to a steady state flux, the complete solution of the point kinetics equations is computed numerically. Also, a realistic solution requires

that the delayed neutrons be divided in (usually up to 6) different groups of respective concentration C_i. The delayed groups are established according to their characteristic decay time constants λ_i.

4.2 Power transient examples

4.2.1 Numerical examples
Consider a step insertion of reactivity of 1 mk in a critical thermal reactor which is at a nominal power P_0. Assume the following typical values:

β = 0.0065 (fresh CANDU fuel)
ρ = 0.001
λ = 0.1 s^{-1} (average for all precursor groups)
Λ = 0.001 s

The solution in terms of the power ratio $P(t) / P_0$ is

$$\frac{P(t)}{P_0} = 1.18 \, e^{+0.0182\,t} - 0.18 \, e^{-5.5\,t}$$

The first and the second term of the solution are plotted in figure 4.1. The prompt jump approximation would consist of the step increase of 18 % occurring at t = 0 as shown by the first term of the solution.

Fig. 4.1:
*Example of a point kinetics numerical solution.*
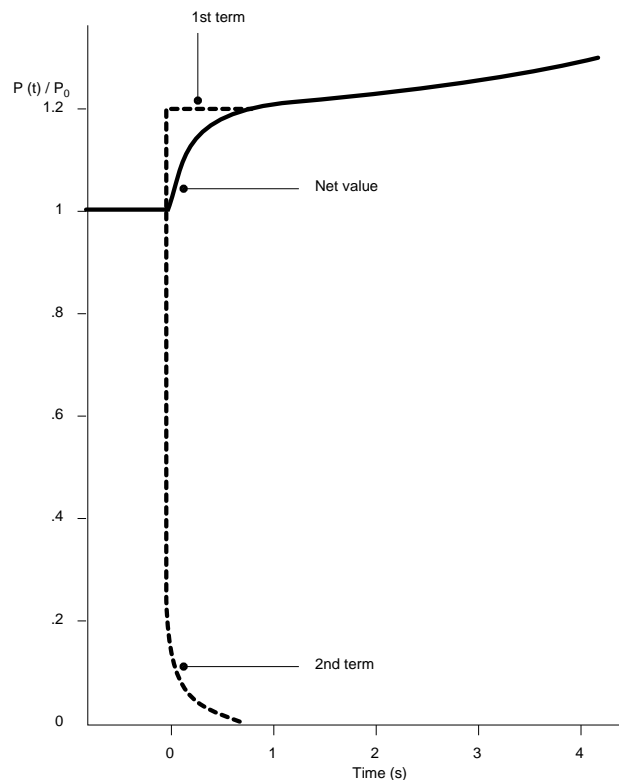
Figure 4.2 compares three different power evolutions following a step insertion of +0.5 mk at t = 0 s: the prompt kinetics, the prompt jump approximation and the actual power increase. In this case the prompt jump appears as a 8.3 % step increase in neutronic power.

Fig. 4.2:
Comparison between different power evolutions.
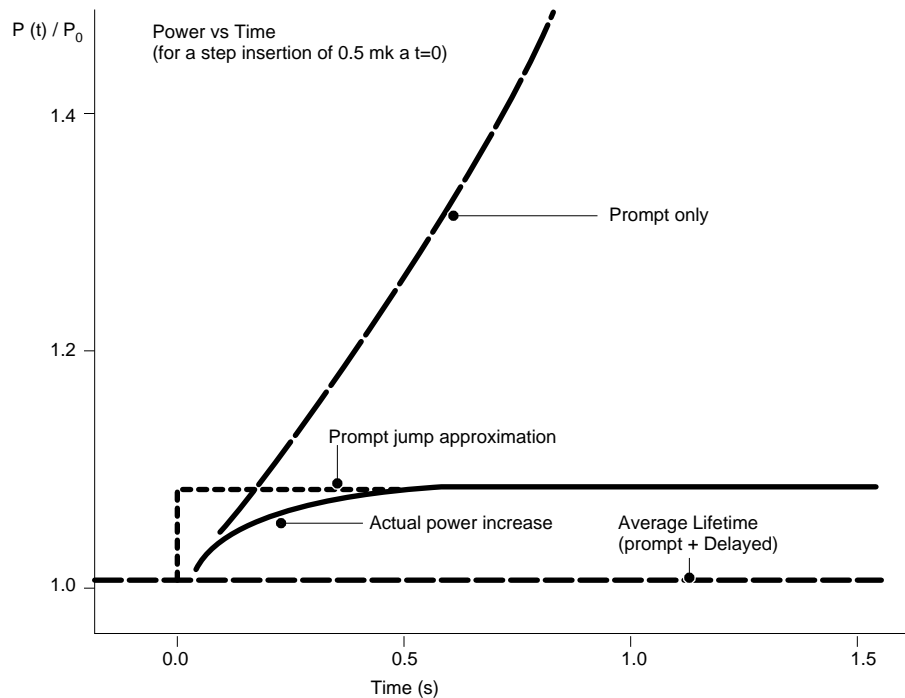
4.2.2 Prompt drop and reactor shutdown

When a negative reactivity is inserted in the reactor core, a sudden decrease of the neutronic power results. Solution (4.1) is still valid and the first term features a prompt drop factor:

$$\text{PROMPT DROP} \equiv \beta / (\beta + |\rho|) < 1 \text{ if } \rho < 0$$

The reactor period τ is still defined as

$$\tau = (\beta - \rho) / \lambda\rho = - (\beta + |\rho|)/\lambda |\rho| \text{ if } \rho < 0$$

and as τ becomes negative, the exponential in equation (4.2) changes from an increasing behaviour (positive exponent) to a damping behaviour (negative exponent). Therefore, the prompt drop is followed by a stable negative period.

For the limiting case of a large negative reactivity insertion, used for instance to trip the reactor, we have:

$$\text{PROMPT DROP (reactor trips)} \approx \beta / |\rho| \text{ if } \rho << -\beta$$
$$\tau \text{ (reactor trips)} \approx -1 / \lambda \text{ if } \rho << -\beta$$

The stable reactor period will be determined by the decay constant of the delayed neutron precursors. It should be determined by the longest lived group

of precursors. According to this argument, the shortest period possible after the prompt drop should be around 80 s for the CANDU reactor. In fact, a significant production of neutron from the photoneutron reaction forces the actual period to be somewhat longer.

4.2.3 Prompt-criticality and design limit

Figure 4.3 shows the variation of the reactor period as a function of the reactivity ρ for a reactor with a prompt lifetime Λ = 0.001 s (typical of CANDU reactors). In order for the reactor to approach prompt-criticality, the positive reactivity insertion ρ has to increase to β = 0.0065 for fresh CANDU fuel (mainly ^{235}U) or to β = 0.0021 for a reactor with only ^{239}Pu. It can be observed that nothing radical happens when the reactor approaches prompt-criticality. The reactor period t simply decreases as the reactor becomes less dependent on delayed neutrons.

Fig. 4.3:
Reactivity insertion versus reactor period.
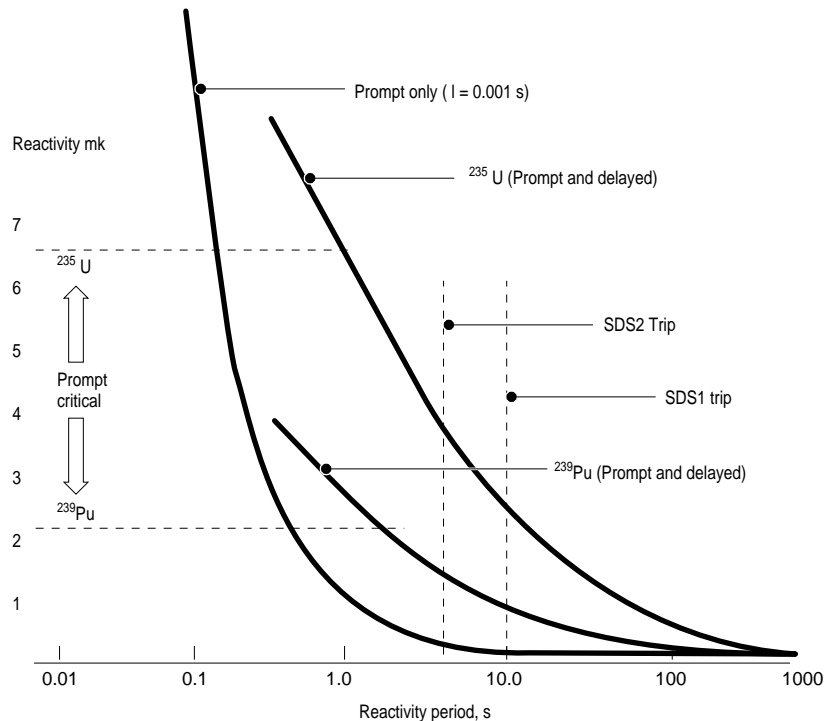
The shutdown systems SDS1 and SDS2 of CANDU reactor are designed to avoid prompt-criticality of the reactor. SDS1 trips the reactor when a reactor period of about 10 s is reached and SDS2 trips the reactor at a reactor period of about 4 s (see figure 4.3). Both of the shutdown systems are tripping the reactor before prompt-criticality which happens when t is around 1 s:

$$\tau = (\beta - \rho) / \lambda \rho \approx < 1 \text{ s} \quad \Rightarrow \rho > \approx \beta/(1 + \lambda) \quad \text{or} \quad \rho \approx \beta$$

It is important to note that the design limit should take into account the type and the evolution of fuel present in the reactor core as indicated here by the value of β (see Figure 4.3). SDS1 and SDS2 should be calibrated to shutdown the reactor for the worst case scenario of any sudden positive reactivity insertion. Equilibrium fuel in CANDU reactor features $\beta \approx 0.0035$.

4.3 Reactivity perturbations during reactor operations

We have seen that using the point kinetics equations to obtain the evolution of the neutronic power requires one to know how the reactor kinetics are perturbed in time in terms of reactivity variation. Any departure from criticality induces a power transient. The state of the reactor is then modified and a steady state will be followed by a transient obeying equations (4.1) to (4.3). We will now investigate the various sources of reactivity perturbations in a thermal nuclear reactor. Finally, we want to stress the use of reactivity devices during normal operations in order to supply positive or negative reactivity addition (recall table 4.1 of lesson II for the reactivity worth and maximum rates of the various CANDU 600 reactivity devices).

4.3.1 Burnup and equilibrium fuel

We have already discussed the fact that the margin to prompt-criticality is related to the nature of the fuel. More generally, the reactivity of the whole reactor core at a given time depends on the nature and on the state of the fuel at that time. Due to the fission process, the fuel isotopic composition is changing with time. The reactivity decreases slowly as a direct consequence of the fuel burnup since the fission products replace the fresh fuel as it becomes more and more irradiated.

Two types of strategies are normally used in the nuclear industry to overcome the reactivity decrease of whole reactor core with burnup.

a) **Cyclic Refuelling**
   The first strategy is associated with cyclic refuelling, typically once per year, used in the light water reactors (LWR). The fuel enrichment and the fuel physical arrangement in the reactor core is made in order to provide a positive reactivity margin which will allow uninterrupted power production between the refuelling. To overcome the excess reactivity of fresh fuel, the core is "poisoned" with an efficient neutron absorber (e.g. liquid Boron in the coolant) which is withdrawn slowly in order to maintain criticality.

b) **On-line Refuelling**
   The second strategy is associated with on-line refuelling, typically once or twice a day, used for instance in the natural uranium reactors (CANDU). The refuelling of given fuel channels in the reactor core supply a quasi uniform reactivity distribution which has to be monitored. A constant and regular strategy using on-line refuelling converges to an equilibrium core distribution of burnup. A small excess reactivity margin is maintained and overcome by the use of reactivity devices in order to maintain criticality.

4.3.2 Fission products poisoning

All fission products can be called "poisons" since they all absorb neutrons. They contribute to a long term reactivity decrease as the fuel burns up. In this respect, Xenon (^{135}Xe) and Samarium (^{149}Sm) are important and they require a special treatment due to their high absorption cross-sections and high production rates. They differ from other fission products since they obey short term variations and induce strong reactivity variations. ^{135}Xe has $\sigma_a = 3.5 \times 10^6$ barns and a total fission product yield of 6.6% (through ^{135}I). ^{149}Sm has $\sigma_a = 4.2 \times 10^3$ barns and a total fission product yield of 1.4%.

The ^{135}Xe and ^{135}I production and decaying cycle is illustrated in figure 4.4.

Fig. 4.4:
Xenon-135 cycle.
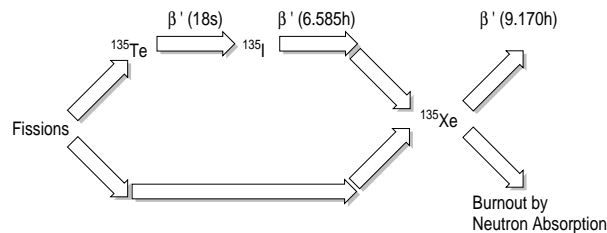
Xenon-135 (often referred to as xenon) is produced in the fuel in two ways:
a) Directly from fission. About 0.3% of all fission products are ^{135}Xe
b) Indirectly from the decay of iodine-135, which is either produced as a fission product or from the decay of the fission product tellurium-135 via the following decay.

$$^{135}_{52}Te \xrightarrow[t\frac{1}{2}\ =30s]{\hat{\epsilon},\gamma} \ ^{135}_{53}I \xrightarrow[t\frac{1}{2}\ =6.7h]{\beta\,\gamma} \ ^{135}_{54}Xe$$
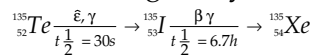
^{135}Te and ^{135}I together constitute about 6.3% of all fission products. Due to the short half-life of ^{135}Te we normally consider the whole 6.3% to be produced as ^{135}I The rate of production of Xenon and Iodine from fission depends on the fission rate.

Xenon-135 is removed (or changed) by two processes:
a) Radioactive decay as follows:

$$^{135}_{54}Xe \xrightarrow[t\frac{1}{2}\ =9.2h]{\beta\,\gamma} \ ^{135}_{55}Cs$$
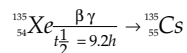
b) Neutron absorption (burnout)

$$^{135}_{54}Xe + ^1_0n \rightarrow ^{136}_{54}Xe + \gamma$$
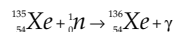
Figures 4.5 a, b and c show the Xenon transient typical behaviours for CANDU reactors. One can see the strong negative reactivity, referred to as Xenon load, which appears following a reactor shutdown (see fig. 4.5c). The "poison out time" corresponds to a period during which the reactor cannot become critical even when using the excess margin provided by the reactivity devices of the reactor.

Fig. 4.5a:

Xenon buildup (CANDU).

A Zero to full power
B 80%
C 60%
D 40%
E 20%

Xenon Activity (Arbitrary Units)

Hours After Startup
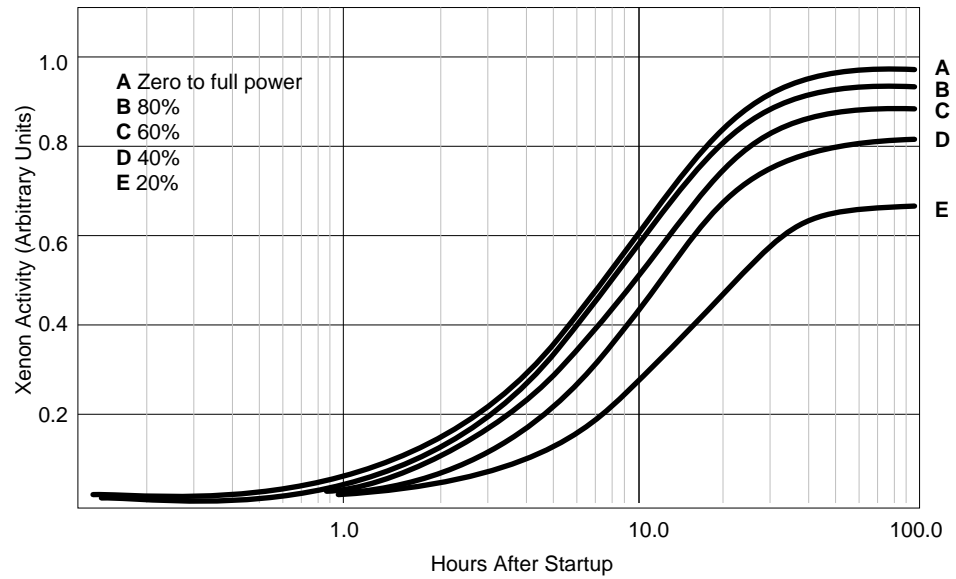
Fig. 4.5b:

Xenon reactivity transients following setbacks from full power (CANDU).

Hours after power setback

Incremental Xenon reactivity (milli-k)

80%

60%

40%

20% - Final power level in
% of nominal
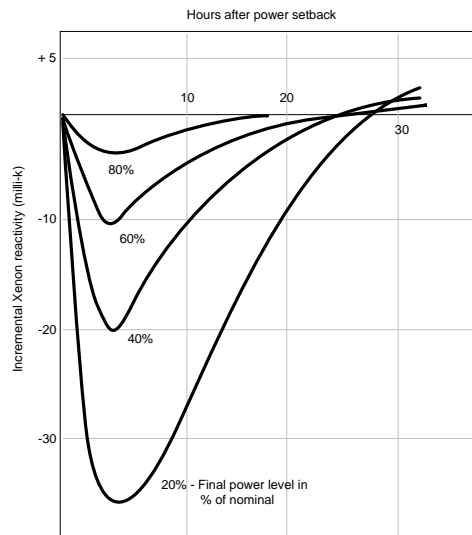
Fig. 4.5c:
Behaviour of Xenon load after a trip from full power (CANDU).
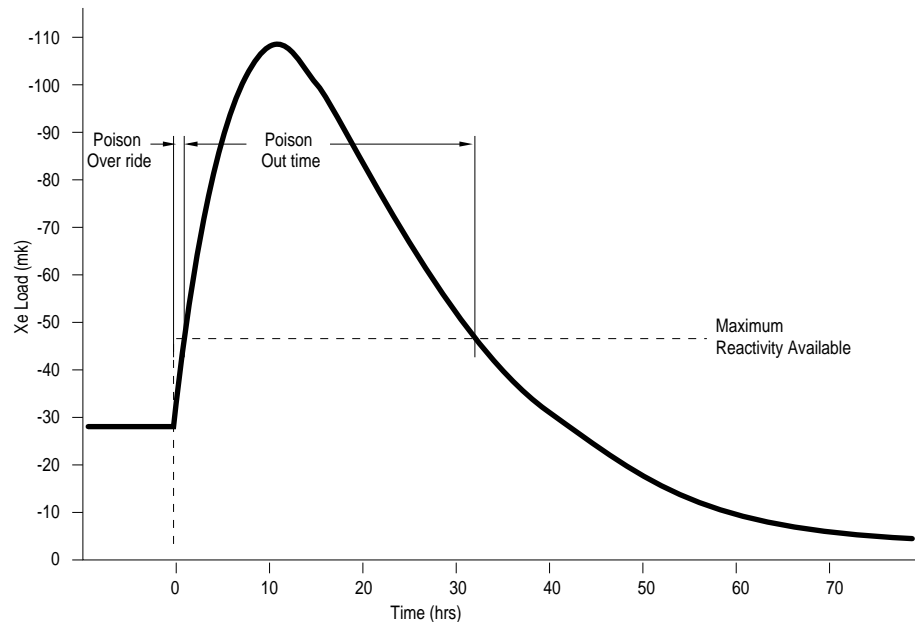
The evolution of the reactivity depicted in figure 4.5 is obtained directly from the mathematical solution of the Xe and I balance equations.

4.3.3 Principal factors affecting the reactivity

The principal factors which can affect reactivity during reactor operations are listed below. We briefly explain how each factor affects the reactivity and how the effect is circumvented or controlled with reactivity device actions or operational strategies for the CANDU reactor. Table 4.1 and 4.2 describe the various factors and illustrate their typical values for Pickering and Bruce nuclear reactor.

a) **Reactor Power Variations:**
   When the power increases from shutdown state to reach full power (pressurized and hot primary circuit), the reactivity decreases due to the increase of fuel and coolant temperatures (characteristic time: minutes). The effect is overcome by liquid absorbent (H_2O) rapid removal from zonal flux controllers.

b) **Coolant & Moderator Temperature Variations:**
   When the coolant and fuel temperatures increase from a cold to a hot primary circuit in a shutdown reactor, the reactivity decreases. The control needed is the same as for a.

c) **New or Equilibrium Fuel Combustion, Xenon Transient:**
The reactivity decreases slowly and regularly (over 6 months period) depending on the burnup history and on the refuelling strategy (see 4.3.1). The effect is overcome by poison relief (moderator) or neutron absorbent withdrawal from the reactor core (mechanical adjusters withdrawal in CANDU 600). The Xenon transient has a shorter characteristic time and is overcome by an excess reactivity margin (mechanical adjusters in CANDU 600).

d) **Flux Oscillation (In Core Zones):**
The power may vary locally in the CANDU reactor core due to channel refuelling and Xenon oscillations (characteristic time: 15 to 30 hours). The effect is overcome by liquid absorbent (H_2O) level adjustments in zonal flux controllers.

e) **Plutonium and Samarium Buildup:**
As the fuel isotopic composition evolves in time, fertile material can be produced as a product of neutron capture. This appears as a net slow change in reactivity (positive for Plutonium and negative for Samarium).

Table 4.1:

Reactivity variations in reactor core.

Sources of reactivity variations in reactor core	Δk (Reactivity variation)	Time intervalle
Power transient, shutdown to full power	moderate (+ve, -ve)	seconds, minutes
Fuel and coolant temperature variations	moderate (+ve, -ve)	seconds, minutes
Temperature variations of the moderator	small (+ve, -ve)	minutes
Fresh fuel burnup (small burnup)	large (-ve)	from 6 to 7 months
Xenon buildup at equilibrium	large (-ve)	40 h
Xenon transient	large (-ve)	12 h
Flux oscillation	moderate (+ve, -ve)	from 15 to 30 h
Fuel burnup at equilibrium (average burnup)	small (-ve)	days (continuous)
Plutonium and samarium buildup	moderate (+ve)	300 h

Table 4.2:
Reactivity loads (CANDU reactors).

Reactivity variations	Pickering A & B	Bruce A & B
(a) Power variation: shutdown (hot) to full power	(1) -7 mk (2) -3 mk	(1) -9 mk (2) -3,5 mk
(b) Fuel and coolant temperature, 25 °C to 275 °C	(1) -8 mk (2) -2,5 mk	(1) -9 mk (2) -3 mk
(c) Moderator temperature coefficient	(1) -0,06 mk/°C (2) +0,08 mk/°C	(1) -0,07 mk/°C (2) +0,09 mk/°C
(d) Fresh fuel burnup	-26 mk	-22 mk
(e) Xenon load at equilibrium	-28 mk	-28 mk
(f) Xenon transient Excess reactivity anti-Xe Period	-98 mk +18 mk 45 min	-105 mk +15 mk 40 min
(g) Reactivity of zonal flux control	5,4 mk	6 mk
(h) Reactivity loss - equilibrium fuel Reactivity gain - central channel refueling	-0,3 mk/day +0,2 mk	-0,5 mk/day +0,5 mk
(i) Plutonium and samarium buildup	+6 mk	+6 mk

(1) Fresh fuel
(2) Fuel at equilibrium

4.3.4 Requirements: Control and Safety

Reactivity devices (recall table 4.1 of lesson II) should obey some requirements depending on whether they are designed to control the reactor or to ensure protection against an accident.

Reactor Control

For the purposes of reactor control, the main requirements are the following:
a) maintain $k_{eff} = 1$ and a constant power;
b) allow for small ρ variations to control reactor power in the adequate time frame;
c) avoid local flux oscillations through fine zonal control of the neutron flux.

Protection and Safety

For the purposes of protection and safety, the main requirements are the following:
a) provide the possibility of adding a negative reactivity, large enough to rapidly shutdown the reactor;
b) insure the maximum and immediate availability and redundancy of two independent shutdown systems.

We now have all the essential elements to understand the basic nuclear reactor physics. I invite the reader to reflect upon the very small distinctions between a controlled and an uncontrolled chain reaction, and upon the fact that the reactor control poses a unique challenge for protection and safety. Indeed, safety should always be treated with the highest priority in nuclear power production. This is the key aspect of the mandate of the nuclear industry regulatory boards in their review of the nuclear power plants' operations.

December 1995

Nuclear Technologies

Training Objectives

The participant will be able to describe or understand:

1   the Candu design,
2   the safety systems,
3   the design related safety issues,
4   the design of a PWR,
5   the design of a BWR,
6   the design of a fast breeder reactor,
7   the design of a graphite reactor,
8   the design of a RBMK reactor,
9   the major design differences between these technologies

Nuclear Technologies

Table of Contents

1. Introduction

In the present lesson we will start to introduce some specific aspects of the **CAN**adian **D**euterium natural **U**ranium (CANDU) design and overall safety features. The lesson will concentrate on the safety aspects with little emphasis on operation. A rapid comparison and description of other nuclear technologies will enable the reader to better identify the originality of the CANDU design and the common features of modern nuclear power plants. The positive and negative aspects of the different designs will be identified from the point of view of safety and operation.

The table 1.1 below shows the relative importance of the main reactor technologies. It can be seen that more than three quarters of the operating reactors are of the Light Water Reactor (LWR) type, either Pressurised (PWR) or Boiling (BWR). The number of Pressurised Heavy Water Reactors (PHWR) is less than 10% of the total reactors.

Table 1.1:
relative importance of reactor technologies

Nuclear Power Units By Reactor Type, Worldwide

Reactor type	Units	MWe
PWR	236	206,883
BWR	88	71,964
GCR	38	12,789
PHWR	31	16,811
LWGR	15	14,785
LMFBR	4	1,178
Total	**412**	**324,410**

On a country basis, Canada ranks 6th for the installed capacity as shown in the table 1.2 below. It can be seen that most other western countries have adopted the LWR type of reactor.

Table 1.2:
Nuclear power generation installed capacity

Country	Units	MWe
USA	108	97,939
France	55	56,488
Japan	42	32,044
Germany	21	22,513
Russia	24	18,849
Canada	20	13,680
UK	37	12,340
Ukraine	14	12,095
Sweden	12	10,002
Korea	9	7,220
Spain	9	7,151
Belgium	7	5,484
Taiwan	6	4,884
Bulgaria	6	3,666
Switzerland	5	2,936
Lithuania	2	2,760
Finland	4	2,310
South Africa	2	1,840
Hungary	4	1,729
Czech Republic	4	1,632
Slovakia	4	1,632
India	8	1,614
Argentina	2	935
Mexico	1	654
Brazil	1	626
Slovenia	1	620
Netherlands	2	507
Kazakhstan	1	135
Pakistan	1	125

A few other countries have installed capacity with reactors that are similar to the Canadian design. These countries are bold in the above table.

2. CANDU Design

The present section will identify some of the specifics of the Candu design and highlight the safety aspects or concerns related to the design. More details on design and operation can be found in the subsequent lessons.

2.1 The pressure tube concept

The major characteristic and originality of the Candu design is the choice of the pressure tube concept for the reactor core.

Figure 2.1 is a schematic of a pressure tube assembly showing the pressure tube, the calandria tube and the garter springs which are designed to maintain the gap separating the calandria tube from the pressure tube.

Fig. 2.1:
schematic of pressure tube assembly
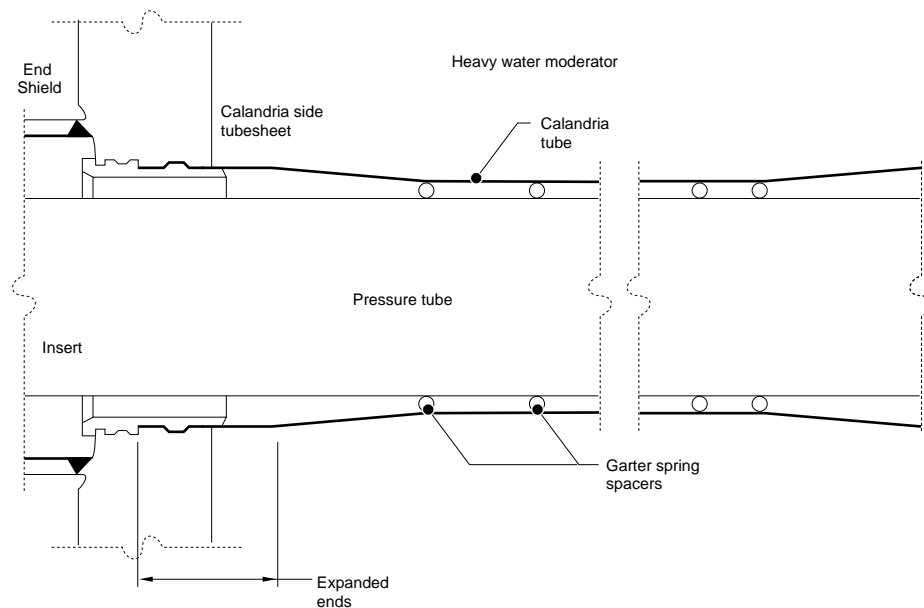
Since liquid is used to remove the heat generated inside the reactor it must be kept at high pressure to reach an appropriate temperature and at the same time avoid boiling. The choice of the pressure boundary is then between a pressure vessel design and a pressure tube design.

One consequence of the pressure tube design is the physical separation of the moderator from the coolant: the coolant flows inside the pressure tube which is itself surrounded by the moderator. The coolant and moderator liquids do not have to be identical and could be of different nature altogether.
The pressure tube concept is therefore the fundamental choice for the CANDU

reactor technology. Furthermore, the manufacture of a pressure vessel for a PHWR at the time the industry started was beyond the available capability of the Canadian steel and manufacturing industry.

2.1.1 Advantages of the pressure tube concept
The pressure tube concept has advantages in relation to the design and safety of the reactor. These advantages will be rapidly surveyed. Some are genuine advantages, some are advantages only when compared to the alternative.

The sudden rupture of a pressure tube would not be a catastrophic event as could be the rupture of a pressure vessel.

Because the coolant and moderator are physically separated, the moderator can be kept relatively cold at near atmospheric pressure reducing the requirements for large structures under pressure.

The large moderator is a potential and efficient ultimate heat sink in case of a severe accident with impaired heat sink capability.

The pressure tube concept allows the regular replacement of fuel in the reactor while on power, precluding the need for periodic shutdowns for refuelling.

On-power refuelling means that the excess reactivity in the lattice is never very high and the requirements for compensating that excess reactivity through absorbing devices are easy to meet.

Another real advantage of on-power refuelling is the possibility to immediately remove defective fuel from the core, preserving thereby the purity of the primary heat transport system.

The calandria tube acts as an isolator between the primary side flowing inside the pressure tube and the moderator surrounding the calandria tube. The low pressure gas between the calandria tube and the pressure tube reduces the conductive heat losses from the primary coolant to the moderator.

Thermalisation of neutrons is achieved away from material that would absorb fast and epithermal neutrons. The fast and thermal spectrums are physically separated.

Figure 2.2 shows the general layout of a typical Candu one figure of eight loop reactor resulting from the Candu pressure tube concept with the horizontal core, the primary cooling system and the moderator cooling system.

Fig. 2.2:
Candu reactor simplified flow diagram
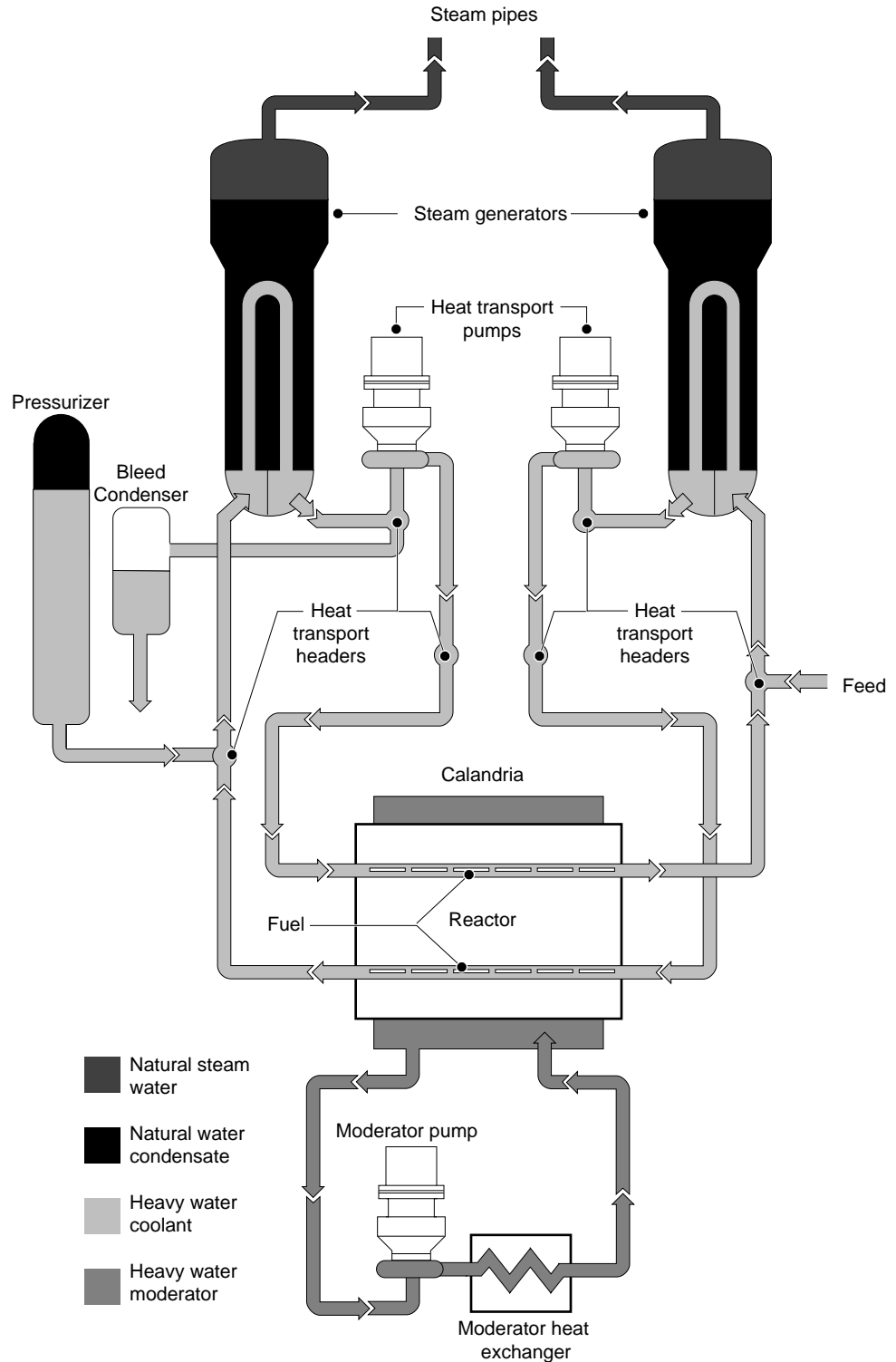
2.1.2 Disadvantages of the pressure tube concept
The main built-in or design specific disadvantages of the pressure tube concept
are briefly analysed below.

Since the calandria tube and particularly the pressure tube act as core supports,
the entire core structure is under maximum γ and neutron irradiation. Therefore
the structure embrittlement and changes in properties under irradiation must be
carefully monitored.

Under irradiation and due to neutron absorption by the zircaloy, the pressure
tubes creep and provisions must be taken to accommodate the pressure tubes
expansion. When necessary the pressure tubes must be replaced to extend the
life of the reactor and reduce the mechanical stresses on the calandria walls.

The pressure tube has to support a channel full of fuel and heavy water along
the entire core length without intermediate core support. Pressure tube sagging
due to the accumulated irradiation will develop with time. If the garter springs
are not located at their prescribed position or if flow induced vibrations dislodge
them from their original positions, local pressure tube calandria tube contact
could occur. The effect would be to create cold spots on the pressure tube wall
that could absorb and concentrate the free hydrogen present in the primary
coolant or in the annular space between the pressure tube and the calandria tube
and weaken the material. Once the hydrogen is absorbed, the material
properties change and embrittlement at low temperature can occur leading to a
pressure tube rupture.

The pressure tube concept coupled with natural uranium fuel requires frequent
opening (typically twice a day) of the heat transport circuit. This constitutes a
systematic but controlled breach of the pressure boundary. At that time, it is
possible that a small **L**oss **O**f **C**oolant **A**ccident (LOCA) or worse a channel flow
blockage could occur.

Fuel dryout must be avoided in all the channels. All channel powers are not
measurable at all times and are the result of a complicated process involving
measurements and calculations. Accordingly the regulation and safety systems
must provide full protection against dryout and require a thorough logic and
redundancy.

The horizontal core does not promote easy thermosyphoning as would a vertical
core under conditions of loss of forced flow (loss of heat transport pumps or total
loss of electrical power). For some channels the horizontal run at the channel
level can be as high as 20 metres. Under certain conditions the flow, if two phase
may stratify and uncover some fuel elements. The result could be high fuel
temperature followed by fuel failure.

For safety and operating reasons limits are imposed on maximum channel power and bundle power. The channel power peaking factor (CPPF) which is a measure of the deviation from an ideal power distribution must be monitored to maintain channel and bundle power limits at all times in particular after refuelling a channel. Each channel refuelling creates a perturbation in the overall power distribution that has to be evaluated before and after each refuelling. In order to calibrate the theoretical calculations, a large amount of detectors have to be installed, monitored and intercalibrated. In addition the analysis of the measurements are complicated.

2.2 The moderator

The function of the moderator is to slow fission neutrons down. As indicated in the previous lessons, the best candidate is a nucleus of hydrogen. Other good potential candidates are light nuclei composed of few protons and neutrons like deuterium, beryllium and carbon.

But it is not sufficient for a moderator to thermalize neutrons, it must do this without absorbing too many neutrons. As a consequence, Hydrogen is not the best choice for a moderator since it has a relatively high neutron absorption cross section in the thermal energy range.

The latest CANDU reactor design is a pressurised heavy water reactor (PHWR) and takes full advantage of the neutron economy provided by the use of deuterium in the coolant and in the moderator. This allows the use of natural uranium fuel and avoids fuel enrichment for an acceptable level of burnup. The use of natural uranium does create a large amount of irradiated fuel bundles that pose a problem of their own in terms of long term storage and disposal. Enriched fuel reduces neutron economy by about 20% but it can also reduce fuel waste by a factor of up to 5.

In order for the neutrons to escape resonance capture in the fuel, it is advantageous that the fuel and moderator not be homogeneously mixed, but physically separated. The CANDU concept enables to create one region of fission with a fast spectrum of neutrons and one of thermalization where the neutrons are slowed down without being heavily absorbed. The neutrons born in the fuel are thermalised away from the fuel and avoid being absorbed without fission in the fuel matrix.

This later separation is an inherent advantage of the CANDU reactor since it promotes a very good neutron economy.

2.3 General reactor layout

The use of expensive heavy water in the heat transport system calls for the design of a very compact reactor and primary heat transport system. The pressure tubes need feeder connections from and to the inlet and outlet headers.

As a consequence the design necessitates numerous pipes and welds on the feeders.

Figure 2.3 shows the elevation differences of the heat transport system where it can be clearly seen that the heat source (reactor core) is well below the heat sink (the steam generators: SG). That layout is extremely important in case of thermosyphoning which can only work under these circumstances.

Fig. 2.3:
Schematic of Candu-PHW reactor
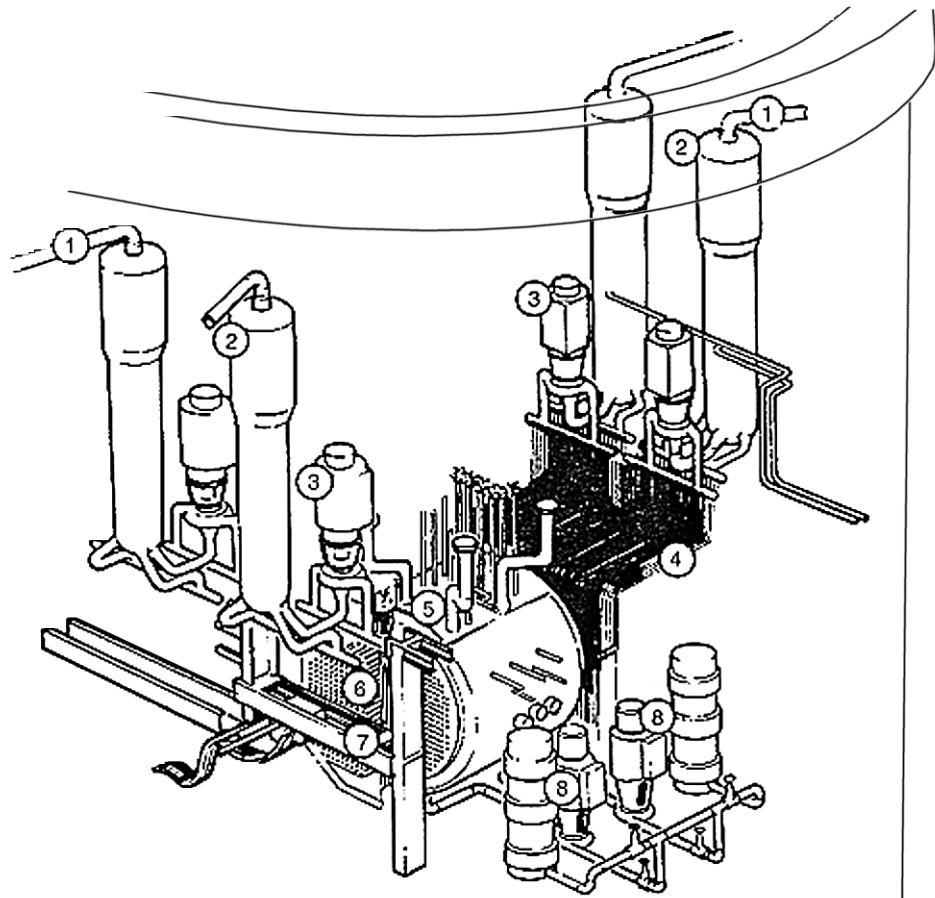
1	Main Steam Supply Piping	5	Calandria Assembly
2	Steam Generator	6	Fuel Channel Assembly
3	Main Heat Transport System Pumps	7	Fuelling Macine Bridge
4	Feeders	8	Moderator Circulation System

The figure also shows that the moderator pumps and heat exchangers are about on the same level than the moderator or the core themselves and in case of moderator cooling interruption no natural circulation flow through the calandria is credible. Nevertheless, the moderator heat capacity is very large and it can accommodate a temporary loss of circulation and heat removal.

In general the Candu reactor is of the two loop concept as shown in figure 2.4.

Two loops separate the core into two equal parts dividing the calandria vertically in the middle.

Fig. 2.4:
Candu heat transport flow sheet
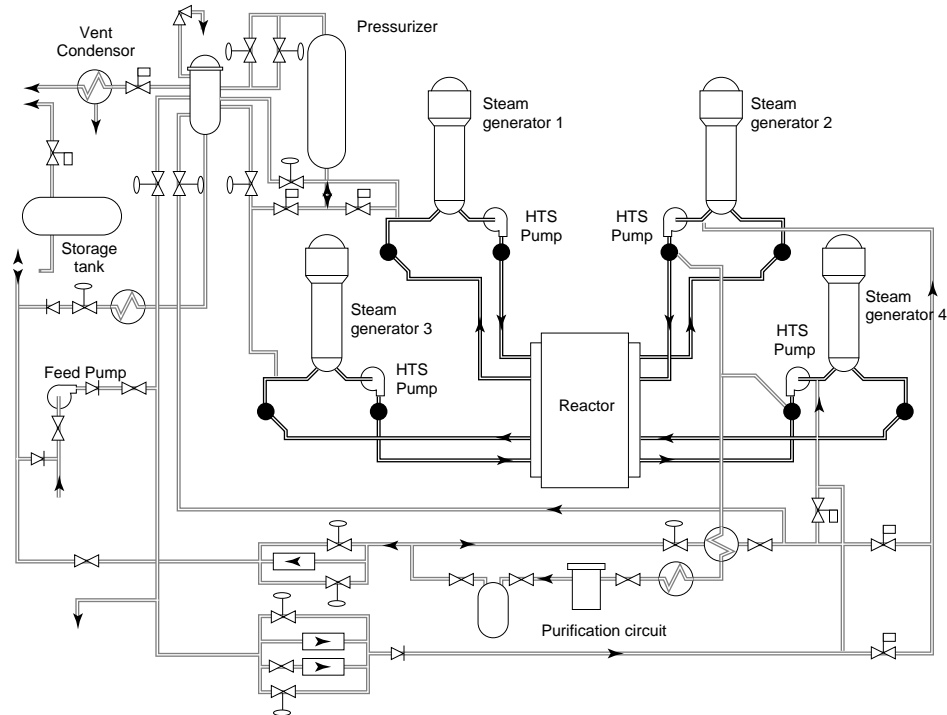
This concept is slightly different for the Bruce station which has inner and outer loops. The outer loop is fed by a higher inlet enthalpy fluid while for the inner loop, containing the high power channels, the inlet fluid passes through a secondary side preheater before reaching the core at a lower enthalpy. The pump arrangement can also vary from one station to the other. The pumps are in series for Darlington in parallel and in series for Bruce and Pickering. As can be observed the loops are only connected to each other through the pressuriser or trough smaller pipes such as the purification system pipes. Some stations may have boiling fluid at the outlet of the channels while other contains only subcooled liquid throughout the heat transport system (Pickering).

A shutdown cooling system dedicated to each loop, as shown in figure 2.5, is capable of replacing the steam generators and the secondary circuit cooling function when the reactor is in its shutdown state. In case of emergency the system can also be activated at full pressure and nominal temperature.

Fig. 2.5:

Shutdown cooling system flow diagram
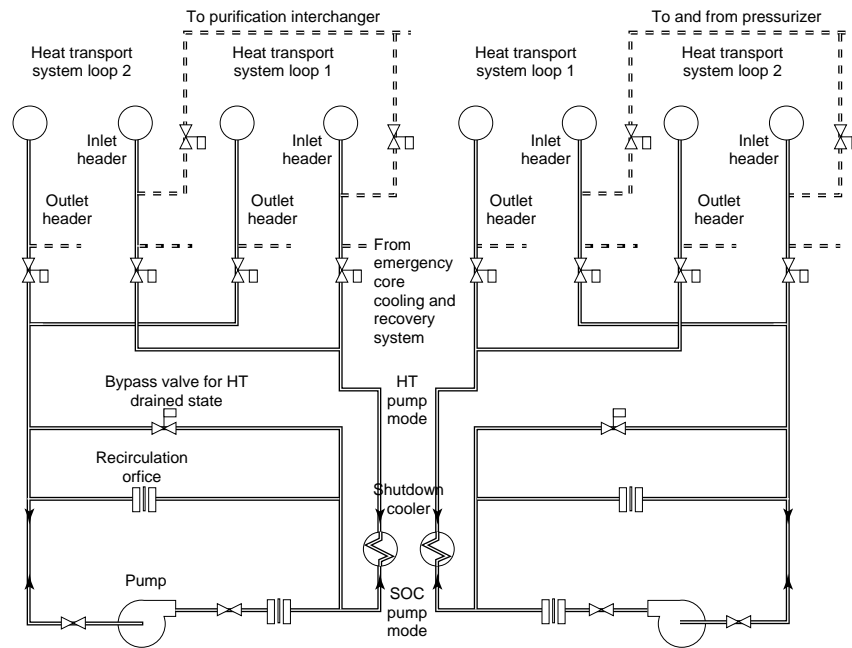
The secondary side system is shown in figure 2.6. One can notice the multiple provisions for rapid steam generator blowdown and therefore primary system cooling though the various steam valves. The steam can be diverted either directly into the condenser or to the atmosphere through valves with staged openings.

Fig. 2.6:

Secondary side system flow diagram
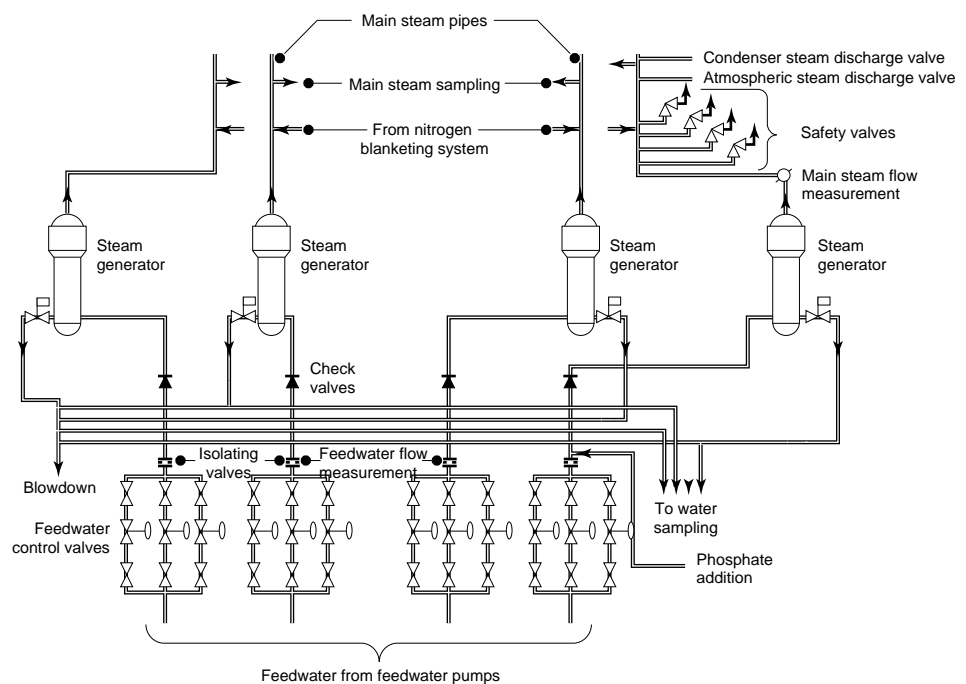
Also of interest is the steam generators check valves whose primary function is to preserve the steam generator inventory in case of an upstream pipe break. Each steam generator is fed by a series of feedwater valves whose position is a control function of steam generator water level and reactor core power. The two 50% main feedwater pumps serve for power operation while the auxiliary pumps can provide up to 5% full power cooling. The secondary side heat removal capacity and heat removal path is of crucial importance to the primary side since it protects the heat transport side against high pressure and promotes fuel cooling.

Under normal operating conditions the moderator cooling must be able to remove about 5% of the core heat. A dedicated system must therefore be designed to fulfil this function as shown in figure 2.7.

Fig. 2.7:
Moderator cooling system flow diagram
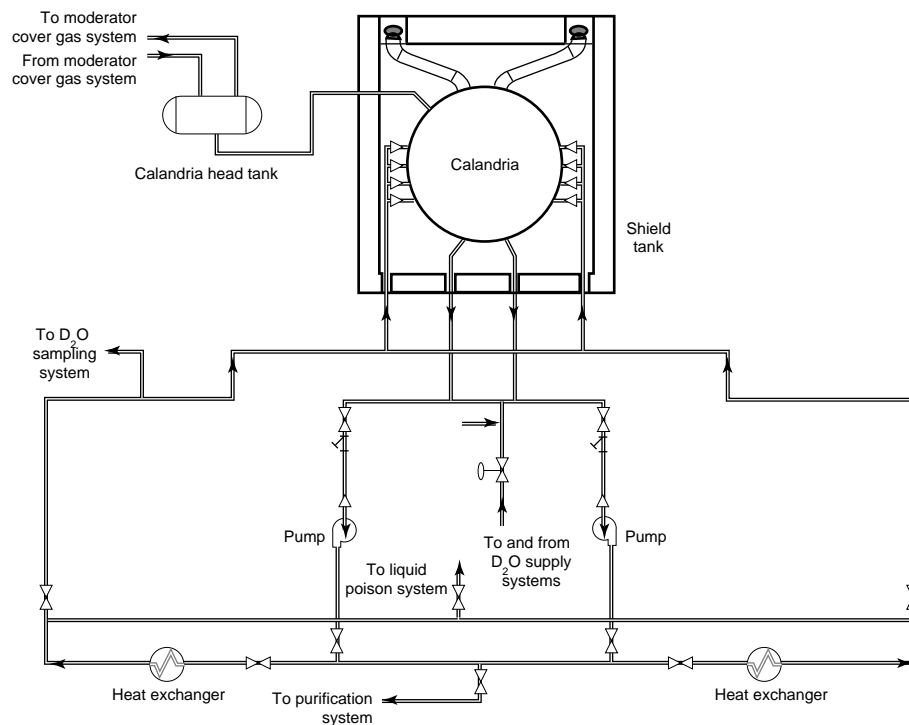
2.4 Special safety systems

The Candu reactor has four special safety systems: two shutdown systems, one emergency core cooling system and the containment system.

2.4.1 Shutdown Systems
In a Candu reactor, two shutdown systems are necessary because of the positive void reactivity coefficient associated with the heavy water moderator and coolant and the natural uranium fuel. It is prerequisite that the reactor be shutdown in all cases of transients. No severe transient will have an acceptable scenario if the reactor is not shutdown.

The availability targets of the shutdown systems is 10^{-3} per year. This means that the shutdown systems could be unavailable when required 8 hours per year. The accepted probability of a severe accident requiring the use of the special safety systems is 10^{-2}. Accidents are declared improbable when their probability falls below 10^{-7}.

Therefore with only one shutdown system the probability to have an accident without shutting down the reactor is 10^{-5}, which is totally unacceptable.

By introducing an additional shutdown system, fully independent from the first one the probability to have an accident without shutting down the reactor falls to 10^{-8} which is beyond the generally accepted credible probability range.

2.4.2 Emergency Core Cooling System
As shown in figure 2.8, the Emergency Core Cooling System (ECCS) consists of 3 stages: High Pressure, Medium Pressure and Low Pressure.

Fig. 2.8:
ECCS flow diagram
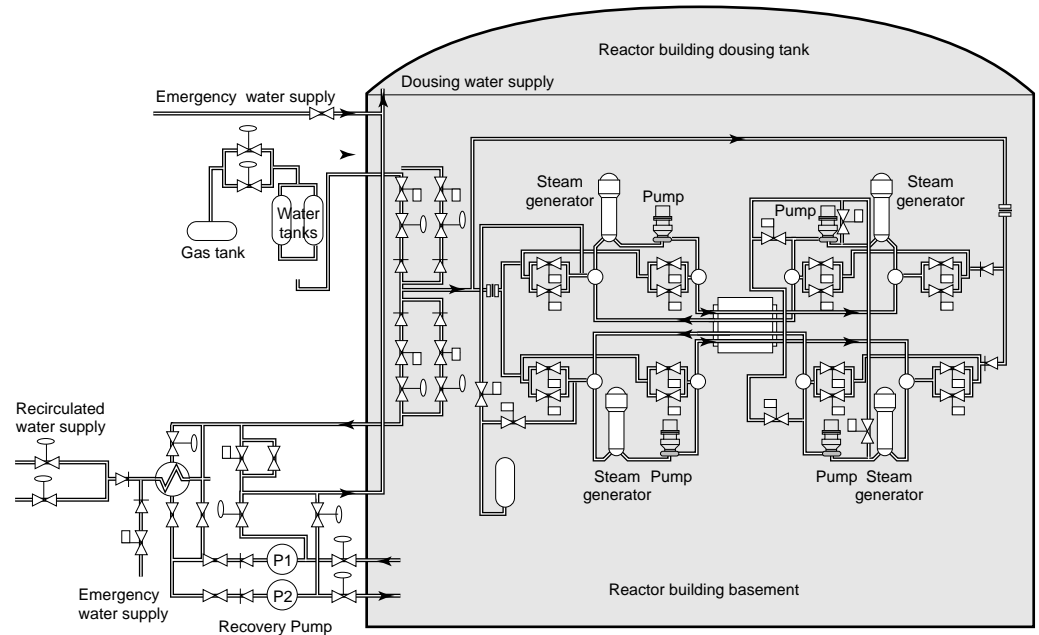
Light water and heavy water mixing concerns render the Candu ECCS complicated through the presence of valves, rupture disks and conditioning signals.

The HPECCS is driven by a pressurised tank of gas which in turn pressurises two water tanks by opening quick acting gas valves. The MPECCS and LPECCS are injected via the same pumps and same injection lines. The source of water of

the MPECCS is the dousing tank located on top of the containment, while for the LPECCS the source is the reactor floor where the water coming from the dousing or the break would eventually have accumulated.

2.4.3 Containment System
The containment system is basically the concrete structure housing all the primary system and part of the auxiliary and secondary systems. It is designed to retain the fission products in case of an accident.

Some stations have a vacuum building in addition to the containment building to retain the fission products and control the containment pressure. In both cases the mechanical integrity of the containment is guaranteed by the dousing of the steam escaping the primary system.

3. Pressurised Water Reactor (PWR)

3.1 Principle

The PWR principle consists of a vertical compact core using enriched uranium with cooling and moderation using the same light water fluid.

3.2 General layout

The typical layout inside and outside the containment is very similar to a Candu reactor as shown in figure 3.1.

Fig. 3.1:
Typical layout of a PWR inside the containment
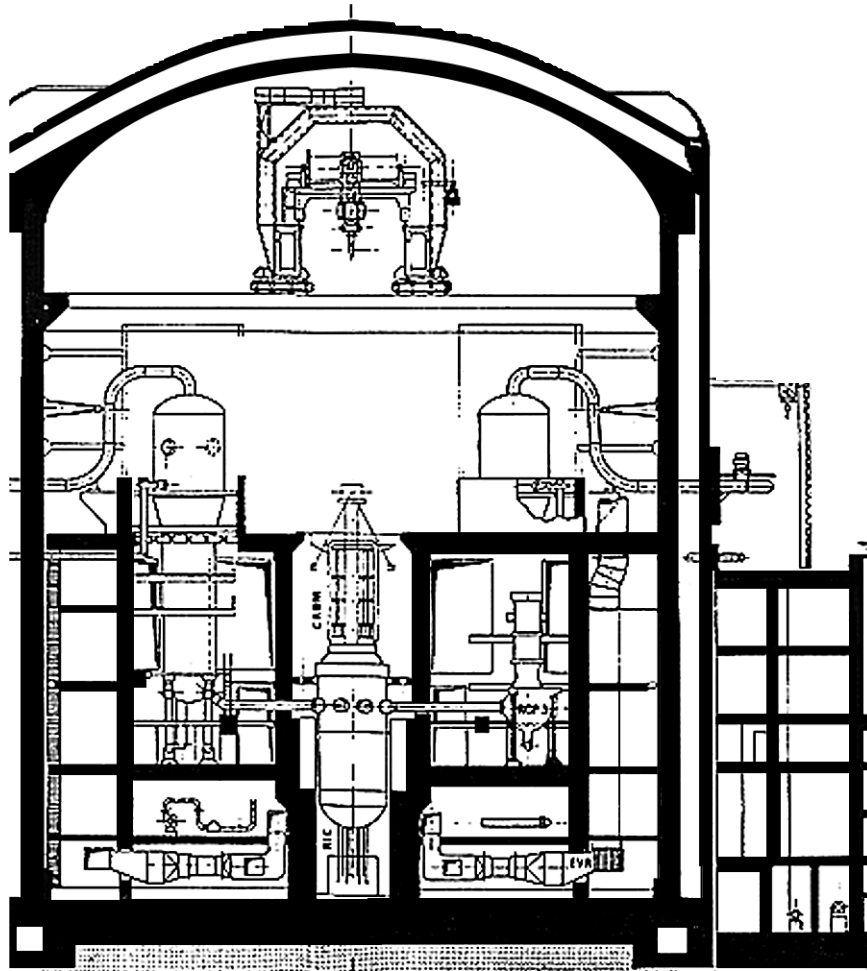
The arrangement of the connection between the core and the steam generators is more simple than in a Candu and only a few large diameter pipes connect the various components as shown in figure 3.2. Since only light water is used the requirement on minimizing water volumes are much less stringent than in a Candu.

Fig. 3.2:
*Typical layout of a three loop PWR*
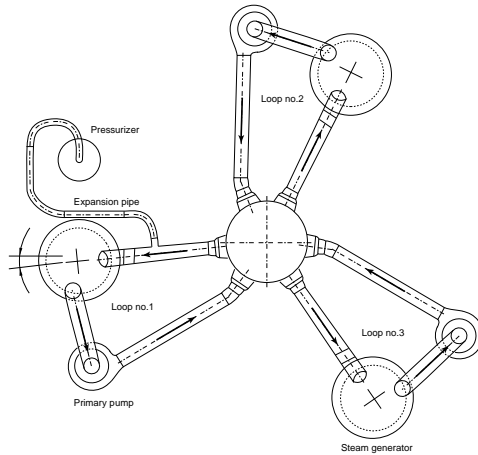

Fig.
3.3: Flow path of a PWR
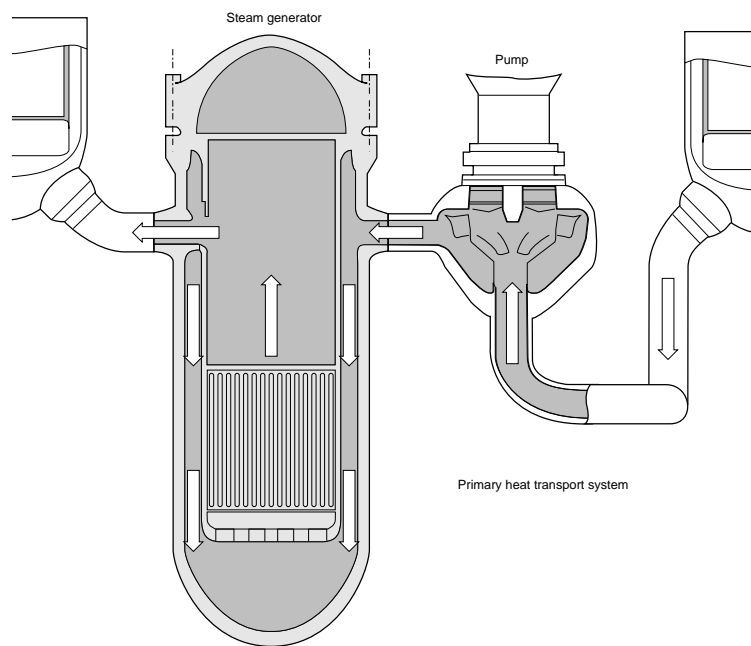
The flow path of the coolant, illustrated in figure 3.3, is quite simple. Starting from the pump suction, the flow is directed toward the vessel inlet where it is redirected downward. The flow then travels up through the core and leaves the vessel to enter the steam generator, goes around the inverted U tubes and back to the pump suction. A small flow enters the top of the vessel to provide adequate cooling of the upper internals.

Depending on the number of heat transport pumps and associated steam generators, the different PWR reactors are of the one, two, three or four loop kind.

The same figure 3.2 also shows that a very large amount of water surrounds the core in the vessel. The reactor arrangement and heat transport system piping are much simpler than in a Candu.

In general PWRs have a double containment as shown in figure 3.4. The outside consists of a concrete wall as in a Candu and the inside of the containment has a steel lining all around. It must be noted that the containment is not technology dependent. The space between the first and the second walls enables the control and the purification of the air that escapes from the inside in case of contamination during an accident. Unlike most Candu reactors, the containment spray water is stored outside the containment and can be recirculated, decontaminated and cooled and is consequently always available. In a Candu 600 reactor, the water is stored in the upper part of containment with no recirculation capabilities and therefore no long term control over containment pressure.

*Fig. 3.4:*
Typical PWR containment
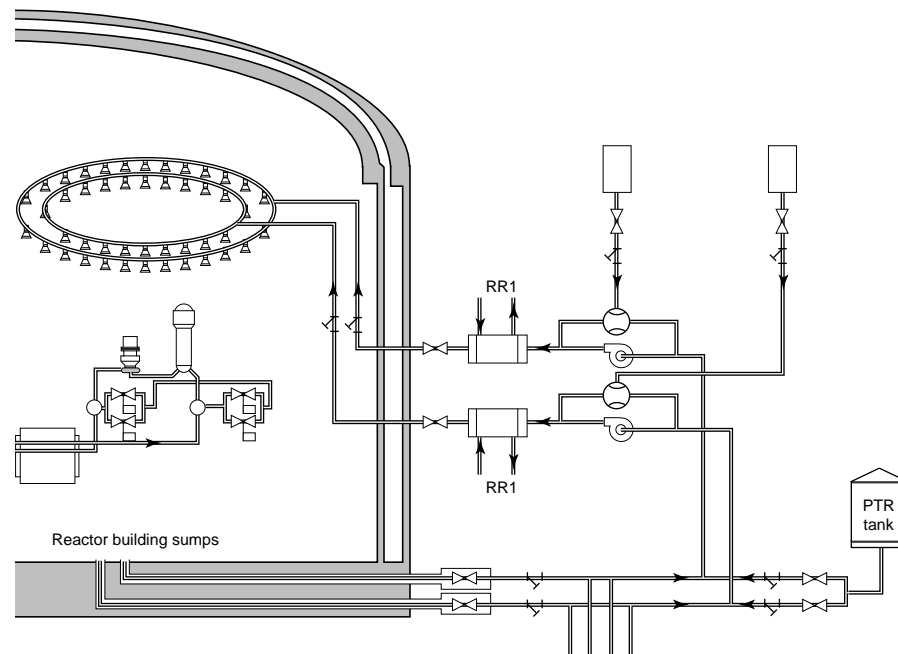
A few PWRs have an ice containment. In that case the steam escaping from a break is condensed by a large amount of ice stored inside the containment. The ice system is kept operating through a very complicated cooling system that increases the size of the containment.

3.3 Pressure vessel

The pressure vessel is shown in figure 3.5. The vessel head itself is held down by giant bolts which are removed to refuel the core. On top of the vessel head are the control rods driving mechanisms which penetrate vertically into the vessel. From top to bottom, the vessel is divided by four plates, the upper plate, the upper core plate, the lower core plate and the lower inlet flow plate. The upper plate delimits the upper core internals and provides support to the various tubes. The top part of the vessel is occupied by the control rod guide thimbles and some instrumentation guides, mainly temperature measurement devices. The core itself consisting of 4 meters high assemblies is contained and held in place between the top and the bottom core support plates. At the bottom of the vessel, the incore instrumentation penetrates the vessel to monitor the flux distribution in the center of the fuel assemblies. The bottom plate also acts as a flow distributor since at the bottom of the vessel, the flow is redirected upwards. A series of shields protect the vessel from irradiation and a lateral core baffle holds the fuel assemblies in place. The core barrel separates the inlet flow from the outlet flow down to the inlet flow plate.

Fig. 3.5:
PWR vessel
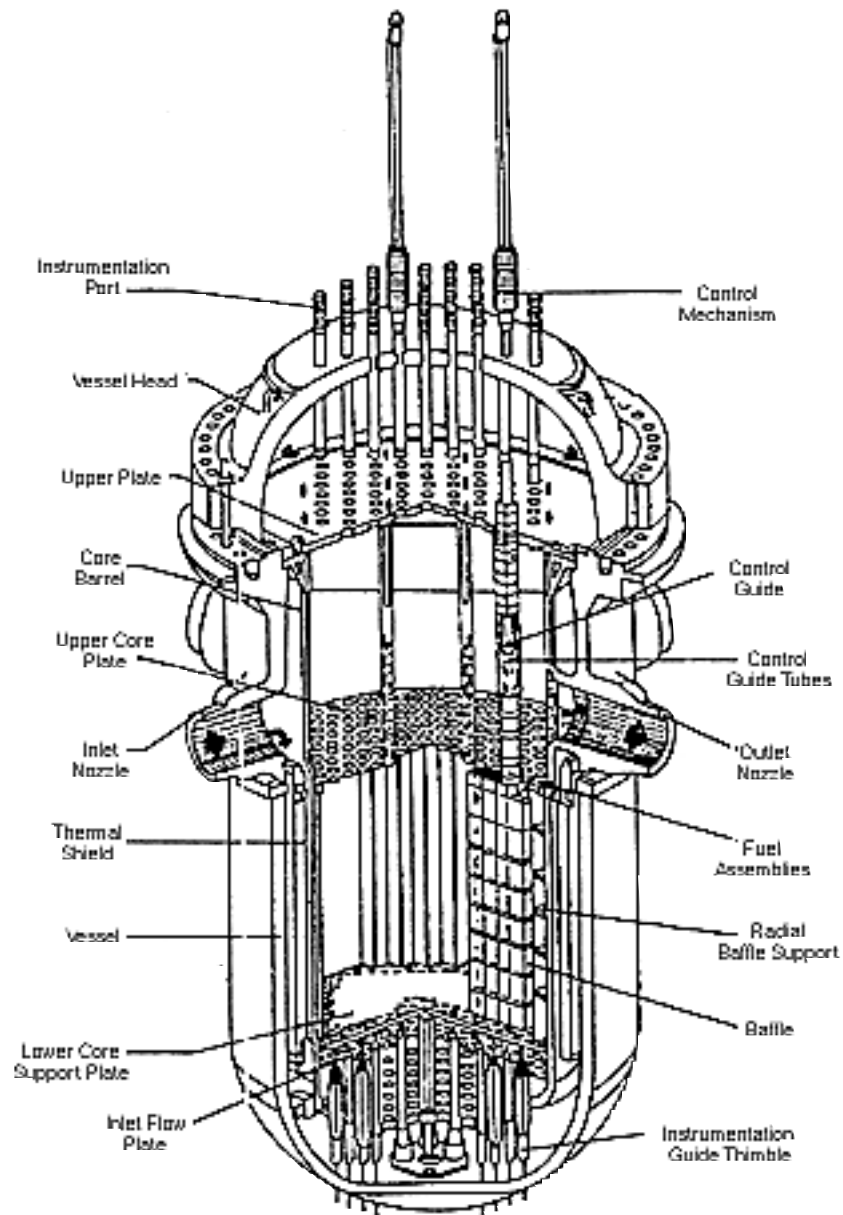
3.4 Fuel

The fuel consists in a square array of generally 17x17 rods with 24 locations for control rods and one central rod for instrumentation as shown in figure 3.6.

Fig. 3.6:
17x17 PWR fuel assembly

Spider

Control Rod

Holdown Spring
Upper Nozzle
Upper Grid

Guide Tube

Fuel Rod

Mixing Grid

Number of Fuel Rods - 264
Number of Fuel Assemblies - 157
(for a 900 MWe station)

Lower Grid

Bottom Nozzle
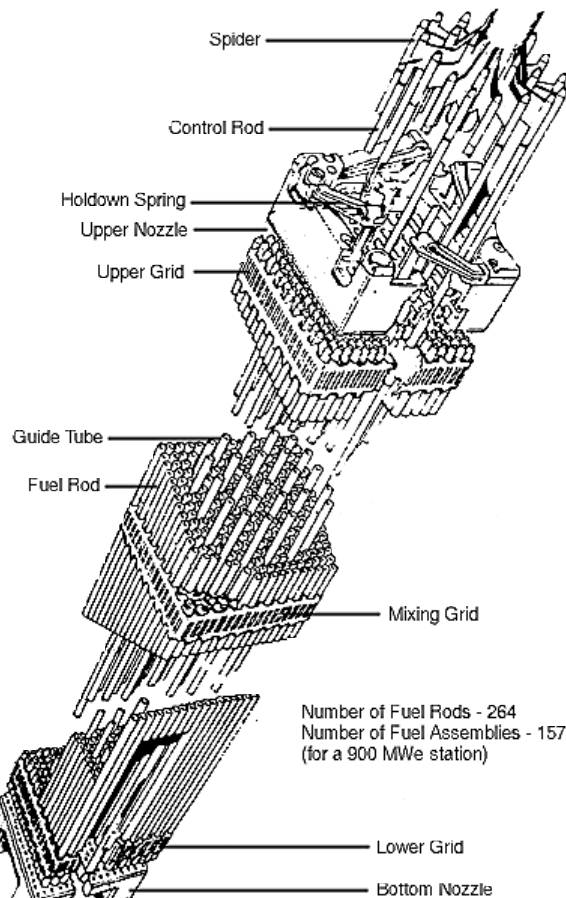
Earlier designs had a 15x15 fuel assembly. Three loop reactors (typically 950 MWe) have 157 assemblies of 12 ft height. Four loop reactors (typically 1300 MWe) have 193 assemblies of 14 ft height.

The fuel rods are held in place by up to 9 spacer and mixing grids. At each grid location four zircaloy or stainless steel springs hold each individual rod in position. The grids are welded to the control guide tubes and to the instrumentation tube. These tubes are in turn attached to the upper and lower fuel assembly nozzles. Holdown springs mounted on the upper nozzle, are used to block the fuel assembly between the upper and lower core plate in the vessel prohibiting any motion of the fuel during normal and abnormal operating conditions.

The figure 3.6 also shows a spider control assembly inserted into the fuel assembly. The downward motion of the spider assembly is gravity controlled while a spring at the centre of the spider is used to decelerate the control rod. Flow restrictions and flow holes provided in the lower part of the control rod guide thimbles also provide a means of dampening the impact of the spider assembly.

4. Boiling Water Reactor (BWR)

4.1 Principle

The BWR principle consists of a vertical compact core using enriched uranium with cooling and moderation using the same fluid without secondary side. The overall design is simpler than the Candu or the PWR since there are no intermediate heat exchangers. The direct cycle at relatively high pressure gives a much better thermodynamic efficiency than cycles with secondary sides.

4.2 Reactor and vessel

The steam and the core heat are produced in the same vessel as shown in figure 4.1. The steam separators which are used to separate the upcoming two phase flow into steam and saturated water are located on top of the vessel. The recirculated water is mixed to the inlet feedwater before being reinjected into the core. In order to promote an adequate fuel cooling and good heat removal jet pumps provide an internal flow through the core. As in a PWR, the vessel head is also removable in order to proceed with the annual refuelling and maintenance of the core internals.

Fig. 4.1:
BWR vessel

Vent and Head Spray

Steam Outlet

Core Spray Inlet

Low Pressure Coolant Injection Inlet

Core Spray Sparger

Jet Pump Assembly

Fuel Assemblies

Jet Pump/Recirculation Water Inlet

Vessel Support Skirt

Control Rod Drives

In Core Flux Monitor

Steam Dryer Lifting Lug

Steam Dryer Assembly

Steam Separator Assembly

Feedwater Inlet

Feedwater Sparger

Core Spray Line

Top Guide

Core Shroud

Control Blade

Core Plate

Recirculation Water Outlet

Shield Wall

Control Rod Drive Hydraulic Lines

The BWR system pressure (typically 10 MPa) is lower than is a PWR (typically 15 MPa) because the direct cycle has a better efficiency by providing a higher steam pressure to the turbine. The feedwater is recirculated in the vessel through a jet pump as sown in figure 4.2.

Fig. 4.2:
BWR inside vessel flow patterns
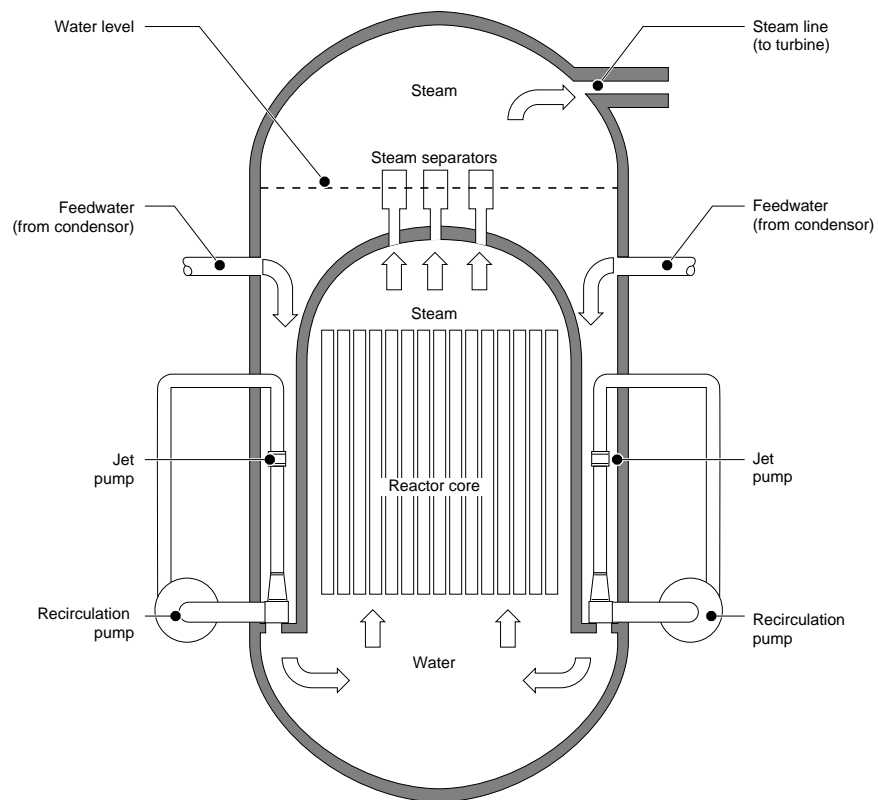
4.3 Fuel

The fuel is contained in canisters as shown in figure 4.3 with four fuel bundles surrounded by a control assembly. In the fuel bundles some empty spaces are left without fuel to flatten the power distribution. Unlike the PWR the lattice of a BWR is not very uniform and graded enrichments of the fuel must be used to compensate for the various water gaps or absorption devices present in the core.

Fig. 4.3: BWR fuel assembly and control rod
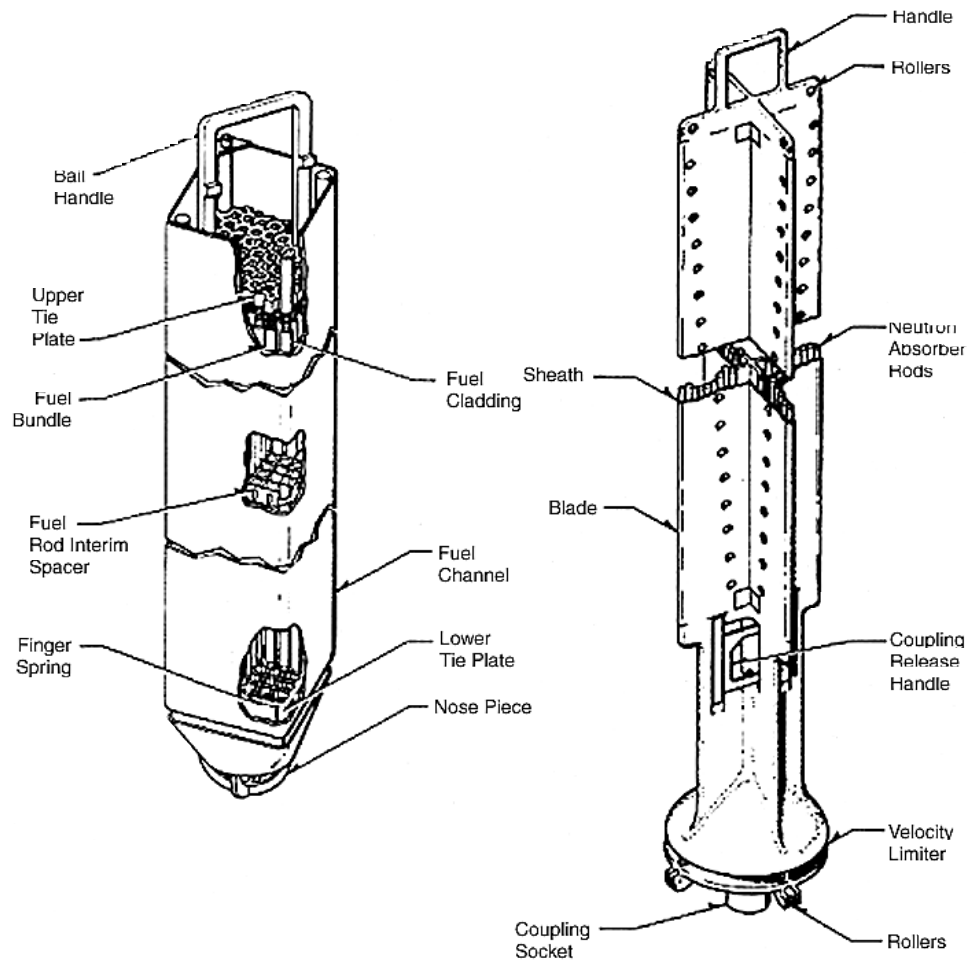
The control rod is cross shaped and must be inserted from the bottom of the core since the top of the core is occupied by the steam production. This means in particular that the insertion of the control rods is counter gravity.

As for the Candu, the BWR has a positive void coefficient, but due to the fuel enrichment and the size of the lattice it has an overall very negative power coefficient.

5. Gas Cooled Reactor (AGR type)

The gas cooled reactor has a fixed moderator (graphite) and a gas coolant as described in figure 5.1. It is a very stable reactor with low power density and on power refuelling. That reactor has been developed in Britain and follows the Magnox type of rectors. Instead of metal uranium, the fuel is made of slightly enriched uranium oxide. The fuel temperature could then be raised such as to obtain an exit gas coolant temperature of about 675 °C instead of 410 °C for natural uranium.

Fig. 5.1:
AGR reactor schematic
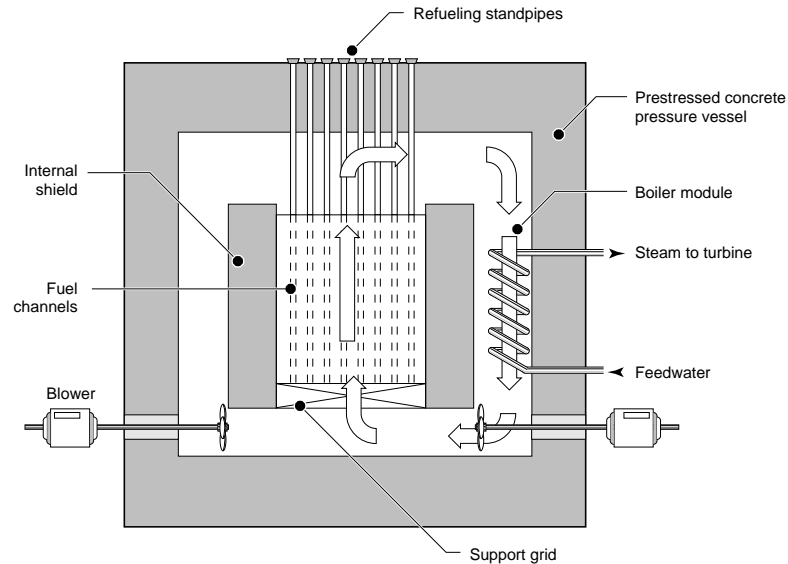
The thermodynamic efficiency of this type of reactor is very high, at about 40% which makes it the most efficient industrial nuclear concept. The on-line refuelling has the same advantages than the ones in a Candu.

6. Fast Breeder Reactor (LMFBR)

The fast breeder reactor is a liquid sodium cooled reactor with two low pressure sodium loops and one light water loop as can be seen in figure 6.1.

Fig. 6.1:
LMFBR schematic
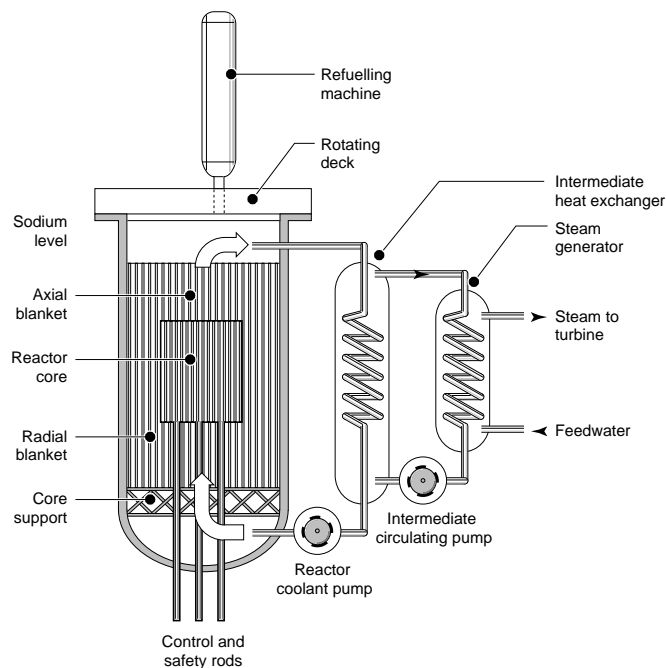
The reactor is highly enriched in plutonium and the uranium blanket has the capability of producing more fissile material than what is consumed in the reactor. It is nevertheless an experimental technology, which enjoys less support than in the early times of development.

One big advantage of the reactor is the size of its core, that can be kept small since no moderator is necessary to slow down the neutrons.

Two big drawbacks of the technology and particularly of its the coolant are: the coolant becomes solid at temperatures lower than 98 °C, and interaction with water must be avoided at all cost even when a water sodium heat exchanger is necessary.

7. RBMK

The RBMK is a vertical pressure tube reactor with a direct cycle as illustrated in figure 7.1.

Fig. 7.1:
RBMK schematic diagram
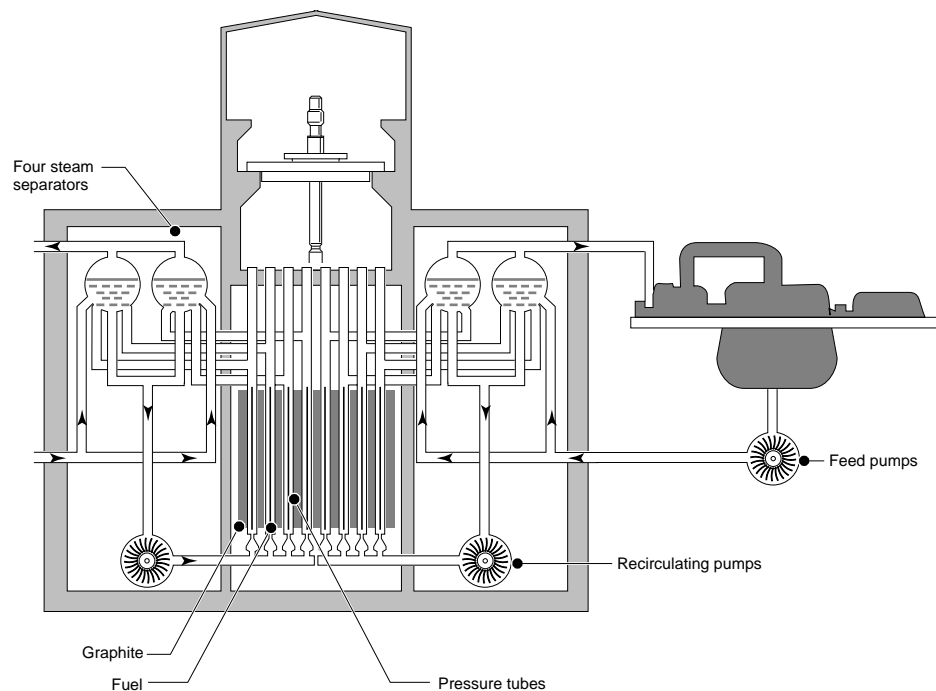
The moderator is high temperature graphite since all the slowing down and gamma ray absorption takes place there. The moderator is a higher heat source than the fuel during normal operating conditions.

The boiling water and the moderating ratio used contribute to the positive void coefficient that ultimately led to the Tchernobyl accident. This technology is typical of the first generation of large Russian power reactors.

Basic Design of a CANDU Nuclear Reactor

Training Objectives

The participant will be able to describe or understand:

1 the CANDU structural design: primary and secondary circuits;
2 elements of the CANDU design: moderator, calandria, fuel, coolant, pressure tube, etc.;
3 the CANDU critical mass considerations;
4 the CANDU primary circuit heat balance;
5 the CANDU operational design and core equilibrium;
6 the CANDU power limits and reactivity regulation;
7 the CANDU overall plant control.

Basic Design of a CANDU Nuclear Reactor

Table of Contents

1 Introduction

It is important to understand the implications of specific design choices in a given nuclear technology. On one hand, these technological choices explain the differences between the possible designs of thermal nuclear reactors. On the other hand many characteristics are the results of the design coherence which is needed to achieve the feasibility, the reliability and the safety of a given reactor technology.

In the present lesson, we will explain in more details the CANDU technology and we want to emphasize the interrelations between the various technological aspects leading to a coherent and safe design. Such a design, where the control and safety processes are integrated with complementary functionalities, should always feature a level of confidence high enough to provide safe power production. In that respect, the nuclear plant design should fulfil the requirement that radiation exposures and contamination risks should be kept as low as possible for the workers and the environment.

2. Basic Aspects of the CANDU Design

2.1 Interrelations between design characteristics

Considering for instance the interrelations between design characteristics one should look to the following interrogations: why is the fuel management one of the most important differences between the CANDU and the Light Water Reactor (LWR) technologies and how does this difference impose the choice of many other design characteristics of the CANDU ?

The main difference between the fuel management strategies of CANDU and LWR nuclear reactors is the type of nuclear fuels which are used: natural uranium in CANDU versus enriched uranium in LWR. Choosing natural UO_2 as the fuel of CANDU nuclear reactors has direct consequences on other aspects of the technology. For instance, the use of natural UO_2 implies that heavy water must be considered as the best (but expensive) candidate for moderator in the reactor core and for coolant in the primary heat transport circuit.

With natural uranium as the nuclear fuel, the on-line refuelling becomes mandatory to provide enough reactivity to allow continuous full power production. The CANDU fuel assembly should indeed be designed to allow the replacement of irradiated fuel bundles by fresh fuel bundles with as few perturbations as possible to other reactor operations at full power. The horizontal pressure tube design is therefore more suitable for the refuelling of individual reactor channels. Moreover, the already mentioned positive void reactivity coefficient (of the CANDU technology) requires the functionality and the complete safety assessment of two independent shutdown systems.

This emphasizes the very close links between the various design characteristics. However, beneath the implementation of a given nuclear technology, the safety systems shall be designed in order to allow operational safety and also to always maintain the consequences of all design basis accidents within acceptable safety limits as defined by the regulatory agencies.

2.2 Comparison between CANDU reactor models

All the CANDU reactors in operation share the same type of design with the following common characteristics:
1)   fuel bundles consisting of natural uranium in the form of UO_2 pellets mounted in fuel pins,
2)   horizontal fuel assemblies contained in pressure tubes surrounded by the calandria tubes,
3)   heavy water coolant circulating in the primary heat transport system,
4)   heavy water present in the calandria acting as the moderator in the reactor core.

Tables 2.1 and 2.2 compare three different CANDU reactor models: Gentilly-2 (CANDU 600 reactor model), Bruce A (initial and uprated designs) and Pickering A.

Table 2.1:

Main characteristics of CANDU design: fuel and reactor core.

	GENTILLY-2	BRUCE 'A' initial design (uprated)	PICKERING 'A'
Unit Electrical Output MWe (net)	640	732 (769)	515
Core and Fuel Data			
No. of Fuel Channels	380	480	390
Design Basis Channel Power MWth	6.5	5.74 (6.5)	5.12
No. of Fuel Bundles/Channel	12	13	12
No. of Elements/Bundle	37	37	28
Nominal Design Basis Bundle Power (kW)	814	(900)	650
Design Basis Fuel Element Rating $\int \lambda d\phi$, kW/m	4.2	3.7 (4.56)	4.25
Fuel Handling			
Previous Similar Design	Pickering 'A'	KANUPP, NPD	Douglas Point, RAPP
Direction of Refuelling	With Flow	Against Flow	With Flow
Major Features	Fuel Separators	Fuel Carrier, Latches	Fuel Separators
Type of End Fitting Closure	Expanding Jaws	Rotating Integral Lugs	Expanding Jaws
F/M Drives	Oil Hydraulics	Electrical	Oil & Water Hydraulics
Spent Fuel Handling	Direct to Elevator	Direct to Elevator	Thru F/T Mechanism
New Fuel Loading	Direct to F/M	Direct to F/M	Thru F/T Mechanism
Reactor			
Calandria Vault	H_2O Filled	H_2O Filled Shield Tank	Air Filled
End Shielding	Steel Balls & H_2O	Steel Balls & H_2O	Steel Plates & H_2O
Min. Pressure Tube Wall Thickness, mm	4.19	4.06	4.06 (unit 4) 4.19 (units 1, 2 & 3) (retubed)
Reactivity Mechanisms			
Adjuster Rods (Absorbers)	21 (stainless steel)	-	8 (cobalt)
Booster Rods (Enriched Uranium)	-	16	-
Control Absorbers	4 (Cadmium)	4 (Cadmium)	-
In-Core Flux Detector Assemblies	33	23 (14)	8

Table 2.2:

Main characteristics of CANDU design: safety and heat transport systems.

	GENTILLY-2	BRUCE 'A' (initial design)	PICKERING 'A'
Safety Systems			
Primary shutdown mechanism	28 shutoff rods	30 shutoff rods	21 shutoff rods (10 adjusters have been converted to shut off rods)
Secondary shutdown mechanism	Poison injection	Poison injection	Moderator dump
Dousing Tank	In reactor building	In vacuum building	In vacuum building
Emergency core cooling	From external tanks (HP) and dousing tank (MP)	From external tanks (HP) and grade level tank (MP)	From moderator system (to be retrofitted with high pressure pumps)
Reactor building design pressure	124 kPag	68.95 kPag	41.37 kPag
Heat Transport System			
Inlet temperature	266°C	251°C/265°C	249°C
Outlet temperature	310.4°C	304°C	293°C
Quality at outlet header	1%	2°C subcooled (0% satured)	5°C subcooled
Inlet pressure	11.3 MPa(a)	10.3 MPa(a)	9.5 MPa(a)
D_2O inventory (main circuit only) m^3/MWe	0.19	0.36	0.27
Number os steam generators	4	8 (4 separate preheaters)	12
Surface area per steam generator	3177 m^2	2369 m^2	1858 m^2
Number of pumps	4	4	12 plus 4 spare
Pump motor rated power	6710 kW	8200 kW	1420 kW
Pressure control	Pressurizer	Pressurizer	Feed and bleed
Purification hall-life minutes	60	65	130
Moderator System			
Number of pumps	2 at 100%	2 at 100%	5 at 25%
D_2O inventory (main system only) m^3/MWe	0.36	0.40 (0.38)	0.41

Besides the number of fuel channels, fuel bundles per channel and type of reactivity devices which vary from one reactor model to the other, the fuel handling method is one significant difference. The CANDU 600 and Pickering A reactors share the same direction of refuelling as the coolant flow. Bruce A is refuelled against the flow of coolant in the reactor channel.

3 CANDU Structural Design

3.1 Core lattice

The CANDU nuclear reactor structure consists in a superposition of lattice cells containing: fuel, moderator, coolant, reactivity devices, structural components, etc. For any reactor to be critical ($k_{eff} = 1$), the designed lattice cell has to be supercritical. Then the multiplication constant for the infinite lattice $k_\infty > 1$ allows for the neutron losses which occur by leakage and absorption in the real case.

Figure 3.1 shows a schematic of the typical configuration of the CANDU core lattice. The vertical reactivity device, either a control rod or a liquid zone controller, is shown inside the calandria vessel. The vertical reactivity device is immersed in the low pressure moderator and passes between the calandria tubes. The fuel and the coolant are contained in the pressure tube which is inside the calandria tube. The tubes are concentric and separated by an annular gas gap.

Fig. 3.1:
*Schematic of a CANDU PHW lattice.*
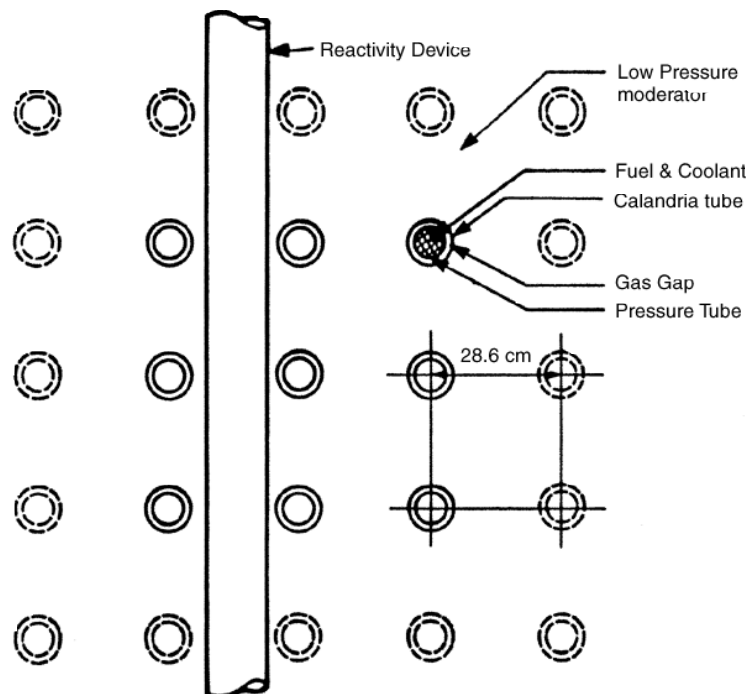
3.2 Moderator

The CANDU moderator consists of heavy water at about atmospheric pressure and at a temperature of 70°C. Due to the high moderating ratio of D_2O, the resulting neutron economy allows to use natural uranium and precludes the need for fuel enrichment. The moderator efficiency increases sharply by a factor of 7.7 going from a purity of 99 % to 100 % (see lesson III, section 2). Isotopic composition of the moderator should be monitored and the reactor grade moderator heavy water should be at least 99.75 weight% D_2O.

Figure 3.2 shows the CANDU 600 reactor assembly with the calandria containing the moderator. The calandria surrounds the cylindrical reactor core with an extra annulus containing also heavy water. This zone acts as a reflector on the neutron flux improving the neutron economy.

Fig. 3.2:
Schematic of a CANDU reactor assembly.
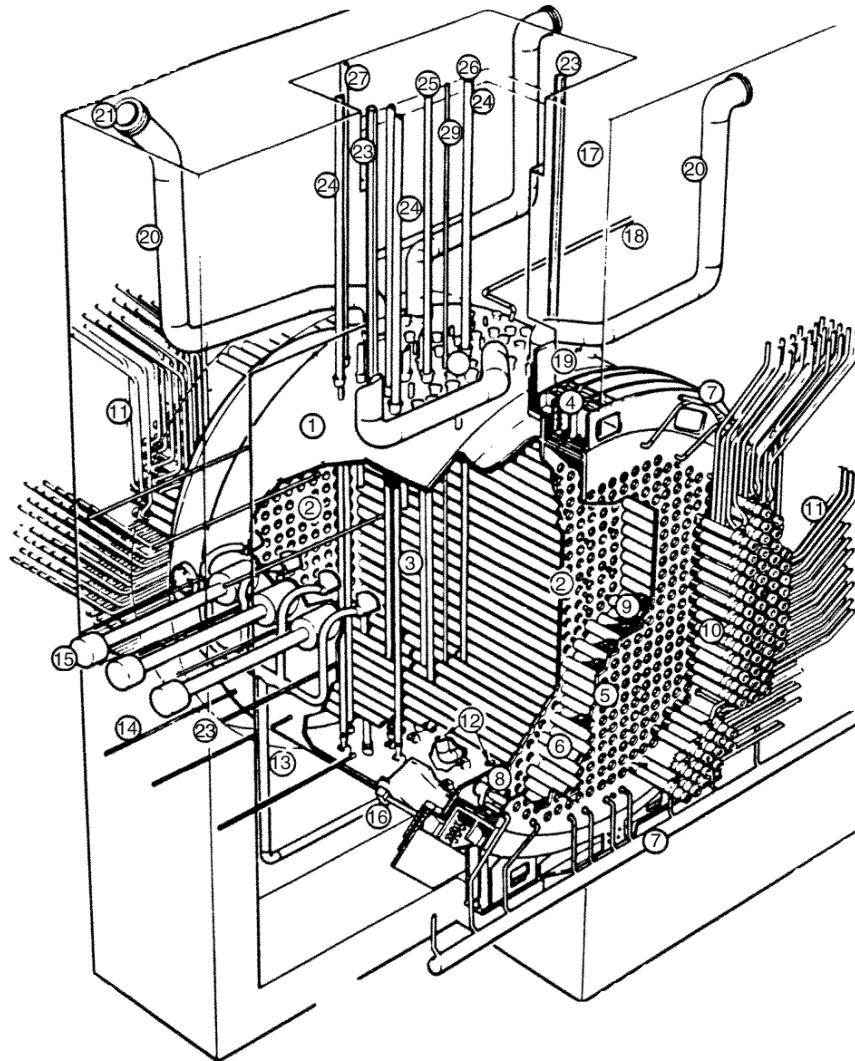
1	Calandria	16	Earthquake Restraint
2	Calandria - Side Tubesheet	17	Calandria Vault Wall
3	Calandria Tubes	18	Moderator Expansion to Heat Tank
4	Embedment Ring	19	Curtain Sheilding Slabs
5	Fueling Machine- Side Tubesheet	20	Pressure Relief Pipes
6	End Shield Lattice Tubes	21	Rupture Disc
7	End Shield Cooling Pipes	22	Reactivity Control Units Nozzles
8	Inlet-Outlet Strainer	23	Viewing Port
9	Steel Ball Shielding	24	Shutoff Unit
10	End Fittings	25	Adjuster Unit
11	Feeder Pipes	26	Control Absorber Unit
12	Moderator Outlet	27	Zone Control Unit
13	Moderator Inlet	28	Vertical Flux Detector Unit
14	Horizontal Flux Detector Unit	29	Liquid Injection Shutdown Nozzle
15	Ion Chamber	30	Ball Filling Pipe

The moderator and the coolant are separated in the CANDU design. It is important to note the benefits and the safety advantage of having in the reactor core a cool moderator whose temperature 70°C, is lower than the coolant temperature, 266 to 312°C, considering the following aspects:

a)   the cold moderator can act as an ultimate heat sink in the case of a loss of coolant accident and of pressure tube rupture accidents;

b)   the moderator provides cooling to the energy absorbent reactivity devices which are immersed in the moderator;

c)   the thermalization efficiency of the moderator depends on its density; a cold moderator is more efficient in slowing down fast neutrons.

3.3 Fuel

The CANDU fuel consists of natural uranium, which contains a fraction of 0.72 % (isotopic abundance) of isotope ^{235}U, the remaining fraction being in the form of ^{238}U. By comparison, the isotopic abundance of ^{235}U of enriched uranium used in LWR, can be increased to typically 3 % or more.

Fig. 3.3:
Basic data for CANDU fuel bundles.

Reactor	N.P.D.	N.P.D. & Douglas Pt.	
Number of Rods/Bundles	7	19	19
Rod Diameter mm	25.4	15.25	15.22

| Reactor	Pickering	Bruce & 600MW
Number of Rods/Bundles	28	37
Rod Diameter mm	15.19	13.08
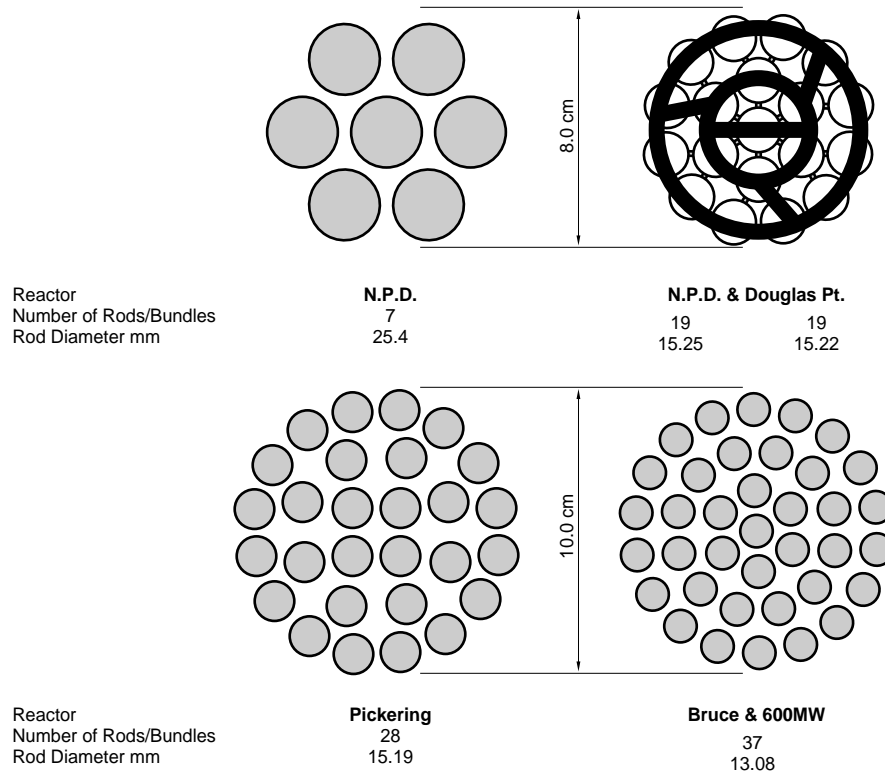
Fig. 3.4:
Schematic of a CANDU 600 fuel bundle.
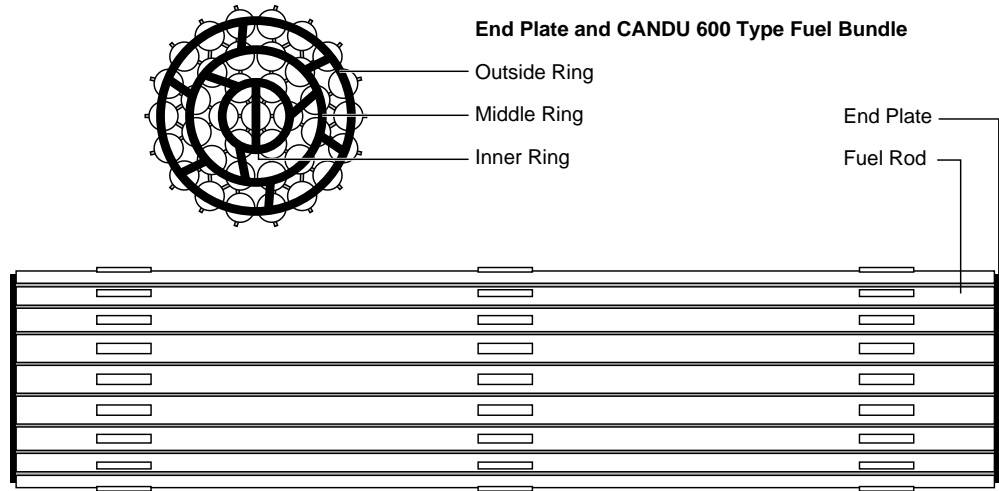
The CANDU 600 fuel assembly consists in a string of 12 fuel bundles contained in a single reactor channel. Each bundle (see Fig. 3.3 and 3.4) has a length of about 0.5 m. It consists of an assembly of 37 elements: the fuel pins (small ZIRCALOY tubes). They contain the UO_2 pellets and are welded to the end-plates of the bundle. Small skates on the surface of the tubes avoid direct contact of the fuel pins with the pressure tube walls leaving open the flow area.

3.4 Coolant

The CANDU Heat Transport circuit coolant is heavy water. It removes heat from the reactor core by circulating in the pressure tubes and cooling the fuel bundles (see Fig. 3.2). The typical variation of coolant temperature is from 266°C at the channel inlet and 312°C at the channel outlet.

Even if the Heat Transport coolant is physically separated from the moderator it also consists of heavy water in order to maintain the neutron economy performance which depends strongly on the thermalisation efficiency of heavy water. The primary heat transport system heavy water coolant inventory is around 150 tons.

3.5 Heat Transport circuit and reactor channel

The CANDU 600 Heat Transport circuit contains 380 reactor channels (see Fig. 3.1) which are distributed in four groups of 95 pressure tubes. Each group of channels is connected to respective inlet and outlet headers via individual feeder pipes. The core is cooled by two distinct circuits, each one including two main coolant pumps and two steam generators. Each circuit is designed as a figure of 8 loop with two reactor passes containing 95 channels per pass (see Fig. 3.5).

Fig. 3.5: CANDU
reactor simplified flow diagram.

Steam pipes

Steam generators

Heat transport pumps

Pressurizer

Bleed Condenser

Heat transport headers

Heat transport headers

Feed

Calandria

Fuel   Reactor

Natural steam water

Natural water condensate

Heavy water coolant

Heavy water moderator

Moderator pump

Moderator heat exchanger
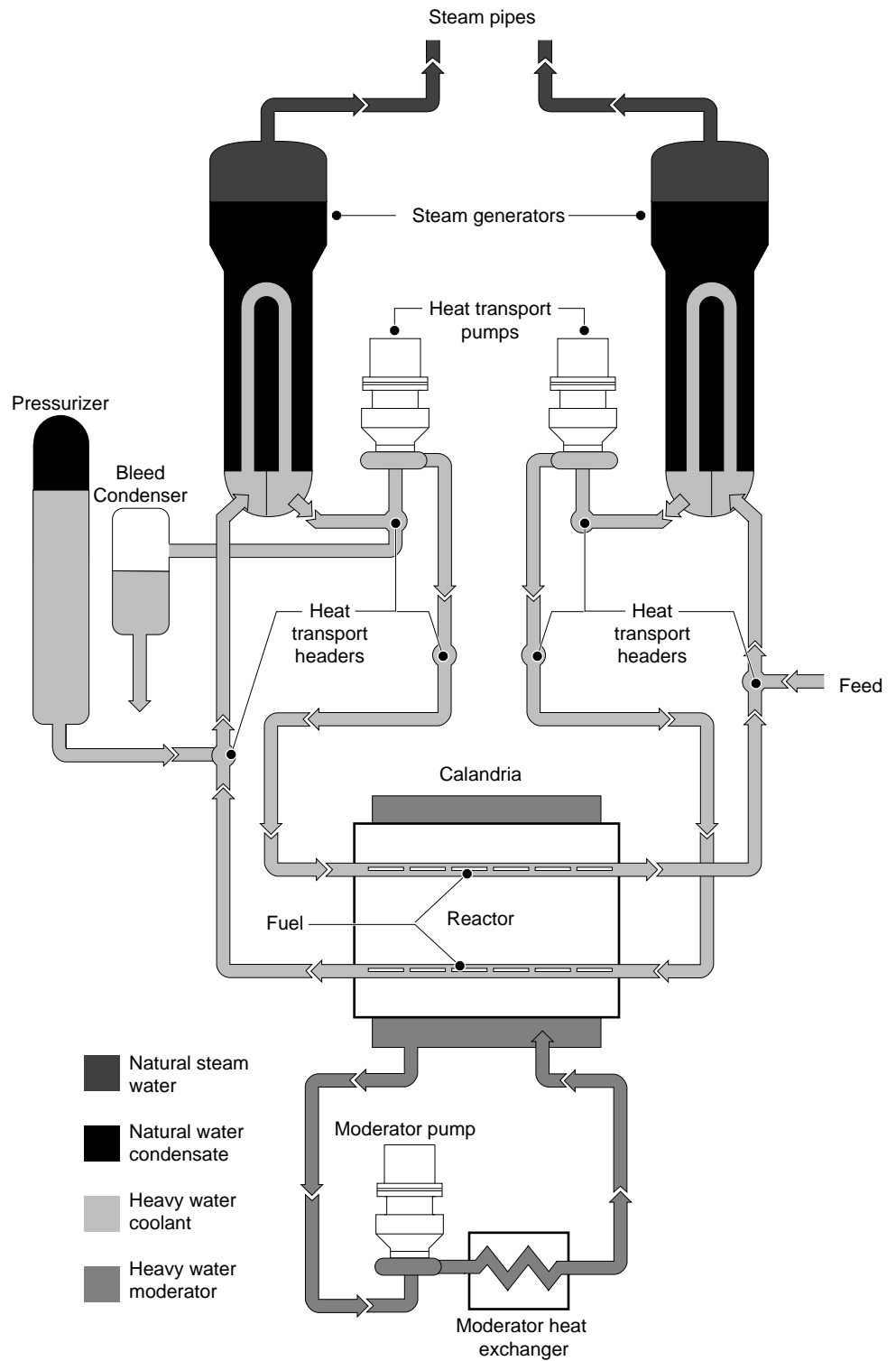
The coolant leaving the reactor core with a coolant flow of 1900 kg/s per pass (CANDU 600) can contain a large void fraction due to boiling at the exit of the channels (see Table 3.1).

Table 3.1:
Coolant conditions and fuel hydraulic data.

1.0	**Coolant Conditions at Full Reactor Power**	
Coolant		D_2O
Coolant chemistry		pD 9.5 to 10.5 by LioH
Coolant temperature - at inlet bundle - at outlet bundle		266 °C 312 °C
Coolant pressure in outer core region - at inlet bundle - at outlet bundle		11.1 MPa 10.3 MPa
Range of time-averaged steam qualities at end of fuel string		0.5 to 4.7%
Range of time-averaged channel flows		10.4 to 26.7 kg/s
Average channel midplane coolant density		800 kg/m^3
Range of channel midplane coolant velocities		4.1 to 10.5 m/s
Coolant viscosity		10^{-4} kg/m.s
Range of Reynolds numbers		2.3×10^5 to 5.8×10^5

2.0	**Fuel String Hydraulic Data for Reference Conditions :**	Channel flow = 23.9 Coolant density = 800 kg/m^3 (single phase)
Maximum pressure drop (with all bundle junctions misaligned at 12° for outer elements)		730 kPa
Most probable pressure drop (due to random bundle loading)		679 kPa

The CANDU reactor channel consists in a pressure tube holding the fuel assembly in the neutron flux of the reactor core. The typical coolant pressure drop across the fuel string is about 800 kPa (see Table 3.1). The pressure tube material is a strong alloy of zirconium. The pressure tube is surrounded by the calandria tube which is in contact with the moderator (see Fig. 3.6).

Fig. 3.6:
End-fitting assembly, calandria and pressure tubes.
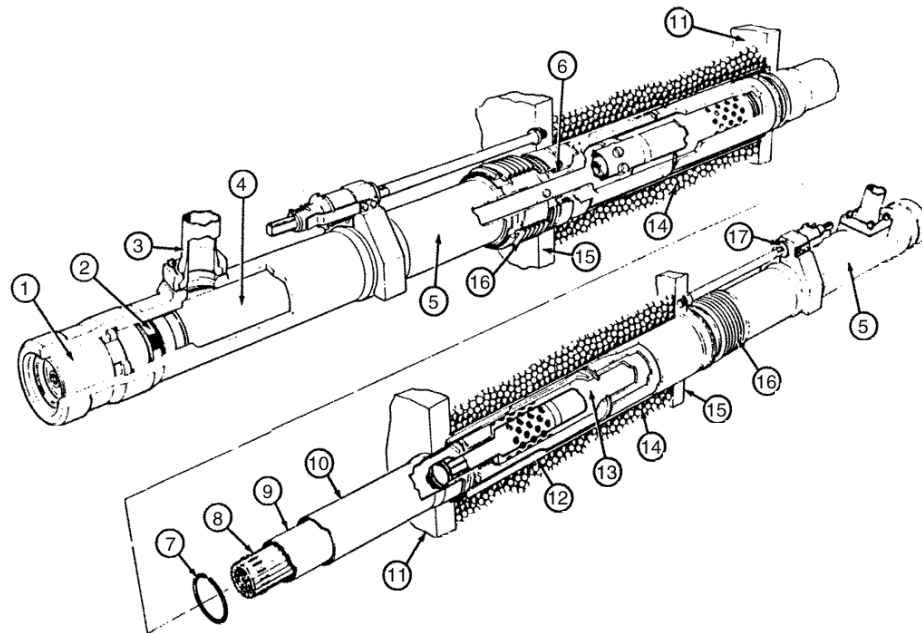
1	Channel Closure	10	Calandria Tube
2	Closure Seal Insert	11	Calandria Side Tube Sheet
3	Feeder Coupling	12	End Shield Lattice Tube
4	Liner Tube	13	Sheild Plug
5	End Fitting Body	14	End Shield Shielding Balis
6	End Fitting Bearing	15	Fuelling Machine Side Tube Sheets
7	Tube Spacer	16	Channel Annulus Bellows
8	Fuel Bundle	17	Channel Positioning Assembly
9	Pressure		

The gas in the annular space between the tubes is monitored for detection of any pressure tube leak. The end-fitting and feeder pipe geometry of a reactor channel is specially designed for the purpose of channel refuelling (see Fig. 3.7). At the beginning of the refuelling sequence, the channel closure and the shield plugs are removed to allow the insertion and removal of fuel bundles.

Fig. 3.7:
End-fitting assembly and reactor channel inlet side during refuelling.

December 1995
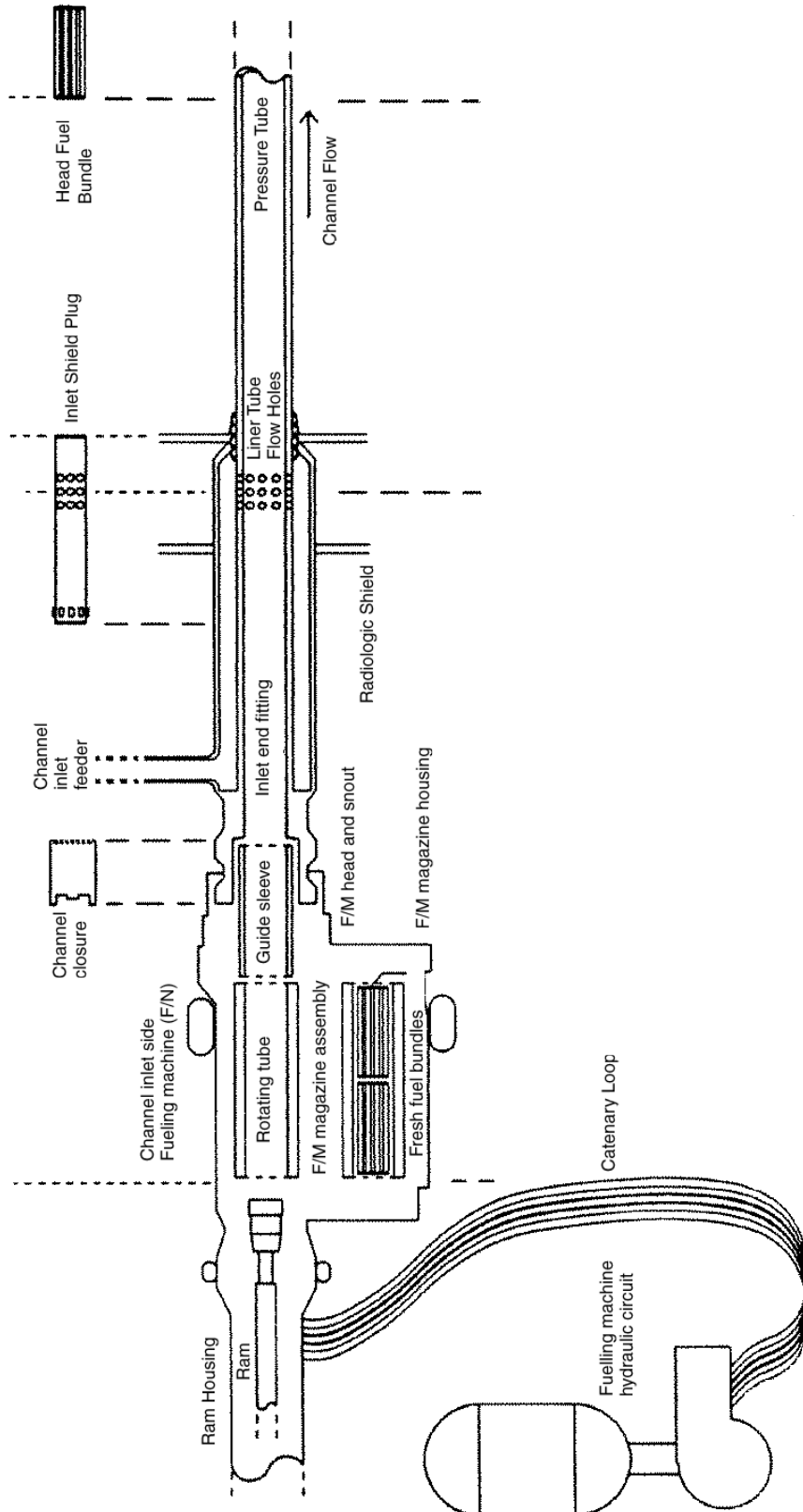
3.6 Reactor core dimension

The reactor core overall dimension is a function of the lattice pitch, the reflector thickness and the total power desired. The CANDU lattice pitch ($\approx$ 28.6 cm) is slightly below the lattice reactivity maximum (see Fig. 3.8). A smaller lattice pitch would require smaller moderator volume compensated by more frequent refuelling. Larger lattice pitch would require a higher moderator volume with less frequent refuelling. The reflector thickness of about 70 cm is close to optimum for most CANDUs.

Fig. 3.8:
Variation of reactivity with lattice pitch for the CANDU-PHW lattice.
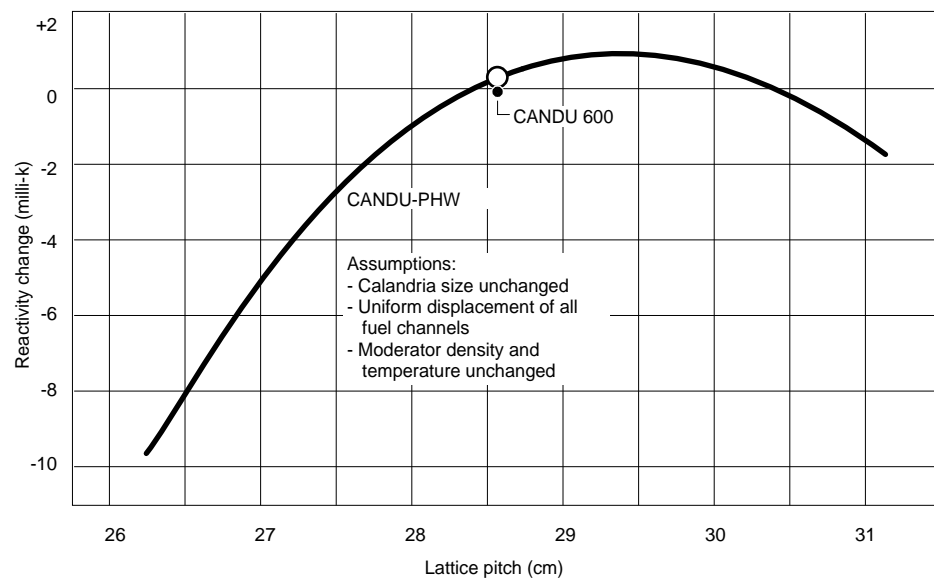
3.7 Secondary side

The secondary side of a CANDU reactor follows almost the same design as any other PWR reactor. It uses light water as coolant in the liquid-vapour cycle. The circuit starts at the upper part of the four steam generators which are connected to a steam main header (see Fig. 3.9). Atmospheric steam discharge valves allow rapid blowdown and cooling of the secondary side. Through the governor valve, the steam main feeds the low and high pressure stages of the turbine. The turbine is connected to the condenser where liquid water is recovered. Through the feedwater pumps and control valves, the cold water is then supplied to the preheater (lower part) of the four steam generators.

Fig. 3.9:
CANDU nuclear power system: secondary side.
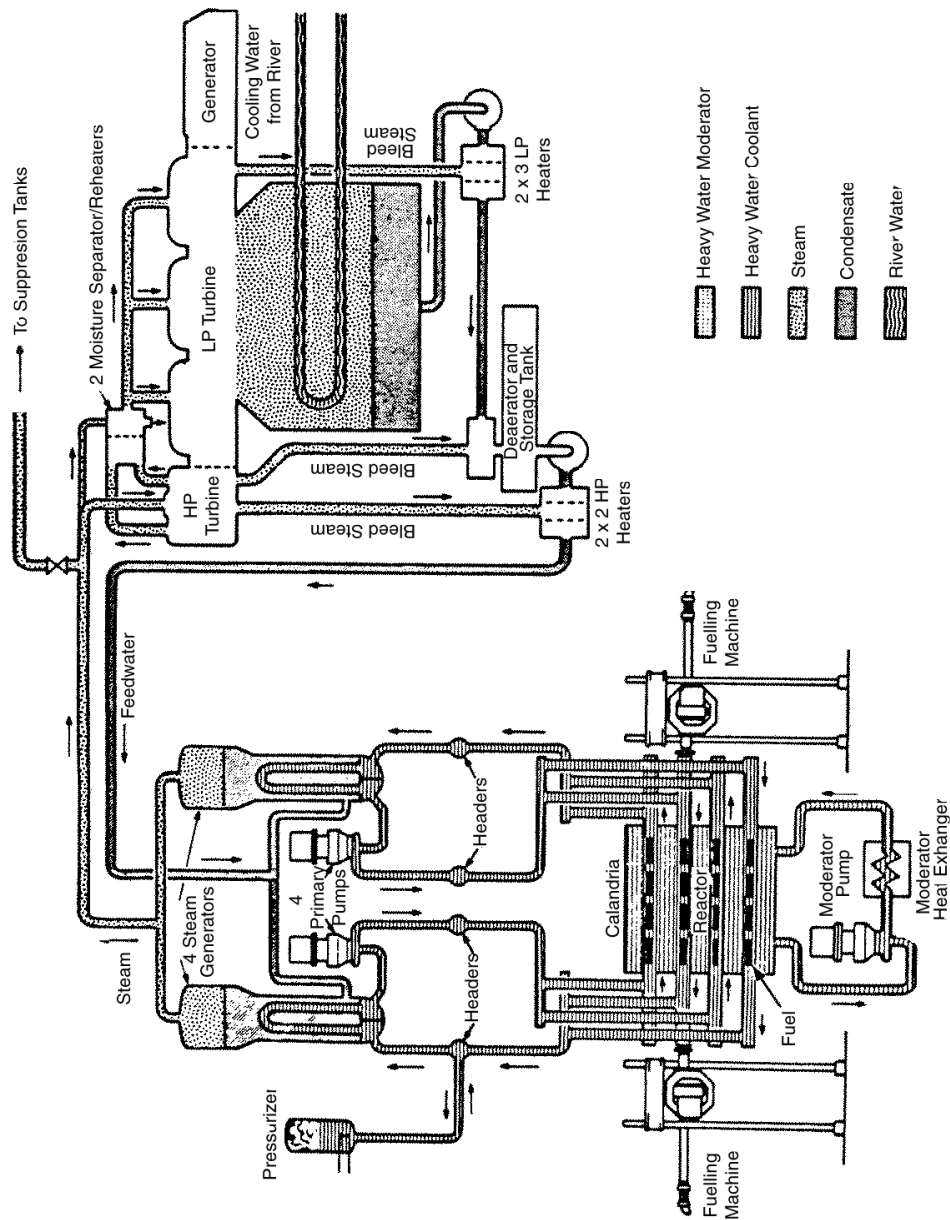
4 CANDU Primary Circuit Heat Balance

4.1 Single phase flow heat balance

Suppose that a nuclear reactor operates without producing steam in the primary circuit. The heat removal power P for the 4 reactor passes depends only on the coolant temperature and is expressed as:

$$P = 4 \ w \ C_p \ \Delta T$$

where:

w is the coolant flow per pass (typical value: w = 1900 kg/s for the CANDU 600),

C_p is the liquid coolant (heavy water) specific heat capacity (C_p = 4.3 kJ/kg/°C),

ΔT is the temperature increase for the coolant passing through the reactor core.

For a temperature increase of 46°C and a coolant flow w = 1900 kg/s (identical in the 4 reactor passes), we calculate the following heat removal power P:

P = 4 (1900) kg/s 4.3 (46) kJ/kg = 1500 MW

4.2 Two phase flow heat balance

4.2.1 Theory

At the channel exit of many CANDU reactors a small amount of vapour is produced (see Table 3.1). It is very efficient for heat removal in the reactor core and energy transport in the primary circuit.

In the presence of a steam quality x (see below) the heat removal power P (for the 4 reactor passes) is expressed by:

$P = 4 \ w \ \Delta h$

$\Delta h = h_{out} - h_{in}$

where the variation of enthalpy h represents the free energy transported per unit of mass of coolant. The calculation requires to establish the outlet to inlet enthalpy balance Δh using the enthalpy of saturated liquid water h_f and the water vapour latent heat of vaporisation h_g which are a function of pressure:

$h = (1 - x) h_f + x h_g$

$x = \dfrac{m_g}{m_g + m_f}$

where the steam quality x is the ratio between the mass of steam m_g and the total mass of water $m_g + m_f$.

4.2.2 Example: application to CANDU 600

Considering the fact that the coolant temperature varies from T_{in} = 266°C to T_{out} = 312°C (see Table 3.1), a thermodynamic table gives the corresponding enthalpies for liquid water and water vapour:

w = 1900 kg/s
h_{in} = 1165 kJ/kg
h_f = 1413 kJ/kg
h_g = 2725 kJ/kg
x = 4 %

and we obtain for the enthalpy variation:
h_{out} = [(1-.04)1413 + (.04)2725] kJ/kg = 1465 kJ/kg

$\Delta h = h_{out} - h_{in}$ = [1465 - 1165] kJ/kg = 300 kJ/kg
Therefore the total power is:
P = 4 (1900) 300 kJ/s = 2280 MW

4.2.3 Boiling consequences

Heat removal by boiling is very efficient since going from a single phase flow to a two phase flow leads to a power increase of 2280 - 1500 = 780 MW which is due to a small (4 %) quality at the channel exit plane. More than 30 % of the heat can be transported by the vapour.

However, too much boiling in reactor channels should be avoided:
1)   too much water vapour may seriously degrade the heat transfer between the fuel and the coolant leading to **Dryout** and eventually overheating of the fuel pins;
2)   a **Power Excursion** may result from a sudden boiling increase due to an immediate addition of positive reactivity (as expressed by the positive void reactivity coefficient) and the resulting prompt jump of neutronic power;
3)   a high void fraction may lead to **Flow Instabilities** and reactor power control difficulties.

In fact, the onset of intermittent boiling provides a design limit and a safety criterion for the reactor thermal-hydraulic behaviours.

5 CANDU Operational Design

5.1 Core equilibrium

Reliable power production requires an adequate fuel management and a monitoring of the irradiation distribution in the reactor core. The CANDU reactor operational design and its on-line fuelling strategy are such that a core equilibrium is achieved and maintained in time.

5.1.1 Average and exit irradiations
Average Irradiation and k_∞: the average in-core irradiation is 0.8 n/kb. Reactivity is high in the fresh fuel-cell and remains positive up to an irradiation of 1.6 n/kb (see Fig. 5.1). Due to refuelling, neutron flux and thus irradiation vary with position in the reactor core. However the core must achieve criticality with a keff equal to 1. Allowing 30 milli-k for leakage effects and about 22 milli-k for reactivity devices and in-core material not accounted in the basic cell, k_∞ must be approximately 1.052.

Fig. 5.1:
Reactivity of 37-element natural fuel: versus irradiation.
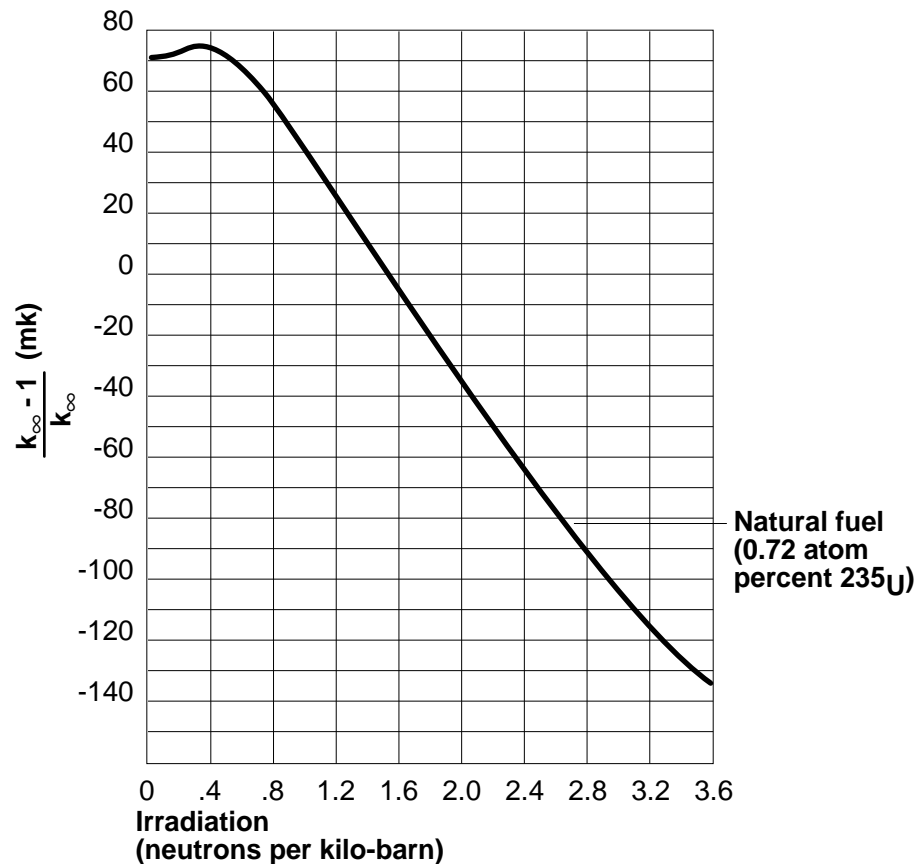
The **Exit Irradiation** of the fuel is about 1.6 n/kb or roughly the double of the in-core average of 0.8 n/kb.

5.1.2 Refuelling and fuel burnup

Refuelling: fuel management establishes the selection of channels to be refuelled in a given day. In a standard CANDU 600, about two channels are refuelled, via an 8-bundle shift (insertion of 8 fresh fuel bundles, see Table 5.1), per full power day of operation.

Table 5.1:

CANDU 600: fuelling and physics data for the reference eight bundles shift.

Estimated fuel position dwell times (time-averaged values)*	
- Maximum (central 124 channels)	160 FPD
- Average (central 124 channels)	150 FPD
- Maximum (outer 256 channels)	300 FPD
- Average (outer 256 channels)	180 FPD
Estimated fuel residence times (time-averaged values)*	
- Maximum (central 124 channels)	320 FPD
- Average (central 124 channels)	225 FPD
- Maximum (outer 256 channels)	600 FPD
- Average (outer 256 channels)	270 FPD
Average number of new bundles loaded per day* (equilibrium refuelling)	
- 80% capacity	14.5 bundles/day
- 100% capacity	18.1 bundles/day
Estimated fuel discharge burnup*	
- Maximum	290 MWh/kgU
- Average	156 MWh/kgU
Bundle sliding distance in channel (including back and forth movements)	
- on pressure tube	15.7 m
- on liner tube	6.7 m
Fuelling times (typical for normal operation)	
- Fuelling machine on channel	60 minutes
- Fuel shifting movements in channel (total)	30 minutes
- Irradiated fuel in fuelling machine (minimum cooling time in D_2O)	30 minutes
- Irradiated fuel transfer time in air	2 minutes
Bundle sliding speed in channel	
- typical	0.015 m/s
- Maximum possible from fuelling machine ram	0.050 m/s

* Since these values are based on physics simulations of an equilibrium core in idealized conditions, the actual maximum values in the operating reactor may be up to 50% higher.

The channel "dwell-time" is in the range 150-200 full power days. Four distinct phases occur during refuelling (see Fig. 5.2): the channel opening to the fuelling machines (C1), the shield plugs removal (C2), the insertion of four pair of fresh fuel bundles (C3) and the removal of irradiated bundles (C4). Figure 5.2 illustrates the successive steps of the flow assisted fuelling (FAF) sequence.

Fig. 5.2:
CANDU 600: phases of flow assisted fuelling sequence.
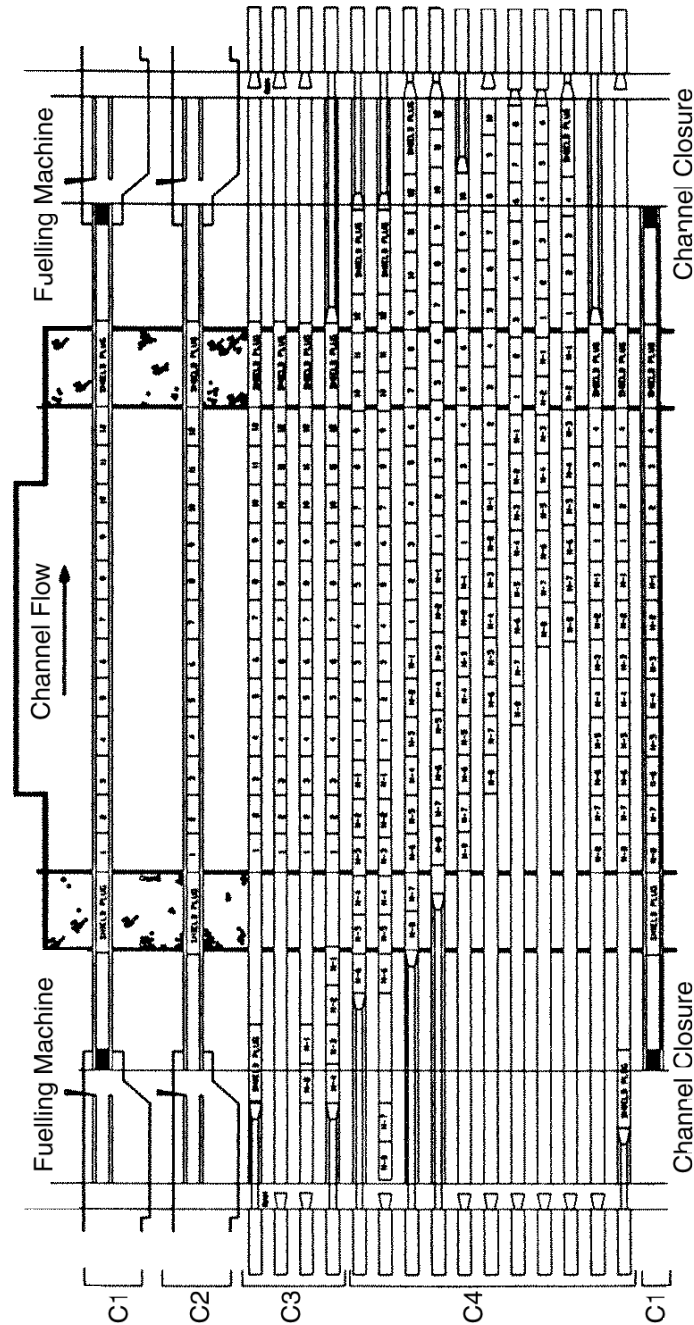
The **Fuel Burnup** is a monotonic, nearly linear function of irradiation (see Fig. 5.3). Typically for CANDU 600, the discharge burnup is about 168 MWh/kg(U). The fuel in-core residence time, the bundle geometry, the reactor core material and the moderator purity affect fuel burnup.

Fig. 5.3:
CANDU fuel burnup as a function of irradiation.

FUEL BURNUP AS A FUNCTION OF IRRADIATION
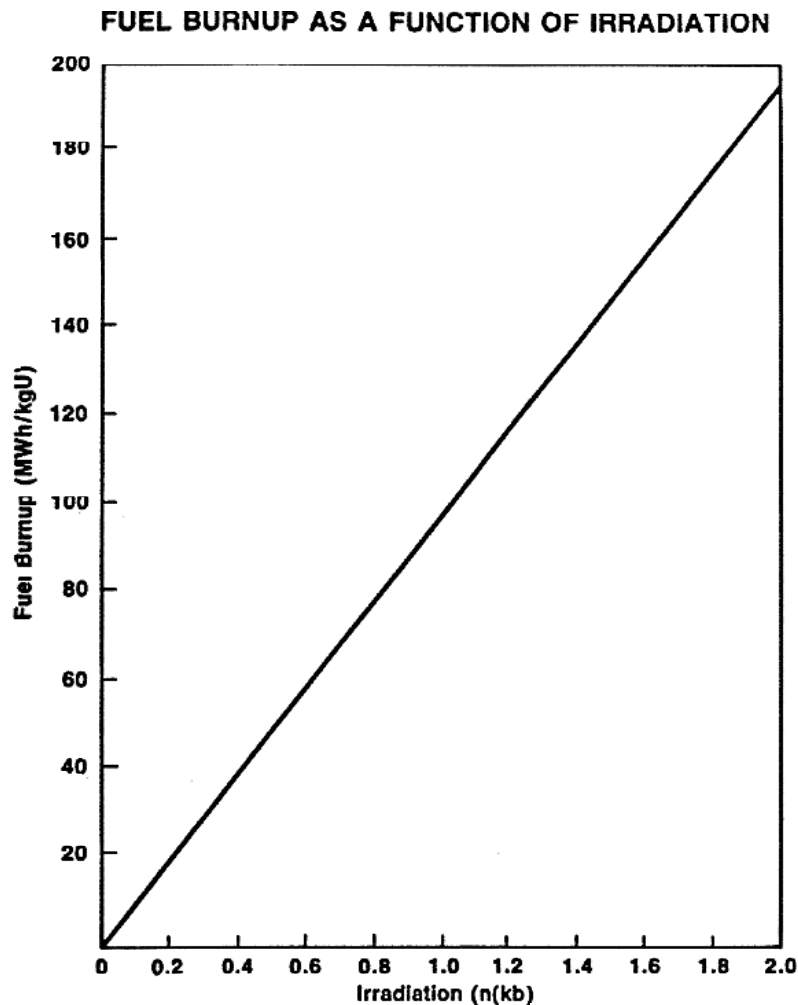
5.2 Power limits and reactor control

Upper **Power Limits** for channels and fuel bundles must be met during the operation of a nuclear reactor (license conditions). For a CANDU 600 reactor using the 37-element fuel bundle, the maximum bundle power is 935 kW. The reference overpower values are given in table 5.2 (for CANDU 600). The maximum channel power is 7.3 MW. The channel power limit is designed to avoid dryout in most accidents while the fuel bundle limit is designed to minimise fission product releases to the environment in case of a fuel element rupture.

Table 5.2:

CANDU 600: thermal performance data.

Number of bundles per channel	12
Number of bundles in core	12 x 380 = 4560
Total Fission power	2180 MW
Average bundle power	451 kW
Nominal design bundle power (peak)	800 kW
Reference overpower bundle power (peak)	900 kW
Reference overpower linear bundle power*	1875 kW/m
Reference over power linear element power*	
- outer ring	57.2 kW/m
- intermediate ring	46.7 kW/m
- inner ring	40.8 kW/m
- centre	38.6 kW/m
Reference overpower surface heat flux*	
- outer ring	1390 kW/m^2
- intermediate ring	1140 kW/m^2
- inner ring	990 kW/m^2
- centre	940 kW/m^2
Reference overpower outer element sheath temperature*	330°C
Reference overpower outer element centre-line UO$_2$ temperature*	1800°C
Ratio of maximum/average element heat flux in bundle (radial)	1.131

* Corresponding to a 900 kW bundle power with an irradiation of 0.4 n/kb.

5.2.1 Reactivity regulation

Reactivity regulation: neutronic power has to be controlled locally and globally in order to maintain the power below the prescribed safety limits, to avoid spurious transients and to ensure a rapid reactor shutdown. In the CANDU 600 operational design (see Table 4.1 of Lesson II) , the main reactivity devices used to control the power are:

ZCU
14 light water filled *zone controller units* (ZCU) allow the adjustment of zonal power. They prevent xenon induced oscillations and other neutron flux instabilities (see Fig. 5.4 a, b and d);

ADJ
21 mechanical *adjusters* (ADJ) are normally inserted to flatten the power distribution (see Fig. 5.4 c and d). Their extraction provide extra reactivity margin to avoid xenon poisoning and enable continuous power operation without refuelling for a certain time (up to three weeks);

MCA
4 *mechanical control adjusters* (MCA)to allow fast reduction of reactor power (stepback) or negative reactivity addition (see Fig. 5.4 d);

BOR / GAD

moderator poison injection and removal to control the criticality approach at startup or the guaranteed shutdown state (see Fig. 5.4 e).

Fig. 5.4a:
*Location of horizontal and vertical reactivity devices.*

NOTES:
1 FACE VIEW FROM PRESSURIZER END. ZONES AND ZONE CONTROLLERS AT OTHER END (AWAY FROM PRESSURIZER) ARE GIVEN IN BRACKETS.
2 ZONE CONTROL DETECTORS ARE 3 LATTICE PITCHES LONG AND LOCATED IN VFDAs 1, 2, 3 AND 24, 25, 26 AXIALLY OUTBOARD FROM THE ZCUs.
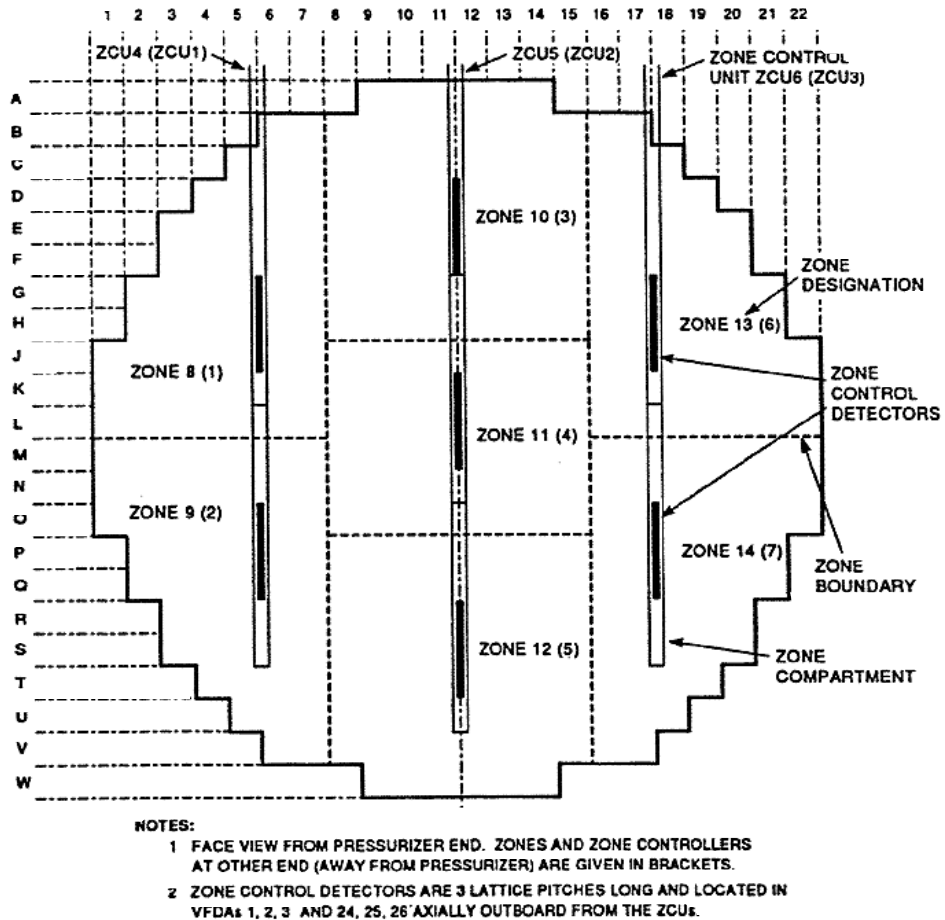
Fig. 5.4b:
*Relation of Zone Control Units*
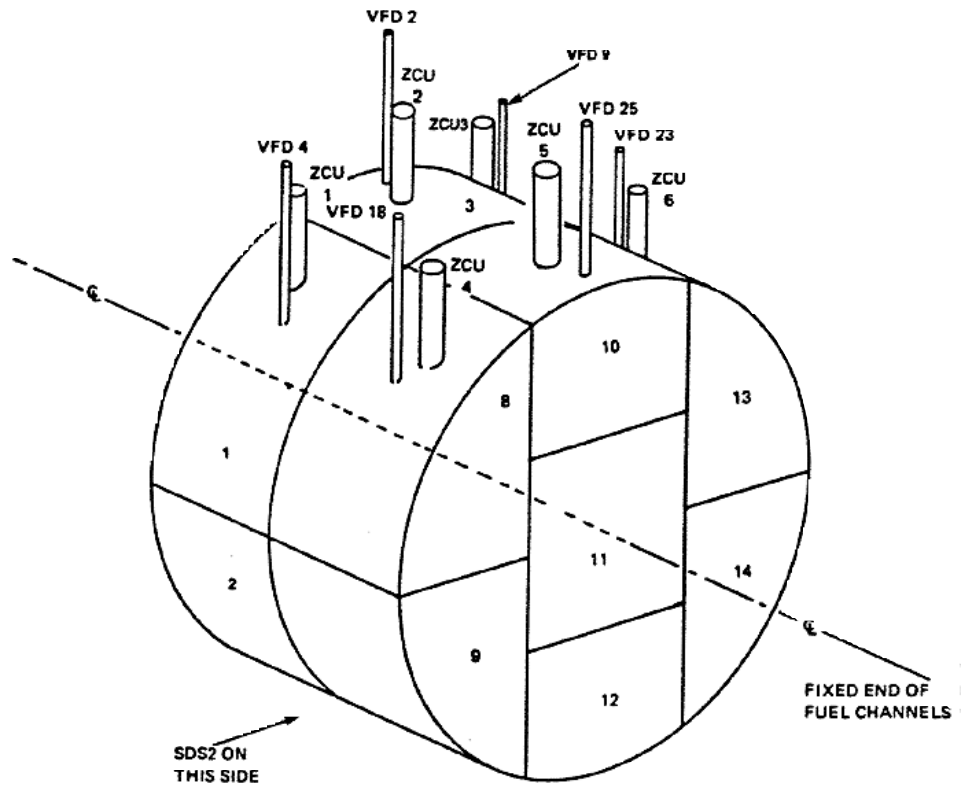
Fig. 5.4c:

*Face view of reactor model*
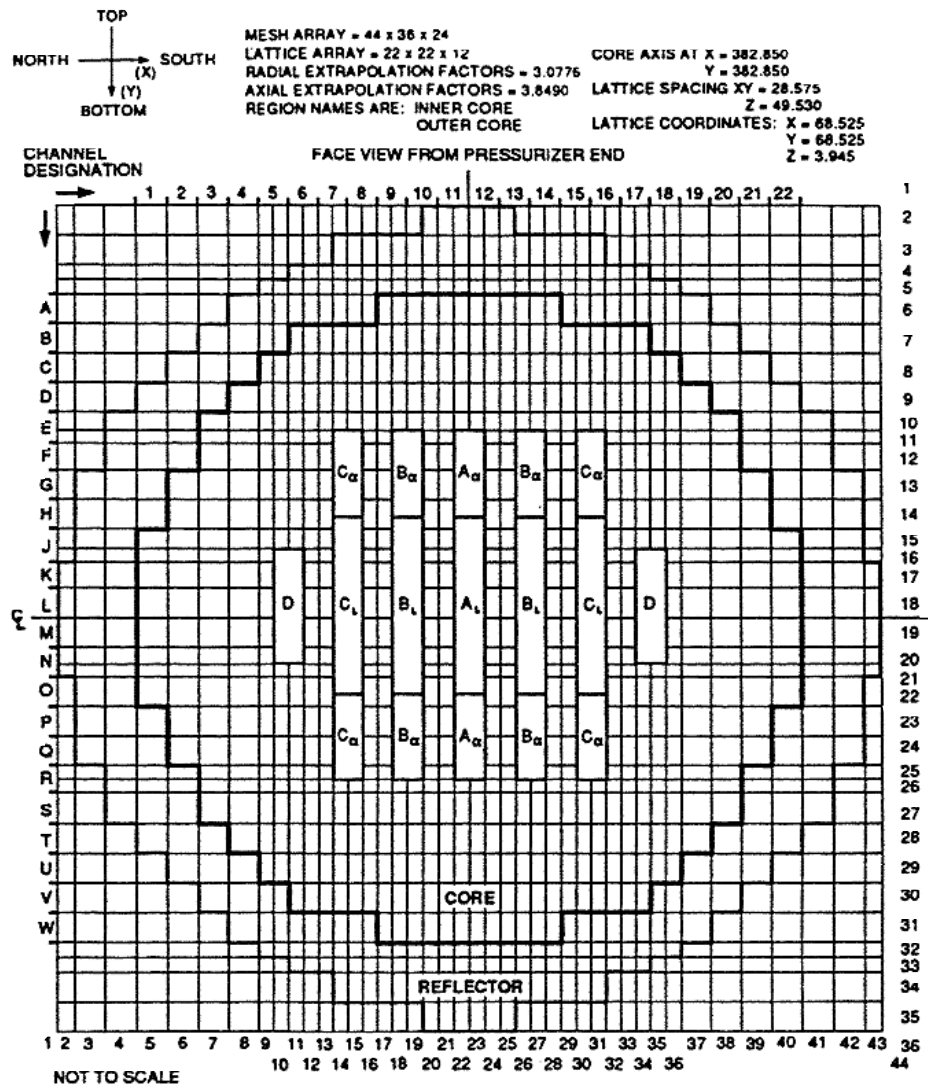
Fig. 5.4d:
*Location of reactivity devices*
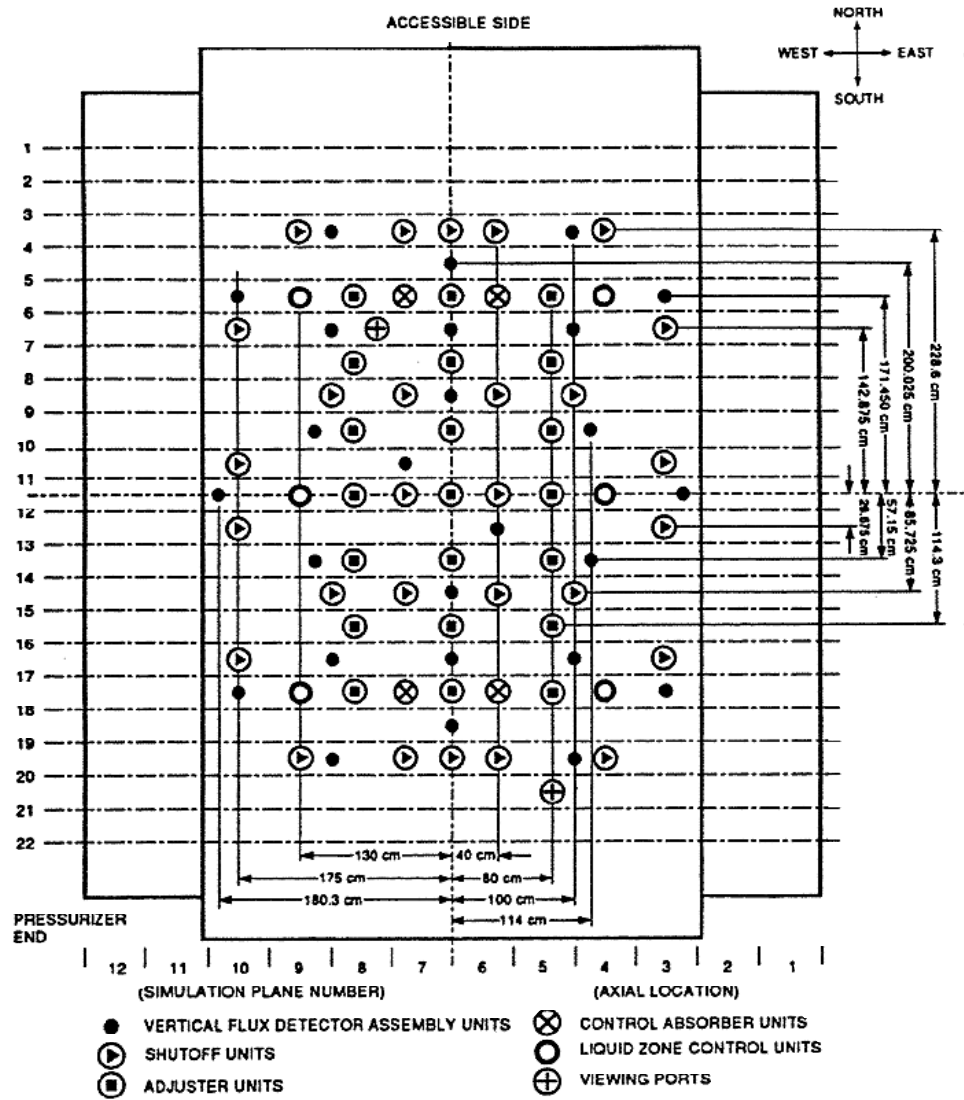
Fig. 5.4e:
Location of horizontal devices
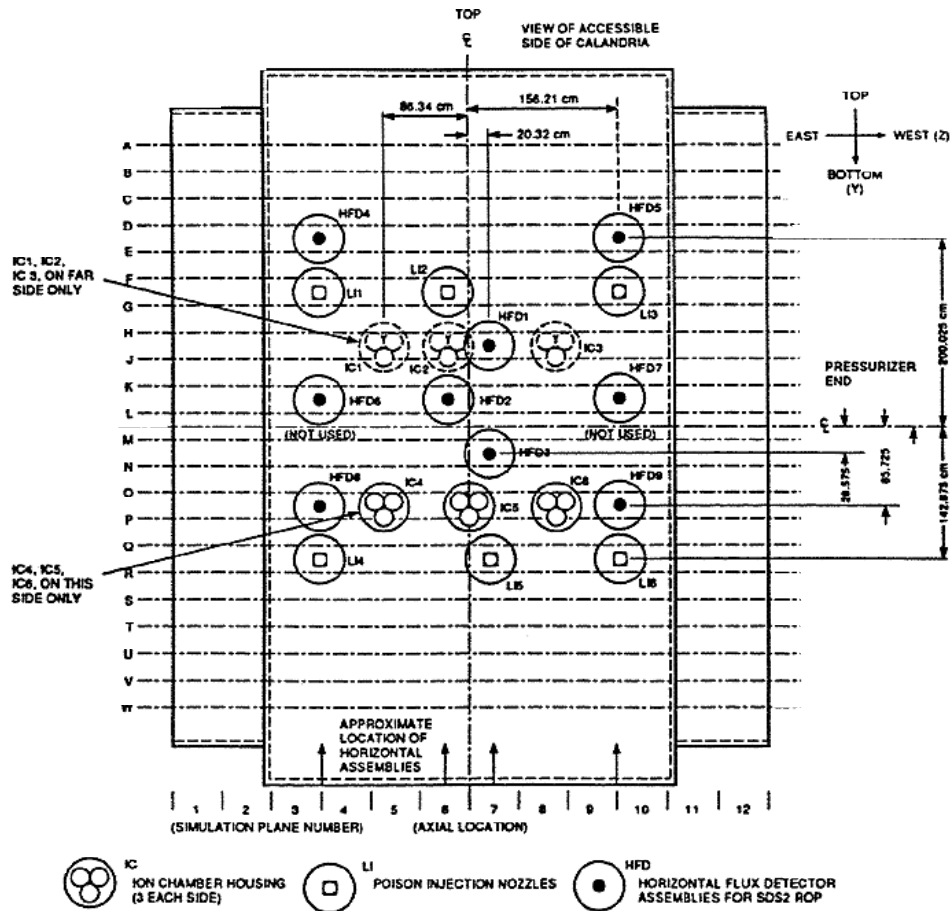
5.2.2 Overall plant control

The overall plant control block diagram is given in Figure 5.5. Two control modes are used in a CANDU 600 reactor:

Normal mode:

the reactor flux control unit controls the power of the plant via a neutronic power setpoint;

Alternate mode:

the unit power regulator (turbine load control) controls the power of the plant via an electrical output setpoint.

Fig. 5.5:
*Overall plant control block diagram reactivity devices.*
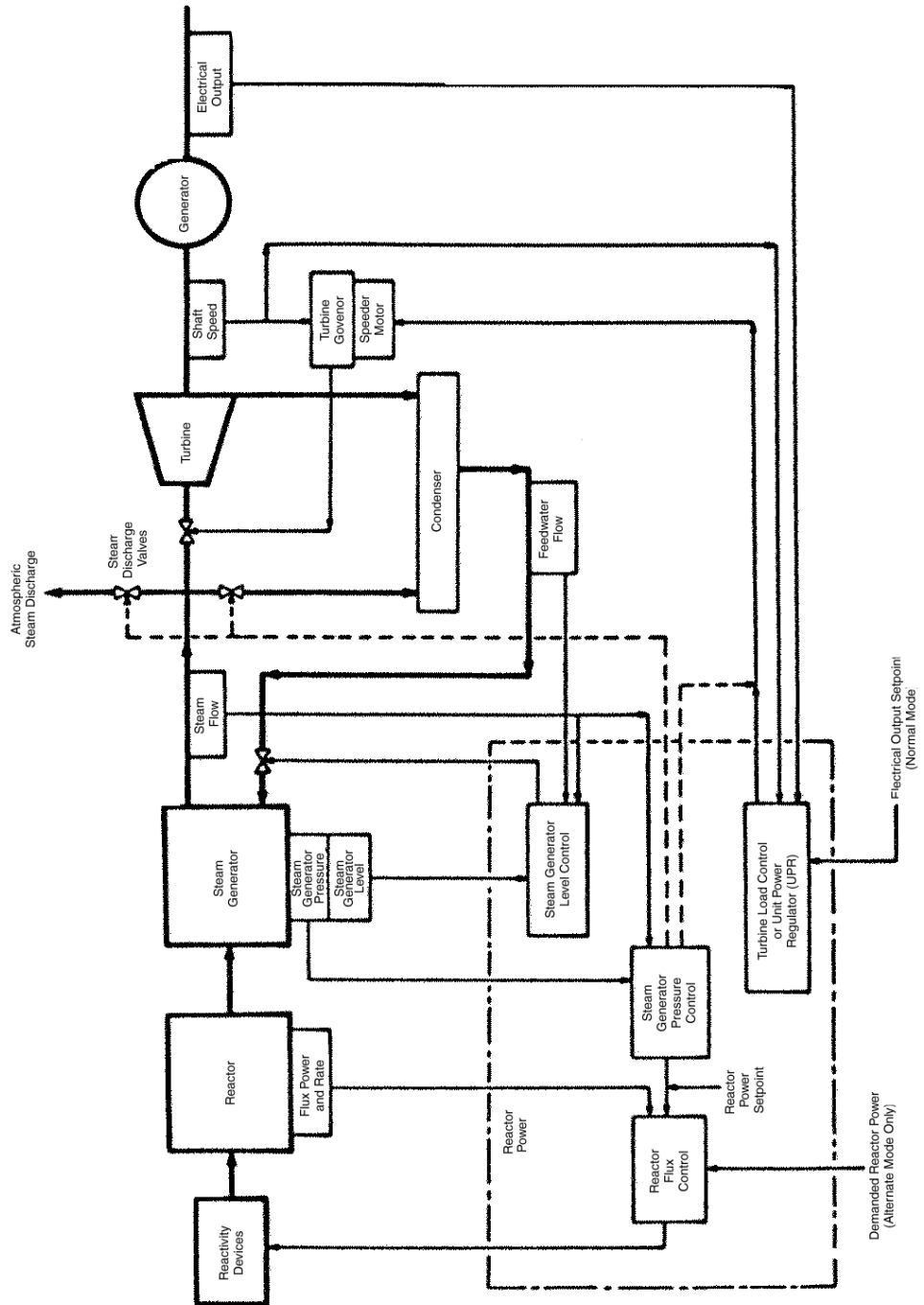
Figure 5.6 gives the names of the different program units which control the reactor power and the generator power. Other control units are also indicated like: pressurizer and heater control (HT), feedwater control (secondary side), boiler level control (secondary side), pressure control (secondary side), etc.

Fig. 5.6:
CANDU 600: unit control.
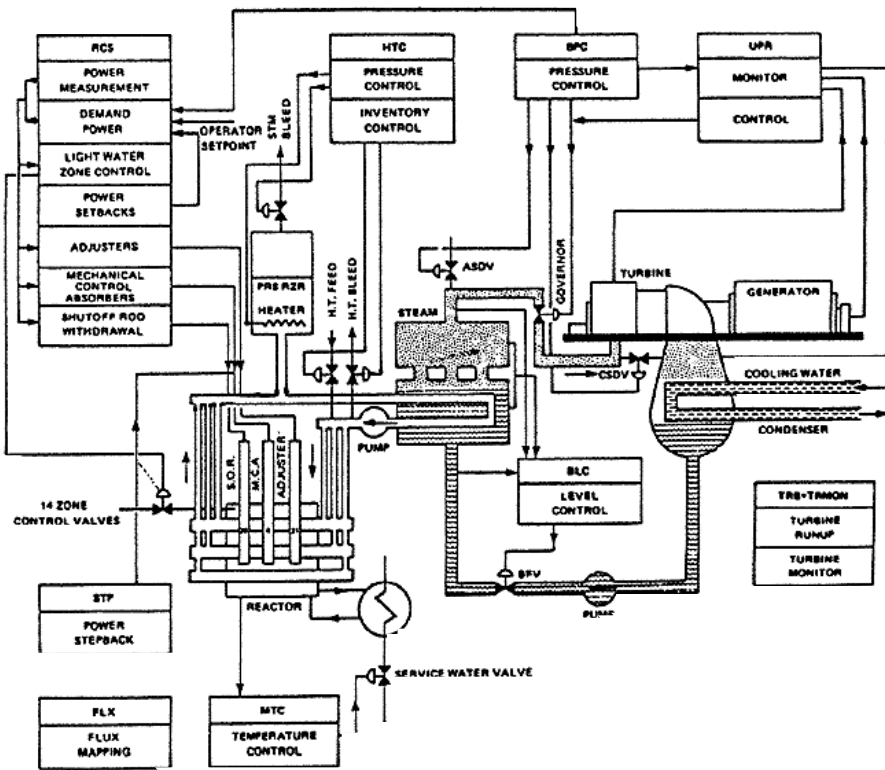
Reactivity Effects In Candu

Training Objectives

The participant will be able to describe or understand:
1   neutron flux fluctuations during reactor operations and
    the reactor reactivity control;
2   the distinction between static reactivity and dynamic reactivity;
3   the local core parameters affecting the reactivity in a CANDU;
4   the definition of a reactivity coefficient;
5   the temperature reactivity coefficients: fuel, coolant and moderator;
6   the void reactivity coefficient;
7   other reactivity effects and safety implications.

Reactivity Effects In Candu

Table of Contents

1 Introduction

To ensure power production in a controllable and stable nuclear reactor, the reactor regulation must control the production and the loss of neutrons. The following balance

$$\begin{bmatrix} \text{net gain} \\ \text{of neutrons} \end{bmatrix} = \begin{bmatrix} \text{production of neutrons} \\ \text{by fission} \end{bmatrix} - \begin{bmatrix} \text{loss of neutrons by} \\ \text{leakage and absorption} \end{bmatrix}$$

should be controlled within precise operation margins to allow safe power manoeuvres. And at a constant power, the regulation system should maintain on average the steady-state critical balance:

Production = absorption + leakage

The production and loss of neutrons are directed by complex physical phenomena. The sources and sinks of neutrons in the reactor core can obey various transient evolutions having different time scales and showing different dynamic characteristics. At all time and in all conditions, the reactor power should be controlled by the regulation and/or shutdown systems.

In the present lesson we are interested in the transient phenomena which perturb the neutronic balance. Since the equilibrium between sources and sinks is lost, the multiplicative constant differs from unity and a reactivity transient is associated. The phenomena under consideration consist in variations of core structures (reactivity device position for instance) or local core parameters (coolant density, fuel temperature, moderator poison, etc.). Their associated *reactivity effects* should be understood and are presented in this lesson. We will discuss in details the most relevant reactivity effects for the CANDU reactor technology.

2 Neutron Flux Fluctuations and Reactor Control

First, we must understand the reasons why neutron flux variations occur during normal reactor operations, then see if these variations are nuclear technology (CANDU, LWR, etc.) dependent.

2.1   Reactor control by reactivity

The average neutron flux varies in the reactor core according to the variations of the effective multiplication factor k_{eff}. If the reactor power is held constant, the *average* neutron flux does not vary in time but different phenomena may force the neutron flux to fluctuate momentarily either locally in various regions within the core or globally over the whole core.

To illustrate this, one has to look at the basic rule of reactor power control which

is called *control by reactivity*. The reactivity mechanisms of the reactor are allowed to move in order that the measured reactor power follows a given power setpoint. In general, a constant reactor setpoint does not mean a steady state of the reactor neutronics. In fact, the neutron flux distribution may vary in time and the reactivity mechanisms are moved to compensate for these variations.

In general there is a power offset called the *power error* which is monitored and evaluated as the difference between the measured power and the power setpoint. Different actions are taken by the regulation system depending on the magnitude and the sign of the power error. When a fluctuation develops in the neutron flux distribution, the associated characteristic behaviour will be an increasing and/or oscillating power error.

The goals of regulation are to keep the power error as small as possible and to react promptly in case the measured power exceeds the power setpoint. In the case of the CANDU reactor, the power distribution is controlled spatially by the automatic adjustments of the water levels in the 14 vertical assemblies of the liquid zone controllers. The levels are moved to compensate the power fluctuations in the corresponding 14 reactor zones (see figure 2.1). If a sudden insertion of negative reactivity is required the regulation system will automatically initiate a power stepback (vertical absorbing rods falling in the reactor core). During the abnormal situation referred to as *slow loss of regulation* the oscillations of the power error may develop and become important enough to require shutdown.

2.2 Causes of neutron flux variations

The local conditions for neutron multiplication varies in the fissile material as a function of the history of the material in the core. For instance, the fuel isotopic composition changes as the fuel burnup increases with fission. This results in a reactivity decrease in time. The burnup distribution is proportional to the neutron flux, following then a cosine profile in the axial direction. Therefore the reactivity decrease is not distributed evenly in the core. Sporadic fluctuations of the neutron flux distributions do occur in the reactor before being homogenized by diffusion.

Shortly after a power transient, the fission products are not at equilibrium concentrations and their specific dynamics may induce reactivity oscillations. In the specific case of xenon, the amplitude of the reactivity fluctuations will grow slowly (referred as xenon instabilities), leading to oscillating power tilts which may tend to diverge if they are not compensated by a local power control within the reactor regions. Reactivity loads evolution characterizes the reactivity effects in this case. Poisons like boron or gadolinium which can be present in the moderator can also perturb the core reactivity. If the reactor power varies suddenly, changes in the core reactivity will result from the temperature variation, from the density variation and from the possible apparition of void in the moderator or coolant. The temperature reactivity effects are characterized by

various coefficients:
- the fuel temperature reactivity coefficient,
- the coolant temperature reactivity coefficient, and
- the moderator temperature reactivity coefficient.

The density variation and apparition of void in the coolant is characterized by the void reactivity coefficient.

Even if the different reactor technologies share similar principles underlying nuclear power production and control, their typical reactivity coefficients may differ considerably. Table 2.2 illustrates the values of the overall core reactivity temperature coefficient for different reactor technologies. Values of Table 2.2 are given at ordinary temperatures which means that the reactivity variation is obtained by the multiplication of the coefficient by the difference between operating and ordinary temperatures. For the Shippingport PWR reactor, for instance, we obtain:

$$230°C * -5.5 \times 10^{-4} °C^{-1} = -0.127.$$

When the temperature coefficient is negative, it indicates a decrease of the reactivity with the increase of temperature. Otherwise, the reactivity would increase with an increase of temperature and may lead to instability. A negative temperature reactivity is desirable since it tends to counteract the effects of transient temperature changes.

Table 2.2:

Examples of overall reactivity coefficient of temperature for various reactor designs

Reactor Name (type)	Moderator	Coolant	T° Coef. °C^{-1}
CANDU 600 (PHWR)	Heavy water	Heavy water	-3.0×10^{-6}
Shippingport (PWR)	Water	Water	-5.5×10^{-4}
Water Boiler (BWR)	Water	Water	-3.0×10^{-4}
Brookhaven (exp. thermal reactor)	Graphite	Water	-4.0×10^{-5}
SRE (exp. thermal reactor)	Graphite	Sodium	$+1.2 \times 10^{-5}$
Calder Hall (exp. thermal reactor)	Graphite	Gas	-6.0×10^{-5}
OMRE (exp. thermal reactor)	Organic	Organic	$+3.5 \times 10^{-4}$
Argonne CP-5 (exp. thermal reactor)	Heavy water	Water	-4.0×10^{-4}
EBR-I (exp. fast breeder reactor)	None	Sodium	-3.5×10^{-5}
Enrico Fermi (exp. fast breeder reactor)	None	Sodium	-1.8×10^{-5}

3 Distinction Between Static And Dynamic Reactivity

3.1 The static reactivity

The *static reactivity* ρ_s characterizes the imbalance between neutron production (represented by the fission term **F**) and loss (represented by the absorption and leakage term **M**). It measures the departure from a steady state critical reactor:

$$\rho_s = 1 - \lambda_{(0)} = \frac{k_{eff} - 1}{k_{eff}} \text{ where } \lambda_{(0)} = \frac{1}{k_{eff}}$$

$\lambda_{(0)}$ being the smallest eigenvalue of the static diffusion equation written for the nth harmonic of the neutron flux distribution $\phi_{(n)}$:

$$M \phi_{(n)} = \lambda_{(n)} F \phi_{(n)}$$

and ρ_s is obtained by the functional bilinear:

$$\rho_s = \frac{\left\langle \phi_0^*, \left(F - M\right) \phi \right\rangle}{\left\langle \phi_0^*, F \phi \right\rangle}$$

The static reactivity ρ_s is typical of a reactor design quantity since it is an average characteristic of the core material for given operating conditions. The reactor design becomes feasible if the reactivity mechanisms can compensate for the remaining small neutron imbalance which may appear during operations.

3.2 The dynamic reactivity

The *dynamic reactivity* $\rho(t)$ includes the variation in time of the imbalance between neutron sources and sinks. A similar definition

$$\rho\left(t\right) = \frac{\left\langle \phi_0^*, \left(F - M\right) \Psi \right\rangle}{\left\langle \phi_0^*, F \Psi \right\rangle}$$

uses the following time varying terms:
– the slow varying flux form Ψ which is used instead   -
   of the neutron flux ϕ, according to the factorisation

$$\phi\left(r,E,t\right) = p\left(t\right) \Psi\left(r,E,t\right)$$

– the sources $F = F_0^{crit} + \Delta F$, $F_0^{crit} = \lambda_0 F_0$
– the sinks $M = M_0 + \Delta M$

where p(t) is defined as a fast varying amplitude according to the point kinetics equations and where ΔM and ΔF are the time dependant perturbations. The 0 index refers to the static calculation corresponding to the unperturbed initial conditions.

The dynamic reactivity has two independent components:

$$\rho\left(t\right) = \rho_{ext}\left(t\right) + \rho_f\left(t\right)$$

-    the first component, $\rho_{ext}(t)$ represents all reactivity perturbations due to an

EXTERNAL CAUSE: reactivity variations adjusted intentionally (to achieve initial criticality at given power P_0) and perturbations resulting from an accident. In all cases it is associated to a structural modification of the reactor core:

$$\rho_{ext}(t) = \rho_{ext}(0) + \delta \rho_{ext}(t)$$

- the second component, $\rho_f(t)$ represents all reactivity perturbations due to FEEDBACK EFFECTS from an internal cause in the reactor and from its automatic control. It includes the INHERENT reactivity changes due to the variation of *local core parameters* ($\delta\rho_{l.p.}$) like temperature, burnup, etc. It includes also the automatic actions of the regulation system and shutdown systems ($\delta\rho_{aut.}$, see examples of reactivity devices in Table 3.1):

$$\rho_f(t) = \rho_f[P_0] + \delta \rho_f(t)$$
$$\delta \rho_f(t) = \delta \rho_{l.p.}(t) + \delta \rho_{aut.}(t)$$

Table 3.1:
CANDU 600 reactivity devices worth and rates

Devices	Function	Total Reactivity worth (mk)	Maximum Reactivity rate (mk/s)
14 Liquid Zone Controllers (LZC)	Control	7.1	± 0.14
21 Mechanical Adjusters (ADJ)	Control	15.3	± 0.09
4 Mechanical Control Absorbers (MCA)	Control	10.8	± 0.075 driving - 3.5 dropping
Moderator poison (BOR)	Control	—	-0.0125 extracting
28 Shutoff Rods (SDS1)	Safety	80	- 50.
Poison Injection (SDS2)	Safety	> 300	- 50.

The initial adjustment of positive reactivity to reach criticality $\rho(t = 0) = 0$ at power P_0:

$$\rho_{ext}(0) = \rho_f[P_0]$$

is related to the *power coefficient*. This adjustment is made as an external contribution to overcome an inherent reactivity decrease. From the design point of view only the operating conditions are changed. That explains why this initial adjustment can be seen as a static reactivity correction to the design values. The adjustment is necessary due to the reactor power and the coolant temperature feedbacks as local parameter variations. From the example of Table 3.2 we can see that both factors are together decreasing the core reactivity as the power and the temperature are respectively increased from 0 %FP and 20°C to nominal values of P_0 and 290°C.

Table 3.2:

CANDU 600 reactivity loads from 0 to nominal power

Core parameter	Fresh fuel core	Equilibrium core
COOLANT T°: 20°C to 290°C $\Delta\rho(T°_{coolant})$	-8 mk	+3 mk
REACTOR POWER: 0 %FP to 100 %FP $\Delta\rho_{Po}$(Fuel T°)	-10 mk	-5 mk
$\Delta\rho_X$ (xenon)	-28 mk	-28 mk

3.3 Local parameters affecting reactivity in a CANDU

Local parameters help to understand the feedback reactivity $\delta\rho_f$ components related to the core evolution. Table 3.3 gives the reactivity variations due to local core parameters and the corresponding feedback time interval.

Table 3.3:

CANDU 600 reactivity and variations of local core parameters

Sources of reactivity variations in reactor core	$\Delta\rho$ (typical variation)	Feedback time (typical interval)
Power variation, shutdown to full power	moderate (+ve, -ve)	seconds, minutes
Fuel and coolant temperature variations	moderate (+ve, -ve)	seconds, minutes
Temperature variations of the moderator	small (+ve, -ve)	minutes
Fresh fuel burnup (small burnup)	large (-ve)	from 6 to 7 months
Xenon buildup at equilibrium	large (-ve)	40 h
Xenon transient	large (-ve)	12 h
Flux oscillation	moderate (+ve, -ve)	from 15 to 30 h
Fuel burnup at equi- librium (average burnup)	small (-ve)	days (continuous)
Plutonium and samarium buildup	moderate (+ve)	300 h

For the CANDU 600 the most important local core parameters are the following:
Fuel Burnup: the fuel burnup is distributed unevenly in the CANDU reactor core due to the power distribution and the refuelling strategy. The fuel isotopic composition varies accordingly and the burnup has to be monitored to follow the core evolution and maintain an equilibrium core.

Fuel Temperature: the fuel temperature affects both the rate of neutron capture and the fission rate within the fuel. This temperature should not exceed the power density rating of the fuel.

Neutron Flux: the neutron flux in the fuel affects directly the concentration of fission products Xe and Sm. Reactivity loads are associated with their concentrations.

Coolant/Moderator Density, Temperature and Isotopic Concentration all these factors affect the different neutron spectrums and the neutron absorption (for instance, poison concentration in the moderator) depending on the region which is considered.

4 Reactivity Coefficients

4.1 The reactivity coefficient definition

The Reactivity Coefficient $\partial\rho/\partial\zeta$ associated to a given parameter ζ is defined in general as a time dependant differential quantity:

$$\frac{\partial\rho}{\partial\zeta}(t) = \frac{\left\langle \phi_0^*, \left(\frac{\partial F}{\partial\zeta} - \frac{\partial M}{\partial\zeta} \right)\phi \right\rangle}{\left\langle \phi_0^*, F\,\phi \right\rangle}$$

where the variations of source (F) and sink (M) terms should be taken into account.

The reactivity load $\delta\rho_\zeta$ associated to a finite parameter change ζ is calculated as a sum over the corresponding time interval t:

$$\delta\,\rho_\zeta(t) = \int_{\zeta(t)} \frac{\partial\rho}{\partial\zeta}\,d\zeta = \int_t \frac{\partial\rho}{\partial\zeta}\,\frac{\partial\zeta}{\partial t'}\,dt'$$

usually an *average* reactivity coefficient is used as the mean slope of the curve $\rho(\zeta)$ as a function of ζ.

The average reactivity coefficient can be inferred from the associated reactivity loads as the variation of the reactivity $\Delta\rho$ over the variation of the parameter $\Delta\zeta$ for the complete domain of variation: $\Delta\rho/\Delta\zeta$. Table 4.1 gives some examples of reactivity loads for different events or local core parameter changes.

Table 4.1:

Reactivity loads associated to various events or local core parameter changes

Sources of reactivity variations in reactor core	$\Delta\rho$ **Pickering A & B**
Power variation: shutdown (hot) to full power	(1) -7 mk (2) -3 mk
Fuel and coolant temperature, 25 °C to 275 °C	(1) -8 mk (2) -2,5 mk
Moderator temperature coefficient	(1) -0,06 mk/°C (2) +0,08 mk/°C
Fresh fuel burnup	-26 mk
Xenon load at equilibrium	-28 mk
Xenon transient	-98 mk
Excess reactivity anti-Xe	+18 mk
Period	45 min
Reactivity of zonal flux control	5,4 mk
Reactivity loss - equilibrium fuel	-0,3 mk/day
Reactivity gain - central channel refuelling	+0,2 mk
Plutonium and samarium buildup	+6 mk
(1) Fresh fuel	(2) Equilibrium fuel

4.2 Temperature reactivity coefficients

4.2.1 General description and individual contributions

The temperature reactivity is related to some distinct physical effects which are the thermal expansion, also a direct nuclear effect called the Doppler broadening and other indirect nuclear effects related to the chain reaction processes.

Thermal Expansion Effect

As the temperature of the coolant or moderator rises its density decreases. The neutrons travel further increasing the probability of escaping (P_f and P_t may both decrease). Also with fewer moderator or coolant molecules there is less absorption and the thermal utilization (f) increases.

Direct Nuclear Effect: Doppler Broadening

Resonance capture occur in ^{238}U for certain neutron energies and depend on the relative velocity of the neutron and the target nucleus. As the fuel temperature rises, the U atoms will vibrate more vigorously. A neutron with higher or lower energy has more chances to encounter an U atom moving at the necessary speed to put their relative velocity in the resonance peak. This causes a decrease in the resonance escape probability p or an equivalent broadening in energy of the resonance capture cross section (see Figure 4.2).

Fig. 4.2:
Illustration the Doppler broadening effect on the neutron population
*with the fuel temperature increase, ^{238}U*
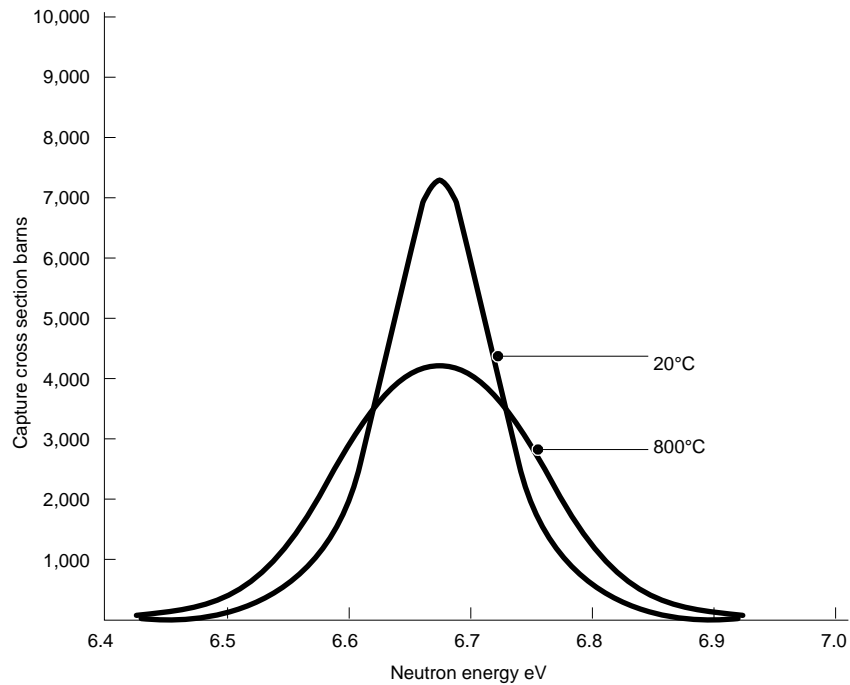
Indirect Nuclear Effect

A thermal neutron is one which is in thermal equilibrium with its surrounding. Any change in the temperature of the moderator, coolant, or fuel will affect the average thermal neutron energy. Thus neutron cross sections being energy dependant are affected. This may affect the thermal utilization (f) and the reproduction factor (η). Figure 4.3 illustrates a sharp rise of η for ^{239}Pu for thermal neutron energy around 0.3 eV

Fig. 4.3:

Illustration of the sensitivity of the reproduction factor as a function of the thermal neutron energy
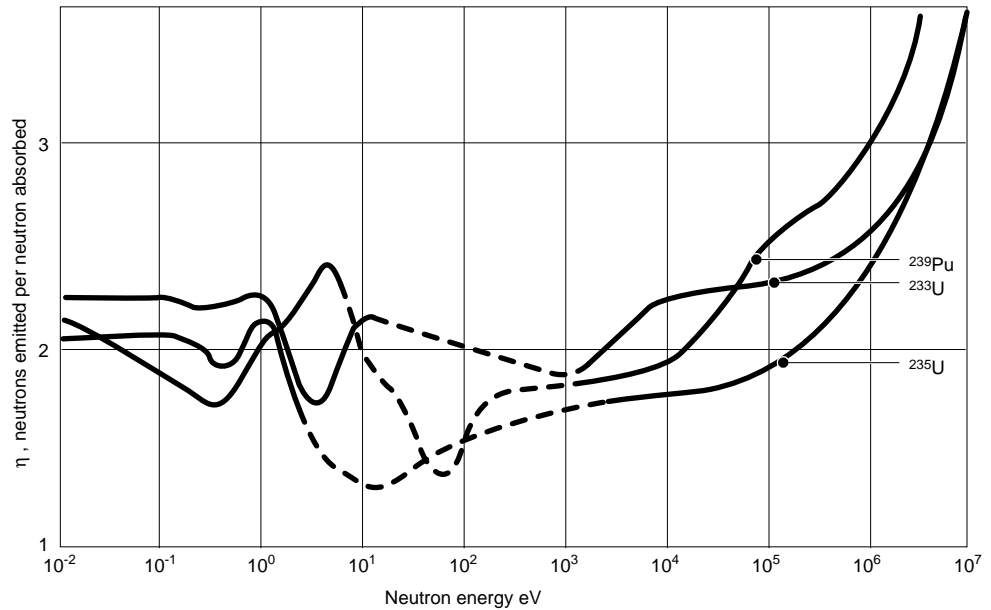
The individual contribution of each effect can be more easily studied if we recall the four factor formula to express the multiplicative constant k:

$$k = \varepsilon \, p \, f \, \eta \, P \quad \text{where}$$

- ε is the fast fission factor which can increase if the number of fast neutrons increases due to a temperature rise;
- p is the resonance escape probability which can be modified due to Doppler broadening associated to a temperature rise (see Fig. 4.2);
- f is the thermal utilization factor which can be modified if the neutron absorption is affected due to a temperature variation;
- η is the thermal reproduction factor which can be modified if the thermal neutron energy range is affected due to a temperature variation;
- P is the non-leakage probability expressed using two energy groups (fast and thermal) as

  $P = P_f P_t$ and can be affected by any variation of the length of the neutron free path in a moderator at a different temperature.

Using this expression leads to the total derivative of k with respect to temperature:

$$\frac{1}{k}\frac{dk}{dT} = \frac{1}{\varepsilon}\frac{d\varepsilon}{dT} + \frac{1}{P}\frac{dp}{dT} + \frac{1}{f}\frac{df}{dT} + \frac{1}{\eta}\frac{d\eta}{dT} + \frac{1}{P_f}\frac{dP_f}{dT} + \frac{1}{P_t}\frac{dP_t}{dT}$$

and the various terms account as individual effects on the variation of k.

For heterogeneous reactor like the CANDU there are always many temperature coefficients because of the physical separations between the fuel, coolant and

moderator. Generally the coefficients differ in magnitude and in sign because of different neutron energy spectrums existing in the separated regions. The various coefficients evolve differently with irradiation. The typical time constants associated with reactivity variations are also different.

4.2.2   Evaluation of the fuel temperature coefficient

Table 4.4 gives the various contributions to the variation of the multiplicative constant k due to a fuel temperature variation.

Two primary effects are related due to a fuel temperature rise:
- a negative resonance escape term (dp/dT) due to Doppler broadening. Fresh and equilibrium fuel values are similar in this case due to the presence of about the same amount of ^{238}U;
- a reproduction factor term (dη/dT) which is negative for fresh fuel due to the presence of ^{235}U as the only fissile material (E < 1 eV in Fig. 4.3), and positive for equilibrium fuel due to the increased concentration of ^{239}Pu (see Fig. 4.3).

The overall result is a negative fuel temperature coefficient which approaches zero with irradiation (see Figure 4.5).

Table 4.4:

Individual effects of the fuel temperature coefficient (Pickering Units 1-4)

Contributions	Fresh Fuel μk/°C	Equilibrium Fuel μk/°C
$(1/\varepsilon)d\varepsilon/dT$	0	0
$(1/p)dp/dT$	-9.33	-9.29
$(1/f)df/dT$	-0.79	+0.34
$(1/\eta)d\eta/dT$	-4.04	+5.33
$(1/P_f)dP_f/dT$	0	0
$(1/P_t)dP_t/dT$	-0.83	-9.43
TOTAL	**-14.99**	**-4.05**

Fig. 4.5:
*Plot of the fuel temperature coefficient as a function of irradiation (CANDU)*
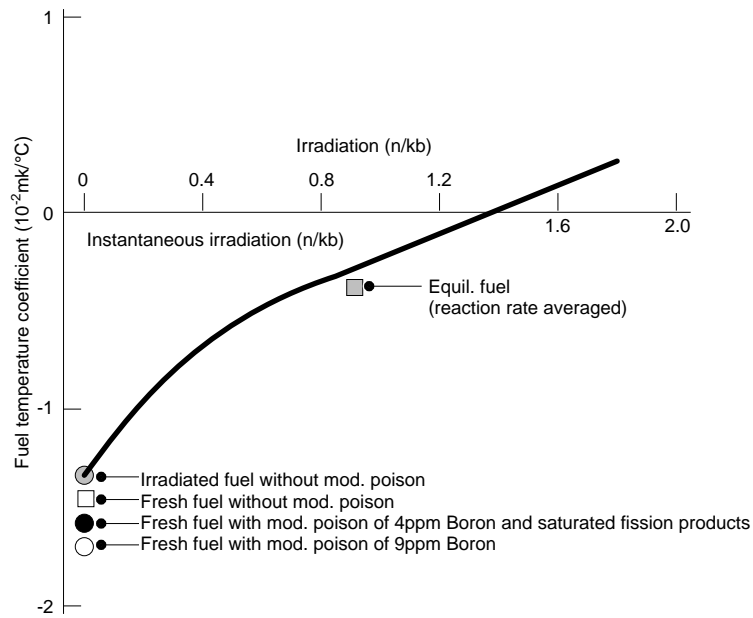
4.2.3 Evaluation of the coolant temperature coefficient

Figure 4.6 shows the variation of the coolant temperature coefficient with irradiation. The overall result obtained from calculation is a positive coolant temperature coefficient (this effect is not observed alone since the coolant temperature cannot be changed without changing the fuel temperature).

The coefficient is positive due mainly to the thermal utilization factor f: a decrease in coolant density results in a decrease in absorption by the coolant.

Fig. 4.6:
Plot of the coolant temperature coefficient as a function of irradiation (CANDU)
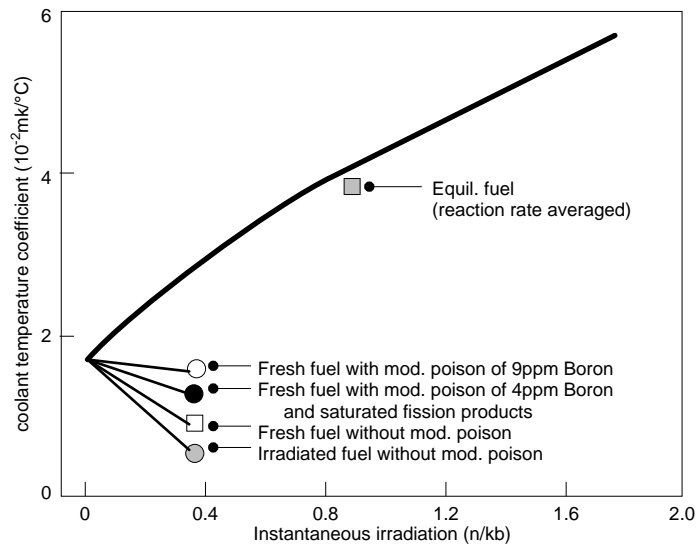
4.2.4   Evaluation of the moderator temperature coefficient

Table 4.7 shows the contributions of individual terms in the reactivity variation. The contributions can be explained by the following effects.

The decrease of moderator density with temperature is responsible for an increase in the distance a neutron travels in slowing down. The consequences are:
- a decrease of the resonance escape probability;
- a decrease of the fast non-leakage probability.

Neutron thermalisation is less efficient at higher moderator temperature. It can be observed as the thermal energy of the neutron increases:
- a reduction in all the absorption cross sections and consequently a change in thermal leakage greater than that in fast leakage;
- a reproduction factor which is decreasing for fresh fuel due to the presence of ^{235}U as the only fissile material (E < 1 eV in Fig. 4.3), or which is increasing for equilibrium fuel due to the increased concentration of ^{239}Pu (see Fig. 4.3).

Table 4.7:

Individual effects of the moderator temperature coefficient (Pickering Units 1-4)

Contributions	Fresh Fuel	Equilibrium Fuel
	μk/˚C	μk/˚C
$(1/\varepsilon)d\varepsilon/dT$	0	0
$(1/p)dp/dT$	-24.0	-23.9
$(1/f)df/dT$	55.4	67.1
$(1/\eta)d\eta/dT$	-59.2	76.0
$(1/P_f)dP_f/dT$	-13.0	-13.0
$(1/P_t)dP_t/dT$	-28.7	-22.0
TOTAL	**-69.5**	**+84.2**

Figure 4.8 shows the variation of the moderator temperature coefficient with irradiation. Note that the temperature of the moderator affects the neutron energy much more than coolant or fuel does. The moderator temperature coefficient is therefore greater than the other two temperature coefficients.

Fig. 4.8:

Plot of the moderator temperature coefficient as a function of irradiation (CANDU)
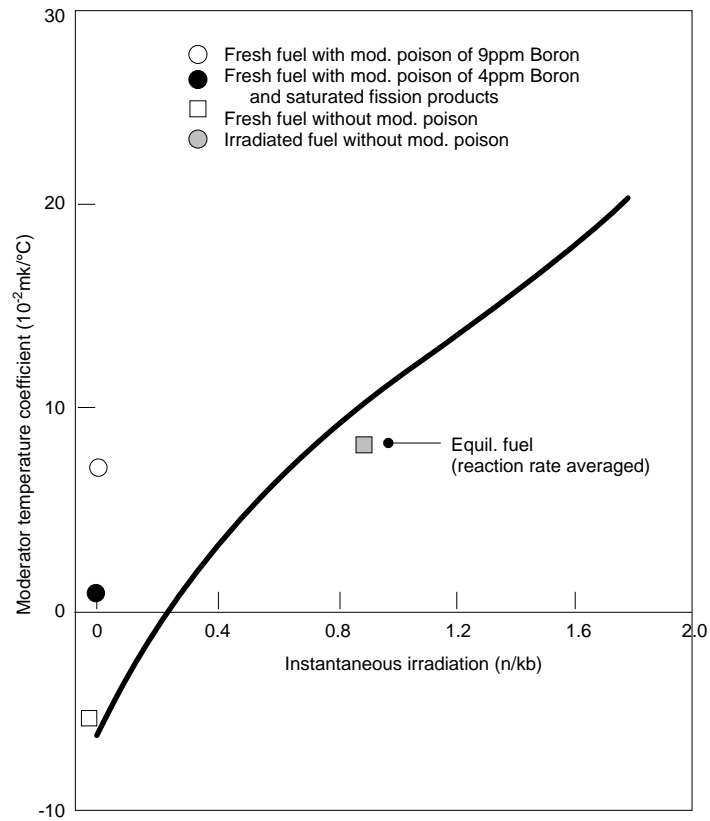
4.3 Positive void reactivity (CANDU)

While the loss of moderator immediately stops the chain reaction, the loss of coolant due to voiding in the channel has different consequences for the CANDU reactor:

- effect on f: a sudden decrease of the coolant density results in a strong decrease in absorption by the coolant;

- effect on p: it occurs through an increase in the resonance escape probability p. This can be understood in the following way: the absence of coolant means that a smaller fraction of neutrons born in a particular fuel element will be slowed down in that cluster into the resonance energy range and, therefore, a smaller fraction will suffer resonance capture in that same bundle;
- effect on η: the absence of hot coolant results in a smaller fraction of the neutrons which enter the bundle from the moderator being scattered up in energy into the resonance range, and thus results in fewer resonance captures;
- effect on ε: the absence of coolant also means that the fast-neutron flux in the fuel will be increased, with a consequent increase in the fast-fission factor ε.

Figure 4.10 shows that the coolant void reactivity of the CANDU reactor is clearly positive and decreases with irradiation. The decrease is partly due to the plutonium and fission products accumulation which are absorbing more neutrons in the equilibrium fuel.

Fig. 4.10:

Plot of the coolant void reactivity as a function of irradiation (CANDU)
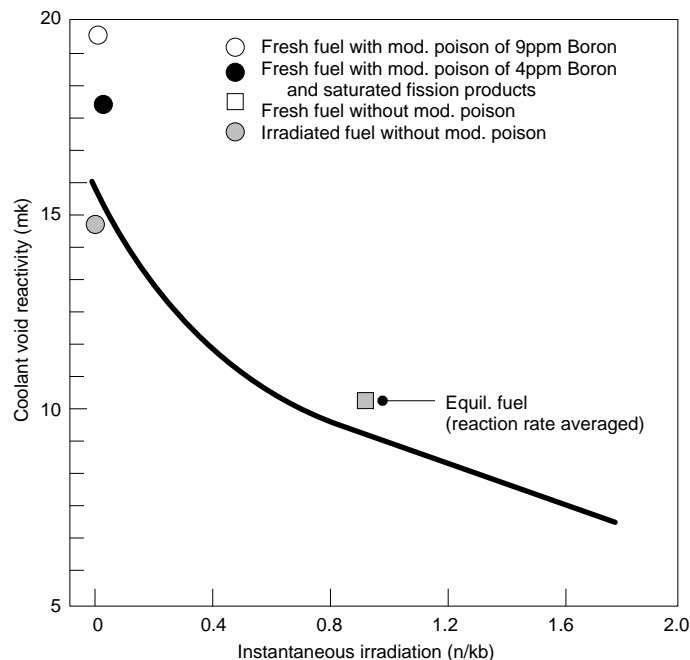
4.4   Other reactivity effects in CANDU

Some other reactivity effects are specific to the CANDU reactor technology and depends on the presence of poisons in the moderator and in the fuel.

Moderator Poisons

Reactivity of the CANDU reactor core changes also by adjusting the concentration of poisons (Boron, Gadolinium) in the moderator.   For instance, Figure 4.11 illustrates the evolution of the boron coefficient of reactivity as a

function of irradiation. The coefficient unit is given with respect to variations of the boron concentration. The variation with irradiation follows the evolution in time of the neutron energy spectrums.

Fig. 4.11:
Plot of the boron reactivity as a function of irradiation (CANDU)
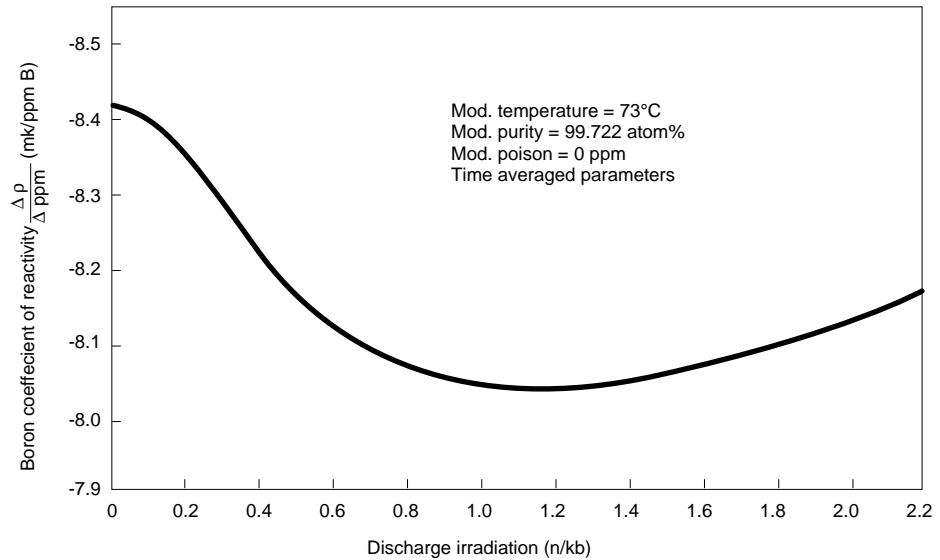

Fission Products

Fission products evolution can determine strong reactivity loads which perturb the neutron flux. These evolutions can be short in time as in the case of xenon loads (see Figure 4.12). They are closely related to the transient evolution of the isotopic composition of the CANDU fuel with the neutron flux intensity. Such reactivity effects depend on the type of fuel in use.

Fig. 4.12:
Plot of the xenon reactivity loads as a function of irradiation (CANDU)
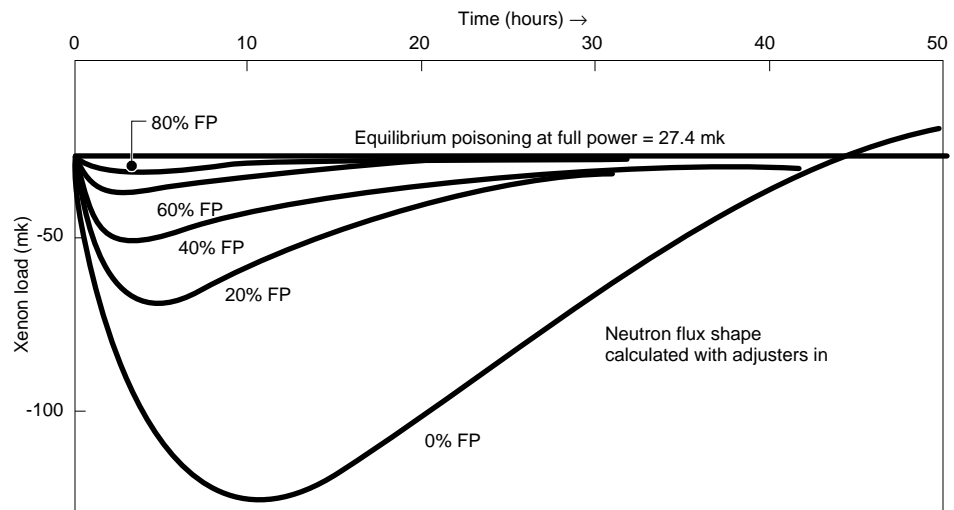
4.5   Safety implications of positive reactivity effects

The neutron balance can be upset by a perturbation to any one of the many core parameters, such as coolant temperature, coolant density, moderator temperature, fuel temperature, moderator poison (boron or gadolinium) concentration, fuel poisons, etc.

The large loss of coolant (large LOCA) is the accident with the potential for the largest reactivity insertion in a CANDU because coolant voiding can happen with its positive reactivity feedback. This design basis accident requires specifically the availability of two independent shutdown systems (SDS1 & SDS2) in the CANDU technology. A massive poison injection due to the trip of the shutdown system SDS2 (see Table 3.1) gives a sufficient protection in the case of large LOCA providing that SDS2 responds very quickly using for instance the log rate detection parameter (logarithmic increase of neutron flux as detected by ion chambers detectors).

Knowledge of the various reactivity coefficients is important from the point of view of reactor control, as the regulating system must be designed to respond to small perturbations in core parameters.

The next lesson will discuss the detailed neutron flux distributions in a typical CANDU reactor core. We will deal with typical transients and examine the control and safety requirements.

Neutron Flux in CANDU

Training Objectives

The participant will be able to understand:
1   the neutron spectrum variations in the unitary cell;
2   the basic cosine flux distribution;
3   the importance of the fundamental mode (time average distribution) and mode flux shapes;
4   the functions and effects of a reflector;
5   the different methods of flux flattening in the CANDU technology;
6   the importance of monitoring the neutron flux distribution in space and in time.

# Neutron Flux in CANDU

Table of Contents

1 Introduction

We have indicated in the last lesson that neutron flux spatial variations have direct consequences on the reactivity effects in CANDU reactors. How are these variations related to the neutron spectrum ? What are the principles behind the neutron flux spatial distribution in the reactor core ?

CANDU reactors are heterogeneous in the sense that fuel, moderator and coolant are physically separated. By comparison, coolant and moderator functions are, in the LWR technology, the same fluid (light water) circulating in the reactor vessel. In the CANDU technology each different physical region presents various thermodynamic conditions like pressure and temperature (see the unit lattice cell of Figure 1.1) and different nuclear properties. During a power transient in the reactor core, the local thermodynamic conditions may evolve differently and lead to different feedback effects due to local actions on the neutron flux spatial distribution. Indeed, the neutron flux interacts with the nuclei present in each region and heterogeneities are then reflected in terms of spatial variations of neutron energy. If thermodynamic conditions change in given regions, feedback effects will be reflected locally on the *neutron flux spatial distribution* and will induce *local variations of the neutron spectrum*. Spatial variations exist between the various physical regions within a given lattice cell but they can exist between different regions in the reactor core, from one lattice cell to another.

Fig. 1.1:
Illustration of the CANDU lattice cell

Lattice Cell Boundary
(Containing D_2O moderator)

Calandria Tube

Annulus (Gas Gap)

Pressure Tube
(Containing D_2O coolant)

Fuel Bundle
(Fuel element made of
UO_2 in a Zircaloy tube)
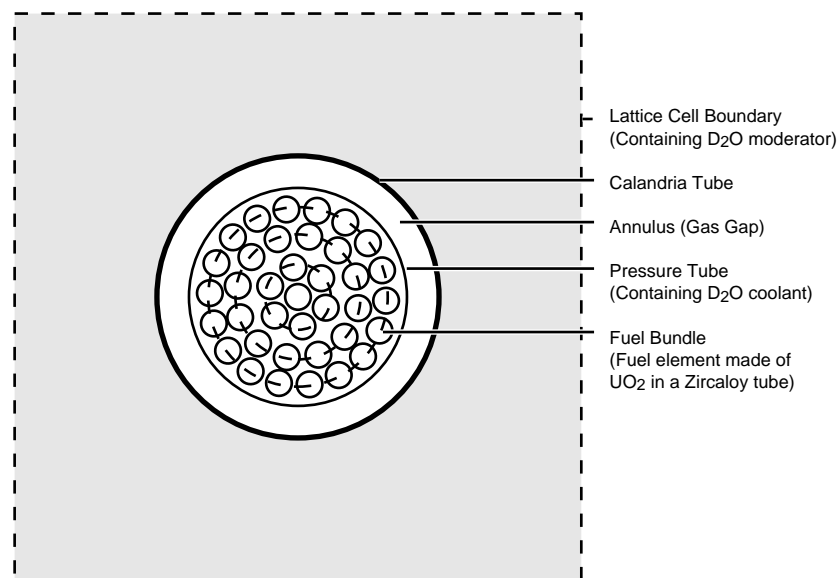
Many physical principles are directing the neutron flux spatial distribution in each lattice cell of the reactor core. In terms of energy spectrum, for instance, neutron energy groups follow mainly distinct rules depending on the characteristic energy range of the group.

High energy (fast) neutrons are linked to the spatial distribution of fission cross-sections properties in the reactor core. High energy neutrons are created in the multiplicative material and the corresponding neutron population is more important near the centre of the fuel bundles (see Figure 1.2).

Fig. 1.2:

Illustration of the variations of the neutron flux spatial distribution in a typical CANDU lattice cell

	Energy Range
Group 1	1.05 MeV - 10 MeV
Group 2	9.12 MeV - 1.05 MeV
Group 3	0.625 eV - 9.12 keV
Group 4	0 - 0.625 eV
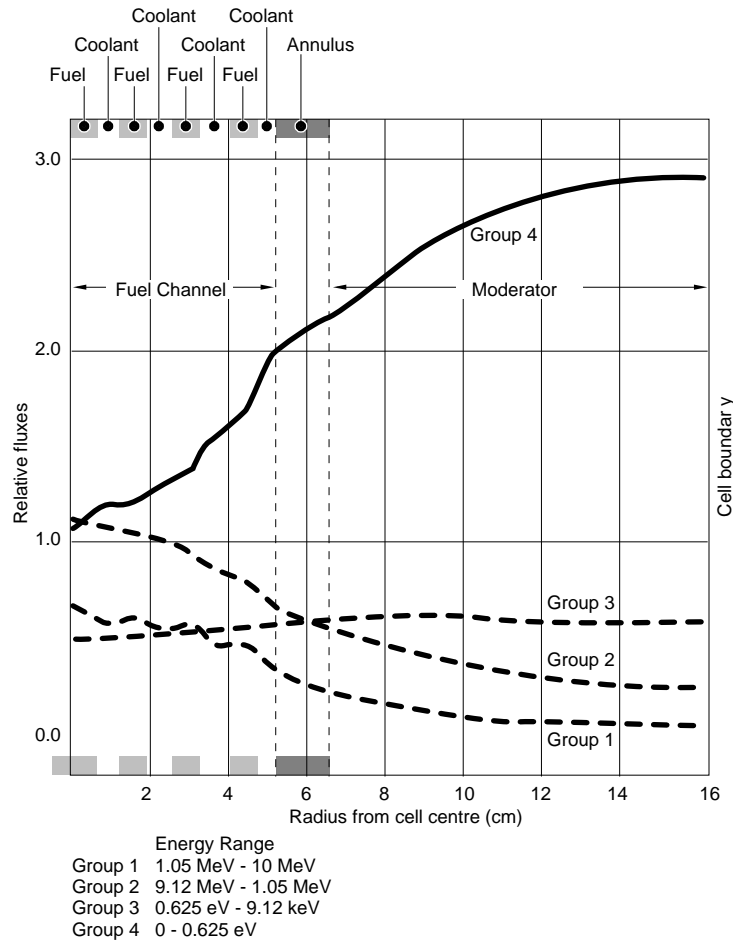
Low energy (thermal) neutrons are linked to the spatial distribution of scattering cross-sections properties in the core. Such properties are typical of the coolant surrounding the fuel pins and of the moderator where the population of thermal neutrons increases (See Figure 1.2).

Parasitic absorption affects the overall neutron population and occurs in the various structural components of the reactor core: pressure tubes, calandria tubes, horizontal and vertical assemblies, etc. Reactivity devices control the reactor by varying the neutron absorption. For instance, adjuster rods are made of "grey" (steel) or "black" (cadmium) materials from the neutronic flux point of view. A local decrease occurs in the neutron flux spatial distribution around the device (see Figure 1.3).

Fig. 1.3:
Illustration of the neutron flux spatial distribution around adjuster rods
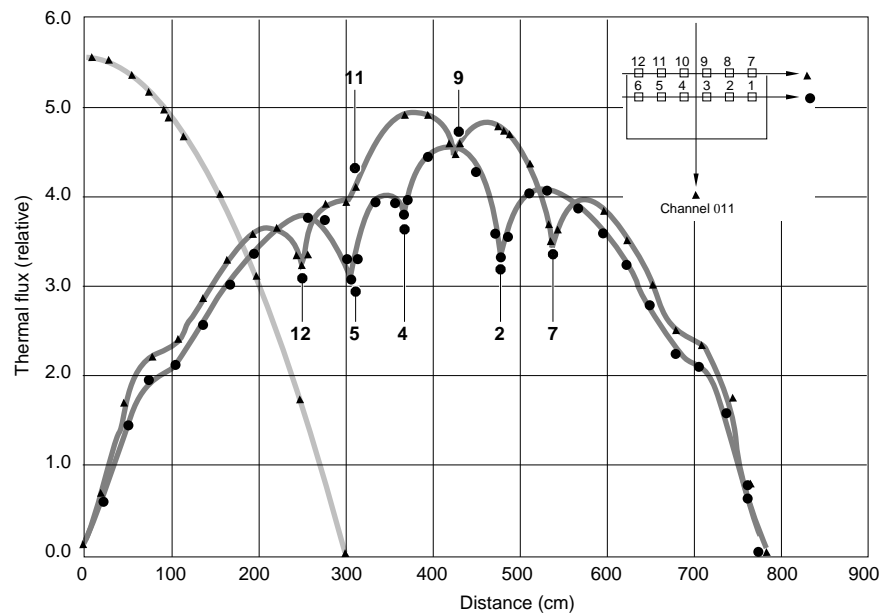
2   Basic Considerations on Flux Distribution

Based on simple assumptions it is easy to deduce the overall typical static flux shape in an homogeneous reactor core. The so-called cosine flux shape is an idealized description of the neutron flux distribution existing in a CANDU reactor core but it is a first approximation which remains satisfactory and useful for simplified reactor models.

2.1   Migration length

The neutron migrates from its point of birth as it slows down and scatters as a thermal neutron. The migration length l_m between neutron production and neutron absorption is about 18 cm in a CANDU.

With the assumption of an homogenous infinite reactor core, the scattering occurs equally in all directions. A typical neutron trajectory can be assimilated to a random walk slowing down in time as the thermalization takes place. The vanishing of the neutron happens on average after it has travelled the migration length. This qualitative description indicates that the process is isotropic and can lead to a statistically uniform distribution of neutrons in an homogenous infinite medium.

With light water instead of heavy water as moderator, the migration length shortens to only a few centimetres in LWR reactors. Since more absorption occurs in light water, the migration length is less than for heavy water.

2.2   Leakage near the core edge

If a neutron is born within l_m = 18 cm of the edge of the CANDU reactor core, it has a high chance of leaking out before producing another neutron. If it is between 18 and 36 cm away, its chance of leakage is significantly less (see Figure 2.1). For a finite reactor core made up of a uniform lattice having a constant migration length, a neutron has the least chance of leakage when it is far away from the reactor boundary. For a cylindrical reactor (CANDU), this is at the centre of the core.

This implies that the maximum of the neutron distribution is located at the centre of the core and that the minimum is located at the edges with a smooth decrease between the maximum and the minimum. The neutron flux distribution will then feature the same symmetry as does the finite reactor core together with its *zero flux* boundary condition at the edge.

Fig. 2.1:

Illustration of the migration length and increased neutron leakage when approaching the core edge

Neutron flux distribution

Reactor core

Migration length
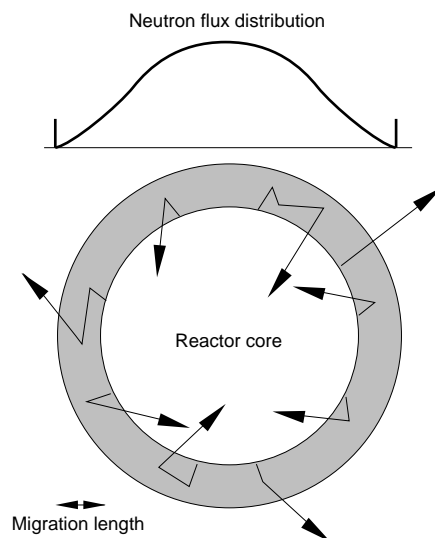
2.3   Flux general profile in the core

We can infer the general profile of the neutron flux in the reactor core based on qualitative arguments on the spatial distribution of loss and source terms throughout the core. These arguments proceed by assuming the existence of:
-    a symmetrical geometry of a cylindrical core surrounded by a cylindrical reflector which defines the reactor core edge (uniform leakage loss term);
-    a quasi-homogeneous description of the reactor core as a regular superposition of basic lattice cells containing fuel (uniform fission source term) and
-    parasitic absorption being almost symmetrically and evenly distributed throughout the core (uniform absorption loss term);

then the static neutron flux basic distribution in the reactor core shall be:
- maximum along the core axial centre (of the cylinder) and
- dropping off symmetrically when going away from the centre due to increased leakage as the reactor boundary is approached;

providing that the total neutron production and removal is balanced, giving a neutron population that is constant in time.

This is illustrated by the typical cosine profiles of Figure 2.2 in the axial and radial directions.

Fig. 2.2:

Illustration of the axial and radial variations of the basic flux spatial distribution in a CANDU reactor core
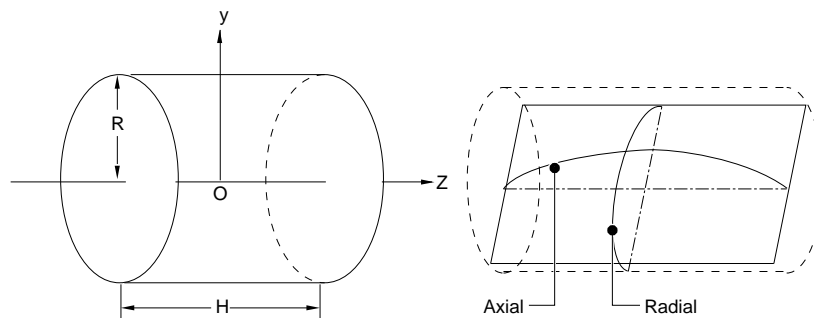
3   Analytical Description and Models

3.1   Neutron flux description

The general directional flux density I which is a function of space r, direction Ω and energy E:

$$\psi\left(r,\Omega,E\right) = v\left(E\right)\ N\left(r,\Omega,E\right)$$

where:
- v(E) is the velocity of neutrons of kinetic energy E;
- $N(r,\Omega,E)$ is the neutron density in phase space such that when considering:
- a small volume dV around the point r,
- a small element of solid angle $d\Omega$ around the direction Ω and
- a small energy band dE containing the energy E. Then the corresponding number of neutrons in the element $dVd\Omega dE$ is given by:

$$\text{number of neutrons} = N\left(r,\Omega,E\right) dV\ d\Omega\ dE$$

The two following basic quantities are derived from I(r,Ω,E):
- the *scalar flux density* ϕ(r,E):

$$\phi\left(r,\, E\right) = \int \psi\left(r,\Omega,E\right) d\Omega \ = v\left(E\right) \int N\left(r,\Omega,E\right) d\Omega$$

which represents an isotropic neutron density
- the *net current density* J(r,E):

$$\vec{J}\left(r,\, E\right) = \int \vec{\Omega}\,\psi\left(r,\Omega,E\right) d\Omega$$

which represents an oriented neutron flow.

3.2   Neutronic transport equation

The exact description of neutron flux distribution within the lattice cell requires the solution of the *general Boltzmann transport equation*. The equation is stated in terms of the directional neutron flux density Φ(r,Ω,E):

$$\frac{1}{v}\frac{\partial}{\partial t}\,\Phi\left(r,\, E,\, \vec{\Omega},\, t\right) =$$

$$-\,\Sigma\left(r,\, E,\, t\right)\Phi\left(r,\, E,\, \vec{\Omega},\, t\right)\,-\,\vec{\Omega}\bullet\vec{\nabla}\Phi\left(r,\, E,\, \vec{\Omega},\, t\right)$$

$$+\int_0^\infty dE'\int_0^\infty d^2\Omega'\, g\left(r;\, E'\to E,\, \vec{\Omega}'\to\vec{\Omega}\right)\Sigma\left(r,\, E',\, t\right)\Phi\left(r,\, E',\, \vec{\Omega}',\, t\right)$$

$$+\,q\left(r,\, E,\, \vec{\Omega},\, t\right)$$

The different terms on the right hand side are:
- neutron losses due to collision which depend on the total cross section Σ(r,E,t);
- neutron losses due to leakage in the direction Ω;
- neutron gains due to collision with the generic differential cross section g(r, E$'\to$ E, $\Omega'\to\Omega$) corresponding to one of the following nuclear phenomena: elastic collision, inelastic collision, radiative capture, nuclear reaction (n, 2n), (n, 3n) ... and fission reaction;
- a neutron source which is independent of neutronic density like spontaneous fission or external source.

The numeric solution of the steady state transport equation which consists in the previous equation with the left hand side $\partial\Phi/\partial t$ equals to 0, is suitable for a refined microscopic description of the relevant nuclear processes and can be achieved using a fine energy discretization (typically up to 69 energy groups).

The solutions of the transport equations serve to homogenize the characteristic properties (cross-sections, diffusion coefficients, etc.) of given unitary lattice cells representative of the reactor core lattice cells.

3.3 Diffusion equation

The formulation based on the diffusion equation constitutes an *approximation* to the transport equation. This approximation is more manageable and economical for a full reactor core description including a realistic representation of the internal components. It is assumed here that the directional neutron flux density features almost *no angular dependence* and can be described by the isotropic scalar flux density ø(r,E) and the net current density J(r,E).

The general diffusion equation is:

$$\frac{1}{v}\frac{\partial}{\partial t}\Phi\left(r, E, t\right) =$$

$$-\Sigma\left(r, E, t\right)\Phi\left(r, E, t\right) - \vec{\nabla}\bullet D\left(r, E\right)\vec{\nabla}\phi\left(r, E, t\right)$$

$$+\int_{0}^{\infty}dE'\Sigma_{s}\left(r, E' \rightarrow E, t\right)\phi\left(r, E', t\right)$$

$$+\chi_{p}\left(E\right)\int_{0}^{\infty}dE'v_{p}\left(E'\right)\Sigma_{f}\left(r, E', t\right)\phi\left(r, E', t\right)$$

$$+S_{d}\left(r, E, t\right) + S\left(r, E, t\right)$$

where the scattering and fission differential cross-sections (Σ_{s} and Σ_{f}) are explicitly given and where the external sources are specified for prompt neutrons (S) and delayed neutrons (S_{d}). By grouping the gain (F) and loss (M) terms, the equation becomes:

$$\frac{1}{v}\frac{\partial}{\partial t}\phi = \left(F - M\right)\phi + S_{d}\left(r, E, t\right) + S\left(r, E, t\right)$$

with the gain due to fission:

$$F\phi = \chi_{p}\left(E\right)\int_{0}^{\infty}dE'v_{p}\left(E'\right)\Sigma_{f}\left(r, E', t\right)\phi\left(r, E', t\right)$$

and the losses due to leakage and scattering:

$$M\phi = -\vec{\nabla}. D\left(r, E\right)\vec{\nabla}\phi\left(r, E, t\right) + \Sigma\left(r, E, t\right)\phi\left(r, E, t\right)$$

$$-\int_{0}^{\infty}dE'\,\Sigma_{s}\left(r, E'\rightarrow E, t\right)\phi\left(r, E', t\right)$$

Note that the *static diffusion equation* without neutron source independent of $\phi(S_{d} = S = 0)$ can be written in an operator form since $\partial\phi/\partial t = 0$:

$$M\phi = \frac{1}{k_{eff}}F\phi$$

where the multiplicative constant k_{eff} is adjusted such that an exact balance is achieved between production and loss of neutrons.

The neutron diffusion approach is analogous to diffusion of heat or diffusion of chemical species along a concentration gradient. Similarly, *neutrons diffuse along a neutron concentration gradient and the rate of diffusion is proportional to this concentration gradient:*

$$\vec{J} = -D\left(r, E\right)\vec{\nabla}\phi\left(r, E, t\right)$$

The constant of proportionality is the *diffusion coefficient* D(r,E) which depends on the homogenized properties of a given lattice cell. For LWR reactors the

diffusion coefficient is < 0.5 cm whereas for CANDU it is about 1 cm.

To obtain the general diffusion equation, the derivation starts by the continuity equation which is stated in terms of two independent variables: the scalar flux density $\phi(r,E)$ and the net current density $J(r,E)$. These two independent variables are then linked together by the former relationship using the diffusion coefficient and the resulting approximation is the general diffusion equation.

Providing that the neutron sources and sinks are homogenized within the various representative lattice cells and correctly distributed in the core, the diffusion approach can be used in static or dynamic neutron flux calculations.

4 λ -Modes of the Static Flux Distribution

4.1 The basic static flux distribution

The static flux distribution is obtained from the solution of the diffusion equations for two or more neutron energy groups. The procedure of dividing the neutron energy continuum in groups is called energy group condensation. The procedure leads to as much equations as the number of energy groups and usually it allows at least two groups (the fast and thermal groups) or more depending on the required discretization. The corresponding equations are not independent since they are coupled by the neutron scattering terms which describe the neutrons going from high energy groups to lower energy ones as they slow down.

The system of equations of the static diffusion equation is written as an eigenvalue problem:

$$\left[M\right]\left[\phi_{(n)}\right] = \left[\lambda_{(n)}\right]\left[F\right]\left[\phi_{(n)}\right]$$

where $[\phi_{(n)}]$ is a nth harmonic vector whose elements are the neutron flux of the various energy groups.

Each harmonic of the λ-Mode set is a *particular solution* which can be *superposed* to obtain the *general solution*. For each harmonic, labelled n there is a corresponding eigenvalue $\lambda_{(n)}$ with the associated *subcriticality* $k_{(n)}$:

$$k_{(n)} = \frac{1}{\lambda_{(n)}} \quad \text{where} \quad k_{eff} = \frac{1}{\lambda_{(n=0)}}$$

The basic flux shape corresponds to the fundamental mode. The highest subcriticality is the multiplicative coefficient k_{eff} and it corresponds to the smallest eigenvalue $\lambda_{(0)}$. The basic static flux distribution for a cylindrical homogenous CANDU reactor is:

$$\Phi\left(r,z\right) = \Phi_m \, J_0\left(\frac{2.405r}{R}\right) \cos\left(\frac{\pi z}{H}\right)$$

and the distributions are illustrated (see Figure 4.1a) for the two energy groups (thermal and fast) at various locations in the reactor (see Figure 4.1b).

Fig. 4.1:

Illustration of the basic static flux distributions for the fast neutrons and thermal neutrons

December 1995
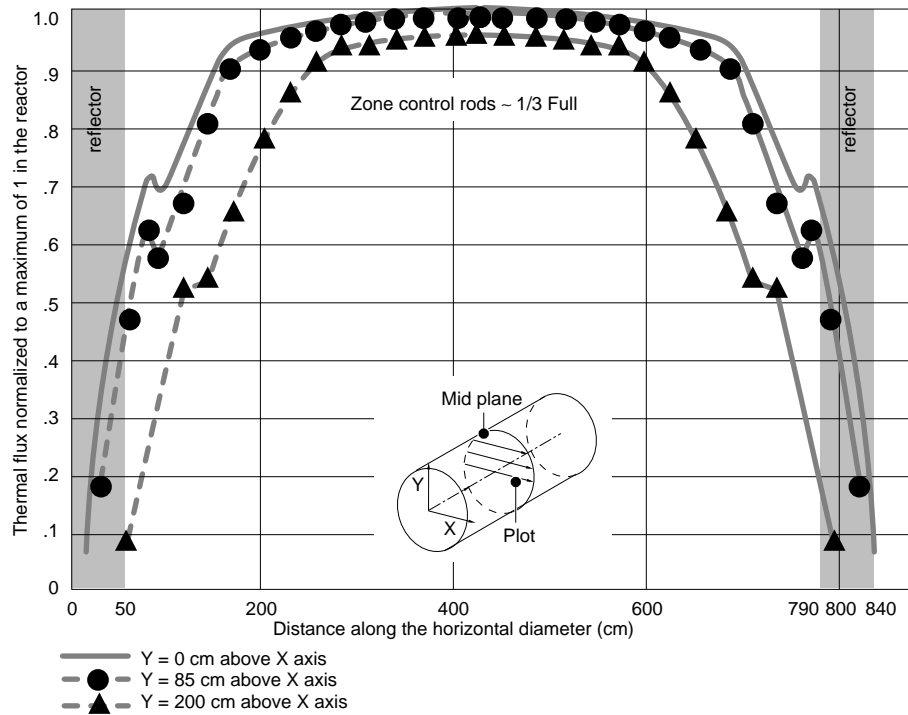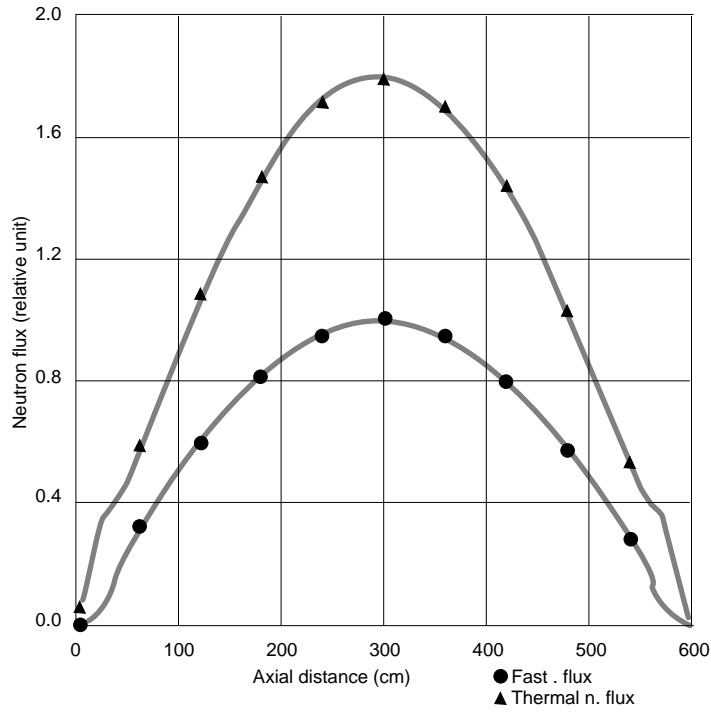
4.2 Harmonic modes and modal synthesis

4.2.1 Perturbations as high harmonic modes

By analogy with a resonant cavity (of a music instrument for instance) higher harmonic modes are mathematically possible and they feature more oscillations than the fundamental mode (see Table 4.2).

All these shapes are partly negative and positive over the spatial domain (see Figure 4.3 for examples of mode number 9 and 10). High harmonic modes are used then to describe *perturbations* which have to be superposed to the fundamental mode.

Table 4.2:

*Flux shapes classification of high harmonics λ-Mode*
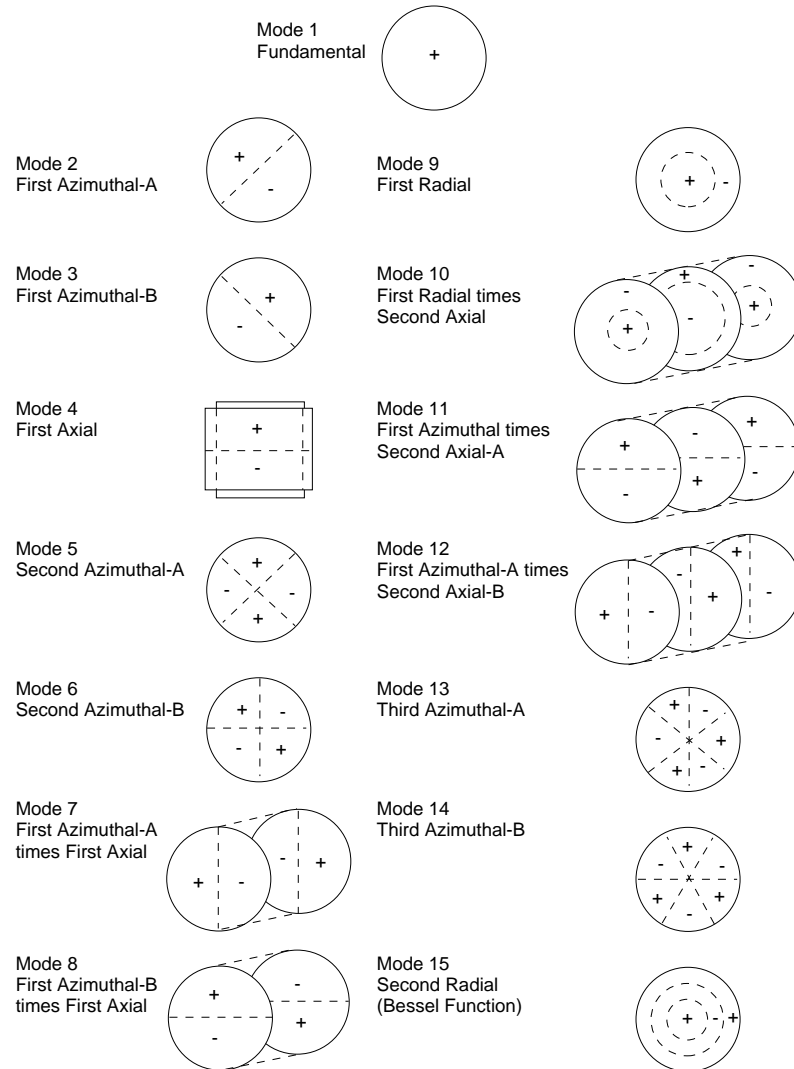
Fig. 4.3:

*Illustration of a high harmonic neutron flux modes 9 and 10*

Mode 9

Mode 10

December 1995
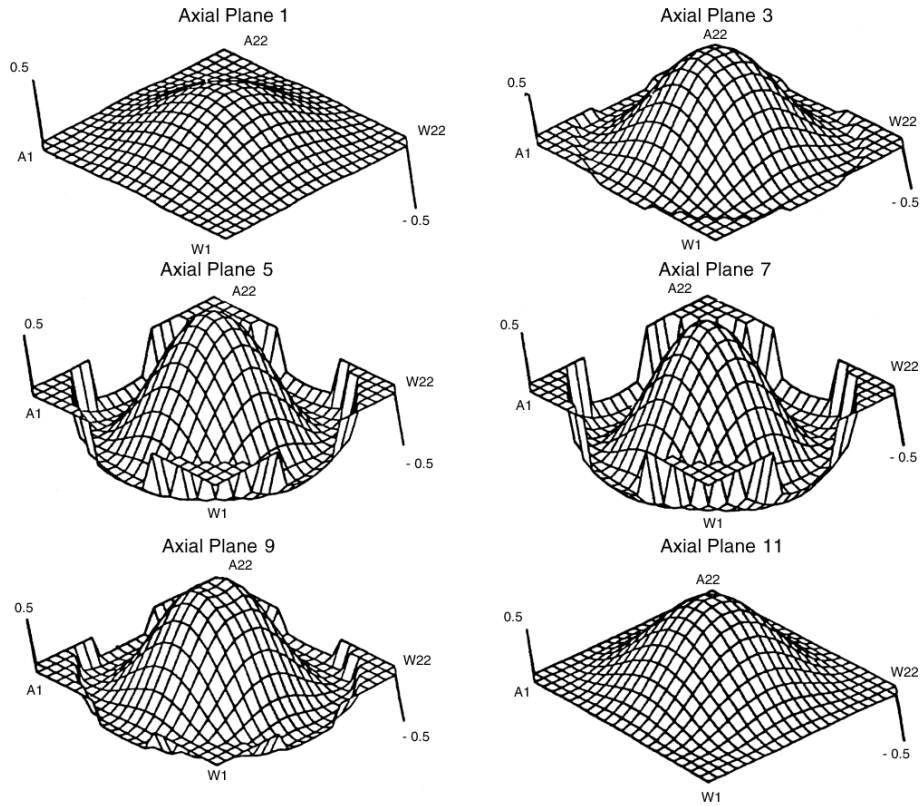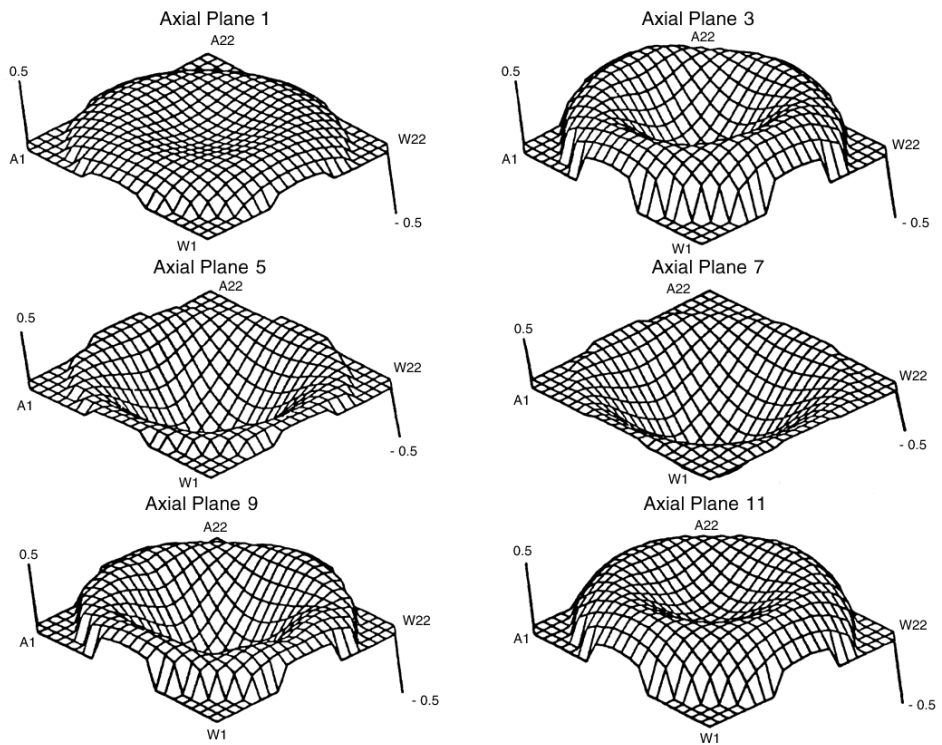
With higher modes, the subcriticalities $k_{(n)}$ are decreasing with increasing eigenvalues (see Table 4.4). This means that an excess reactivity should be added to the core to allow the existence of the associated high harmonic perturbation.

Table 4.4:

Example of subcriticality associated to harmonics λ-Mode

Mode Number	Designation	Subcriticality mk	Mode schematic (idealized)
0	Fundamental	0	
1	First Azimuthal-A	16.2	
2	First Azimuthal-B	16.9	
3	First Axial	27.1	
4	Second Azimuthal-A	44.0	
5	Second Azimuthal-B	47.0	
6	First Azimuthal-A times First Axial	46.9	
7	First Azimuthal-B times First Axial	47.7	
8	First Radial times First Axial	66.3	
9	First Radial times Second Axial	30.6	
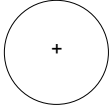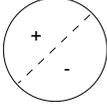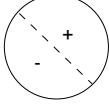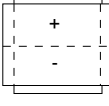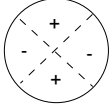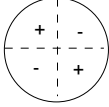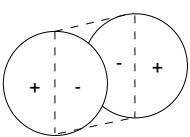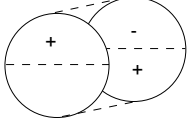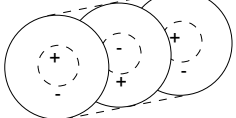
4.2.2   Modal synthesis

An arbitrary reactor core flux shape can consist of a *linear superposition* of the fundamental mode plus a linear combination of harmonic modes.

Using a procedure called *modal synthesis* (see Figure 4.5), a sufficient description can be achieved with a relatively small set of orthogonal modes providing:
-    that the "natural" modes used have high subcriticalities to represent the most usual *perturbations* of the steady state which may happen naturally (like power tilts for instance), and
-    if the modes were to be used for transient neutronics, providing that they are representative of the *typical perturbations induced by the action of the reactivity devices*. For instance such modes are used in the flux mapping control program when the mechanical adjusters move.

Fig. 4.5:
Illustration of flux modal synthesis with an simple example of superposition of modes
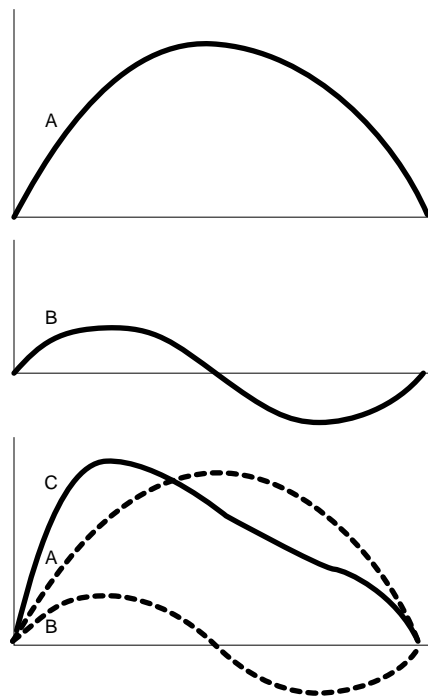
5   Flux Flattening in CANDU

5.1   The needs for flux flattening

The CANDU reactors are designed with a large core. A high lattice pitch provides enough space between fuel channels to allow for refuelling manoeuvres. This provides also room to accommodate the moderator in the calandria, too much space in fact since the reactor is overmoderated (see Figure 5.1).

Fig. 5.1:
Illustration of the moderation as a function of the lattice pitch
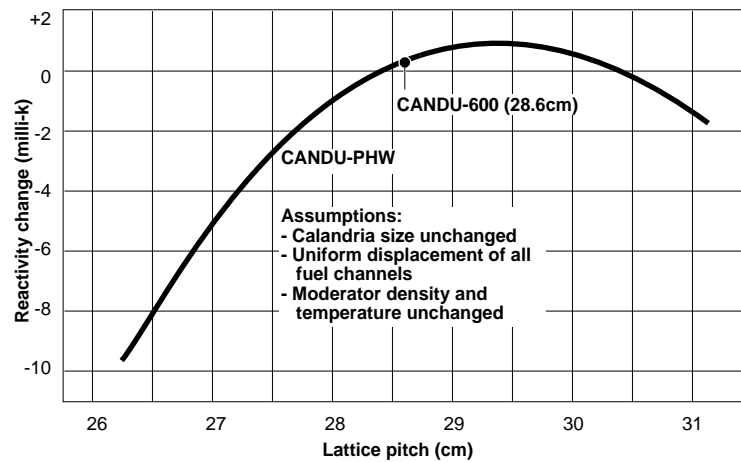
A large core implies important neutron leakage at the reactor core boundaries. A direct consequence of the previous homogenous reactor calculation of the flux distribution is a small value of the *average to peak flux ratio:*

$$\frac{\Phi_{avg}}{\Phi_{max}} = 27.5 \text{ \% } \text{ with } \Phi_{max} = \Phi_m = MAX\left[\Phi\left(r, z\right)\right]$$

The *total power output* of the reactor depends on Φ_{avg} and Φ_{max} is limited by the *maximum fuel heat rate* which is reached near the centre of the reactor.

One way of increasing Φ_{avg}, hence the total power, is to increase Φ_{max} up to the allowable fuel heat rate limit. Due to the flux shape as indicated by the 27.5 % average to peak ratio, the fuel burnup will not be evenly distributed and the combustion in outer regions will not be optimal.

Another way is to *flatten the flux distribution* over part of the reactor. This can be achieved by modifying the distribution of neutron sources and losses.

Neutron Loss Modifications:
- decrease the leakage at the core edges;
- adjust the overall flux shape and damper or redistribute Φ_{max} near the centre by parasitic absorption of adjuster rods.

Neutron Source Modifications:
- axial flux flattening due to bi-directional refuelling strategy;
- radial flux flattening due to differential burnup criteria in the channel selection rules of the refuelling strategy.

5.2 The effects of adding a reflector

Since leakage is controlling the flux shape near the core edges, a leakage reduction will help to increase Φ_{avg}. In this respect, the effects of a reflector around the core are:

- neutron flux is "flattened" radially: the ratio of average flux to maximum flux is increased (see Figure 5.2). Fast neutrons escape into the reflector where they are thermalized, creating a hump in the curve;
- because of the higher flux at the edge of the core, fuel utilization is improved;
- neutrons reflected back into the core become available for fission.

Fig. 5.2:
Illustration of the action of a reflector on the thermal neutron flux distribution
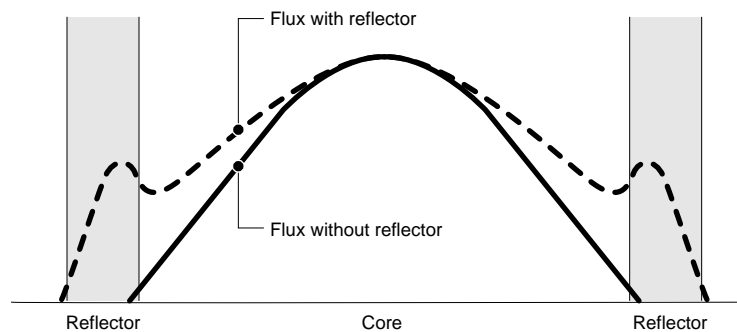
In the CANDU technology the reflector is part of the moderator.

5.3 Bi-directional refuelling

In CANDU reactors, adjacent fuel channels are fuelled in opposite directions leading to flux flattening in the axial direction (see Figure 5.3).

Fig. 5.3:
Illustration of the effect of bi-directional fuelling
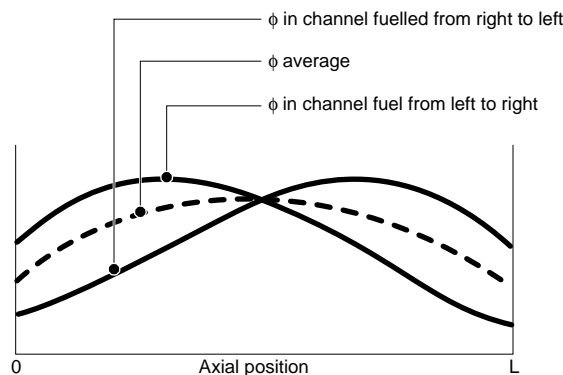
New fuel, freshly inserted at the input end of the channel, generates a higher flux than the burned up fuel at the exit end. The degree of flattening depends on how many bundles are replaced during refuelling. From the point of view of flux flattening, the fewer the better: however, other considerations largely determine the number of bundles replaced (channel opening frequency, reactivity needed per zone, channel power output, etc.).

All the refuelling schemes currently used provide some flux flattening. For CANDU 600 reactors, 8 irradiated fuel bundles are removed from the 12 bundles contained in a fuel channel and are replaced with 8 fresh fuel bundles *(8-bundle shift scheme)*. With partial channel fuelling, bi-directional fuelling prevents the flux distribution which would result from uni-directional fuelling (see Figure 5.4).

Fig. 5.4:
Illustration of the effect of uni-directional fuelling

φ with uni-directional refueling

φ with bi-directional refueling

0   Axial position   L
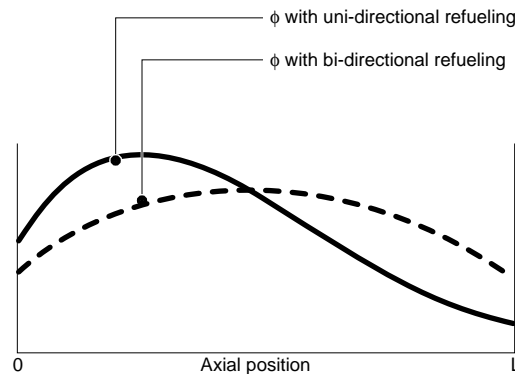
5.4   Flux shape adjustment: adjuster rods

Adjusters are rods of a neutron absorbing material (Cobalt or steel) which are normally inserted into the central regions of the reactor core to *dampen or redistribute the flux peak*. Being symmetrically distributed in banks around the core centre, they affect both radial and axial flux shapes (see Figure 5.5). Figure 5.6 shows the radial flux distributions with and without adjusters; both distributions feature the same maximum. The *use of adjusters enables a higher total power output for the same maximum flux.*

Fig. 5.5:

Illustration of the adjuster rod positions and bank assignation in a CANDU 600 reactor

Adjuster bank #	Rods
1	1,7,11,15,21
2	2,6,18
3	4,16,20
4	8,9,13,14
5	3,19
6	5,17
7	10,12
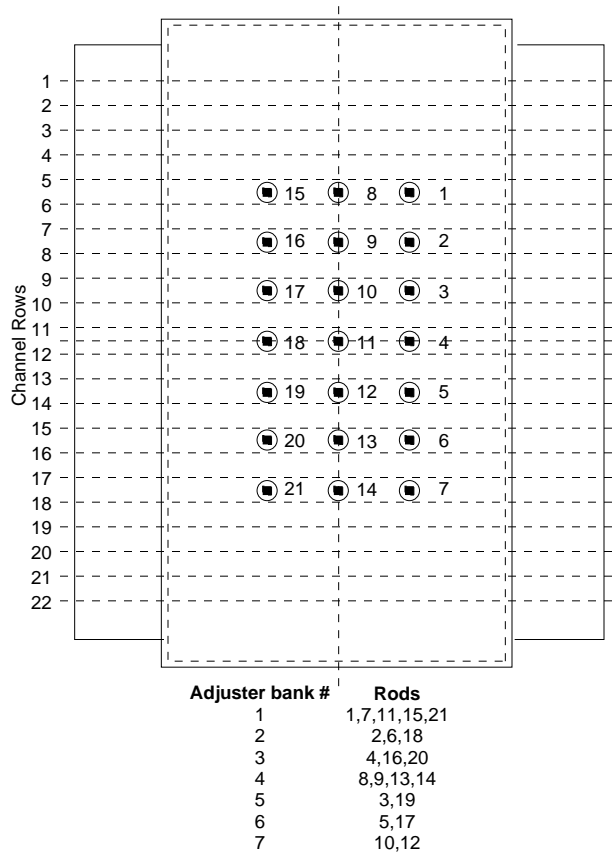
Fig. 5.6:

Illustration of the effect of adjuster rods on flux distribution
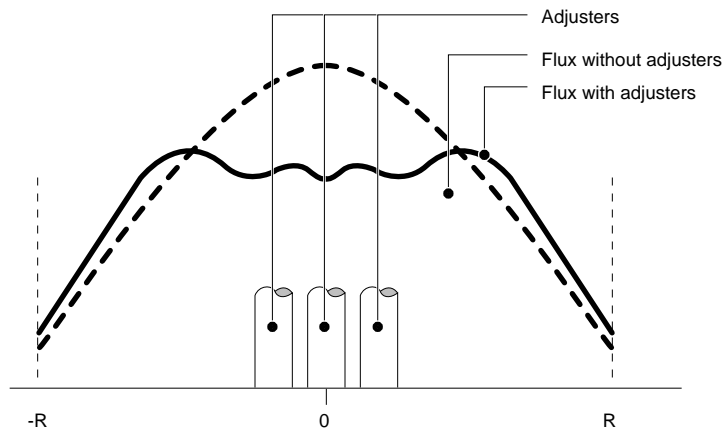
Parasitic absorption around the core centre changes the dominant contribution of neutron leakage at the edge in the diffusion approach applied to an homogenous core. Instead of a cosine profile, the diffusion calculation will now lead to a *truncated cosine* type of flux shape when the adjusters are in the core.

Inasmuch as adjuster rods are normally inserted in the reactor at full power, they

represent a negative reactivity contribution. To overcome this the CANDU utilities must increase the fuel replacement frequency by approximately 10 %.

In addition to flattening the flux, adjuster rods are withdrawn successively one bank after the other *to add positive reactivity for xenon override or to allow extended power production without refuelling* (for instance, when a fuelling machine is unavailable).

Since CANDU reactors are allowed to operate at reduced power *"in shim modes"* which means with given number of adjuster banks withdrawn, static calculations of flux distribution are performed to describe the steady states of the corresponding core configurations. This gives a set of *perturbation modes which are precisely excited by adjusters withdrawal*. This set of modes is used accordingly if required by the reactor regulating system (RRS).

5.5 Differential burnup

Differential burnup is a method of flux flattening which acts radially in the reactor core. For this purpose, the reactor is divided radially in two concentric regions usually called *inner zone* and *outer zone* (see Figure 5.7). The refuelling strategy changes from one region to the other.

Fig. 5.7:
Illustration of differential fuelling zones in CANDU 600
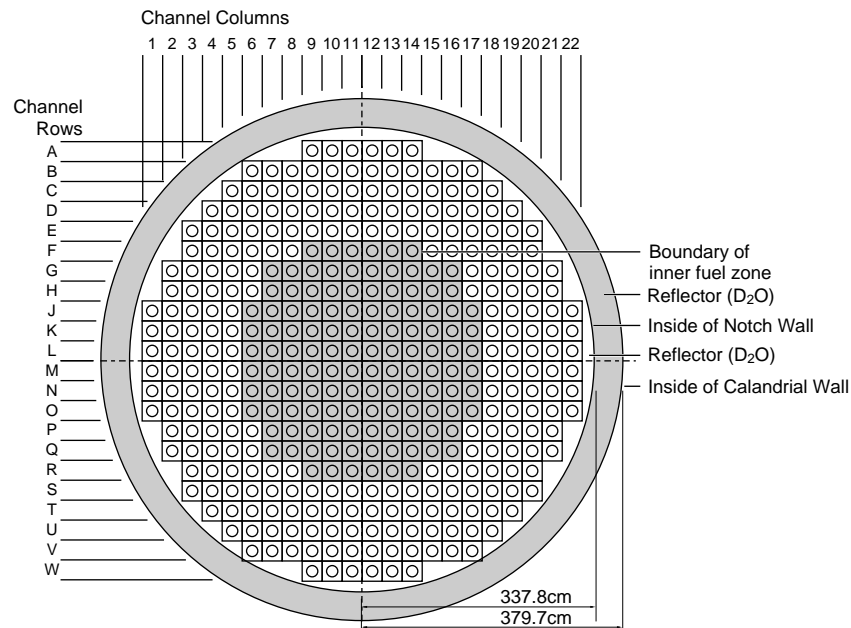
The fuel in the outer zone is allowed to burn out approximately 2/3 the period of the fuel in the inner zone. This means an increase of the fuel replacement frequency. With fresher fuel in the outer regions of the core there are more fission reactions taking place, hence higher flux (see Figure 5.8). This strategy should also reflect in slightly higher fuel costs.

Fig. 5.8:
Illustration of the effect of differential fuelling on the flux shape
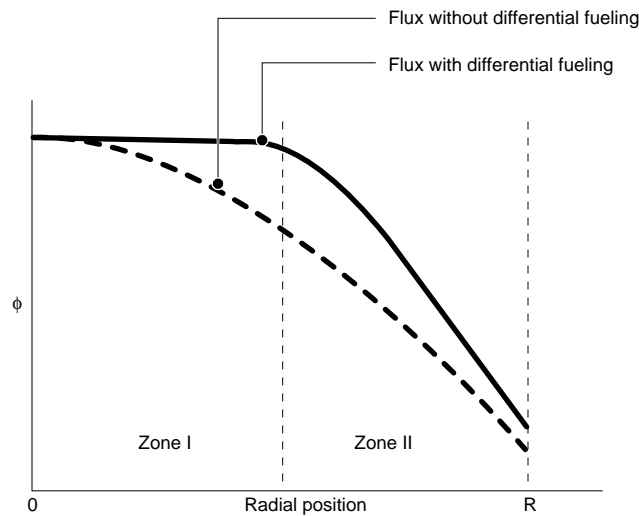
5.6   Importance of flux monitoring

Monitoring in Space: Flux Shapes
Table 5.9 lists for the various CANDU reactors, the methods of flux flattening
used and the resultant average to peak flux ratios. The total power of a CANDU
reactor is related to the average thermal flux by the following expression:

$$P_{tot} = \kappa \, V \, \Sigma_f \, \Phi_{avg} \; = \frac{\Phi_{avg}M}{3 \times 10^{12}}$$

where P_{tot} is the total power (in MW) and M is the total mass of uranium fuel (in
tons of U). The value of 3×10^{12} is obtained for the typical CANDU as the ratio of
the mass M of uranium to the product of the following three factors: the energy
release per fission κ, the reactor volume V and the macroscopic fission cross-
section Σ_f.

The ultimate justification for flux flattening is an economic one. With the various
flux flattening strategies in the CANDU technology, it is possible to increase the
average flux from 27.5 % to more than 55 % of the maximum (see Table 5.9). The
economic gain in terms of the power supplied by the reactor is of the same order.
It is clear then that increasing the average flux without increasing the maximum
flux has enormous economical benefits.

Table 5.9:

Flux-flattening methods for different CANDU reactors

	Reflector	Bi-directional fuelling	Adjusters	Differential burnup	$\dfrac{\phi_{avg}}{\phi_{max}}$
Pickering-A	axial & radial	X	X		57%
Pickering-B	radial	X	X		60%
Bruce-A	radial	X			~59%
Bruce-B	radial	X	X	X	~60%
Darlington	radial	X	X	X	~60%
CANDU 600	radial	X	X	X	~60%

Therefore flux flattening:
- drives the flux shape away from the cosine profile which was inferred from the homogenous static case, and
- is used by the utility to drive the flux shape toward the allowable maximum limit (according to fuel heat rate) in a larger region around the centre (see Figure 5.10),

since operational procedures are allowed to modify the flux shape of the CANDU reactor technology, therefore flux shape monitoring is mandatory.

Fig. 5.10:

Illustration of the time average radial flux distribution for the CANDU 600 reactors
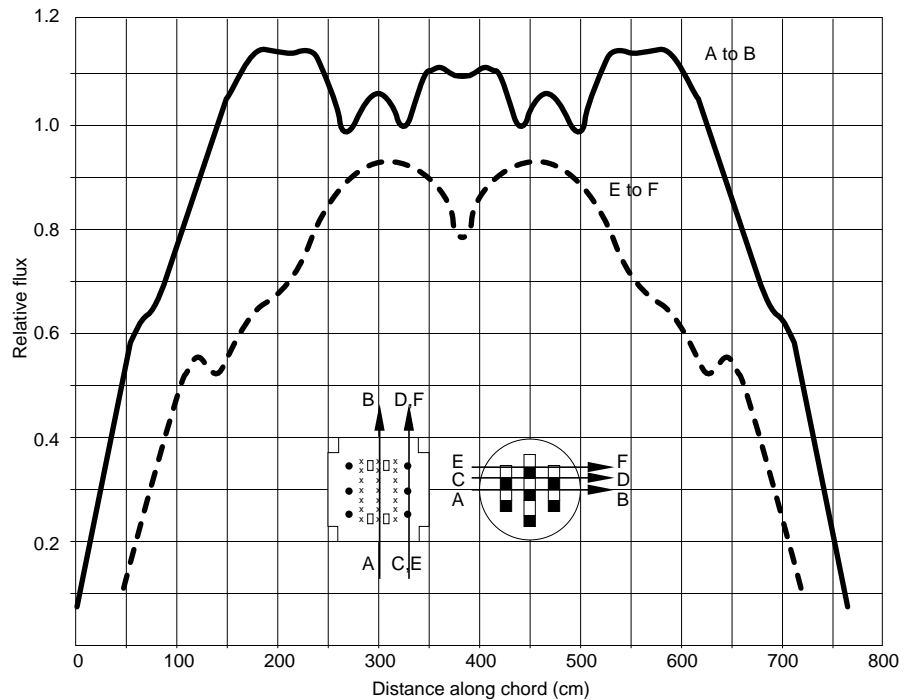
In the case of the CANDU 600, a design basis set of allowable configurations is defined. The set contains a large number of flux configurations under which operations are allowed under various handswitch positions (HSP1, 2 & 3). The regional overpower system (ROP) ensures the required protection of the shutdown systems in case of a slow loss of regulation.

December 1995

Reactor Regulation and Control Instrumentation

Training Objectives:

The participant will be able to understand or to describe:

1   the principles of CANDU reactor regulation;
2   the functional requirements of regulation;
3   the principles of the various regulating routines;
4   the actions of the reactivity control units;
5   the control instrumentation of the CANDU reactor;
6   the start-up instrumentation, the ion chambers and the in-core flux detector systems.

Reactor Regulation and Control Instrumentation

Table of Contents

December 1995

1.0   Introduction

1.1   Presentation of the reactor regulation system

The *reactor regulating system* is that part of the overall plant control system that controls reactor power, and manoeuvres reactor power between specified setpoints. The *reactor power setpoint* can be entered by the operator (in the *alternate mode*) or it can be calculated automatically by the steam generator pressure control program (in the *normal mode*, or load following, mode). The description presented here refers to a CANDU 600 reactor.

The reactor regulating system (RRS) is composed of:
* input sensors (ion chambers, in-core flux detectors),
* reactivity control devices (adjusters, light water zone controllers, mechanical control absorbers),
* hardware interlocks, and a number of display devices.

Except for extremely low power levels (below 10^{-7} of full power), reactor regulating system action is fully automatic, by digital computer controller programs which process the inputs and drive the appropriate reactivity control and display devices. The *operator* is responsible for *long-term reactivity balance* via refuelling and moderator poison control.

A general block diagram of the reactor regulating system is shown in Figure 1.1 c. The *power measurement and calibration* routine uses measurements from a variety of sensors (self-powered in-core flux detectors, ion chambers, process control instrumentation) to arrive at calibrated estimates of bulk and zonal reactor power. The *demand power* routine computes the *desired reactor power setpoint* and compares it with the measured bulk power to generate a bulk power error signal that is used to operate the reactivity devices.

Fig. 1.1a:
Block diagram of the unit control
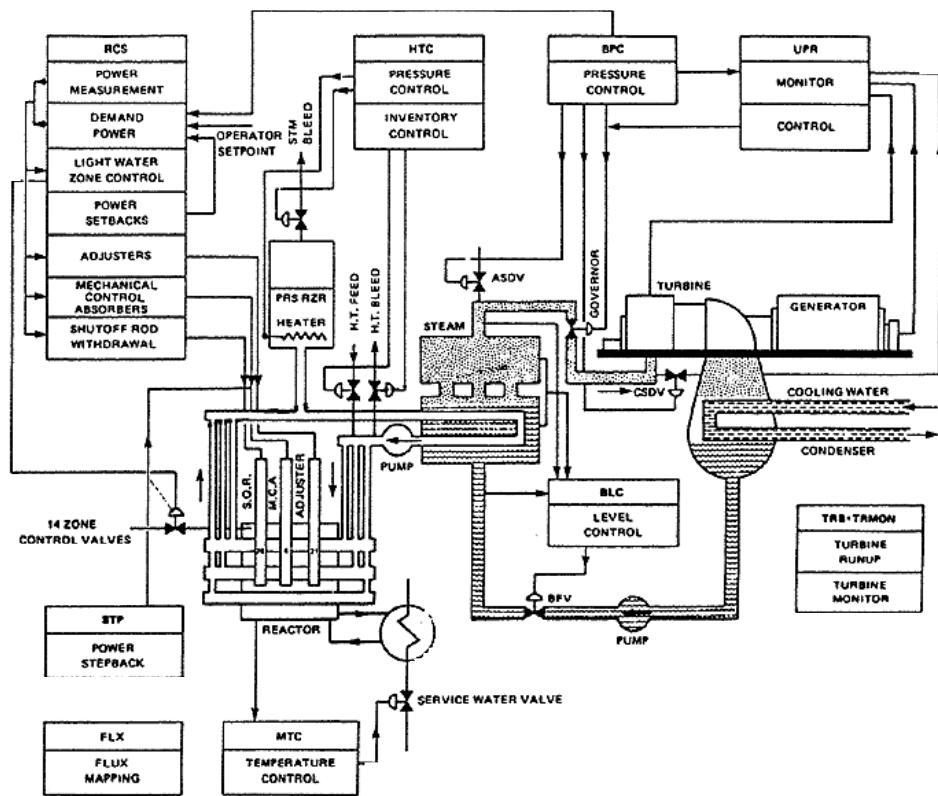
Fig. 1.1b:
Block diagram of the overall plant control
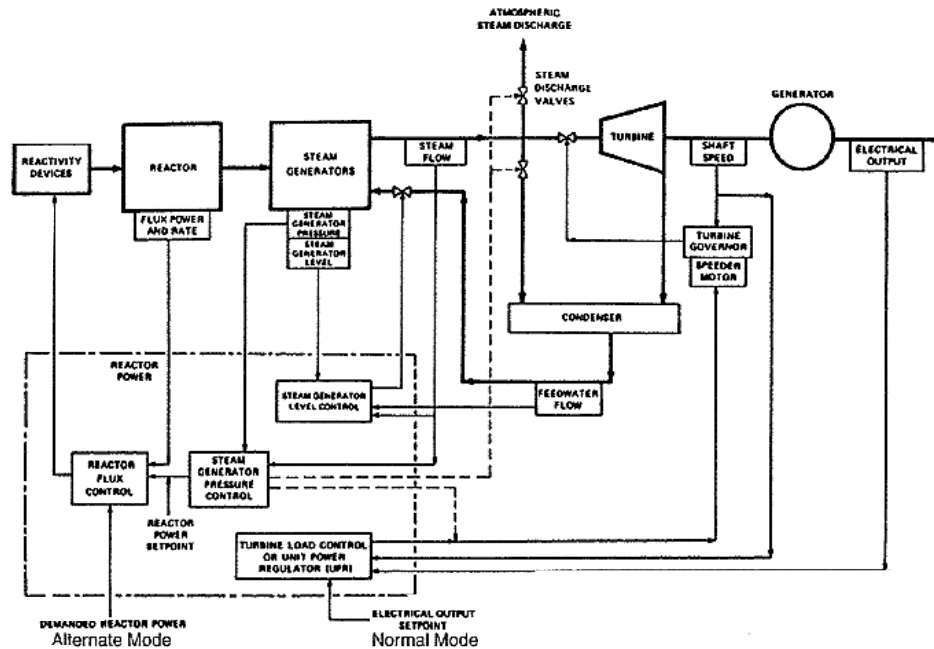
Fig. 1.1c:
Block diagram of the reactor regulation system
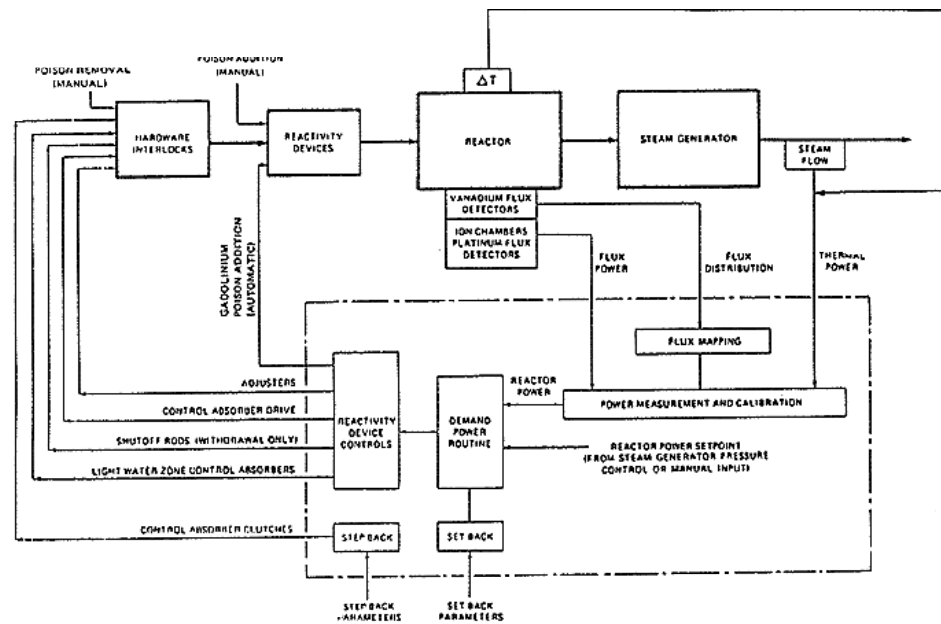
The primary control devices are the 14 light water zone control absorbers. Their reactivity worth is varied in unison (for bulk power control) or differentially (for tilt control). If the reactivity required to maintain reactor flux power at its specified setpoint exceeds the capability of the zone control system, the reactor regulating system programs call on the other reactivity devices. Adjusters are removed for positive reactivity shim (this function is inhibited if the reactor power setpoint is above 97%). Negative reactivity is provided by the mechanical control absorbers or by poison addition to the moderator. The movement of these devices is dictated by average zone controller level and the effective power error as shown in Figure 1.2. The approximate reactivity worths of these devices, and the highest average rates at which the reactivity can be added or removed, are shown in Table 1.3. The general arrangement of reactivity devices is shown in Figure 1.4.

Fig. 1.2:
Limit control diagram of reactivity devices
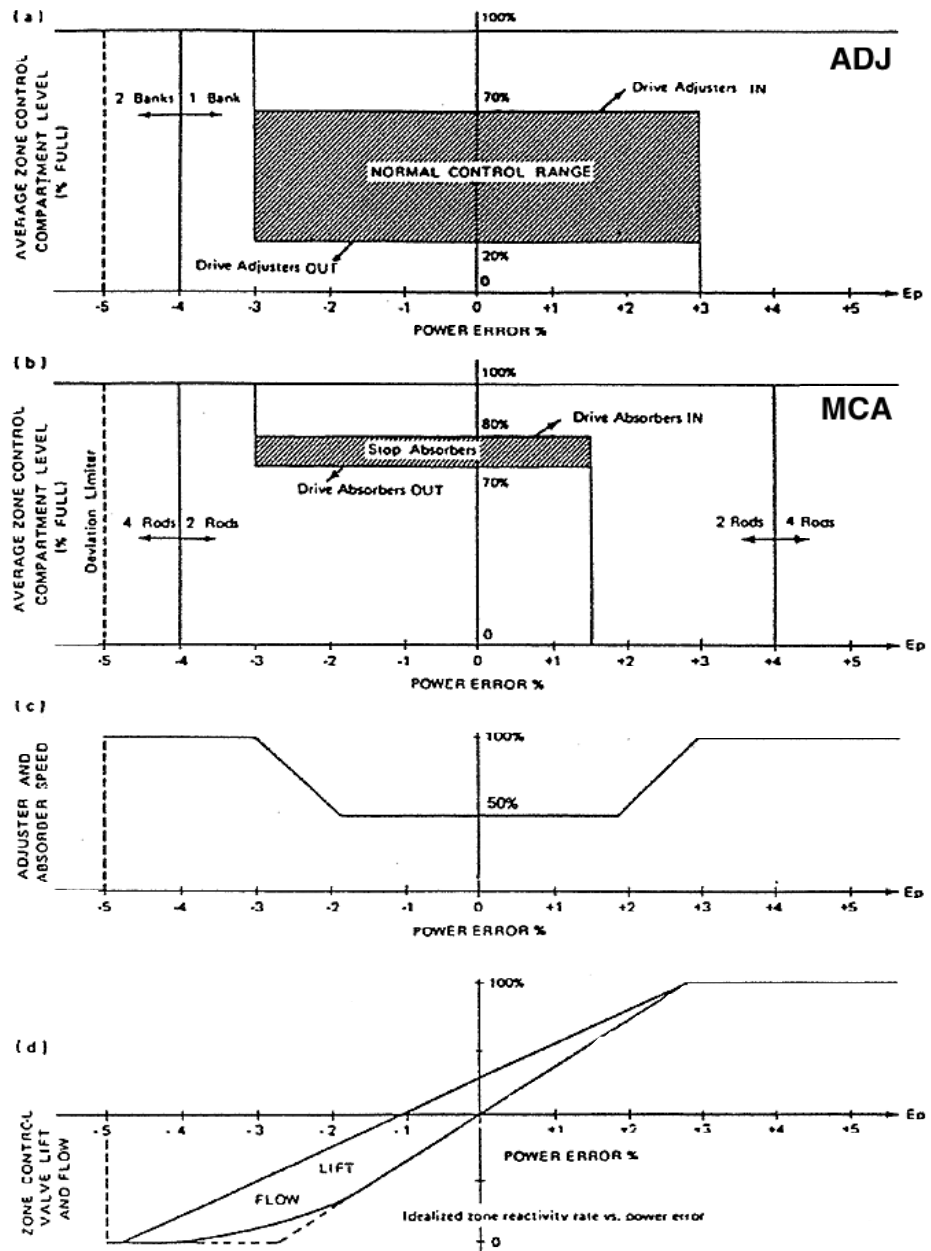
Table 1.3:

Design worths and rates of RRS reactivity devices

Device	Worth (mk)	Highest Average Rate (mk/s)
Liquid Zone Control Absorbers	7.5	± .14
Mechanical Control Absorbers	10.3	±.07*
Adjusters	15.0	±.08
Automatic Poison Addition		-.0125

*   *When dropped, the control absorbers are fully inserted in the core in about three seconds. The rate of ± .07 mk/s is that available when driven at their maximum speed.*

Fig.   1.4:

Layout of RRS and SDS reactivity mechanisms
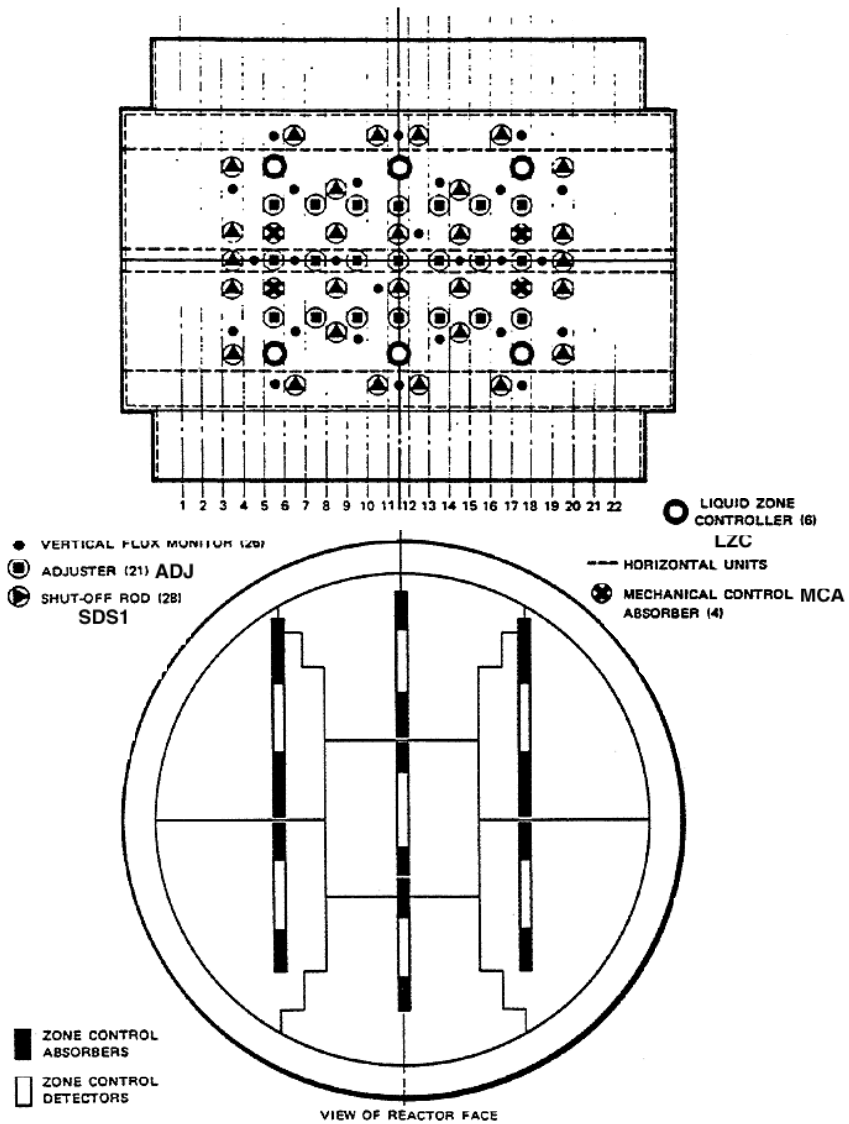
In addition to controlling reactor power the reactor regulating system monitors a number of important plant variables and reduces reactor power, if any of these variables is out of limits. This power reduction may be fast *(stepback)*, or slow *(setback)*, depending on the possible consequences of the variable lying outside its normal operating range. Stepbacks are accomplished by dropping the mechanical control absorbers, while setbacks are effected through the normal action of the control system by reducing the reactor power setpoint at a controlled rate.

The *reliability* of the reactor regulating system is of the utmost importance. The frequency of serious process failures associated with the reactor regulating system *(losses of regulation)* must be kept to a minimum. The design intent is that there be no loss of regulation during an earthquake of intensity less than or equal to the *design basis earthquake.* Both these requirements are met through the stepback function.

1.2　　　Functional requirements of RRS

The reactor regulating system (RRS) is required to:

a. Provide automatic control of reactor power to a given setpoint at any power level between 10^{-7} full power (FP) and full power. The setpoint may be specified by the operator (ALTERNATE mode) or by the boiler pressure control program (NORMAL mode, see control modes in Fig. 1.1 b).
b. Manoeuvre reactor power at controlled rates between any two power levels in the automatic control range (above 10^{-7} FP).
c. Insert or remove reactivity devices at controlled rates to maintain a reactivity balance in the core. These devices compensate for variations in reactivity arising from changes in xenon concentration, fuel burnup, moderator poison concentration, or reactor power. This requirement actually follows from (a) and (b).
d. Maintain the neutron flux distribution close to its nominal design shape, so that the reactor can operate at full power without violating bundle or channel power limits. This requirement, along with the natural spatial instability of the core, dictates the need for spatial control.
e. Monitor a number of important plant parameters and reduce reactor power quickly when any of these parameters is out of limits. Parameter limits may be specified for economic or safety related reasons.
f. Withdraw shutoff rods from the reactor automatically when the trip channels have been reset following a reactor trip on shutdown system No. 1 (SDS1).

2.0 Reactor regulating programs

This section describes the main features of the reactor regulating system programs and follows the logic of Figure 1.1 c.

2.1 Power measurement and calibration program

The reactor regulating system requires power measurements to control zone power and total reactor power. Measurements of zone power and total reactor power with minimum delay are obtained from 28 self-powered, in-core *platinum flux detectors* (Pt, two per zone). These measurements are used for *control of reactor power* (above 5% FP) and for *control of flux tilts* (above 15% FP).

Estimates of total reactor power based on the platinum flux detectors are adjusted by comparison with thermal measurements. Additionally, *vanadium flux detectors* are used to perform a *slow calibration of the platinum detectors* in each zone so that they more truly reflect average zone power.

In the *low power range*, total reactor power estimates are based on measurements from *uncompensated ion chambers with logarithmic amplifiers*. The ion chamber signals are calibrated against thermal power measurements at power levels where reliable thermal measurements are available (above 10% FP). The regulating program is designed to fail safe on irrational control signals (e.g. if at less than 15% FP the median ion chamber signal is irrational). During a reactor startup, the operator manually raises power to -6 decades at which point the computer automatically takes over control. Special software provisions facilitate a smooth transition between operator and automatic control.

In the *high power range* (greater than 5%FP), self-powered in-core flux detectors (Pt) are used to provide accurate power and flux tilt information not available from the ion chambers. The signals from the ion chambers, situated on one side of the core, depend on the concentration of poison in the moderator, and on flux tilts.

Flux measurements are obtained from (see Fig. 1.4):
a. three ion chambers (IC) located on one side of the calandria
b. fourteen pairs of in-core platinum flux detectors, one pair in each of the reactor's fourteen power zones
c. 102 Vanadium flux detectors distributed throughout the reactor core.

Ideally, power measurements shall be fast, absolute, and able to provide spatial average; spatial average means either an average over the entire reactor core or over some specific zone, depending upon the intended use of the signal. The signals originating from platinum flux detectors, although fast, do not reliably indicate average power because each detector is more or less a point and is therefore subject to local disturbances. Ion chamber measurements are strongly

influenced by poison in the moderator and platinum flux detector characteristics change with irradiation. Vanadium detectors, although accurate, are too slow ($\tau \approx 5$ min) to be directly used in the flux control loop.

The approach taken in the CANDU 600 reactors, uses ion chambers and platinum flux detectors to generate fast, approximate measurements of zone power and reactor power. These measurements generate short-term error signals to drive the zone controllers and stabilize the core. Over the long time span, these signals are slowly calibrated to agree with more accurate estimates of reactor and zone power.

2.1.1 Calibration of Reactor Power

The fast, approximate estimate of reactor power is obtained by either taking the *median ion chamber signal* (at powers below 5% FP), *or the average of 28 in-core platinum flux detectors* (above 15% FP) *or a mixture of both* (5%-15%). These signals are filtered and calibrated by comparison with estimates of reactor power based on thermal measurements from one of the following two sources:

a. Twelve pairs of Resistance Temperature Detectors (RTDs) are located on the reactor inlet and outlet headers. Each pair measures the temperature rise across the reactor. The average temperature rise generates an accurate estimate of reactor power, which is used to calibrate the platinum flux detector signals below 50% FP. Reactor thermal power is directly proportional to average primary heat transport system (HT) flow. The calculation of reactor power therefore requires an estimate of HT flow[1].

b. Above approximately 85% FP boiling commences in the channels and in the reactor outlet header. The average temperature rise across the reactor is no longer a good estimate of reactor power, and flow variations become significant. For calibration purposes, reactor power estimates above 70 % FP are therefore based on a number of secondary side measurements. Boiler steam flow, feedwater flow and feedwater temperature are measured and reactor power estimated from enthalpy/flow calculations. Secondary side measurements are used above 70% FP and RTD measurements apply below 50% FP. In the intermediate power range (50%-70% FP) a linear combination of both types of measurements is utilized as the calibrating signal.

2.1.2 Spatial calibration

Short term spatial control is based upon fast, approximate measurement of zone power obtained by taking the average of the platinum flux detectors in each zone. *Accurate estimates of average zone flux* are obtained by processing the vanadium flux detector measurements through the *flux mapping routine*. These estimates slowly calibrate the fast zone power measurements to give accurate long-term spatial control.

---

[1]   Since the regulating program in the CANDU 600 reactors does not have access to HT flow measurements, a constant value based on off-line calculations and commissioning measurements is used. In the power range of interest (below 50% FP) there is no boiling, and HT flow does not vary significantly with power.

Spatial Calibration Using Flux Mapping:

The *flux mapping* routine collects readings from 102 vanadium flux detectors distributed throughout the reactor core and *computes a best fit* of this data with respect to flux modes expected for the given core configuration. Flux mapping procedure provides an accurate estimate of average zone flux in each of the fourteen zones. These estimates are available once every two minutes (flux mapping sampling interval) and lag the neutron flux by approximately five minutes (vanadium detector time constant). Spatial calibration in a zone is done by matching the average zone flux estimate generated by flux mapping with appropriately filtered ($\tau \approx$ 5 min) zone platinum flux detector readings. This *spatial calibration is only relative* - the average of all zone fluxes is removed - so that flux mapping calibration cannot affect reactor power.

The flux mapping routine rejects individual detectors whose readings disagree with the rest of the detectors. The net result is a smoothed accurate steady state estimate of relative zone power.

2.2   Demand power routine

The demand power routine serves three functions (see Fig. 1.1 a and c):

a.   it *determines the mode of operation* of the plant,

b.   it *calculates the reactor setpoint*, and the *effective power error* that is used as the driving signal for the reactivity control devices,

c.   it *adds poison* to the moderator if required.

The source of the requested power depends upon the selected operating mode:

- In the *normal mode*, where the reactor follows the turbine, the request comes from the steam generator pressure control program. Reactor manoeuvring rate limits are built into the demand power routine. This mode will be preferred to perform turbine power manoeuvres.

- In the *alternate mode*, where the turbine follows the reactor, the requested power is set by the operator who also selects the manoeuvring rate. This mode is used on plant upsets or at low power when the steam generator pressure is insensitive to reactor power. It can also be used in steady state operations of the plant.

- In the *setback mode*, the demand power routine receives a negative manoeuvring rate from the setback routine. Should the reactor be already reducing power at a greater rate, the setback rate is ignored; otherwise the setpoint is ramped down at the setback rate.

The *effective power error* is calculated as a weighted sum of the difference between the set and measured flux powers, and the difference between the set and measured rates. If the effective power error is large, and if the rate of power increase is positive, the demand power routine adds gadolinium poison to the moderator at the normal poison addition rate. This action protects against a loss of regulation (LOR) resulting from a decreased reactivity load due to the decay of xenon, when the plant has been shut down for extended periods.

A shortage of negative reactivity is indicated by high average water level of the liquid zone controller (LZC) and/or a large positive power error. In this case the mechanical control absorbers (MCA) are driven into the core in one or two banks. In the case of a shortage of positive reactivity, indicated by low average zone controller water level or a large negative power error, adjusters (ADJ) are driven out in banks according to a fixed sequence. A *deviation limiter* contains special logic to prevent the power setpoint from exceeding 1.05 times the actual power, thus preventing power increases at large rates.

Adjusters and mechanical control absorbers are driven out at a speed proportional to power error. This reduces the normal shim reactivity rate and should enable the zone controllers to offset the inserted reactivity with minimum power disturbances (see Fig. 1.2).

Reactor Power and Manoeuvring Rate Limits
The demand power routine manoeuvres the flux set point at adjustable rates up to a maximum of 1% FP per second above 0.25 fractional full power (FFP), 4% present power per second between 0.25 FFP and 0.1 FFP, and 1% present power per second below 0.1 FFP in NORMAL mode (in ALTERNATE mode, rates below 0.1 FFP remain at 4% present power per second). All manoeuvring rates are linear above 0.25 FFP and logarithmic below 0.25 FFP. At the cross-over point, the maximum rates are equal.

The primary heat transport circuit is designed to operate with 4% quality in the reactor outlet header at full power. Boiling commences in the channels at about 85% FP. If a high manoeuvring rate is used in this region for lengthy manoeuvres, the pressure, both in the channels and in the degasser condenser begins to rise rapidly.

Simulation indicates that in the NORMAL mode, step increases in turbine load of up to 10% can be handled by the reactor manoeuvring at 1% FP/s at the high power levels. Step increases in turbine load greater than 10% are prevented by the Unit Power Regulator (UPR see Fig. 1.1 a) . For large excursions in the normal mode, the rate is determined by the turbine loading rate, its maximum being 0.15 FP/s. The reactor can maintain this rate over long periods.

2.3   Setback routine
The setback routine (see Fig. 1.1 a and c) monitors a number of plant variables and reduces reactor power in a ramp fashion if any variable exceeds acceptable operating limits. The rate at which reactor power is reduced and the power level at which the setback ends, are chosen to suit each variable. The setback clears either when the end point is reached or when the condition clears. A list of the setback parameters and their end points in given in Table 2.1.

Table 2.1:

Setback conditions

Variable	Rate	Endpoint (%FP)
High Local Neutron Flux	0.1%/s	60
Spatial Control Off Normal	0.1%/s	60
Zone Control Failure	0.2%/s	60
Low Deaerator Level	0.5%/s	2
High Steam Generator Pressure	0.5%/s	8
Manual	0.5%/s	2
High Moderator Temperature	1.0%/s	2
Low Differential Pressure Across Moderator Pumps for More Than Eight Seconds	1.0%/s	2
High Condenser Pressure	0.2%/s	30
Loss of Endshield Cooling	0.5%/s	2

2.4   Stepback routine

The *stepback routine* (STP, see Fig. 1.1 a and c) checks the values of the variables and, should a *power stepback* be necessary, opens the clutch contacts of all four mechanical control absorbers (MCA). The *absorbers fall into the core, resulting in a rapid decrease of power*. While the absorbers are dropping, the program monitors reactor power at frequent intervals and closes the clutch contacts when the power has diminished to a preset value associated with the condition causing the stepback or when this condition has cleared. To avoid possible spurious stepbacks, both computers have to request a stepback for one to occur. Should one of the computers be unavailable, its clutch contacts are opened; a stepback then occurs on the demand of the other computer. Table 2.2 is a list of plant upsets causing stepbacks, and the terminal power associated with each input.

Table 2.2:

Stepback conditions

Condition	Endpoint
Heat Transport Pump Failure	60% of Current Power
Turbine Trip, Loss of Line	60% Full Power
High Heat Transport Pressure	0%
Low Steam Generator Level	0%
High Log Rate	0%
Reactor Zone Power	0%
Reactor Trip	0%
Low Moderator Level	0%

The stepbacks on high neutron flux and high log rate serve to prevent a *loss of regulation* (LOR). In these particular cases the computers also inhibit outdrive of the adjusters until reset by the operator.

Protection Against LOR During An Earthquake
Protection against *loss of regulation during an earthquake* is accomplished by *seismic qualification of the stepback* function. Computer failure during an earthquake will be detected by the timer causing the transfer of control logic to open the digital outputs from the failed computer to the clutches and allowing the absorbers to drop in shutting down the reactor. A potential loss of regulation caused by failure of equipment other than the computer is detected by the stepbacks on high flux and/or high log rate. As the entire chain from the digital outputs to the clutch coils is seismically qualified, the stepback will operate and avert the loss of regulation.

The stepbacks on high flux and high log rate also disconnect the supply of power to the adjusters. This is done as the adjusters have a greater worth than the control absorbers and could, if spuriously driven out, add an excess of positive reactivity. Power to the adjusters is restored when the operator depresses a pushbutton located on a seismically qualified panel.

The following are also seismically qualified:
a. the platinum detectors (Pt), amplifiers and cable runs
b. the ion chambers (IC), amplifiers and cable runs
c. the computer watchdog timer
d. the absorber rod (MCA) drop logic
e. the digital outputs and associated wiring from the computer to the absorber rod drop logic
f. the transfer of control interlocks associated with the digital outputs
g. the digital output and its associated wiring to interrupt the power supply to the adjusters.

2.5 Flux mapping routine

The *flux mapping routine* (FLX, see Fig. 1.1 a and c) uses measurements from the vanadium detectors to calculate the spatial distribution of reactor power. This is done:
a. to guard against locally overrating the fuel; and
b. to calibrate the zone power detectors to properly reflect the spatial flux distribution.

The algorithm, which is outlined in the next section, is based on the assumption that the normal flux shape, and deviations from this shape due to a given set of reactivity disturbances, can be calculated from physical data. The disturbances considered include perturbations from the mechanical control absorbers, the light water zone control absorbers and the adjusters.

During situations when some or all adjusters are withdrawn to provide positive reactivity (*shim operation, startup*), the flux shape is distorted and some derating may be required. The distorted flux shape is mapped by the flux mapping routine, and a setback initiated if there is local fuel overrating. If, for some reason (high average zone level, for example) control absorbers are inserted at high power, derating is again achieved in the same manner.

The vanadium flux detector measurements are periodically calibrated when the reactor is at a power level that is accurately known and the flux shape is undistorted. This is done to offset the 4% per year deterioration of detector sensitivity with irradiation.

The operator can obtain maps of flux at selected axial locations, values of flux at the safety system detector locations, maps of channel power, and the location of peak flux in the core. A typical flux map is shown in Figure 2.3, and a channel power map in Figure 2.4.

Fig. 2.3:
Typical CANDU 600 flux map

FLUX MAP (PLANE 4)
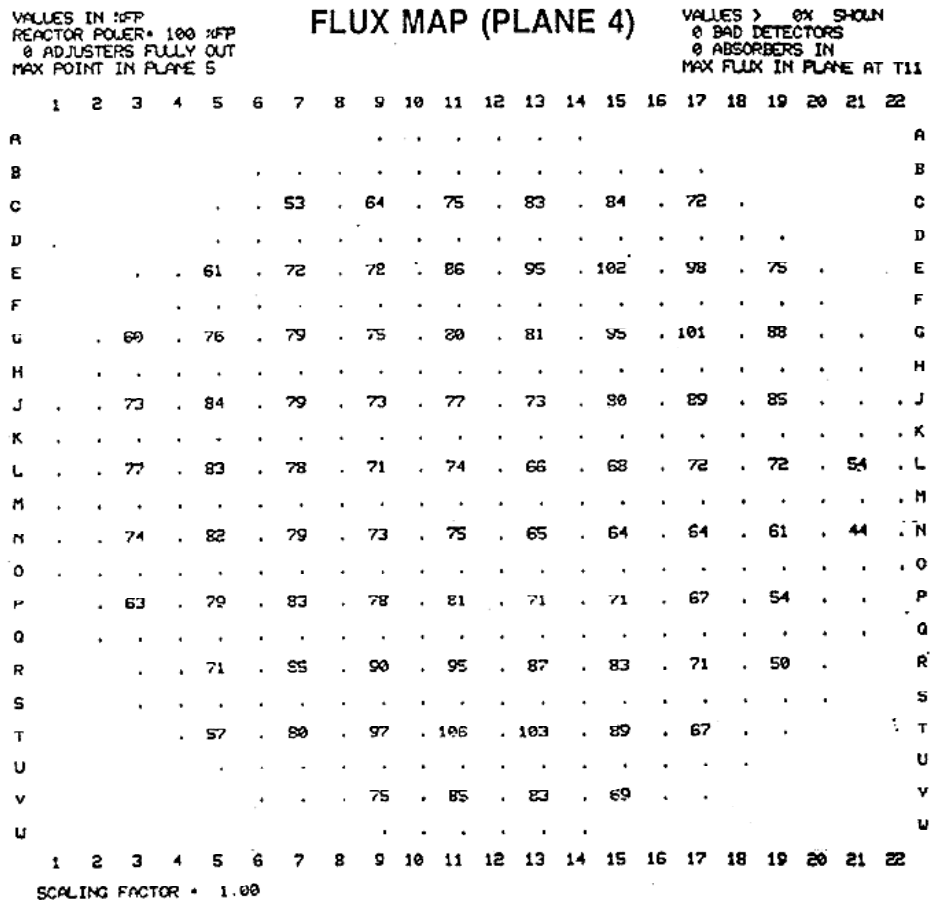
Fig. 2.4:
Typical channel power map

```
REACTOR POWER= 100 %FP        CHANNEL POWER MAP         0 BAD DETECTORS
  0 ADJUSTERS FULLY OUT                                  0 ABSORBERS IN
VALUES IN MW                                            VALUES >  0MW SHOWN
MAX CHANNEL AT S10

      1   2   3   4   5   6   7   8   9  10  11  12  13  14  15  16  17  18  19  20  21  22

A                                     2.6 2.9 3.1 3.2 3.2 3.1                                    A
B                             2.5 3.0 3.4 3.7 4.0 4.2 4.4 4.5 4.4 4.2 3.8 3.2                    B
C                         2.9 3.5 4.0 4.5 4.8 5.0 5.1 5.3 5.5 5.5 5.4 5.0 4.4 3.6                C
D                     3.2 3.8 4.5 5.0 5.4 5.6 5.8 5.8 6.0 6.3 6.4 6.3 6.0 5.4 4.5 3.7            D
E                 3.2 4.0 4.7 5.4 5.8 6.1 6.2 6.3 6.3 6.4 6.6 6.8 6.8 6.5 6.0 5.3 4.4 3.4        E
F                 4.0 4.9 5.5 6.0 6.4 6.5 6.5 6.3 6.4 6.4 6.5 6.7 6.8 6.6 6.2 5.6 4.9 3.9        F
G             3.7 4.7 5.6 6.1 6.5 6.8 5.8 6.7 6.5 6.5 6.5 6.3 6.5 6.6 6.5 6.1 5.7 5.1 4.3 3.3    G
H             4.3 5.4 6.3 6.6 6.9 7 1 7.0 6.8 6.5 6.5 6.4 6.1 6.2 6.3 6.2 5.9 5.5 5.1 4.4 3.4    H
J   3.5 4.8 6.0 6.7 7.0 7.1 7 2 7.1 6.9 6.5 6.5 6.3 5.9 5.9 5.8 5.7 5.5 5.2 4.9 4.3 3.4 2.4    J
K   3.8 5.2 6.3 7.1 7.2 7.3 7.3 7.2 6.9 6.5 6.3 6.0 5.6 5.5 5.4 5.2 5.0 4.7 4.6 4.0 3.2 2.4    K
L   4.0 5.4 6.5 7.3 7.5 7.5 7.5 7.2 6.9 6.5 6.3 5.9 5.5 5.2 5.0 4.8 4.6 4.4 4.2 3.7 3.0 2.2    L
M   4.0 5.3 6.5 7.4 7.6 7.6 7.6 7.3 7.0 6.5 6.3 5.8 5.4 5.1 4.8 4.6 4.4 4.1 3.9 3.4 2.7 2.0    M
N   3.7 5.1 6.3 7.2 7.5 7.6 7.6 7.4 7.1 6.6 6.4 6.0 5.4 5.1 4.8 4.5 4.3 4.0 3.6 3.1 2.5 1.8    N
O   3.4 4.7 5.9 6.9 7.4 7.6 7.6 7.5 7.2 6.8 6.6 6.2 5.6 5.3 4.9 4.6 4.3 3.9 3.5 2.9 2.2 1.6    O
P       4.2 5.3 6.3 7.0 7.4 7.6 7.5 7.3 7.0 6.9 6.5 5.9 5.5 5.2 4.8 4.3 3.8 3.2 2.6 2.1        P
Q       3.6 4.6 5.6 6.3 6.9 7.4 7.5 7.5 7.2 7.1 6.8 6.2 5.9 5.5 5.0 4.3 3.6 3.0 2.4 1.7        Q
R           4.0 4.9 5.7 6.5 7.2 7.5 7.6 7.5 7.5 7.2 6.7 6.3 5.9 5.2 4.4 3.6 2.9 2.3            R
S           3.2 4.2 5.0 6.0 6.8 7.4 7.7 7.8 7.6 7.4 7.2 6.7 6.1 5.3 4.4 3.5 2.7 2.0            S
T               3.4 4.3 5.3 6.2 6.9 7.3 7.5 7.4 7.2 7.1 6.6 6.0 5.1 4.2 3.3 2.5                T
U                   3.5 4.4 5.3 6.0 6.5 6.2 6.8 6.6 6.5 6.0 5.4 4.5 3.6 2.8                    U
V                       3.2 4.1 4.8 5.3 5.7 5.8 5.7 5.5 5.0 4.5 3.7 2.8                        V
W                               3.9 4.2 4.4 4.4 4.1 3.7                                        W

      1   2   3   4   5   6   7   8   9  10  11  12  13  14  15  16  17  18  19  20  21  22

SCALING FACTOR = 1.00      CALIBRATION FACTOR =  9.785
```

2.6   Flux mapping algorithm

Flux mapping is based on the premise that any spatial flux distribution $\phi(r)$ which can be achieved in the reactor, can be approximated by a flux $\phi_{MS}(r)$ obtained by a procedure called *modal synthesis* (see lesson 7). The procedure consists in superposing high harmonic perturbation modes to the fundamental mode which corresponds to the time average flux distribution. The superposition is done using a linear combination of basis orthogonal functions called λ-modes $\phi_j(r)$:

$$\Phi\left(r\right) \approx \Phi_{MS}\left(r\right) = \sum_{j=1}^{NM} A_j \, \Phi_j\left(r\right)$$

where A_j is the amplitude of the jth mode $\phi_j(r)$. Using a least squares technique, modes are fitted to the readings from the vanadium flux detectors in order that the spatial flux distribution can then be synthesized. Zone average fluxes, in particular, can be estimated by using the appropriate linear combination of mode amplitudes.

To fit the modes from the 102 readings of the vanadium detectors which are distributed through the reactor core, we must estimate the mode amplitudes A_j from the vector [D] of measured flux at the detector sites r_{di}. Thus, we would like to solve for the vector [A] in the equation:

[D] = [M] {A}

where $[M]_{ij} = \phi_j (r_{di})$. Since the number of detectors is larger than the number of modes, the matrix [M] is not invertible. The generalized inverse of M given by $([M]^T [M])^{-1} [M]^T$ is used instead and gives a least squares fit of flux at the detector sites. The amplitude vector [A] is then calculated as:

$[A] = ([M]^T [M])^{-1} [M]^T [D]$

and the solution is sorted in the on-line reactor control computer. A special feature in the flux mapping algorithm is an error detection/correction routine which rejects anomalous detector readings (assumed failed), and recalculates the flux map. This gives improved immunity to detector failures. Simulation of mapping with failed detectors indicates that the mapping algorithm is tolerant of up to ten randomly distributed failed detectors.

The number of flux modes is kept to a minimum for the concept to be practical. A restricted set of lower-order reactor eigenfunctions (i.e., λ-modes of the steady-state reactor diffusion equation), supplemented by specific perturbation modes (for particular device configurations) gives acceptable performance. Measurements at operating stations indicate flux errors (differences between calculation and measurement) of less than 5% overall.

Flux mapping provides an accurate three-dimensional picture of the relative power (neutron flux) distribution in the CANDU 600 reactor. The following on-line flux information is available to the operator on request:
- flux at the site of each mapping detectors, of each ROP safety detector and at 500 selected fuel bundle sites in the high power region of the core;
- axially integrated flux for all fuel channels and average flux in each spatial control zone.

2.7 Reactivity control and flux shaping principles

The functions of *reactivity control and flux shaping* are performed by the light water zone control absorbers, the adjusters and the mechanical control absorbers.

The primary method of short term reactivity control is by varying the levels in the 14 light water zone control absorbers. Normally, adjusters are fully inserted, mechanical control absorbers are fully withdrawn, and the average zone level is between 20% and 70% full. The light water zone control absorbers program converts the calculated (by the demand power routine) power errors into lift signals to the light water zone control valves. The total lift signal to a given light water zone control valve consists of a signal proportional to the effective power

error, a differential component proportional to the zone level error, plus a constant value (bias), which correspond to the valve lift required to maintain constant level in a zone controller compartment.

Bulk and Spatial Reactivity Control
CANDU reactors require spatial control due to loosely coupled core. For an equilibrium core at full power, the reactor is close to neutral stability - the feedback of fuel temperatures, coolant density and moderator temperature almost cancel each other. This section will describe in more detail the calibration of the fast acting platinum flux detectors and how the *calibrated measurement is used in the control of bulk and zone powers*.

The requirement for spatial control necessitates distribution of sensors and reactivity devices throughout the core. The sensors are self-powered platinum and vanadium detectors. The main reactivity devices (and the only one used for spatial control) are the 14 light water zone control compartments located in six vertical assemblies in two axial planes of the reactor (see Fig. 1.4). Light water is a very strong absorber of neutrons in CANDU reactors. Water is forced into these compartments by pumps through individual control valves. The cover gas in the compartments is pressurized to provide a constant outflow from each compartment. Varying the valve lift alters the rate of change of the amount of water in the compartment and thus alters reactivity.

For control purposes the reactor is divided into 14 zones of approximately equal power (see Fig. 1.4). A zone controller and two platinum detectors are located in each zone. The detector readings are compared, and if sufficiently close, are averaged to provide an estimate of zone power. If the readings differ significantly, the higher is taken as indicating zone power. The zone powers are then averaged to form an estimate of bulk power. As the platinum detector signals lag fuel power, and are not absolute, they require calibration.

About 94.4% of the total response is sufficiently rapid for use in control. The remainder is slow. To provide a fast measure of reactor power, the detector output is multiplied by a factor of 1.06 (1/.944 to compensate for the prompt fraction being less than unity) and a corrective term ADAF subtracted.

ADAF is derived as follows: the platinum detector readings for the 14 zones are averaged to form a quantity PDA. PDA is then filtered by a 20 second time constant to approximate the thermal and hydraulic delays between fission heat and steam generation in the boilers. The filtered output is subtracted from an estimate of average boiler power to yield a quantity ADA. ADA, filtered by a three minute time constant, gives ADAF. This time constant is chosen to suppress noise, to smooth out relatively quick transients and yet make ADAF change slowly compared with the dynamics of the flux control loop so as not to affect stability.

If P_{LIN} is the calibrated linear power based on platinum detectors then
$$P_{LIN} = 1.06 \, P_{DA} + A_{DAF}$$

The process is illustrated in Figure 2.5. Boiler power is calculated for each of the four boilers as:
$$PBi = WSiC \, (HS - HF) + WFi \, (HF - HFW) \, / \, PBin$$
where,

WSiC is the calibrated steam flow from boiler
= WSi x KSi where WSi is the uncalibrated steam flow from boiler and KSi = WFi / WSi is the calibration factor which is calculated off line, when the plant is in steady state.

HS is the steam enthalpy in kJ/kg at nominal boiler pressure and 0.25% wetness

HF is the enthalpy of saturated liquid at nominal boiler pressure

WFi is the sum of the feedwater flow to boiler and one quarter the total reheater drains flow

HFW is the enthalpy of the feedwater in kJ/kg calculated as -21.58 + 4.36 x feedwater temperature in °C at inlet to boiler

PBin is the nominal thermal power generated at full power in each boiler.

KSi makes the steam flow out of the boiler equal to the total feedwater flow when the plant is in the steady state and compensates for any errors in calibrating the elbow taps used for steam flow measurement.

Fig. 2.5:
*Bulk power measurement at high power*
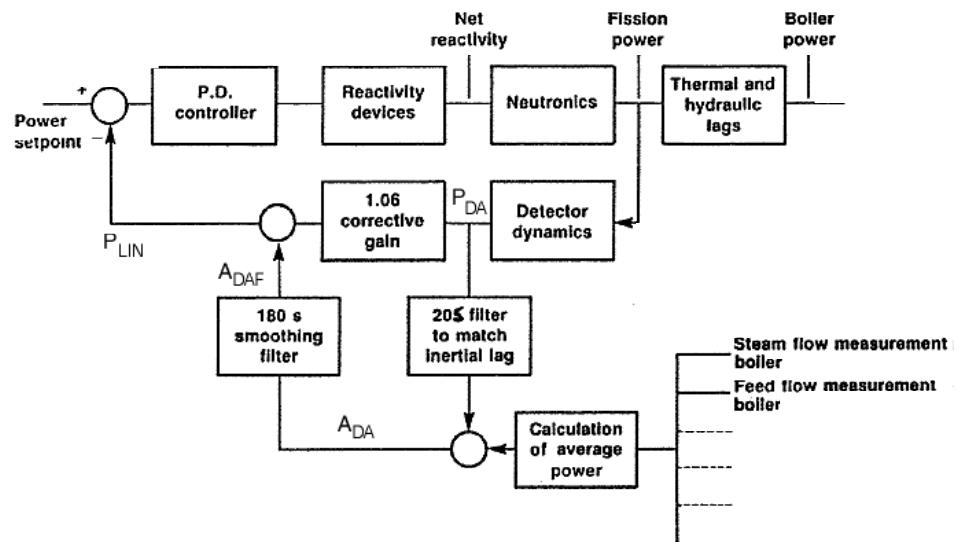
Figure 2.6 shows the bulk control loop. An effective power error is computed as the weighted sum of the error between flux and its setpoint and the rate of change of flux and its setpoint. Control is implemented by making zone controller valve lift proportional to power error.

Fig. 2.6:
The flux control loop (for bulk control)
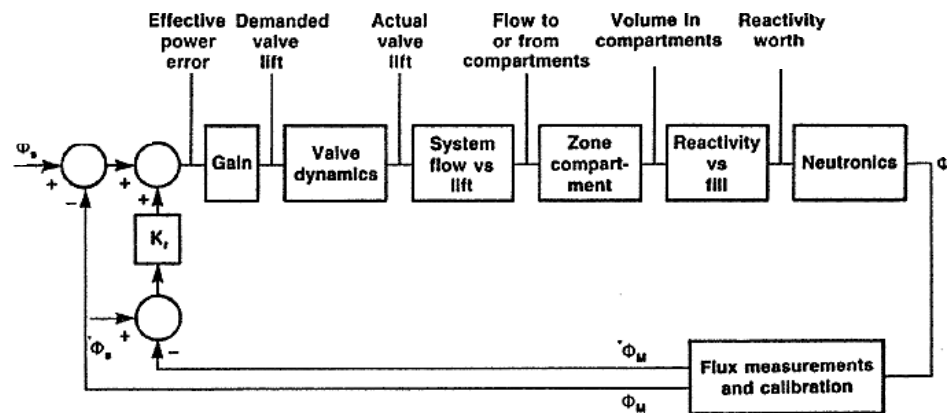
Tilt control is similar but the measure of tilt is derived quite differently. The flux mapping routine computes the average power Φ_i in each of the 14 zones, and normalizes them by dividing each by the nominal value of power for that zone, ϕ_{inom}. Call the normalized values ϕ_{in}.

The uncalibrated zone powers are each multiplied by a factor of 1.06 and filtered with a 325 second time constant to provide signals of zone power, P_{iuF} (the F indicating filtered), calculated from the platinum detectors, but having dynamics similar to those of vanadium detectors. An additive calibration A_{Di} is computed for each zone, as:

$$A_{Di} = \phi_{in} - P_{iuF}$$

Let $\overline{AD}$ be the average of the good values A_{Di}. Call the differences between each calibration term and the average A^*_{Di}. Thus $A^*_{Di} = A_{Di} - \overline{AD}$. A^*_{Di} is filtered with a 180 second time constant for the same reasons as ADA was filtered in the bulk calibration process, and the individual calibrated zone powers Pic calculated as:

$$P_{ic} = 1.06 P_{iu} + A^*_{DiF} + A_{DAF}$$

where A^*_{DiF} is the filtered value of A^*_{Di}, and A_{DAF} the bulk calibration correction term.

The process is shown in Figure 2.7. Tilt is calculated as $P_{ic} - P$, where P is bulk power. The tilt control is similar to bulk control - a tilt error is calculated as $P_{ic} - \overline{P_{ic}}$ (the bar indicating an average over the 14 zones) and the tilt valve lift for zone i calculated proportional to tilt error.

Fig. 2.7:
Zone power calibration
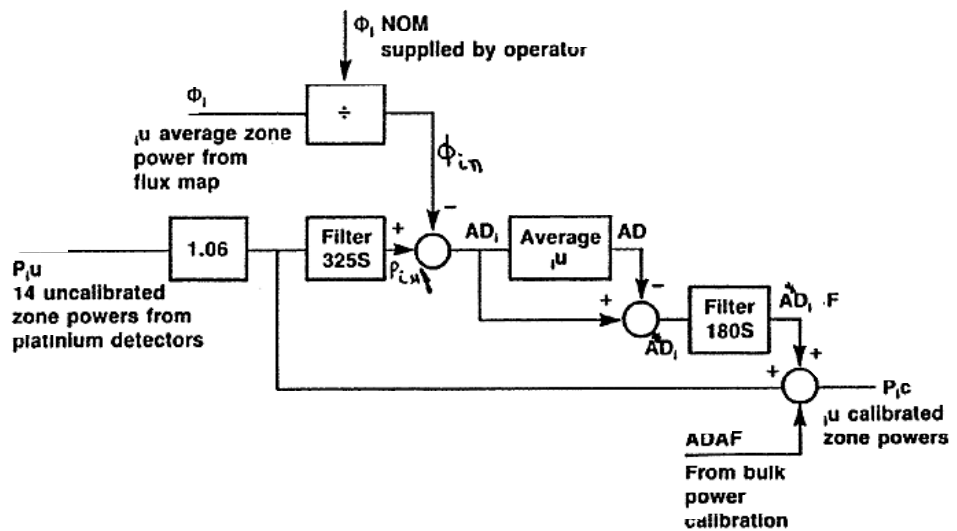
The total valve lift to a compartment is the sum of:
a. a bias term to make inflow equal to outflow,
b. the bulk lift proportional to effective power error,
c. a tilt lift proportional to tilt error.

The *flux loop must handle perturbations caused by burn up, refuelling and xenon transients*. The zone control system has ± 3 mk available. Burn up is about 0.4 mk/day. Refuelling provides about 0.25 mk for an eight bundle shift. Xenon perturbations are much larger. To provide some xenon override capability, CANDU 600 reactors have 21 adjusters in core. Their withdrawal provide about 17 mk. The adjusters are designed to flatten the core flux, allowing higher bulk power for a given peak flux (see lesson 7). CANDU 600 reactors also have control absorbers normally out of core, that can be dropped or driven in to provide additional negative reactivity. Like the adjusters they are equipped with variable speed drives. The adjusters and absorbers are used for bulk control only.

The regulating system calls upon these devices when it finds itself unable to adjust reactivity at the required rate or depth. Low average zone controller level indicates a dearth of reactivity: as average zone level drops, first the absorbers and then the adjusters are driven out of the core. Conversely, high average zone level indicates a surfeit of reactivity: as average zone level rises, first the adjusters and then the absorbers are driven in.

If the regulating system is not supplying reactivity at the required rate, the power error builds up. The speed of adjuster and absorber drive is proportional to the absolute value of the effective power error. Ultimately the power error

determines device drive - at high positive power errors the adjusters and absorbers are driven in. At large negative values of power error the absorbers and adjusters are driven out. At very large negative power errors, two banks of adjusters are driven simultaneously. Figure 1.2 shows how all the bulk flux controls operate.

3.0   Actions of the Reactivity Control Units

Three types of reactivity devices, as described below, together with moderator poison addition and removal, are used for reactor control. In addition, it should be noted that withdrawal of the safety system shutoff rods is carried out under computer control by the Reactor Regulating system. In this section we will describe the actions of the different reactivity control units.

3.1   Light water zone control absorbers

The light water zone control absorbers (LZC) are the primary devices for control of reactivity. Six tubes within the reactor core (see Fig. 1.4) contain 14 compartments into which the light water is introduced. The quantity of water in each compartment is controlled by manipulating the compartment's inlet valve. The water is forced out of the compartment at a constant rate by the helium cover gas pressure. Figure 3.1 shows a liquid zone control unit.

Fig. 3.1:
Liquid zone control unit
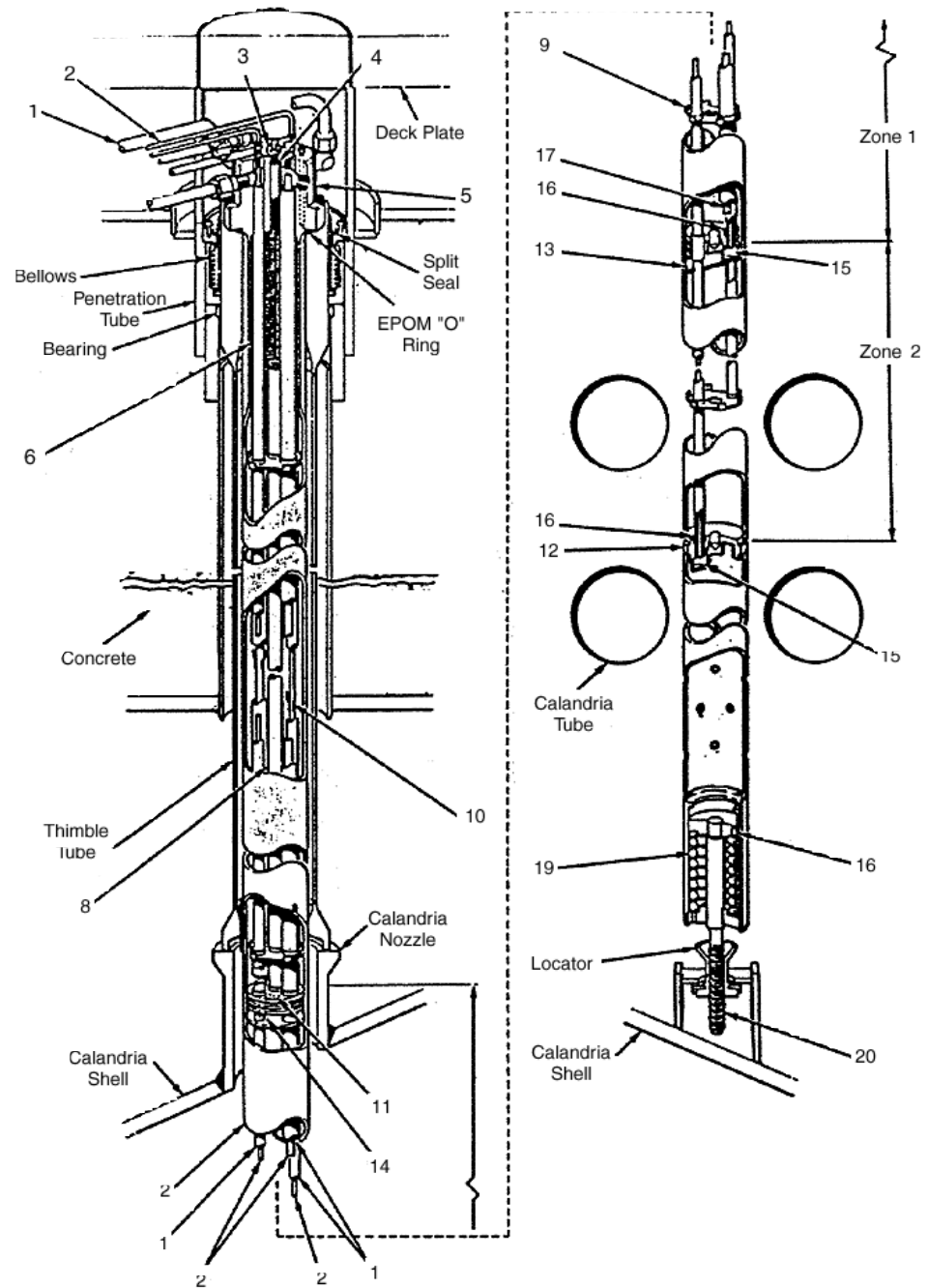
1	Water	2	Helium	3	Nut
4	Crush Washer	5	Terminal Block	6	Shield Plug
7	Zone Control Tube	8	Water and Helium Tubes	9	Tube Support
10	Tube Spring	11	Water Inlet	12	Bulkhead
13	Baffle	14	Helium Outlet	15	Helium Inlet
16	Water Outlet	17	Helium Balance Line	18	Key
19	Spring	20	Locator Thread		

The difference in reactivity between all compartments empty and full is about
7.5 milli-k. The rate of change of reactivity when all 14 absorbers are filling or
draining in unison at their maximum rate is about ± 0.14 mk/second.

A typical compartment and its connection to the remainder of the system is shown in Figure 3.2. Each water pump and helium compressor is capable of supplying the requirements of the system. A tank provides a five-minute delay for the decay of 0-19 and N-16 to acceptable levels. Hydrogen and oxygen produced in the helium by radiolytic dissociation are combined in the recombination unit.

*Fig. 3.2:*
Liquid zone control system
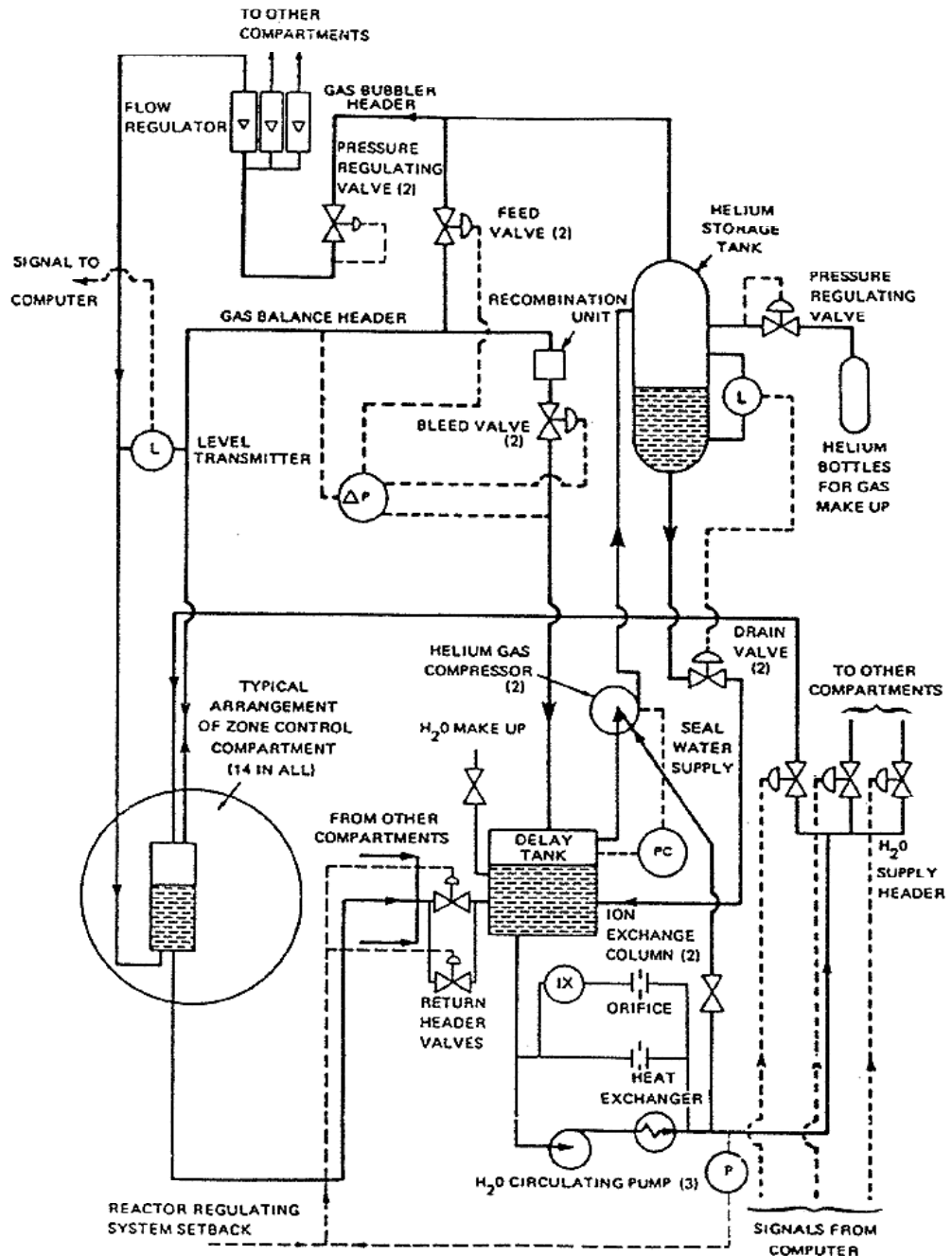
3.2 Mechanical control absorbers

The four mechanical control absorbers are mechanically similar to shutoff rods, but controlled by the regulating system. They can be driven in or out at variable speed, or they can be dropped under gravity by releasing a clutch. These absorbers are normally out of the core, and are driven in to supplement the negative reactivity from the light water absorbers, or are dropped to provide a fast reactor power reduction (stepback). The mechanical control absorbers have sufficient reactivity worth to compensate for the fresh fuel temperature coefficient of reactivity on shutdown from full power. The control absorbers also prevent the reactor from going critical on shutoff rod withdrawal. This is to enable the first shutdown system to be repoised before criticality.

The reactivity change when all absorbers go from the fully inserted to the fully withdrawn state is approximately 10 mk. The average reactivity rate when driving the rods at full speed is ± 0.07 mk/s. When dropped, the rods take approximately three seconds to go fully in. By re-energizing the clutch while the rods are dropping, a partial insertion to any intermediate position can be achieved. Figure 3.3 shows a control absorber unit.

Fig. 3.3:
*Shutoff and control absorber unit*

December 1995
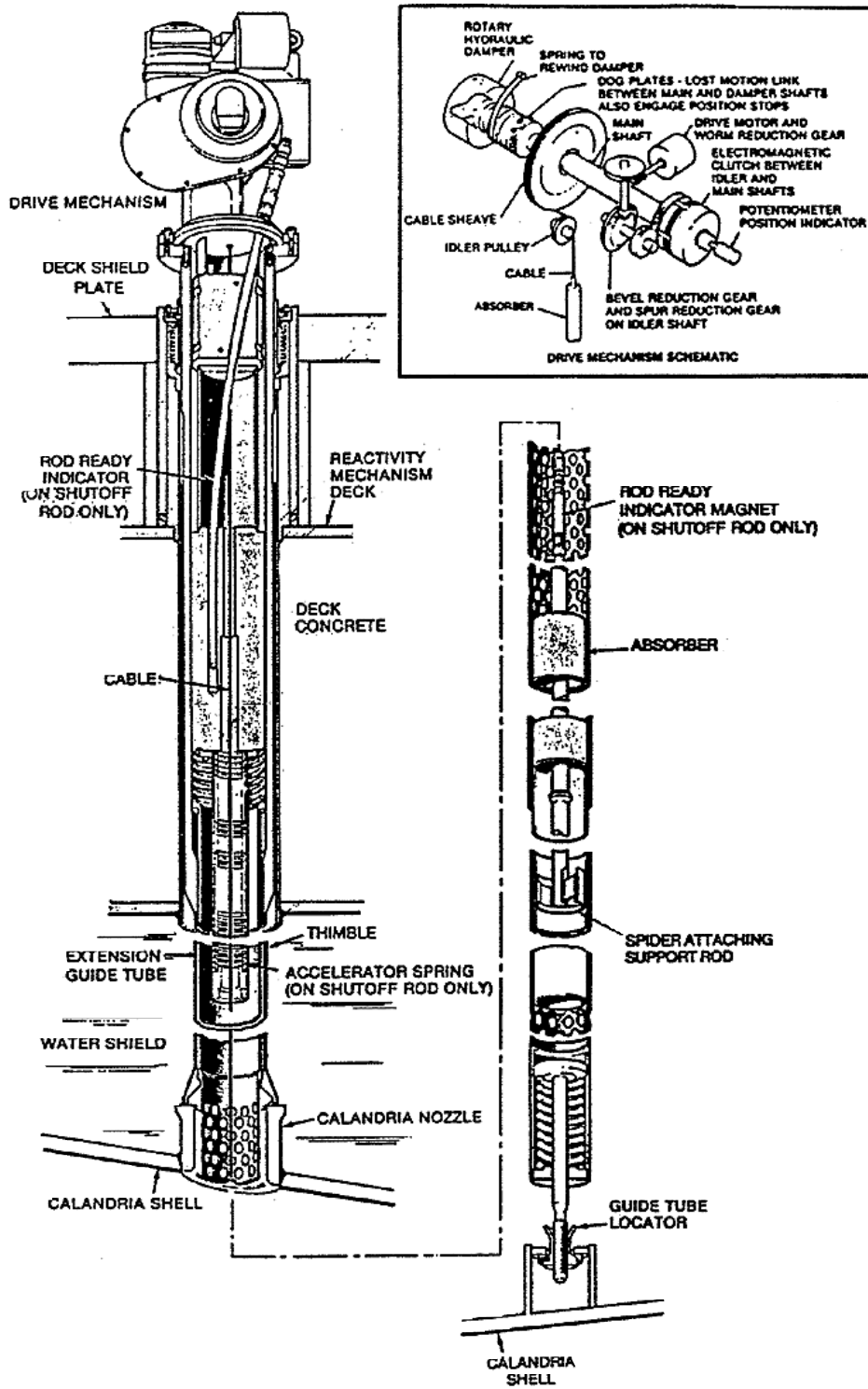
3.3 Adjusters

The reactor has 21 *adjuster rods* normally fully inserted for flux shaping purposes, capable of being driven in and out at variable speed to provide reactivity shim as required by the control system. The adjusters are normally driven in banks, the largest bank containing five rods.

The reactivity change when all adjusters go from the inserted to the withdrawn state is approximately 15 mk. The average reactivity rate when two banks of adjusters are driven at full speed is approximately ± 0.08 mk/s. Figure 3.4 shows an adjuster unit.

Fig. 3.4:
Adjuster unit
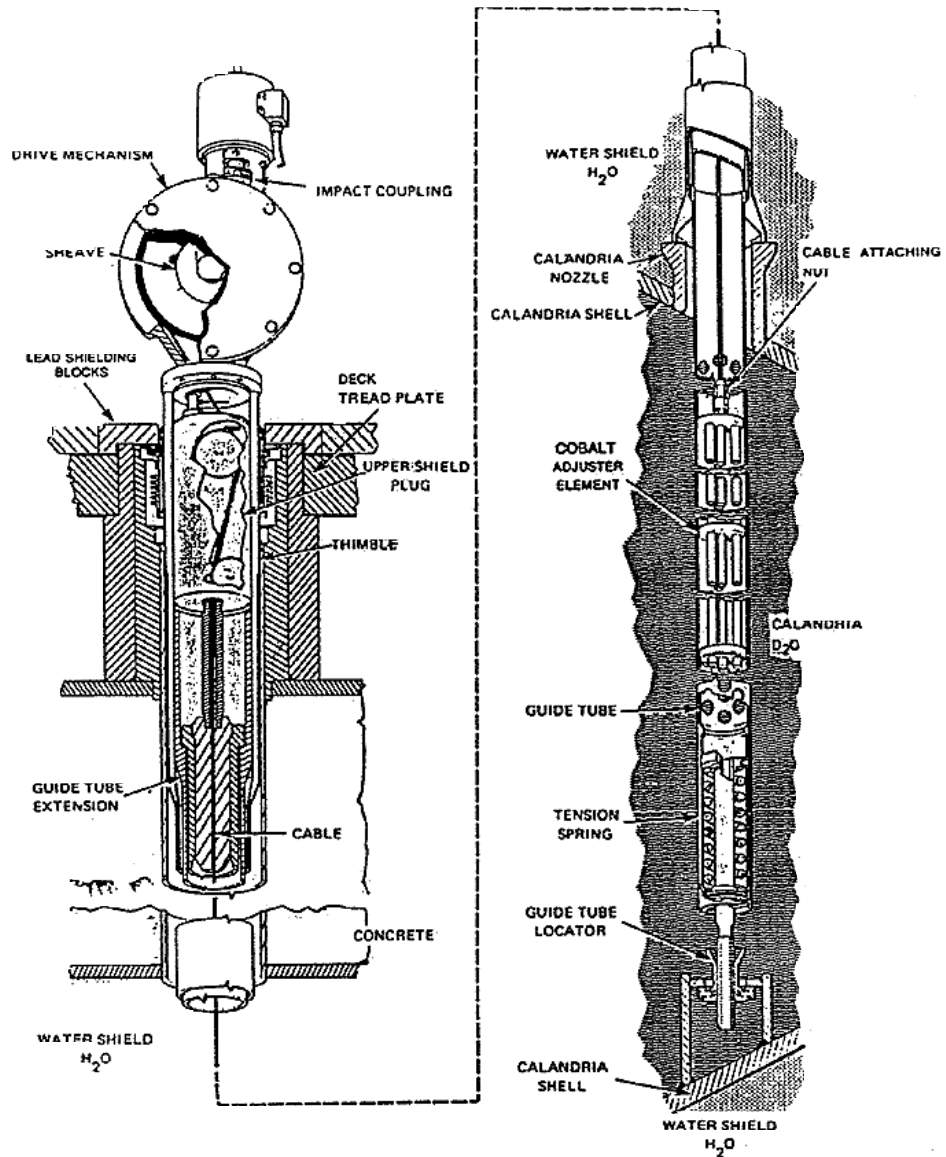
3.4   Poison addition and removal

A *reactivity balance can be maintained by the addition of soluble poison to the moderator*. *Boron* is used to compensate for an excess of fresh fuel as it does not burn out rapidly. *Gadolinium* is added when the xenon load is significantly less than equilibrium (as happens after prolonged shutdowns).

An *ion exchange system removes the poisons from the moderator*. Addition and removal of poison is normally done by the operator. The reactor regulating system does, however, have the capability of adding gadolinium, if needed, to compensate for gross errors in the reactivity balance.

3.5   Hardware interlocks

The reactivity mechanisms are subject to a number of interlocks external to the control computers (see Fig. 1.1 c) to limit the consequences of a gross loss of regulation.

When the reactor is in a tripped state (either SDS1 or SDS2 not *poised*), the adjusters and mechanical control absorbers are inhibited from being withdrawn, and poison removal is prohibited, to prevent the addition of positive reactivity. The same devices are similarly inhibited until a sufficient number of shutoff rods have been fully withdrawn to prevent the reactor from being started up with insufficient shutdown capacity available.

The adjusters are further interlocked to prevent more than a limited number of high worth adjusters from being withdrawn at the same time. This is to limit the maximum rate of addition of positive reactivity. With the exception of the light water zone controllers, which are controlled only from the computer, the reactivity control units (the adjusters and the mechanical control absorbers) can also be manually controlled from the control room panel. When manual mode is selected, the mechanisms are unavailable to the reactor regulating system (except for the drop function of the control absorbers which always remains available for a stepback).

3.6   SDS1 and SDS2

Although not part of the reactor regulating system, two more reactivity control devices should be mentioned. These are the *shutoff rods associated with* SDS1 and the *liquid injection nozzles associated with* SDS2 and basically control reactivity in one direction only.

Fig. 3.5:
General layout of SDS1 and SDS2
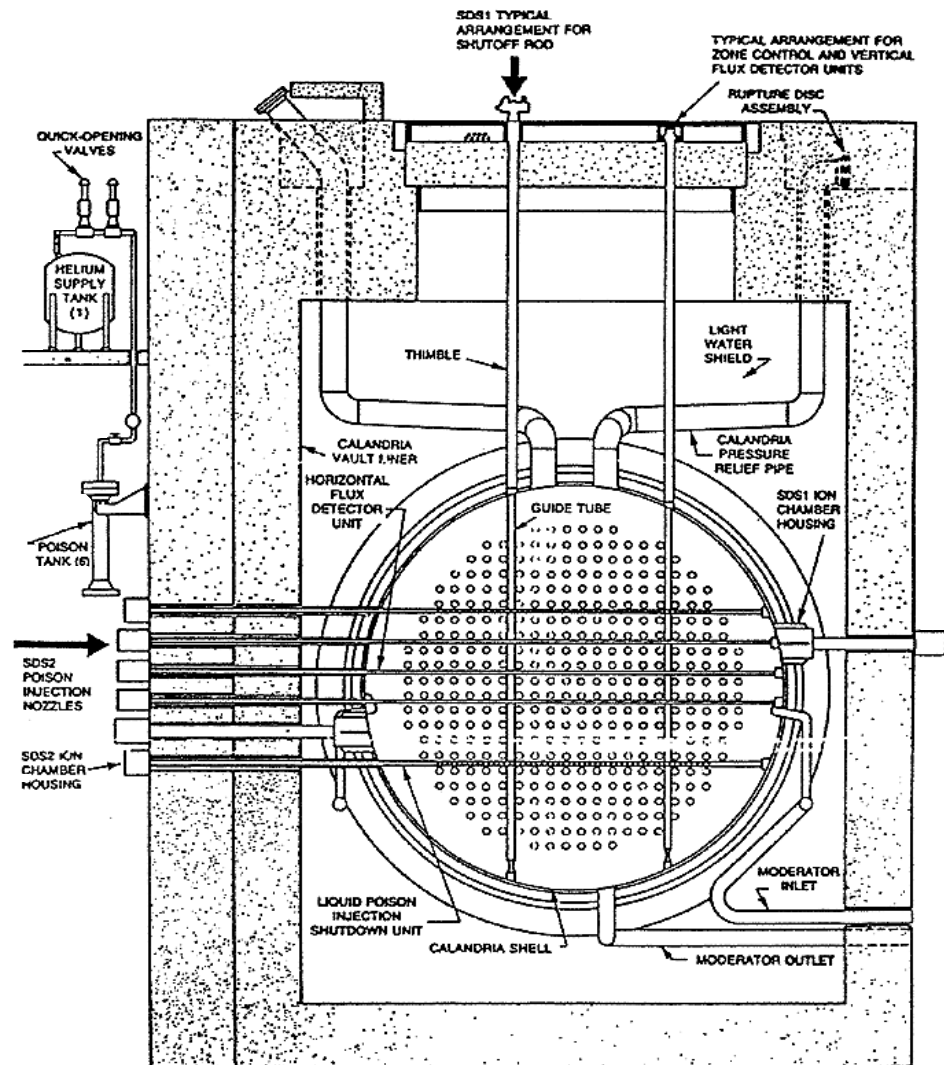
3.6.1   SDS1 Shutoff Rods
The SDS1 shutoff rods utilizing cadmium absorber elements are provided to quickly shut down the reactor under normal and emergency conditions. The rods, being diverse in design principle and orientation from SDS2, hang above the core, suspended from the reactivity mechanisms deck. Typical locations are shown in Figure 1.2 for CANDU 600 reactors which use 28 rods. The absorber elements fall into the reactor under gravity, inside a perforated zirconium alloy guide tube within the core, in response to a shutdown signal. A helical *spring* secured to the top of the thimble is compressed in the rod's parked position, *to provide* it with *initial acceleration upon release*. Typical shutoff rod construction is illustrated in Figure 3.3.

The stainless steel cable that suspends the cadmium absorber element, is wound on a cable sheave inside the shutoff rod drive mechanism. This mechanism is mounted on top of the reactivity mechanism deck directly above the absorber. The vertical location of the absorber element is determined from a position indicator, fastened to the sheave shaft. In addition, a set of reed switches, actuated by a magnet in the top of the shutdown element, signals when the element is in the up or *poised* position. The cable sheave is driven by an electric motor through a gear train, engaged by an electromagnetic friction clutch. When the clutch is de-energized the sheave is released and the element falls, unwinding the cable. When the clutch is energized, the element may be motor-driven in or out. Shutoff rod withdrawal is normally done under control of the reactor regulating system. Thus the shutoff rods can be considered as providing reactivity control as part of the reactor regulating system when being operated this way. When the clutch is released, the drive is disconnected from the sheave and the motor drive so the regulating system cannot influence the safe operation of the shutdown system.

3.6.2 SDS2 liquid injection shutdown system

The second shutdown system operates by injection of the neutron absorber, gadolinium, directly into the moderator. Figures 3.6 and 3.7 show a schematic of the liquid injection system and location of the injection nozzles respectively for CANDU 600 reactors. The Zircaloy-2 nozzles penetrate the calandria horizontally and at right angles to the fuel channels. A solution of gadolinium nitrate in heavy water forms the poison that is injected from each nozzle. Holes are drilled in the nozzle along its length to form four rows of jets which inject the poison upward, downward, and to the sides. The poison solution is stored in the cylindrical tanks mounted vertically on the outside wall of the reactor vault. Each tank is connected to its own nozzle by piping which traverses the vault and shield tank.

Fig. 3.6:

Liquid injection shutdown system
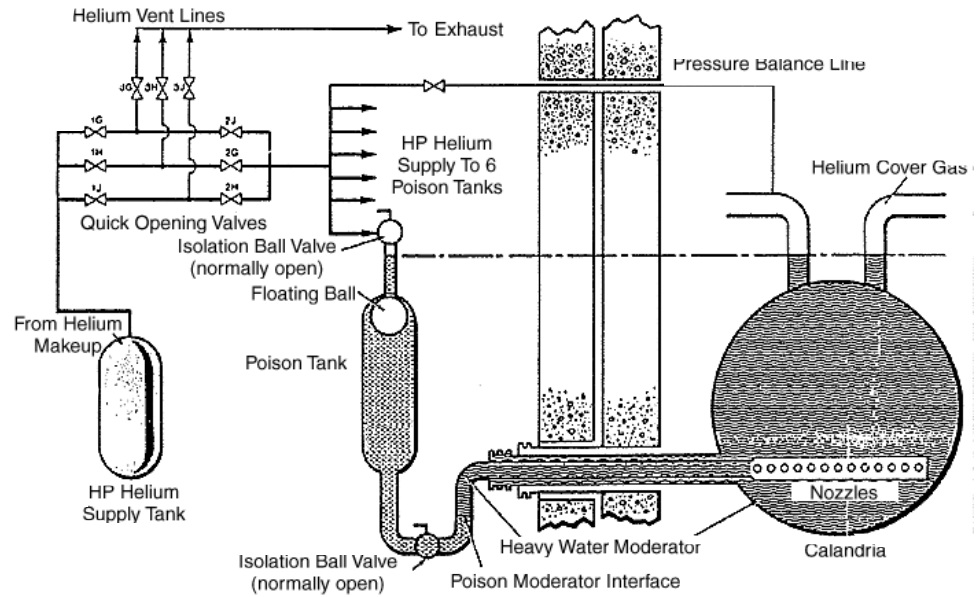
Fig. 3.7:

Location of horizontal reactivity devices
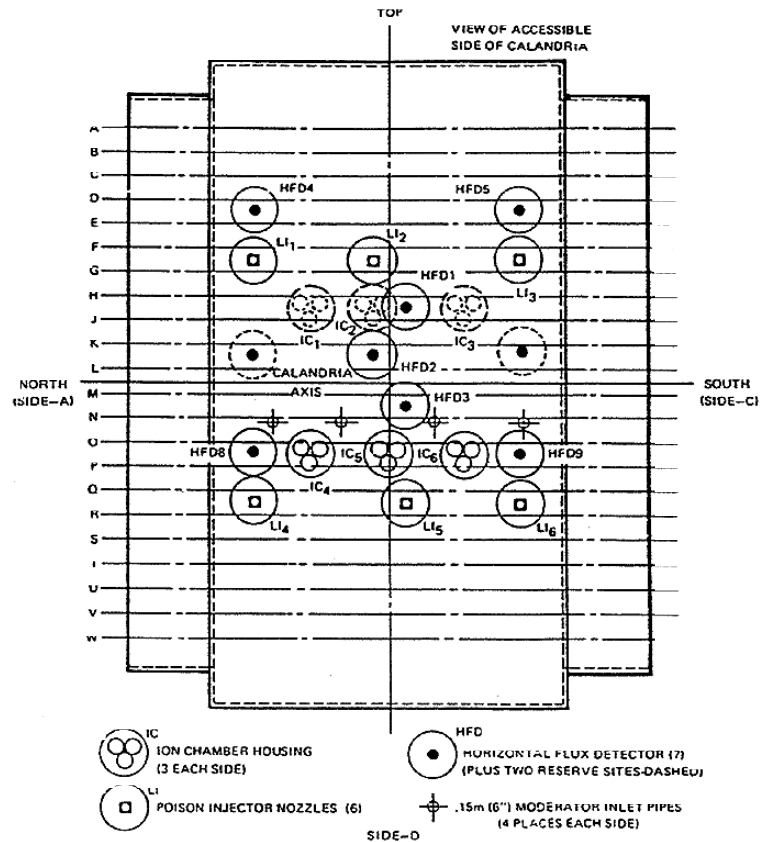
A small diameter pipe is routed from the top of each poison tank to a helium header and thus to a pressurizer helium tank. With a normal operating pressure of 8.27 MPa(g), this tank supplies the source of energy for a rapid injection. Typically the header is isolated from the helium tank by six quick-opening valves which are mounted in a triplicated array.

A small line with a valve connects the helium header to the moderator cover gas. Any small leak from the helium tank to the header cannot influence poison level which will stay equal to that of the moderator in the calandria relief ducts. A polyethylene ball floats at the top of the poison tank. On firing it is swept to the bottom of the tank where it seats, preventing helium leaking into the calandria. This prevents the calandria relief duct bursting disks from failing. As an added precaution, a volume tank is connected to the calandria and relief ducts to increase the helium volume. Each poison tank can be isolated for maintenance or sampling using two valves, one on the helium side and one on the liquid side. The former valve protects the operator in case a firing occurs during maintenance. The latter valve prevents loss of heavy water. Both valves require a key for closure; a key that cannot be removed while the valve is closed. A key interlock arrangement provides a warning should more than one poison tank be unavailable at a time.

4.0   Control Instrumentation

Neutron flux in a CANDU reactor spans numerous decades. *Flux in a fresh core prior to first criticality is approximately* 10^{14} *times lower than flux in an equilibrium core at full power*. Because of this large range, different types of instruments are required depending on the power level (see Figure 4.1). These measurements are required both for control of reactor power and for reactor protection.

Fig. 4.1:
Range of sensitivity for reactor power measurement
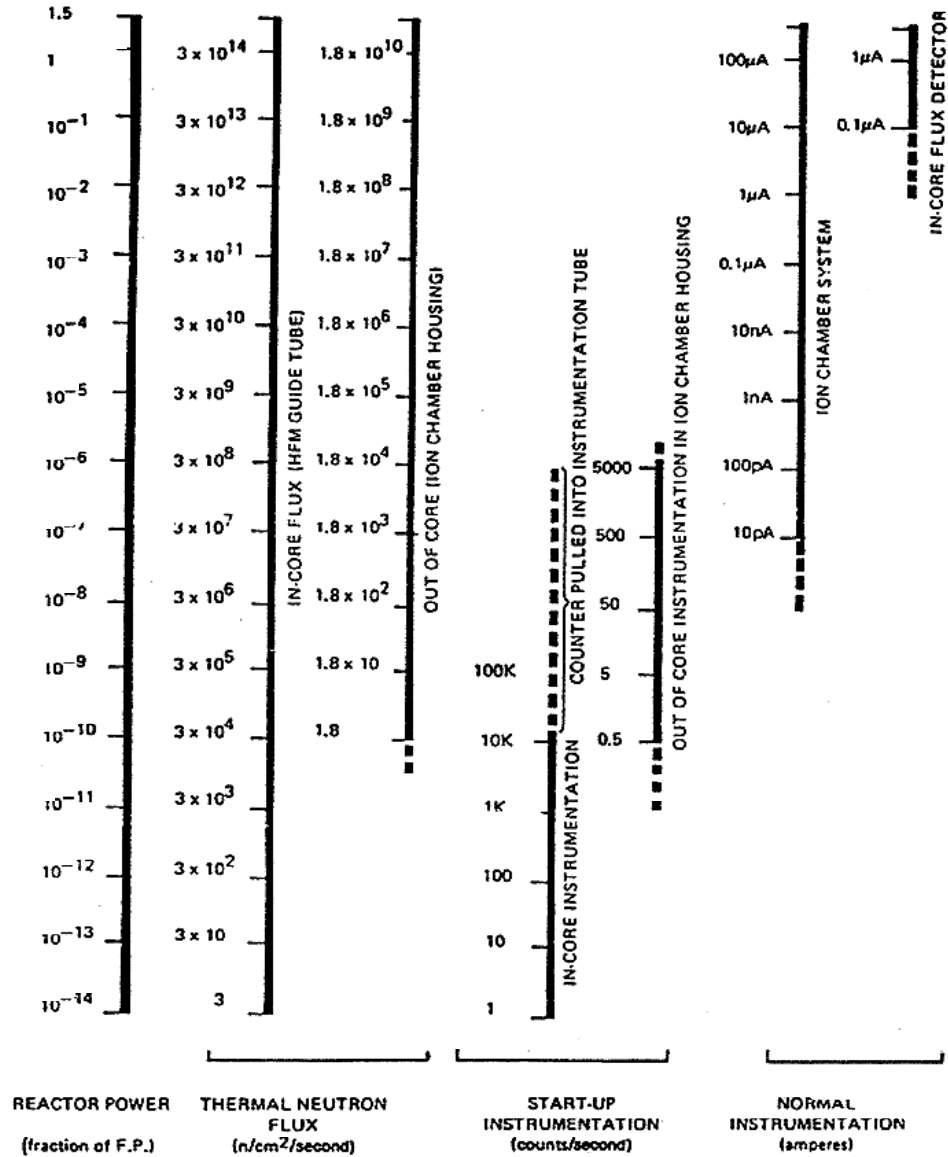
At very low power levels (below 10^{-6} of full power), power is measured by boron trifluoride (BF_3) counters located temporarily in-core in the viewing port, and out-of-core in the SDS2 ion chamber housings. The in-core counters are needed only for the initial reactor start-up; the out-of-core counters may be needed for restarts following extended reactor shutdowns as well as for the initial start-up. At power levels of about 10^{-7} times full power, the permanently installed out-of-core ion chambers start coming on scale. At 10^{-6} power, the ion chambers are well on scale and the start-up counters are reaching the end of their range. The ion chambers span a range of operation from 10^{-7} to about 150% FP , but they are

used only at relatively low reactor powers, below 10% FP, because they are not very accurate and give no flux tilt information. At high power levels, spatial control is necessary, requiring distributed measurements by the platinum flux detectors.

4.1   Start-up instrumentation

The start-up instrumentation provides a continuous indication of the reactor power from the initial spontaneous fission power level up to the threshold of sensitivity of the ion chamber system (with a decade of overlap). High accuracy of calibration is not required since it is sufficient to obtain an indication approximately proportional to the actual reactor power. However it is important that an output be provided which is always on-scale and responds promptly to changes in the power level. The instrumentation must trip SDS1 if reactor power or rate-of-change of power exceed preset limits, or if the instrumentation or its power source should fail.

### 4.1.1   Instrumentation description

The required range of sensitivity is from $\sim 10^{-14}$ to 10^{-6} of FP, with rate-of-change indication from -15% to +15% per second. The following outputs are provided:
• visual indication of the power on linear and logarithmic scales with the corresponding chart records as a function of time,
• trip outputs (for the three channels of SDS1) on high power, high rate and instrumentation failure.

To monitor a power range of *eight decades*, without saturating the counting capability of the instrumentation, both in-core and out-of-core detectors are employed. As shown in Figure 4.1, the in-core counters are used from $\sim 10^{-14}$ to 10^{-10} of FP where the count rate is between ~8 and 80,000 counts per second. The counting equipment is connected to the out-of-core detectors, when they *come on-scale* (at $\sim 5 \times 10^{-11}$ FP), and their count rates are monitored to a power level of $\sim 10^{-6}$ FP (~70,000 counts per second). At this point, the ion chamber system should be on-scale and control can be transferred from the operator to the automatic reactor regulating system.

To provide the necessary redundancy for reliable operation and the independent trip inputs for SDS1, the instrumentation is grouped into three independent channels corresponding to the SDS1 channels. A spare channel is provided for monitoring or replacement purposes (see Figure 4.2).

Fig. 4.2:
Block diagram of startup instrumentation
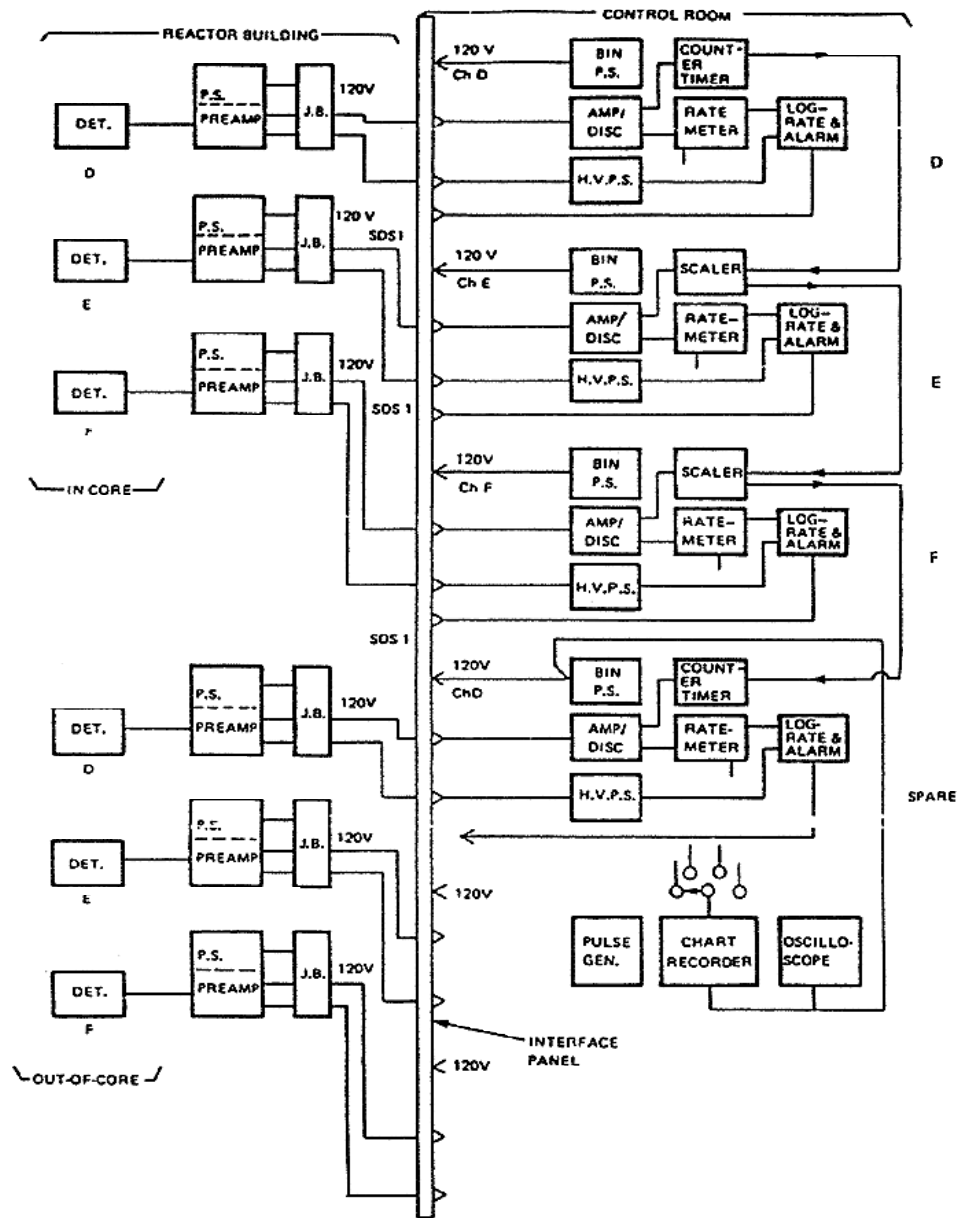
Standard boron trifluoride (BF3) gas counters, having a sensitivity of four counts per second per unit flux are used to detect and count thermal neutrons. The electronics are standard items except for a special log-rate and alarm module which has been designed to meet the specific reactor trip requirements of this system. Figure 4.3 shows the arrangement of the start-up instrumentation. Three neutron detectors are located in-core in a dry thimble which has been inserted temporarily through a viewing port in the reactivity mechanisms deck.

This instrumentation tube will be removed during a later shutdown, before the reactor is brought to high power. After a few days of low power operation there should be sufficient photoneutrons present in the reactor core to allow monitoring of any subsequent start-ups to be carried out with the out-of-core detectors, rather than the in-core ones. The three out-of-core detectors are inserted in the three spare cavities of the SDS2 ion chamber housings. On completion of the start-up phase, the detectors, preamplifiers, and cables (shown by a solid line in Figure 4.3) are removed.

Fig. 4.3:
Arrangement of startup instrumentation
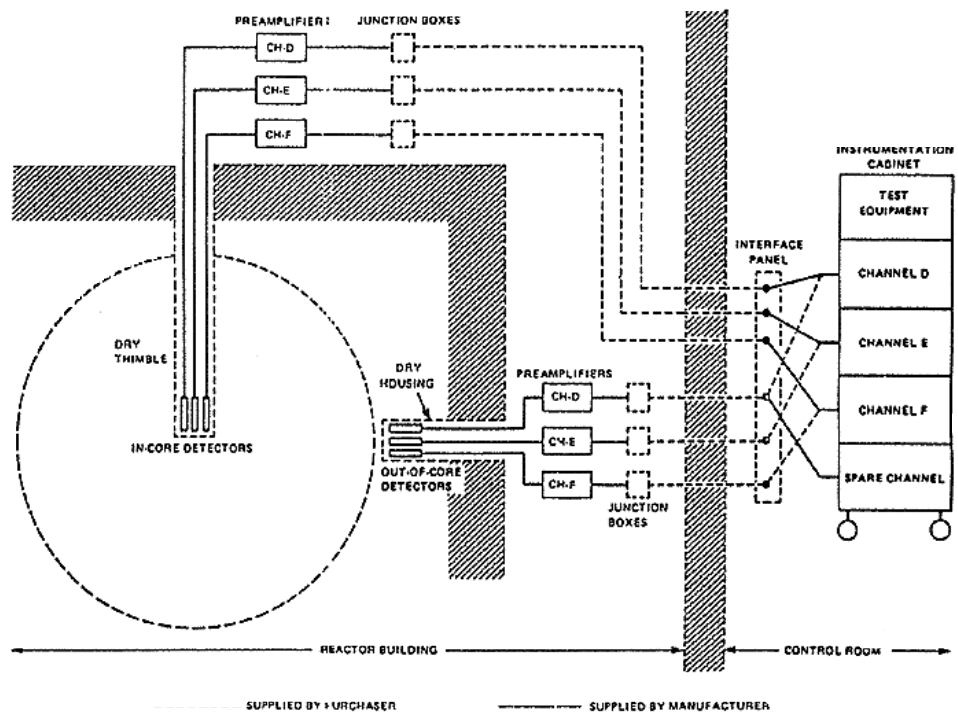
4.1.2 Operation: approach to criticality

The start-up instrumentation is put into operation prior to the *initial approach to criticality*, or *after a very long shutdown during which the ion chamber system has gone off-scale*. When reactor power is not being monitored, the reactor is put into a *guaranteed shutdown state* (GSS). When fuel is loaded or when moderator poison is being removed the neutron flux must be monitored and SDS1 armed.

When the fuel has been loaded into the core, it should be possible to measure, with the in-core detectors, a neutron count rate of the order of 1 count per second or higher depending on the boron concentration in the moderator. When the instrumentation is operational, it is connected into the SDS1 trip system by removing the shorting plug from the interface panel in the control room and

connecting the corresponding trip alarm output cable from the start-up instrumentation. This should be done one channel at a time to avoid tripping the reactor. The trip settings on the count rate alarm unit should be correctly set and enough margin must be allowed to ensure that they are not tripped by normal statistical fluctuations of the count rate. One of the out-of-core detectors is connected to the spare channel at this time.

On the approach to criticality, the operator removes boron from the moderator and records the neutron count rate from each of the three channels at regular time intervals. The counter/timer module of channel D is used to control the counter/timers of the other channels. A suitable preset time is selected so that a statistically significant neutron count (> 100 counts) is accumulated on each of the counter modules. In addition to recording these counts, the inverse of the count rate is computed (for one of the channels) and plotted on graph paper against time, as the boron removal progresses. The graph is a useful tool in predicting when criticality will be achieved. As the reactor power increases, the high log counts per second trip setpoint is periodically raised for each channel to avoid a trip. The low log counts per second trip can be raised as required to provide protection against instrument failure.

The initial power in the reactor core is about 1×10^{-14} full power based on core physics calculations. Using this information and the initial count rate before poison removal, the operator can determine the calibration factor between measured counts and reactor power. The relationship will be linear up to about 30,000 cps, i.e., over four decades, before pile up effects will affect the linearity.

When the count rate has reached 25,000 cps, an out-of-core counter which was being monitored on the spare channel should be on scale. When the counter is well on scale, the removal of poison by the ion exchange columns should be stopped, and the instrument channel transferred from the in-core to the out-of-core detectors, one at a time to avoid tripping SDS1. With each transfer the amplifier output should be checked to ensure the signal is valid, and the discriminator and high and low log setpoints adjusted. At this time the relationship between out-of-core count rates and reactor power can be established, and should be approaching about 5×10^{-10} FP.

Poison removal continues, using progressively fewer ion exchange columns until with one column in use, the reactor is within a few minutes of going critical. Fine control of reactivity is now required since the count rate from the start-up counter about doubles for each one minute of ion exchange column activity. This is done using the control rods to raise reactor power until the regulating system ion chambers come on scale and the RRS control programs take over, as evidenced by slight changes in the water levels of the zone controllers. The start-up instrumentation high log and high log-rate trips are still operational, and remain connected to SDS1 until the shutdown system ion-chambers have been

commissioned and are capable of performing the necessary protective functions. The start-up instrumentation should be removed after the reactor has operated for an adequate period of time so that the power level will not drop below the sensitivity of the ion chamber system.

4.2   Ion chambers

The *ion chambers* (IC) *consist of two concentric cylindrical electrodes*, whose facing surfaces are coated with boron-10, housed in a gas filled vessel. A high voltage is supplied across the electrodes. The output current is proportional to the thermal neutron flux over a range of seven decades. The signal is processed to provide an *output voltage proportional to the logarithm of the thermal flux*, and to its rate of change. The ion chamber spans a range of operation from 10^{-7} to about 150% FP.

The ion chamber signals are sensitive to the amount of poison (neutron absorbing material) in the moderator. Also, since the ion chambers are located at the side of the reactor, their signals are affected by flux tilts. They provide a reasonable measure of total reactor power over several decades, but they are not sufficiently accurate to be used for control at high power.

Three uncompensated ion chambers, located in separate housings are provided for each shutdown system. For SDS1 each housing also contains one RRS regulating system ion chamber, but in a separate cavity within the housing. The design minimizes the possibility of ingress of light water from the reactor vault, into the ion chamber cavities. Figure 4.4 shows a typical housing with three cavities, two for ion chambers and one for a test shutter. The SDS2 ion chamber housings are located on the poison injection system side of the calandria. The SDS1 housings are usually located on the opposite side of the calandria except for some CANDU designs (such as BRUCE), where they are located at the top. Figure 3.5 shows the location of SDS1 and SDS2 ion chamber housings for CANDU 600 reactors.

December 1995

Fig. 4.4:
Ion chamber housing
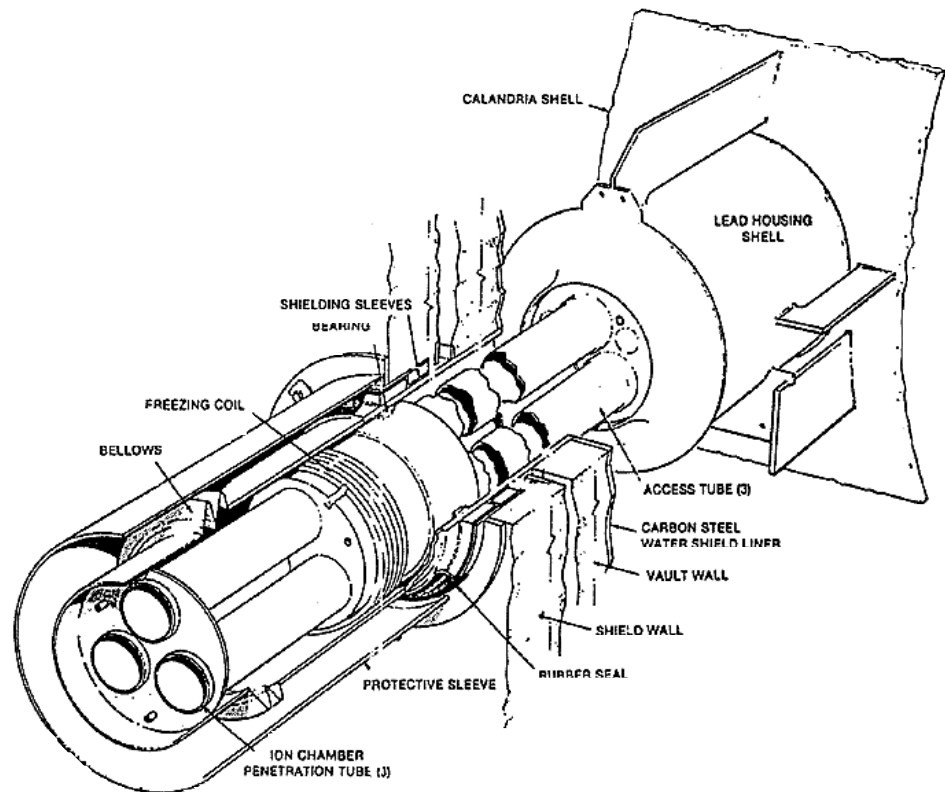
The output current from each ion chamber goes to an amplifier, which produces log neutron power, linear neutron power, and log-rate signals. *The log-rate signal is a direct trip parameter*. The log and linear power signals are used as conditioning signals for other trip parameters.

4.2.1 Ion Chamber Theory

An ion chamber consists basically of two cylindrical electrodes, which, when a DC voltage is applied between the electrodes, collect electrons and ions produced by ionizing particles travelling in the gas. The ion chamber is a current source, dependent on the quantity of ion-pairs collected, not on the resistance of external circuitry used to amplify the current. The electrodes are coated with boron-10. The ionization in the chamber is due to the following reaction between thermal neutrons and boron-10:

$$^{10}B_5 + {}^1n_0 \rightarrow {}^4He_2 + {}^7Li_3 + 2.85\,\text{MeV} \quad (7\%)$$

$$\rightarrow {}^4He_2 + {}^7Li_3{}^* + 2.4\,\text{MeV} \quad (93\%)$$
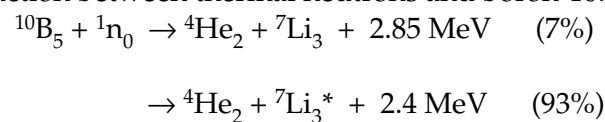
The energetic helium and lithium nuclei ejected from the boron coating cause ionization in the gas volume between the anode and cathode. The current

collected increases with applied voltage, as the recombination of ions is progressively overcome. Above a voltage called the saturation voltage, the collected current remains constant. The operating voltage of the ion chamber is set well above the saturation voltage to accommodate some deterioration of the saturation curve with time, without affecting the output signal. The operating voltage is selected such that all the primary ions produced by the ionizing radiation are collected. The *current is linearly proportional to the thermal neutron flux at the location of the ion chamber*. This *linearity holds over seven decades* of reactor power.

The ion chamber is also sensitive to gamma-rays. Gamma radiation impinging on the chamber ejects high energy electrons into the active volume. This also causes ionization. To obtain an ion chamber which is sensitive to reactor power over a range of seven decades, it is necessary that the signal component due to gamma radiation be small. This is because the gamma flux in the location of the ion chamber does not vary proportionally with reactor power, especially after a shutdown. The signal due to gammas is kept small by surrounding the ion chambers with a lead (Pb) housing to attenuate the gamma flux. This permits the use of non-compensated ion chambers. The gamma rays produce an unwanted signal. The gamma rays originate from the reactor core, activated ion-chamber cavity materials, and activated ion chamber materials. The activation of the cavities and chamber materials leads to significant background signal noise when the neutron flux is small, such as during a reactor start-up at 10^{-6} full power.

The neutron/gamma sensitivity ratio is determined by the design and materials used in the uncompensated chamber. The ion-chamber body is made of high purity aluminium because of its low neutron cross-section, short half-life of activated products, and its low atomic weight which minimizes gamma interaction. The filling gas, chamber volume, electrode spacing, boron thickness and gas pressure, are selected for optimum differentiation of ionization produced by the lithium and helium particles from the neutron interactions, and the electron particles from the gamma interactions with the chamber walls and electrodes.

4.2.2 Ion Chamber specifics

The environmental conditions at the location of the ion chambers are given in Table 4.5. The major characteristics are given in Table 4.6.

Since the ion chambers are measuring the thermal neutron flux in their vicinity, the power indication cannot therefore represent very accurately the total power generated in the reactor. Fluctuations of as much as 60% have been observed in the ion chamber signals in Pickering reactors due to local refuelling operations or adjuster rod movement. Shutoff rod movement will also affect ion chamber signals. Calculations for the CANDU 600 reactor indicate that ion chamber

signals can be perturbed by a factor of three by shutoff rod withdrawal, at approximately constant reactor power. Furthermore, significant log-rate signals (~7%/s) can be expected when both SOR banks are withdrawn simultaneously. These rates do not correspond to real power changes.

Moderator poison depresses the ion chamber signals. Boron poison, dissolved in the moderator to compensate for fresh fuel, will decrease the ion chamber current for a given power level. A concentration of 2 ppm will depress the current by ~11%; 5 ppm will cause a ~24% perturbation.

Table 4.5

Nuclear and environmental conditions at the location of the regulating ion chambers

Conditions	Full Power	10^{-7} Full Power
Thermal Neutron Flux (boral sleeve retracted) n.cm^{-2}.s^{-1}	2.2×10^{10}	2.2×10^{3}
Fast Neutron flux (E>1 MeV) n.cm^{-2}.s^{-1}	6.2×10^{8}	
Gamma Dose Rate R/h	1.1×10^{4}	5.1
Temperature °C	54	
Relative Humidity %	<1%	

Table 4.6

Major ion chamber characteristics

Ion chamber characteristics

- Type Reuter Stokes   co-axial, uncompensated,
  RS-C2-0808-107   boron-10 lined
- Thermal Neutron Sensitivity 0.8×10^{-14} A/n.cm^{-2}.s^{-1} ±20%
- Gamma Sensitivity $\leq 3.4 \times 10^{-12}$ A/R/h
- Residual Current (40 hr after $\leq 1.3 \times 10^{-12}$ A
  shutdown from full power)
- Operating Flux Range 1×10^3 to 5×10^{10} n.cm^{-2}.s^{-1}
- Seismic Qualification Level ≤ 2 g, 6-33 Hz

The reactor regulating ion chamber (RRS-IC) system is a triplicated system consisting of three independent channels A, B and C. Each channel has the following instruments:

a. a co-axial, uncompensated IC with output current proportional to thermal neutron flux in the ion chamber housing;

b. a regulated high-voltage DC power supply capable of providing sufficient polarizing voltage for the IC to saturate throughout the flux range;

c. a logarithmic amplifier capable of accepting at least seven decades of current from the IC and producing an output voltage (log signal) proportional to the logarithm of the chamber current;

d. a band-limited differentiator whose voltage output is proportional to the rate of change of the logarithm (log-rate signal) of the IC;

e. a linear amplifier whose output is proportional to the IC current.

As indicated in Figure 4.7, each channel provides one set of outputs (log, lograte and linear signals) to DCCX, one set to DCCY and a third set to three chart recorders used to record all three signals continuously. All amplifier outputs are short-circuit proof and buffered.

Fig. 4.7:
Block diagram of regulating system ion chamber
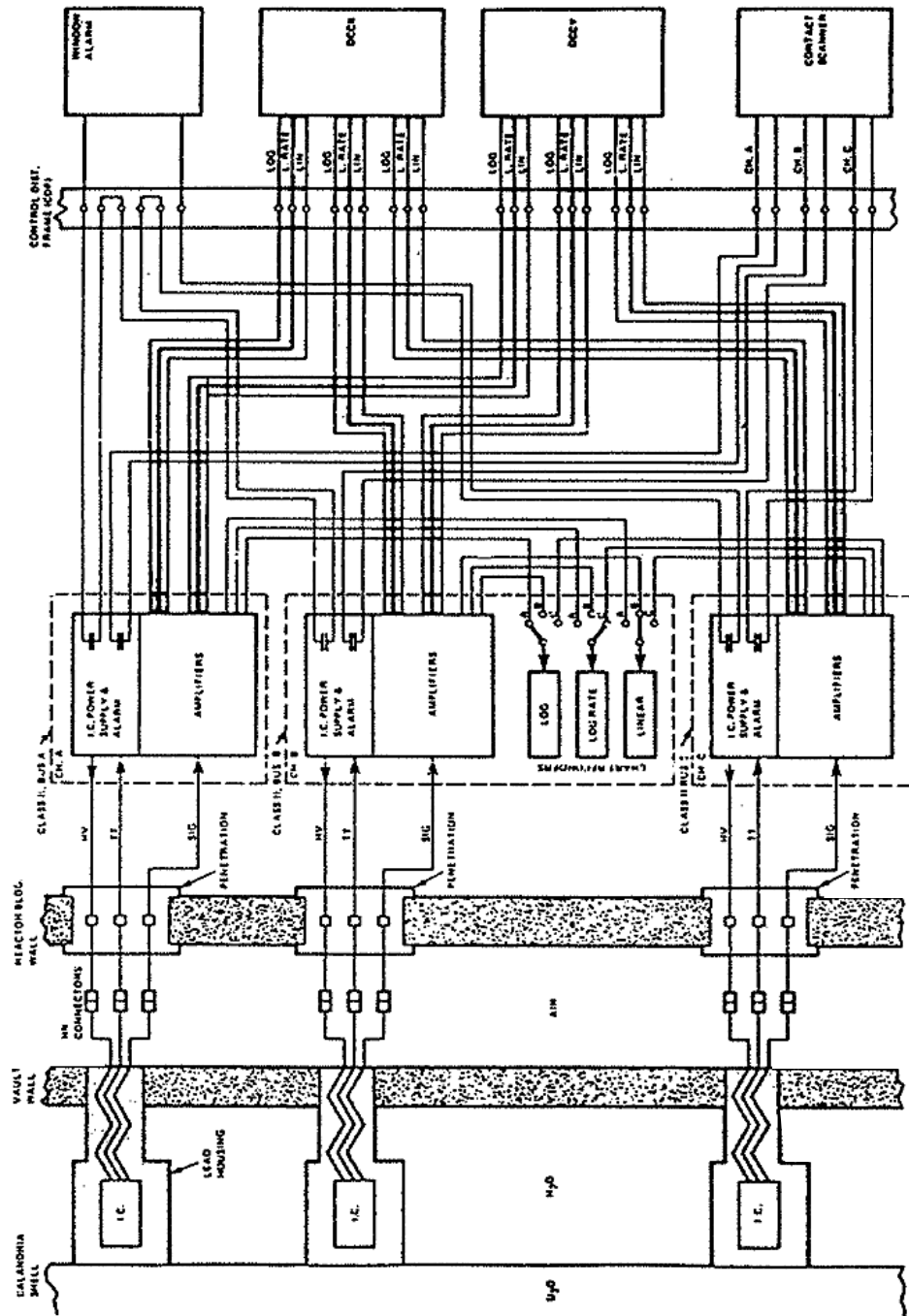
At full power, the thermal neutron flux of 7.8×10^{13} n.m^{-2}.s^{-1} inside the ion chamber cavity will result in a current output of about 180 μA. The gamma flux of 5×104 R/h in the ion chamber cavity at full power will generate a current of about 0.15 μA, i.e., three decades below the neutron sensitive component.

On a shutdown neutron flux decreases gradually to a value of 10^{-7} FP over a period of about 81 days. This flux results from photoneutron production in the D_2O

moderator by gamma rays from long-lived fission products. It is important to ensure that the ion chamber system remains neutron-sensitive and responsive to fission power during this period so that the reactor can be easily restarted with automatic power monitoring. Otherwise start-up instrumentation must be set up and monitored by the operator.

4.3   In-core flux detector systems

Only in-core self-powered flux detectors are used in CANDU reactors during normal operation at high power levels (see Fig. 4.1). This type of detector is essentially a coaxial cable consisting of an inner emitter electrode, and an outer collector electrode separated from each other by an annular insulator. It is *self-powered* because it does not require an applied bias voltage to separate and collect ionization charge to derive a signal. Exposure to radiation causes the emission of energetic electrons from both the emitter and collector, some of which penetrate the solid annular insulator and reach the opposite electrode. This results in a net deficiency of electrons in the emitter and hence a positive charge on the inner electrode. At full power with the detector disconnected from external circuitry, the voltage on the emitter will be of the order of 100 to 500 volts. On connection to an amplifier, the electron deficiency in the emitter is made up by a flow of electrons from the collector to the emitter via the amplifier. The electron flow maintains the emitter at collector (reactor ground) potential. Therefore the *flux detector acts as a current source* (for small loads), *dependent only on radiation intensity*.

In-core flux detectors consist of two types, vanadium and platinum. Vanadium detectors are almost totally neutron sensitive but have a slow dynamic response, while platinum detectors have a response which is mainly prompt. Platinum detectors are therefore employed for the reactor control and protection systems, while the vanadium detectors are used for neutron flux mapping. The in-core detectors associated with the reactor regulating system (28 platinum and 102 vanadium detectors) are mounted (coiled) on twenty-six vertical flux detector assemblies inserted down into the core from the reactivity mechanisms deck, see Figures 1.4 and 3.5. A vertical flux detector assembly for coiled in-core detectors is shown in Figure 4.8. The vertical assemblies also contain the thirty-four high neutron flux trip detectors (and their spares). The corresponding SDS2 detectors are mounted on horizontal in-core assemblies of similar construction.

Fig. 4.8:
Flux detector unit

DECK SHIELD/
TREAD PLATE

ELECTRICAL
CONNECTION

DETECTOR ASSEMBLY
(SEALING PLATE)

COVER GAS
CONNECTION

BELLOWS
ASSEMBLY

DECK
STRUCTURE

DECK
CONCRETE

SHIELD PLUG
(UPPER)

SHIELD PLUG
(LOWER)

GUIDE TUBE
EXTENSION
ST. STEEL

THIMBLE

CALANDRIA
NOZZLE

CALANDRIA
SHELL

LEAD
CABLE

LEAD
CABLE

DETECTOR COIL

CALANDRIA TUBES

ZIRCALOY
CARRIER
TUBE

ZIRCALOY
CAPSULE

ZIRCALOY
GUIDE TUBE

GUIDE TUBE LOCATOR

CALANDRIA SHELL

The detectors and mounting hardware have to withstand the environment in the core without significant corrosion, radiation damage, mechanical stress or other deterioration, for the required operating lifetime. The in-core environment is

circulating heavy water, the chemistry of which is carefully controlled, with a controlled helium moderator cover gas. The maximum concentrations of D_2 and O_2 allowed in the cover gas are ~4% and ~2% respectively. The moderator temperature is maintained at about 71°C; the pressure is near atmospheric. The maximum temperatures inside the assembly are calculated to be about 180°C. The in-core radiation environment normally does not exceed:

Thermal neutron flux	3×10^{14} n.cm^{-2} s^{-1}
Fast neutron flux (E > 1 MeV)	2×10^{13} n.cm^{-2} s^{-1}
Gamma dose rate	2×10^{8} R/h

The in-core materials have a low thermal neutron cross-section so as not to incur a significant fuel burn-up penalty. They cause a negligible perturbation to the neutron flux distribution in their vicinity.

4.3.1 Flux Detector Theory

A *self-powered detector consists of a coaxial cable*. The metallic centre conductor called the emitter is separated from the metallic sheath (collector) by a layer of insulation (see Figure 4.9). The detector signal arises from three important interactions.

Fig. 4.9:

Platinum and vanadium in-core flux detector

A) PLATINUM SELF-POWERED IN-CORE FLUX DETECTOR

B) VANADIUM SELF-POWERED IN-CORE FLUX DETECTOR
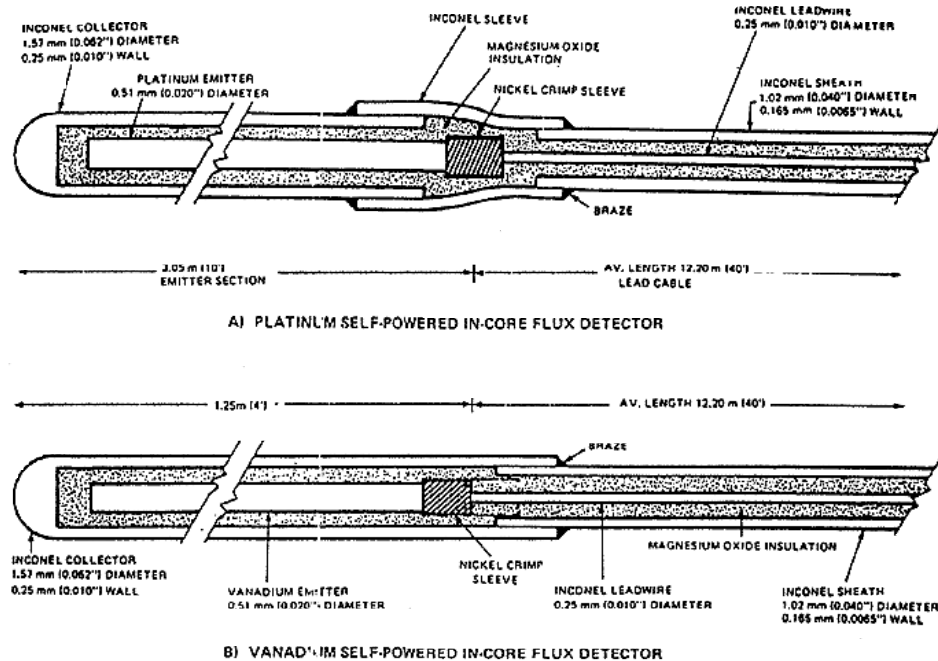
Neutron capture in certain isotopes in the detector *causes the emission of an energetic, charged particle*. The nature and energy of the charged particle depends on the nuclide, but for the vast majority of nuclides, it is an *energetic electron*.

This neutron interaction, culminating in the emission of an electron, is termed the (n,β) interaction. The electron emission is delayed relative to the neutron capture event, the delay being governed by the half-life of the particular nuclide. Typical half-lives of most interest in flux detector materials range from seconds to days. The frequency of capture events depends on the neutron flux and on the capture cross-sections of the materials. Since the capture cross-section is a function of neutron energy, the total interaction rate depends on the energy spectrum of the neutrons.

Gamma-rays propagating through the detector may transfer some of their energy to the electrons of the detector materials, thus producing prompt energetic electrons through the (γ,e) interaction. The interaction rate depends in a complex way on the energy of the gamma rays, on the number density of the electrons, and on the electronic structure of the particular materials used in the detector.

Neutron capture in the detector causes the emission of capture gamma rays through the (n,γ) interaction. These emitted gamma rays then lead, through the (γ,e) interaction, to the production of prompt energetic electrons. The combined effect is referred to as the (n,γ,e) interaction. It should be noted, however, that the original (n,γ) interaction and the subsequent (γ,e) interaction generally do not occur at exactly the same point in the detector. In fact, the gamma ray may escape the detector without interacting.

Since the gamma rays that interact in the detector arise from two sources, the gamma flux from the reactor and from neutron capture events in the detector, it is important to distinguish between the two sources. The former source truly reflects the reactor gamma flux, while the latter actually reflects the neutron flux. Consequently, the (γ,e) notation is reserved for interactions with gammas external to the detector, i.e., the reactor gamma flux, while the internally-generated gammas in the detector materials are included in the (n,γ,e) interaction.

The three interactions are effectively harnessed to produce a current by employing the coaxial structure shown in Figure 4.9. Electrically, the detector is connected to an amplifier. The sheath is grounded at the reactor, and the current generated by the emitter is directed, via a coaxial or twisted pair twin axial lead cable, to the amplifier. The same interactions that occur in the detector also occur in the in-core section of the lead cable. By a proper choice of materials and geometry, the sensitivity per unit length of the lead cable can be made much smaller than that of the detector. Nevertheless, the lead cable signal is not negligible, being of the order of 1 to 4% of the total signal, because the length of lead cable exposed to high flux is much greater than the detector length.

The net current I can be expressed as the sum of four distinct components:

$$I = I_n\gamma + I_n\beta + I_{\gamma e} + I_e$$

where
- $I_n\gamma$ results from (n,γ,e) interactions in the detector,
- $I_n\beta$ results from (n,β) interactions,
- $I_{\gamma e}$ results from interactions with external gammas, and
- I_e results from an impinging electron flux due to (n,γ,e), (n,β) and (γ,e) interactions in the hardware surrounding the detector.

The I_e component induced by the externally generated electron flux is negative and generally small, relative to the electron flux generated within the detector. The polarity and magnitude of the other three components depend on the construction material and geometry of the emitter, insulator, and collector.

The relative importance of the four components also determines the dynamic response of the detector, i.e., the time response of the net detector current I due to changes in reactor power. The dynamic behaviour of a flux detector signal, relative to the neutron flux, is given by the transfer function

$$D(s) = F_p = \sum_{i=1}^{m} \frac{a_i}{1 + \tau_i s}$$

where
- s is the Laplace transform variable,
- Fp is the prompt fraction, and
- a_i is the amplitude of the ith delayed component having a time constant τ_i.

Normally five or six delayed components are sufficient to describe the delayed response with sufficient accuracy. Since D is normalized, the a_i obey

$$\sum_{i=1}^{m} a_i = 1 - F_p$$

The expression for D given before is an *engineering approximation* to the true response. The amplitudes and time constants depend on two effects, namely on the (n,β) interactions in the detector and on the delayed reactor gamma flux. The (n,β) components are an intrinsic property of the detector, while the delayed gamma flux is a function of the particular reactor and indeed of the detector location within the reactor. Generally, most of the gamma flux (about two-thirds) is prompt, arising mainly during fission of the fuel and neutron capture in ^{238}U, while the remaining one-third arises from the decay of fission fragments and, less importantly, from neutron activation of the reactor hardware, and are delayed.

Thus the choice of emitter material determines both the absolute sensitivity and the dynamic time response of the detector. With irradiation, the isotopic and elemental composition of the detector materials changes, due to neutron capture. Thus the signal properties change with time, the rate of change with time depending on the neutron flux level and on the magnitude of the neutron

capture cross-section. Since the original material is consumed, the phenomenon is referred to as *detector burn-out and detector burnup*. The gamma sensitivity, for a given detector geometry, depends mainly on the atomic numbers of the detector components, and, therefore the sensitivity is only a very weak function of detector burn-out. Thus the relative magnitudes of the neutron-dependent and gamma-dependent signals vary with irradiation. Since the neutron signal ultimately decreases with irradiation, the total sensitivity and the n/γ ratio also decrease with time. The magnitude of the delayed component amplitudes will change with burn-out, thus modifying the dynamic response of the detector.

4.3.2   Detectors Used In CANDU Reactors

For reactor control and shutdown action at high power, CANDU reactors use four types of in-core detectors: vanadium, platinum, Inconel, and Inconel clad with platinum. In the original design of the CANDU 600 reactors, vanadium and platinum detectors are wound spirally at specific locations on zircalloy carrier rods sealed in a capsule containing 100% helium and then inserted into the core. Spare detectors are provided on each assembly since individual detectors cannot be replaced.

4.3.2.1   Platinum Detectors

The outer sheath of the detector cable, which forms the collector electrode, is fabricated from reactor-grade Inconel-600. The outer diameter of the sheath is 1.5 mm. The insulation is compacted magnesium oxide. Magnesium oxide, ~99.4% pure, was selected because of its excellent insulating characteristics (high, stable resistance $>10^{13}$ ohms) under intense radiation and its low noise properties. The emitter electrode is a solid platinum wire 0.51 mm in diameter and 3.04 m long. To this sensitive portion of the detector is spliced the leadcable consisting of a long mineral insulated, Inconel-600 coaxial cable 1 mm in diameter. The diameter of the Inconel core wire of the lead cable is 0.25 mm. The construction of a platinum self-powered detector is shown in Figure 4.9.

For the regulating system two of these detectors, each three meters long, are wound together (bifilar) on the carrier tube over a three lattice pitch distance (33-3/4 inches) in the centre of each zone. This is to smooth out, to some extent, the local flux perturbations and make the detector less sensitive to the effects of fuelling. The SDS detectors are wound similarly at various locations on the assemblies.

The platinum detector is sensitive to the local radiation intensity. For a fixed reactor geometry in a steady state core, the neutron and gamma fluxes are proportional to one another. Both are related to fission rate or reactor power. About one-half of the signal from a platinum detector is due directly to the thermal neutron flux. The other half results from the gamma dose rate. The detector response to the radiation is almost totally prompt. However, since the gamma signal in a reactor is partially delayed (~30% from β-active fission

products), the prompt response of the detector to changes in power is about 84% (1 second after a step change). This composition of the signal follows from CRNL data which indicate that neutron capture is the source of 46% of the current generated in the detector. This permits calculation of the prompt fraction of the detector signal with the following assumptions:

a. the detector responds promptly to γ-rays
b. 30% of the reactor γ-rays are delayed
c. the current due to β-decay of activation products in the detector is considered negligible.

Using the above information, the predicted prompt fraction is 0.84, of which 55% of the prompt signal is due to neutron capture.

The platinum detector provides a signal output of about 1.5 μA in the peak flux at full power. The dimensions of the leadcable have been chosen to minimize its contribution to the total signal. The background contribution of the leadcable is usually less than 3% of the total signal. The detectors themselves depress the local thermal neutron flux by about 2%. The sensitivity of a platinum detector is estimated to decrease by 50% over the lifetime of the reactor, with the prompt fraction dropping to about 70%.

4.3.2.2   Vanadium Detectors

At the interstitial locations between the fuel channels in a CANDU reactor, the neutron energy spectrum is closely represented by a Maxwellian distribution. As the absorption cross-section of vanadium is inversely proportional to the neutron velocity (a good 1/v detector), the output current will be a direct measure of the thermal neutron flux in its vicinity.

Vanadium detectors are not suitable for direct use in safety or control systems. They have a dominant time constant of 325 seconds. In response to a step increase in power the vanadium detector signal will take 25 minutes to indicate 99% of the power increase. However, they are suitable for neutron flux mapping in CANDU reactors, because a vanadium detector is essentially neutron sensitive.

The primary nuclear reaction for converting the incident radiation into a current signal is:

$$^{51}V + N \quad \rightarrow \quad ^{52}V^* + \gamma \quad \rightarrow \quad ^{52}Cr + \beta^-$$
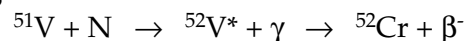
The neutron capture product $^{52}V^*$, has a half-life of 3.75 minutes. Ninety-nine percent of the β⁻ decays are to the first excited state of ^{52}Cr. This yields beta particles with a maximum (endpoint) energy of 2.545 MeV.

After conversion from vanadium to chromium, the emitter nuclei can no longer contribute significantly to the output signal. Hence exposure to a neutron flux

results in the gradual loss of sensitivity of a vanadium detector. Initially, the sensitivity of a new vanadium detector is 1.0×10^{-20} A/(n cm^{-2} s^{-1}). In an average thermal neutron flux of 3×10^{14} n cm^{-2} s^{-1} the output signal will be ~3 mA. After continuous exposure to this average flux, the loss in detector sensitivity (based on a simple exponential model) will be 21% after five years and 50% after fifteen years. This is still within the range of the amplifiers.

The physical dimensions of the vanadium detector, Figure 4.9 are similar to the platinum detector except for the emitter length, which is 1.25 m. The emitter portion is coiled over one lattice pitch (28.6 cm) to provide approximate "point" measurements to the flux mapping routine.

The flux mapping routine requires an individual relative sensitivity value for each vanadium detector. The detectors, before being wound on the carrier rods, are calibrated relative to a standard vanadium detector. This calibration is carried out in a thermal neutron flux, generated by the ZED-2 reactor at CRNL. From this irradiation a relative sensitivity factor is calculated for each detector. Experience in producing detectors of uniform response has been good. Standard deviations from the mean value of the relative sensitivities are normally of the order of ± 1 to ± 2%.

December 1995

Reactor Simulations and Power Manoeuvring

Training Objectives

The participant will be able to understand or to describe:

1   the simulation tools for CANDU reactors;
2   the distinction between neutron and thermal power;
3   the neutron source effects in a subcritical reactor;
4   the approach to criticality and power manoeuvring;
5   the xenon transients and spatial oscillations as a consequence of power manoeuvring;
6   some thermalhydraulic simulations of the overall plant with its regulating and safety systems.

Reactor Simulations and Power Manoeuvring

Table of Contents

1 Simulation of Reactor Physics

This lesson is an introduction to the field of reactor simulation. Reactor physics and thermalhydraulics analysis integrate many levels of modelling and calculation. They require therefore precise methodologies (safety analysis, probabilistic and deterministic assessments, accident scenario, etc.) and specialized tools (like computer codes, large nuclear databases, etc.) to approach the specific simulation goals. The basic principles are common between the various technologies of nuclear power production (see Figure 1.1). However due to the current level of safety requirements in western countries, the specific tools and methodological details are highly dependent on technologies.

Fig. 1.1:

Relations between reactor physics and related fields
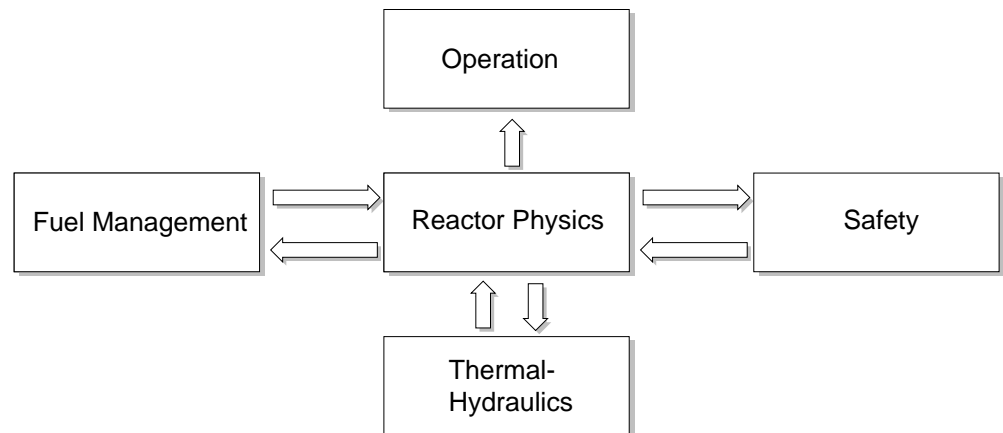
The first section of the present chapter introduces specific simulation tools of the CANDU reactor technology. The second section will distinguish between thermal and neutron power and illustrate the fact that thermal power is used to control the reactor power under nominal conditions. The remaining sections will deal with typical reactor transients and the associated power manoeuvres: approach to criticality transients, xenon transients and some examples of thermalhydraulic simulation of the overall nuclear plant behaviour.

1.1 CANDU reactor physics analysis and computer codes

Reactor physics has to take into account all the effects of importance, and must model:
- the physics of the basic lattice cell,
- the perturbing effect of reactivity devices,
- the static (time-independent) picture of the finite-reactor core,
- dynamic (time-dependent) phenomena,
- the effects of refuelling,
- the thermalhydraulics effects related to the various hydraulic circuits of the plant under specified operations (normal operations or accident).

To carry out these tasks, reactor-physics analysis is heavily dependent on a multitude of computer programs. Figure 1.2 shows the various roles of these programs in the overall analytical scheme. These roles will be discussed below. However, we first discuss the various methods available to the reactor physicist.

Fig. 1.2

Chart of the physics analysis of CANDU reactors

Reactor Design Requirements:
- Fuel channel
- Power limitations
- Temps, materials, etc.

Lattice codes:
- Powderpufs
- Latrep
- Transport codes

Reactivity Device Simulations:
- 3D diff codes
- 2D trans codes

1

Core Design Control Devices Shutdown Systems
- CHEBY

Kinetic Studies:
- CERBERUS

Reactor Control Transients Due To Perturbations:
- SHORGHUM
- CHEBXEMAX

2

Fuel Management Studies:
- FMDP

4

3

5

Overall Plant Thermalhydraulic Simulations

Outputs:
1
- Cross sections vs Burnups
- Isotopic composition
- Void effect (point model)
- Reactivity coefficients
- Power distribution in fuel bundles etc.
2
- Control devices layout
- Power distribution in the core
- Shutdown systems
- Void effect, etc.
3
- Xe oscillation studies
- Zonal overpowers and detector locations
- Sequences of withdrawal or insertion of control devices etc.
4
- Power pulse
- Adequacy of shutdown systems etc.
5
- Fuelling schemes
- Simulations

⇨ Indicates feedback information from experimental and power reactors

1.1.1   Basic reactor-physics methods

During the process of slowing down, neutrons lose energy and change their direction of motion at the same time. To understand a reactor in detail we must know simultaneously the energy distribution of the neutrons and the spatial distribution of the reactions arising from neutrons born at a certain point.

There are three basic methods for obtaining this information, namely diffusion theory, transport theory and Monte Carlo methods.

Diffusion theory makes two major assumptions: (i) the probability of scattering is much greater than that for capture or fission, (ii) scattering is isotropic (the probability of the scattered neutron going off in any direction is constant). The solution of the diffusion equation relates the neutron flux at any position in a region to the material properties (macroscopic cross sections) of the region and the neutron sources in that region, and to the leakage rate into or out of the region. The form of the solution is dependent on the geometry of the assembly and a set of boundary conditions must be specified.

Transport theory does not make any assumptions and in principle gives exact results. However, it is too complicated to solve the transport equation exactly, so that various approximations have to be made. In particular, modifications to diffusion theory based on transport theory can be made which increase the accuracy.

The multi-group method is at present the most practical technique of considering the spatial distributions of neutrons as they slow down. Neutron energies are divided into groups (30 or more) to approximate a continuous energy distribution. Within any group, the neutrons are assumed to obey diffusion theory with transport corrections, or transport theory. Neutrons slowing down below the lower energy limit of any group are treated as being absorbed with respect to that group and as being a source in one of the lower energy groups. For heavy water natural uranium reactors, a two-group calculation usually gives sufficient accuracy. In two-group theory, the neutrons are divided into a thermal group and an epithermal group in which neutrons are slowing down. This gives two diffusion equations solved simultaneously.

An alternative to the multi-group transport-theory method is the Monte Carlo method. In this approach the particular life history of a typical neutron is followed. The distance that a particular neutron travels between two collisions, the particular type of reaction which occurs and the change in direction and energy, upon scattering, are regulated by chance. Fast computers are required since, to obtain sufficiently high statistical accuracy, tens or hundreds of thousands of neutron histories are necessary.

As an alternative to the diffusion method, the modal methodology can be used to calculate the three-dimensional flux distribution in the core. The basis of this method is to expand the flux as a linear superposition of precalculated basis functions (flux modes). The system equations are written in terms of the mode amplitudes, which are the unknowns of the problem. The flux modes used are precalculated harmonics of the static diffusion equation; 10-20 harmonics are typically used. Because of the small number of unknowns, the equations can be

solved very quickly. This is done at the expense of accuracy. The speed of calculation makes the modal method eminently suitable for application in reactor simulations.

1.1.2 Lattice codes

The lattice (or cell) code provides the neutronics of the basic lattice. It calculates the infinite-lattice multiplication constant k_∞, and may also give the individual parameters in the four-factor formula. It provides the cell-averaged two-group nuclear cross sections to the finite-reactor code.

The lattice code also provides information on the variation of fuel isotopic composition and lattice cross sections with irradiation (or burnup). It also provides information on the spatial flux distribution in the basic cell, and perhaps on the expected distributions of power among the various rings of pins in the fuel bundle. The lattice code is sometimes used to calculate the reactivity coefficients of the core in an approximate way without a full reactor calculation.

Some lattice codes, e.g. WIMS, base their modelling and calculations on fundamental methods of neutron transport theory. POWDERPUFS-V, on the other hand, is a semi-empirical code which makes use of various correlations collected from experiments on heavy-water-moderated lattices in Chalk River research reactors such as ZEEP and ZED-2. POWDERPUFS-V was specifically designed for CANDU modelling, and is the lattice code routinely used for the design and analysis of present-generation CANDU reactors.

1.1.3 Reactivity-device codes

This type of code determines how reactivity devices perturb the properties of the nuclear lattice in their vicinity. It provides "incremental cross sections" which are used to correct the bare-lattice cross sections for the effect of a reactivity device. These incremental cross sections are fed, together with the bare-lattice properties, to the finite-reactor codes. Examples of such programs are MULTICELL and SHETAN.

1.1.4 Finite-reactor codes

These codes treat the entire region of the reactor core. Two decades ago approximate two-dimensional calculations were done, but present-day finite-reactor codes almost always perform calculations in three dimensions. Most finite-reactor codes are based on two-energy-group neutron-diffusion theory. However, flux-mapping and modal-methods codes are also used.

Finite-reactor codes can be subdivided roughly into the following categories:
- Static codes,
- "Quasi-Static" codes,
- Kinetics and thermalhydraulics codes,
- Fuel-management codes.

Static Codes

These codes analyze the steady-state three-dimensional reactor core. They calculate the spatial distribution of neutron flux in the core, and the associated power distribution. They provide the value of the reactor multiplication constant $k_{eff.}$

Static codes can be used to calculate the reactivity worth of various reactivity devices, by calculating the values of system reactivity with the device first inserted in the core, and then withdrawn. Such calculations also provide information on the spatial flux and power distortion associated with device movements. An example of a static finite-reactor code is CHEBY, which is based on two-group diffusion theory.

Quasi-Static Codes

"Quasi-static" codes are similar to the static codes in the sense that they do not solve the time-dependent diffusion equation. However, they may be used to predict the static core conditions at specific times in a slow transient, such as that associated with changes in ^{135}Xe concentration. CHEBXEMAX is such a code.

CHEBXEMAX is similar to CHEBY in that it solves the two-group time-independent neutron diffusion equation. However, it contains in addition the capability to solve the time-dependent ^{135}I/^{135}Xe kinetics equations. These equations can be used to follow the time variation of the spatial distribution of ^{135}Xe concentration following an assumed power manoeuvre, device movement, or refuelling operation. The change in ^{135}Xe concentration affects the spatial distribution of neutron absorption (i.e., of lattice properties) in the core. CHEBXEMAX can be used to study such ^{135}Xe transients. A sequence of snapshot calculations at selected times can be performed, with the ^{135}I and ^{135}Xe distribution updated between snapshots. In this way the flux and power distribution associated with specified power manoeuvres or device movements can be analyzed.

Another useful feature of CHEBXEMAX is its capability to reproduce, in an asymptotic manner, the actions of the zone-control system. CHEBXEMAX is not a time-dependent code and thus cannot model precisely reactor regulating system (RRS) action. However, it can model the long-term or asymptotic bulk-control and spatial-control functions of RRS in the following way:

- It can calculate the uniform (bulk-control) change in zone-control-compartment fill required to maintain criticality (i.e., a constant k_{eff}) following a change in lattice conditions or device movement, and
- It can be used to predict the differential (spatial-control) changes in the zone-control-compartment caused by a change in lattice conditions or device movement. It does this by searching for the zone fills which will best restore the three-dimensional flux distribution to the desired reference distribution.

CHEBXEMAX is therefore typically used to analyze in three spatial dimensions the consequences of a power manoeuvre (such as shutdown or reactor setback followed by a power recovery) and the associated changes in Xenon-135 distribution, zone-control-compartment water fills, and flux distribution.

Kinetics and Thermalhydraulics Codes
Kinetics codes analyze the time-dependent behaviour of the flux distribution within the reactor. The main application of these codes is in the study of the consequences of hypothetical events such as a large-loss-of-coolant accident or a pressure-tube rupture. To accurately model power transients which follow such events, kinetics codes must take into account delayed-neutron effects.

Examples of kinetics codes are CERBERUS and SMOKIN. CERBERUS solves the time-dependent neutron diffusion equation in two energy groups, and provides the most accurate method of analyzing three-dimensional reactor kinetics in CANDU. The capabilities of CERBERUS to perform realistic analysis of LOCAs have further been enhanced by coupling it to a thermalhydraulics code such as FIREBIRD, CATHENA or SOPHT. The coupled reactor-physics-thermalhydraulics-code packages have been used to study a large number of LOCAs from different initial reactor conditions and with different break sizes and locations. Other studies may require a detailed thermalhydraulic description of the plant with the regulating and safety systems together with a neutronic model (like the point-kinetic model) of the reactor core. For instance typical safety report studies like : loss of class IV, loss of HT pumps, small LOCAs, steam header break, fall into this category.

SMOKIN is another example of kinetics code. The advantage provided by SMOKIN is that it is a modal code, so that it can execute in a small fraction of the execution time of CERBERUS. However, this is at the expense of loss in accuracy. Another useful feature of SMOKIN is that the reactor regulating system (RRS) algorithms have been programmed into it and the code can be used to predict the RRS response to various lattice perturbations or device movements.

Fuel Management Codes
Fuel-management codes are used for core design from the fuel management point of view, and to track reactor operating histories. Fuel management codes

in use at AECL are FMDP (Fuel Management Design Program) and its offshoot RFSP (Reactor Fuelling Simulation Program). At Ontario Hydro the fuel-management codes used are SORO for core tracking and OHRFSP (the Ontario Hydro version of FMDP) for design. At Hydro-Quebec (Gentilly-2) HQSIMEX is used.

All these codes have the capability to solve the two-group neutron diffusion equation. The flux-mapping methodology is also incorporated in HQSIMEX and RFSP. In this methodology the flux distribution is synthesized as a linear superposition of flux modes, using the readings of in-core detectors to determine the mode amplitudes.

In its design mode, FMDP can be used to study the effect of various axial fuelling schemes or various subdivisions of the core into different burnup regions. It establishes the time-average flux and power distribution used as a target by the fuelling engineer. It also calculates the expected fuel burnup and the refuelling rates in the various core regions. A core-tracking code keeps track of each bundle's irradiation individually. It models core burnup steps, updating the irradiation distribution and taking into account channel refuellings, as well as device movements. It calculates the flux and power distributions, enabling the fuel engineer to monitor the channel and bundle powers and the CPPF (channel power peaking factor). This and other results of the core-tracking code assist the fuelling engineer in selecting channels for refuelling in the subsequent few days of operation.

1.2 Thermal power and neutron power transients

The power referred to most frequently in reactor physics is neutron power which is equivalent to the fission rate. However, the actual output of the reactor is in the form of heat and the heat output is called reactor thermal power. Normally the instruments are calibrated such that 100% neutron power corresponds to 100% of the thermal power required from the reactor to provide the design heat input to the turbine cycle. The power of the overall unit is the gross electrical power output of the generator. By way of example, CANDU 600 reactors produce 680 MW(e), gross generator output, for a thermal power from the reactor of 2061.4 MW(th).

1.2.1 Thermal power lag

Thermal power Q is generally evaluated by measuring the primary heat transport flow rate (w in kg/s) and temperature change ($\Delta T = T_{out} - T_{in}$) in selected coolant channels (called instrumented channels). The single phase flow balance is expressed in terms of the coolant specific heat (C_P) :

$$Q = \ w \ C_P \ \Delta T$$

Neutron Power is measured either by ion chambers located outside the calandria and by in-core flux detectors.

Thermal power has the advantage of being the actual, useful power output of the reactor. The measurements have the disadvantages of having an excessive time lag between neutron power changes and detected thermal power changes (around 25 s) and a non-linear relationship with neutron power especially at low power levels (below 10 %FP). The importance of the time lag may be seen by calculating the neutron power change that would occur in the time before there is any detected change in the channel ΔT. With an insertion of reactivity ρ = +1 mk at equilibrium fuel and assuming the time lag to be about 5 s, we find using the neutron power equation (point kinetics description, see lesson 3):

$$\frac{P(t)}{P_0} = \frac{\beta}{(\beta - \Delta\rho)} \; e^{+\frac{\lambda\rho}{(\beta - \rho)}t}$$

that neutron power would increase by a factor of 1.7 before detected thermal power even started to change (using β = .0035 and λ = 0.1). it should be clear that thermal power measurement is incapable of protecting the reactor from a rapid increase of reactivity, in fact it is rather slow even for normal control.

The non-linearity between thermal power and neutron power is due principally to fission product decay heat. Approximately 7 % of the total reactor thermal power is produced by the β, γ decay of the fission products. Thus in a reactor operating at 100% of rated thermal output, 7 % of the thermal power is due to decay heat. Even if it were possible to instantaneously stop all fissioning (zero neutron power), the thermal output would still be 7 % of full power and would decay over a long period of time. Figure 1.3 is a graph of a typical rundown of neutron power and thermal power after a reactor trip. Note that after a minute the neutron power makes little contribution to the thermal power.
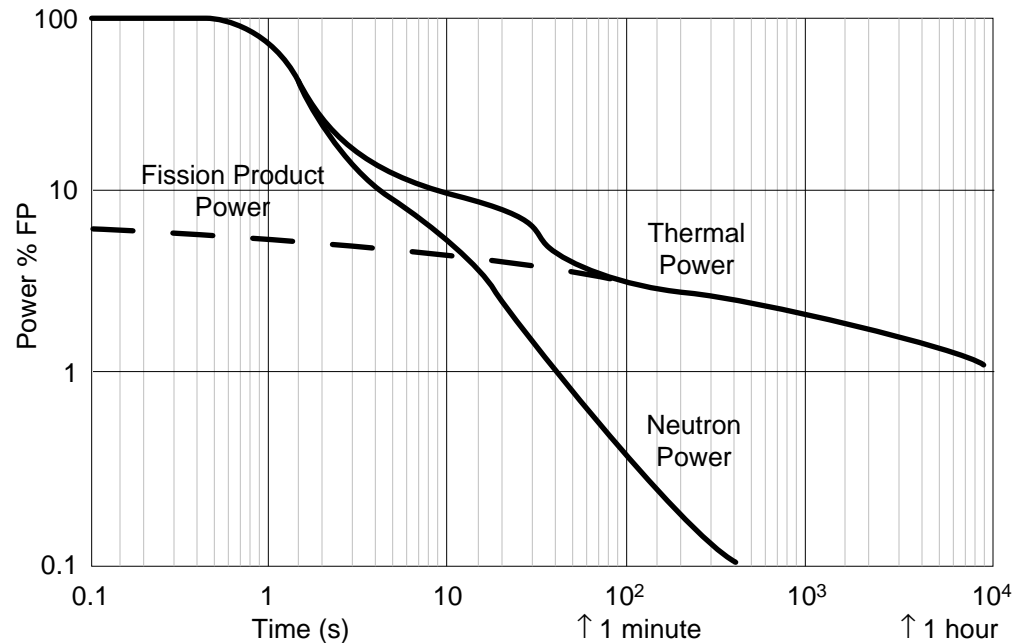
A second source of non-linearity is the heat lost from the coolant channels to the moderator (ex.: ~4 MW[th] at BRUCE-A). The amount of heat lost is a function of the temperature difference between the coolant and the moderator and is, therefore, relatively independent of the power.

A third source of non-linearity is the heat generated by fluid friction. About two-thirds of the pressure drop in the heat transport system occurs in the coolant channels. This means that about two-thirds of the heat input of the heat transport pumps shows up in the coolant channels (ex.: ~13 MW[th] at BRUCE-A). This depends only on coolant flow rate and is independent of reactor power level. Because of these non-linearities neutron power must be recalibrated to thermal power when the power level is changed.

1.2.2   Power monitoring when shutdown

As illustrated in Figure 1.3, thermal power and neutron power are not proportional when power is < 10 %FP. To protect the reactor against criticality accidents neutron power must be monitored, especially at low power levels.

Assume a protective system which uses thermal power as the control variable. The reactor is slightly subcritical (k_{eff} = 0.999) and the neutron power is 10^{-5} %FP. Since the response time of the ΔT detector is about 25 s, thermal power would lag neutron power such that, about 25 s after neutron power reacted, 1 % thermal power would indicate 1%. Now assume the reactor is inadvertently made supercritical (k_{eff} = 1.003). For equilibrium fuel, +3 mk gives a reactor

period of ≈2 s. Thus 22 s after the reactivity addition, neutron power will reach 1 %, ≈25 s after that, thermal power will reach 1 % and begin to show a rapid rate of change. In those intervening 25 s neutron power will reach ≈27,000 %.

If this reactor has been monitored for neutron power and rate of change of neutron power, the excursion could have been terminated long before power reached 1 %. Typically SDS1 trips at a reactor period of 10 s and SDS2 trips at a period of 4 s.

Assume a Candu reactor is running at 100% full power, with equilibrium fuel and a reactor trip inserts -40 mk of reactivity. Figure 1.4 shows the theoretical behaviour of the total neutron power.

Fig. 1.4
Neutron power rundown after shutdown
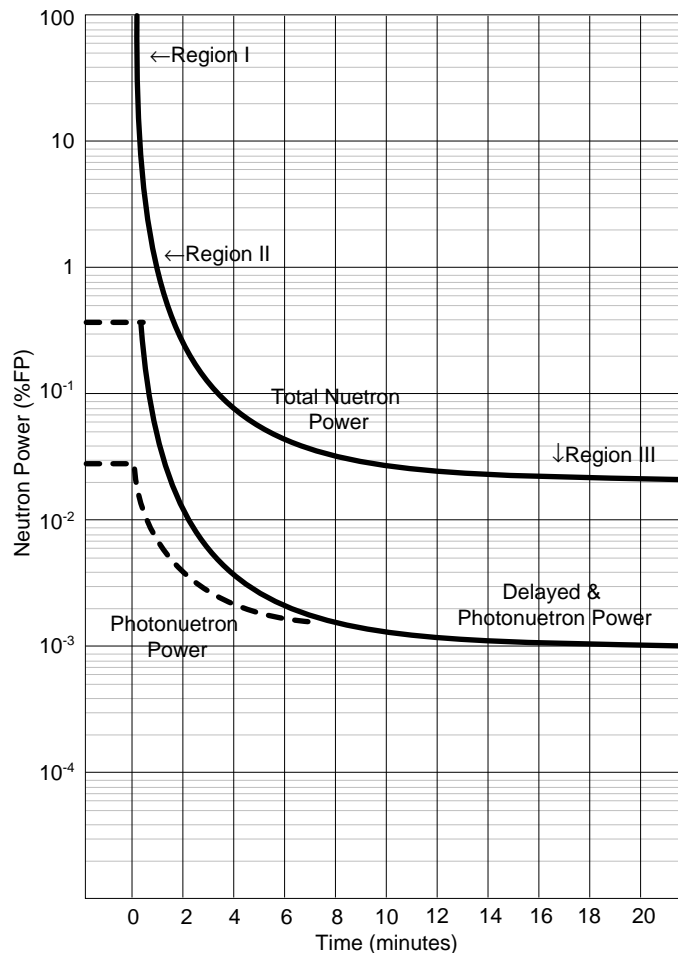
1.2.3 Neutron power rundown

We will divide the power rundown into three regions. In region I the prompt neutron population is rapidly collapsing. With k_{eff} = 0.96 (using typical shutdown reactivity $\Delta\rho$ = -40 mk) the original prompt neutron population would decrease by a factor of 0.96 each generation. In 100 generations it would be less than 2 % of its original value. Using in fact the relationship of neutron generation by iterative multiplication: $n/n_0 = k^n$, then it comes that $0.96^{100} = 0.017$ (~ 2 %).

With a prompt neutron lifetime of 0.001 s, this decrease would take 0.1 s. Because of the delayed and photoneutrons, the actual neutron power will, however, not drop this fast nor will it drop this far. Just before the reactivity insertion, delayed neutrons made up 0.35 % (fraction β) of the neutron population (ie, 99.65 % of the fissions were caused by prompt neutrons, 0.35 % were caused by delayed neutron.). Immediately after the insertion, if we assume the prompt neutrons disappear we have a source of neutron giving 0.35 %FP in a subcritical reactor. We can use the equation for neutron power after the prompt drop, which in this case gives:

$$\frac{P(t=0)}{P_0} = \frac{\beta}{(\beta - \Delta\rho)}e^0 = \frac{0.0035}{(0.0035 + 0.04)} = 0.08$$

Note that the power level of 8 %FP is higher than the source power level because of the multiplicative material. Therefore, the delayed neutrons present at the time of the trip will not let the neutron power drop initially below ~ 8 %FP as shown in Figure 1.4 (the actual drop is always determined by the value of β and the amount of inserted reactivity $\Delta\rho$).

As the reactor is subcritical, the power drop appears throughout regions II and III. In region II the source of neutrons is the decay of the delayed neutron precursors which were present prior to shutdown. This source decreases rapidly at first as the short-lived precursors decay until the longest-lived group ($t^{1/2}$ = 55 s) controls the rate of power decrease.

As was pointed out in Lesson 3, the reactor period after a large insertion of negative reactivity may be approximated as:

τ (reactor trips) $\approx$ - 1 / λ if $\Delta\rho << -\beta$
where, λ is the decay constant for the delayed neutron precursors.

The division between regions II and III is somewhat arbitrary. As the longer-lived delayed neutron precursors decay, the photoneutrons are now the only important source of neutrons. Twenty minutes after shutdown, the photoneutrons become the controlling source. From then on the power decreases at a rate determined by the decay of the fission fragments producing the 2.2 MeV photons required for the photoneutron reaction. As the longest-lived photoneutron producing fission fragments have half-lives of ~ 15 days, this source takes about 3 months to reduce to 10^{-7} FP.

1.2.4 Thermal power rundown

At full power ~ 7 % of the total thermal power is produced by the decay heat of the fission products (see Lesson 1). Although the fission rate can decrease very rapidly, the heat produced by decay of fission products (called decay heat) will only decrease at the decay rate of the fission products. Fission products have half-lives ranging from fractions of a second to thousands of years. Thus we expect a slow decrease in thermal power. Typically thermal power will take about a day to decrease to 1% of full power (~ 29 MW[th] for a BRUCE reactor).

The actual thermal power rundown will depend on the fission product inventory. A reactor at equilibrium fuel will have more fission products than one with relatively fresh fuel. Therefore, it would produce a greater decay heat. This difference in production of decay heat will become more pronounced as time passes and the longer-lived fission products become more significant.

2 Approach to Criticality

2.1 Source neutron effects

The source neutrons available in CANDU reactors are those from spontaneous fission and those from the photoneutron reaction with deuterium. Spontaneous fission produces a neutron flux which represents approximately a fraction of 10^{-14} of the full power flux (spontaneous fission has an order of magnitude less than 10^2 n.cm^{-2}.s^{-1}). The strength of the photoneutron source depends on the number and energy of the photons present. At significant power levels (> 10 %FP) the gamma flux is directly proportional to the power level; thus, the photoneutron reaction produces a photoneutron flux which is proportional to the total neutron flux present. At low power levels and particularly when shutdown, the strength of the photoneutron source depends on the inventory of fission products which produce the high energy (> 2.2 MeV) gammas required for the photoneutron reaction. The longest lived relevant fission product decay chain has a half life of about 15 days; thus the photoneutron source persists for several weeks after shutdown, decreasing exponentially from approximately 10^{-5} %FP one day after shutdown. We will see that the values given for the actual neutron fluxes in the reactor due to the photoneutron source do not include any fission multiplication of this source.

2.1.1 Effect of neutron sources on the total neutron population

In a critical reactor with no neutron sources other than induced fission, the neutron population in the reactor remains constant from one generation to the next since absorption and leakage balance exactly the excess neutrons generated by fission that are not required to keep the chain reaction going.

Suppose that a neutron source emitting S_0 neutrons in each neutron generation time is inserted into the reactor, and let this reactor be subcritical ($k < 1$).

The number of neutrons present at the end of the first generation will be S_0. At the end of the second generation, these S_0 will have become S_0k neutrons, and another S_0 neutrons will have been added by the source, giving a total of $S_0 + S_0k$ neutrons. At the end of the third generation, these $S_0 + S_0k$ neutrons will have become $(S_0 + S_0k)k$ neutrons, and again another S_0 neutrons will have been added by the source to give a grand total of $(S_0 + kS_0 + k^2S_0)$. Continuing the argument indefinitely and using the fact that $k < 1$ lead to a final neutron population $S\infty$ given by :

$$S_\infty = S_0 + kS_0 + k^2S_0 + k^3S_0 + k^4S_0 + ...$$
$$= S_0 (1 + k + k^2 + k^3 + k^4 + ...)$$
$$= S_0 / (1 - k)$$

where we used the convergent sum of the geometric series:

$$1 + k + k^2 + k^3 + k^4 + ...$$
$$= 1 / (1 - k) \quad \text{if} \quad k < 1$$

Example 1 :
Subcritical Constant Neutron Population
If S_∞ = 5000 neutrons per generation and $k = 0.8$, these 5000 neutrons will become $k S_\infty$ = 4000 neutrons after one more generation. Since $k < 1$, this means that $(S_\infty - S_\infty k)$ = 1000 neutrons have been removed and these are made up by $S0$ = 1000 new emitted neutrons.

Using the following expression for the reactivity ρ :

$$\rho = (k - 1) / k \quad \text{then} \quad \Delta\rho \approx k - 1$$

we can write in terms of neutron population S or neutron power P :

$$S_\infty = -S_0 / \Delta\rho \quad \text{or} \quad P_\infty = -P_0 / \Delta\rho$$

Example 2 :
Subcritical Multiplication
Even when the reactor is well below critical (ex.: -40 mk, typical of reactor trip) the equilibrium source level S_∞ is greater than the actual photoneutron source and the factor $1/(1 - k)$ is the subcritical multiplication factor:

if $\Delta\rho$ = -40 mk then $S_\infty = S_0 / (1 - k) = S_0 / (1 - 0.96) = 25\,S_0$

if $\Delta\rho$ = -20 mk then $S_\infty = S_0 / (1 - k) = S_0 / (1 - 0.98) = 50\,S_0$

In a subcritical reactor without a neutron source the neutron population would totally collapse; however, when a source is present it is not the major constituent of the equilibrium neutron population (provided $k > 0.5$).

2.1.2 Subcritical reactor

The value of k can be easily obtained in a subcritical reactor in the following way. Suppose a reactor is shutdown with a constant indicated power of 2×10^{-5} %FP. The operator inserts +1 mk by withdrawing an adjuster and power stabilizes at 3×10^{-5} %FP. Let's find the original value of k.

Before and after the reactivity addition we have respectively

$P_{\infty i} = P_0 / (1 - k_i)$ and $P_{\infty f} = P_0 / (1 - k_i - \Delta\rho)$

leading to

$k_i = 1 - \Delta\rho (1 - P_{\infty i} / P_{\infty f})^{-1}$

and we obtain for the example $k_i = 0.9970$. This means that we can always find the value of k in a shutdown reactor by changing the reactivity and noting the power before and after.

In a subcritical reactor the power will increase to a new equilibrium value each time positive reactivity is added. The magnitude of the increase and the time it takes for power to stabilize will depend on the value of k. The closer k is to one the larger the power increase for a given reactivity increase, and the longer the time for the power to stabilize:

$P_{\infty f} = P_{\infty i} [1 - \Delta\rho / (1 - k_i)]^{-1}$

The Figure 2.1 illustrate the power increase in a subcritical reactor where we start with $P_{\infty i} = 10^{-5}$ %FP and $k_i = 0.90$ and add reactivity in $\Delta\rho = +10$ mk steps allowing P_{∞} to stabilize after each reactivity addition.

Fig. 2.1
Power increase in a subcritical reactor

10 mk step changes

Times in neutron generations
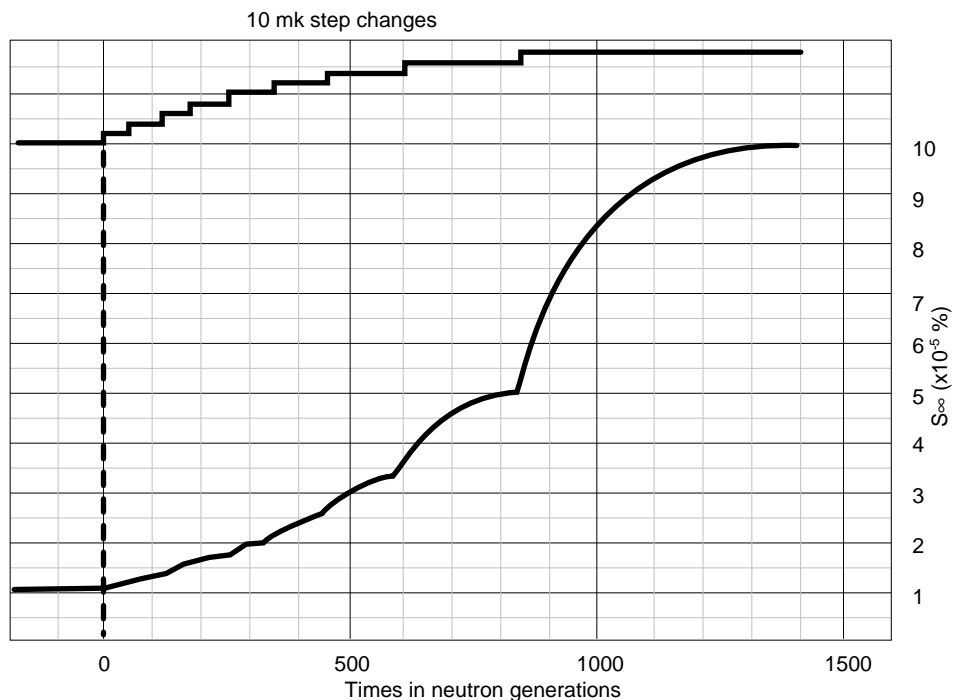
2.2   Approach to criticality transients

During the approach to criticality the reactor will, by definition, be subcritical. Therefore, we have to consider the behaviour of neutron power in a subcritical reactor. The approach to critical with regulating system instruments off scale represents a "transition" state, in which the reactor is neither under the control of the reactor regulating system, nor is it in a guaranteed shutdown state. One must carefully monitor and control any changes in reactivity. Since operating history of the core is different for every outage, any procedure to make the reactor critical should be carried out with extreme caution.

The following sections look at different transients: the initial approach to criticality, an approach to criticality following a poison outage, and an approach to criticality following an extended outage.

2.2.1   Potential hazards during the initial approach to criticality

The initial approach to criticality is a procedure undertaken with great caution, because the reactor is in a potentially dangerous condition. The reasons for this are:

1. Available reactivity is near its maximum value since there has been no fuel burnup and there are no fission products present. This excess positive reactivity is compensated for by moderator poison; however, the poison is removable, hence the possibility of a large positive reactivity insertion exists.
2. Normal nuclear instruments (ion chambers and flux detectors) will be "off scale" at their low end (10^{-7} FP); therefore, the regulating system will not automatically control the reactor.
3. The count rate from the startup instrument is used to monitor reactor power while under manual control at very low powers. This instrumentation enables to see the effect of reactivity changes and determine if the reactor has gone critical. Without monitoring, the reactor could be made supercritical at a very low power level. And, it is possible that positive reactivity addition could continue, resulting in a rapid power increase.
4. If startup instruments were not used, an uncontrolled power rise could only be terminated after the normal SDS instruments come on scale. Although startup instruments (He-3 or BF3 detectors) would be wired into the shutdown systems to provide trip coverage, their response is slow at the very low power levels being measured. Therefore, if a very rapid power rise took place, an unacceptably large power excursion could occur before the reactor is shutdown.
5. The critical value of the control variable is not precisely known. For example, if the approach to criticality is being made by removing moderator poison, the critical poison concentration is only a design estimate.

2.2.2 Methods to achieve/predict criticality

Early Candu Units

The method for early CANDU units was to raise moderator level until enough fuel was covered to sustain a chain reaction. More precisely, k_∞ was fixed and the leakage was gradually reduced until k was exactly 1.

The approach to criticality was monitored by devising linear plot which could readily be extrapolated to predict the critical moderator level. From section 2.1 recall that:

$$P_\infty = P_0 / (1 - k) = - P_0 / \Delta\rho$$

Since the count rate on any detector is proportional to P_∞, we can now write:

$$1 / \text{count rate} \propto (1 - k) \propto \Delta\rho$$

Since $\Delta\rho$ is a direct function of moderator level (as level increases, k increases), we can plot the reciprocal count rate versus moderator level as shown in Figure 2.2.

Fig. 2.2
Approach to critical graph
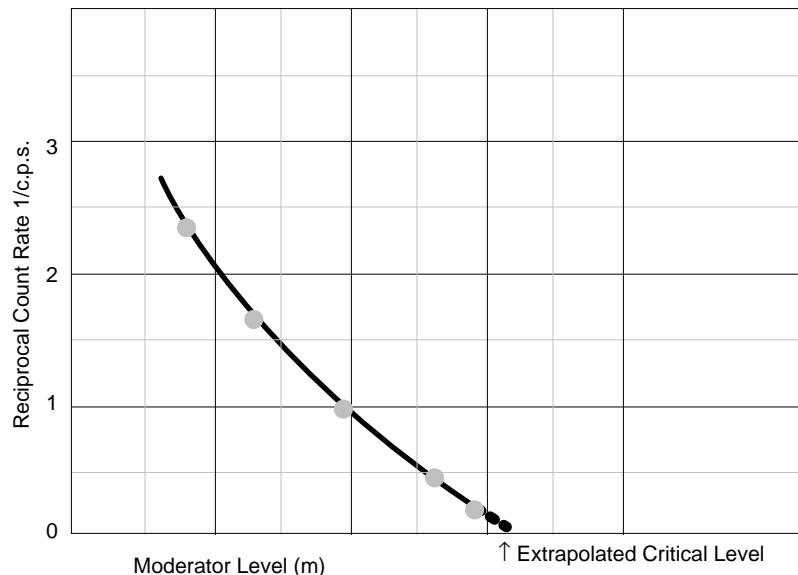
The intercept of this curve with the moderator level axis gives the critical level.

Newer Candu Units

Alternatively, you could begin in the guaranteed shutdown state. The calandria is nominally full of moderator and overpoisoned to ensure that criticality is not possible. The poison is gradually removed until criticality is reached. In this case, the leakage is nearly constant, and k is increased by raising the value of f, the thermal utilization factor, until k equals 1.

Pickering A, Unit 3 and all subsequent CANDU units obtained initial criticality by removing poison (boron or a combination of boron and gadolinium) from the moderator. In these cases the moderator was full throughout the startup. The

reactivity ($\Delta\rho$) is proportional to poison concentration (1 ppm boron = 8.85 mk; 1 ppm gadolinium = 31.42 mk). Because of this, total poison load may be calculated from the measured poison concentration. A plot of poison load versus inverse count rate is a straight line. Figure 2.3 shows a plot of inverse count rates from the incore detectors for the Bruce A, Unit 1 initial criticality. The measured values fall in a straight line, that can be extrapolated to predict the poison concentration at criticality.

Fig. 2.3
Inverse count rate as a function of the poison load
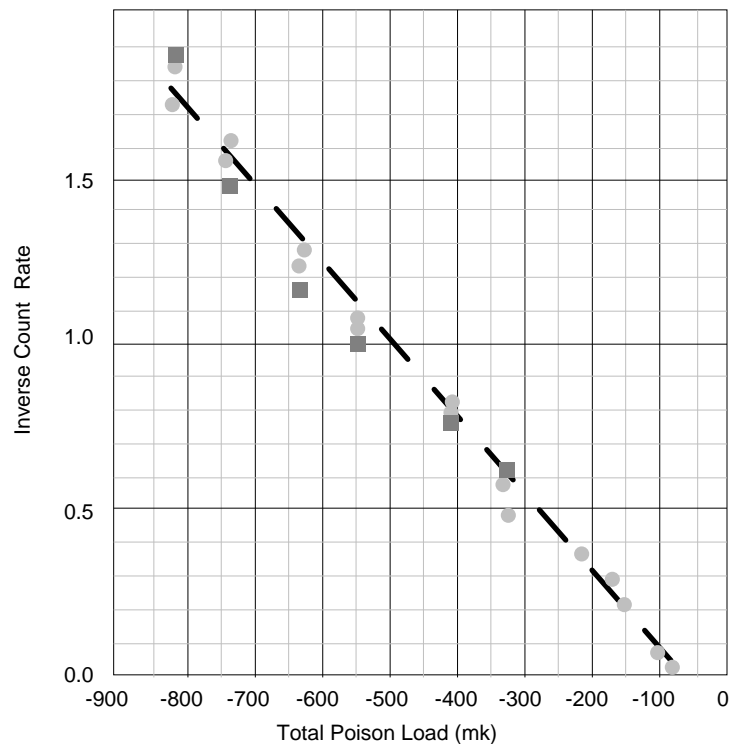
These types of approaches do not have to be repeated for every startup. Once sufficient fission products have been built up to give a significant photoneutrons source, (actual neutron power > 10^{-5} %FP) the reactor may be started up using installed instrumentation and automatic regulation.

Power Doubling Rule
A method used for approaching criticality is the power doubling technique. When starting with a subcritical reactor, the power doubling rule states:
• when an addition of reactivity causes a doubling in subcritical reactor power (count rate), then a further addition of the same amount of positive reactivity will make the reactor critical.

If 1 mk has been added to a subcritical reactor, and has caused subcritical reactor power to double, then the addition of another 1 mk will cause the reactor to go critical.

This is a simple concept, but why does it happen? The relation between the power level, the source strength and the degree of subcriticality is:

$$P_\infty \ = \ P_0 \ / \ (1 - k) \ = \ - P_0 \ / \ \Delta\rho$$

When RRS is requested to increase power, it will add reactivity, making $\Delta\rho$ in the formula smaller. If possible (i.e. within the control range), RRS adjusts $\Delta\rho$ in the formula until the new setpoint is reached. A request to double power (or to double P_∞) requires RRS to add enough positive reactivity to cut $\Delta\rho$ in the formula in half (i.e. substituting $\Delta\rho/2$ for $\Delta\rho$ in the above formula).

Since power doubling occurs when half of the $\Delta\rho$ has been added, adding the same amount again makes the reactor critical ($\Delta\rho$ is reduced to zero, so $k = 1$).

Another way of looking at this is that we start with a subcritical core with a neutron multiplication constant k and equilibrium power P_∞. We then add core reactivity by an amount equal to x mk (i.e. either by changing zone level or by removing moderator poison), causing the power to double to $2P_\infty$.

Since we can assume the source power (P_0) is constant, then:

$$P_\infty \ (1 - k_1) \ = \ 2 \, P_\infty \ (1 - k_2) \ = \ 2 \, P_\infty \ (1 - k_1 - x)$$
$$\text{therefore,} \ \ k_1 \ = \ 1 - 2 \, x$$
$$\text{then,} \ \ k_2 \ = \ (1 - 2 \, x) + x \ = \ 1 - x$$

So if we now add an additional reactivity by the amount of "x" to k2, then k becomes unity, and consequently the reactor is in a critical state.

$$k_{crit} \ = \ k_2 + x \ = \ (1 - x) + x \ = \ 1$$

If the reactor is deeply subcritical (i.e. poisoned), the power doubling will be observed during poison removal. From the amount of poison removed to cause a power doubling, we can estimate the approximate poison concentration when the reactor will reach criticality.

The ease of this method is shown when the reactor is only slightly subcritical (one or two mk), where requests to the regulating system to double power can be handled within the available control range of the liquid zones. From the above examples, we can see that if we continue to request RRS to double reactor power, we will never actually reach criticality, we just move closer and closer to it. This method ensures that the approach to criticality is done in a progressive and safe manner. From a practical viewpoint we can say the reactor is "critical" if a power doubling request results in only a small change in liquid zone level (for example, less than a 5 % change in zone levels allowable zone level change will be specified in operating documentation).

2.2.3   Approach to criticality after a poison outage

For this discussion, we assume that there are sufficient source neutrons to keep the reactor regulating system instruments on scale, and RRS is available to control reactor power.

As the xenon decays in the reactor, the ion chamber signals increase until the reactor power reaches its setpoint. At this point, RRS will take control of bulk reactor power. As more xenon decay occurs, the liquid zones will start to fill to maintain the reactivity balance. Once the liquid zones reach their control limit, and the xenon decay continues, reactor power would increase in the absence of further control action. Poison addition and/or adjuster insertion (if they are out) will be required to maintain the liquid zones in control range.

There are certain aspects of a poison outage that have to be considered.
1) During a poison outage, reactivity changes are not under direct control. The reactivity changes are affected mainly by the xenon transient.
2) The characteristics of the xenon transient following a reactor shutdown are highly dependent on the operating history of the reactor prior to shutdown. If this was not considered, this may result in reaching criticality earlier than one would expect. This is undesirable, since the operator must be ready to verify that RRS has taken control/maintains control of reactor power, otherwise a rapid power increase could result.
3) During the reactor poison outage, the reactor starts off with reactivity decreasing, making the reactor more subcritical. When the xenon concentration starts decreasing, the reactivity starts to increase, making the reactor less subcritical. Careful monitoring is required!

2.2.4   Approach to criticality after extended outages

For an approach to criticality after an extended shutdown, we must use the same degree of caution as we do for the first approach to critical. The reasons for this are:
1) In this very low power situation, the RRS and SDS ion chamber power readings are not correct, because they are heavily influenced by the background γ-radiation levels. Startup instrumentation is required.
2) Available reactivity is high, and will be uncertain. Iodine has decayed to xenon, and the xenon has also decayed. Other neutron absorbing fission products have decayed. The amount of fissile ^{239}Pu increases due to the decay of ^{239}Np, introducing positive reactivity into the core. The samarium growth after shutdown (from the decay of ^{149}Pm) has introduced negative reactivity into the core, the amount depending on Pm concentration in the fuel prior to shutdown (but not enough to cancel the positive reactivity of ^{239}Pu). The sum of all of the above factors can only be estimated.
3) Reactivity worth of moderator poisons is uncertain. Chemical sampling indicates chemical concentration, but will not indicate isotopic of the neutron absorbing isotopes. If a poison shim was in used prior to the outage, some of

the absorbing material will be burned off (ex.: Gadolinium isotope [1] *see note 1*).

4) The rate of poison removal during the approach to criticality will be uncertain. The reactivity is under the control of the operator by manual poison removal. The operator has an indication of purification system flow, but rate of poison removal also depends on the condition of the ion exchange resins and concentration of moderator poisons.

3 Xenon Transients

3.1 Effects of Xenon-135 poison

The xenon isotope ^{135}Xe plays an important role in any power reactor. It has a very large absorption cross section for thermal neutrons and represents therefore a considerable load on the chain reaction. The ^{135}Xe concentration has an impact on the power distribution, and in turn is affected by the power distribution, by changes in power, and by movements of reactivity devices.

3.1.1 The Xe-I kinetics

The ^{135}Xe/^{135}I kinetics are shown in Figure 3.1.

^{135}Xe is produced to some degree directly in fission, but mostly as the result of the beta decay of its precursor ^{135}I (which has a half-life of 6.585 hours). ^{135}Xe is destroyed in two ways:
- through its own radioactive decay (^{135}Xe has a half-life of 9.169 hours), and
- by absorption of neutrons to form ^{136}Xe.

---

1 *Note that Gadolinium-155, on absorbing a neutron becomes a non-absorbing isotope. Since chemical analysis cannot distinguish between isotopes, high Gd concentration does not necessarily mean a high value of negative reactivity.*

Fig. 3.1
Illustration Xe-135/I-135 kinetics
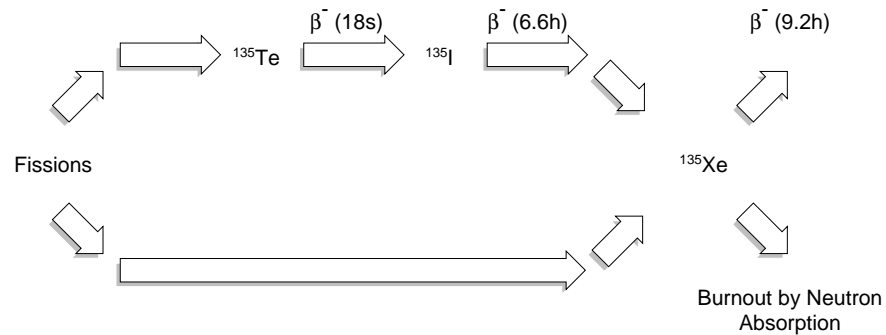
^{135}I is a direct product of fission, but can also appear through the radioactive decay chain ^{135}Te → ^{135}Sb → ^{135}I. As ^{135}Te and ^{135}Sb have very short half-lives (19.0 s and 1.71 s) compared to those of ^{135}I5 and of ^{135}Xe, it is sufficient to model the decay of ^{135}Te and ^{135}Sb as "instantaneous" and add their yields in fission to that of ^{135}I.

The ^{135}Xe/^{135}I kinetics in any particular fuel bundle can thus be represented by the following equations:

$$\frac{dI}{dt} = \gamma_i \, \hat{\Sigma}_f \, \hat{\phi}_F - \lambda_i \, I$$

$$\frac{dX}{dt} = \gamma_x \, \hat{\Sigma}_f \, \hat{\phi}_F + \lambda_i \, I - \lambda_x \, X - \hat{\sigma}_x \, X \, \phi_F$$

where
$\quad$ X $\;=\;$ average concentration of ^{135}Xe in the bundle in atoms.cm^{-3}
$\quad$ I $\;=\;$ average concentration of ^{135}I in the bundle in atoms.cm^{-3}
$\quad$ γ_x $\;=\;$ direct yield of ^{135}Xe per fission (averaged over all fissions)
$\quad$ γ_i $\;=\;$ direct yield of ^{135}I in fission, including yields of ^{135}Te and ^{135}Sb
$\qquad\quad$ (averaged over all fissions)
$\quad$ λ_x $\;=\;$ decay constant of ^{135}Xe in s^{-1}
$\quad$ λ_i $\;=\;$ decay constant of ^{135}I in s^{-1}
$\quad$ $\hat{\phi}_F$ $\;=\;$ average flux in the fuel in the bundle in n.cm^{-2}s^{-1}
$\quad$ $\hat{\Sigma}_f$ $\;=\;$ macroscopic fission cross section of the fuel in cm^{-1}
$\quad$ $\hat{\sigma}_x$ $\;=\;$ microscopic ^{135}Xe cross section in cm^2

In the above equations, the term $\;\gamma_i \, \hat{\Sigma}_f \hat{\phi}_F$ gives the ^{135}I production rate, while λ_iI gives the ^{135}I loss rate (and the production rate of ^{135}Xe by iodine decay). Similarly, the term $\;\gamma_x \, \hat{\Sigma}_f \hat{\phi}_F$ gives the production rate of ^{135}Xe due to direct fission, while λ_xX gives its decay rate. The term $\hat{\sigma}_x \, \hat{\phi}_F$ presents the burnout rate of ^{135}Xe due to neutron capture. Because of the comparable magnitudes of the various terms, the ^{135}Xe concentration is very sensitive to changes in flux level. The large absorption cross section of ^{135}Xe does significantly affect the value of reactivity of the reactor.

3.1.2   Reactor startup

On starting up a reactor ^{135}Xe will build up according to the equations derived above. In Figure 3.2, the variation of reactivity as a function of time following startup is given for different steady state power levels. It can be seen that it takes ~40 hours for equilibrium ^{135}Xe to be established.

Fig. 3.2

Illustration of Xe buildup after startup
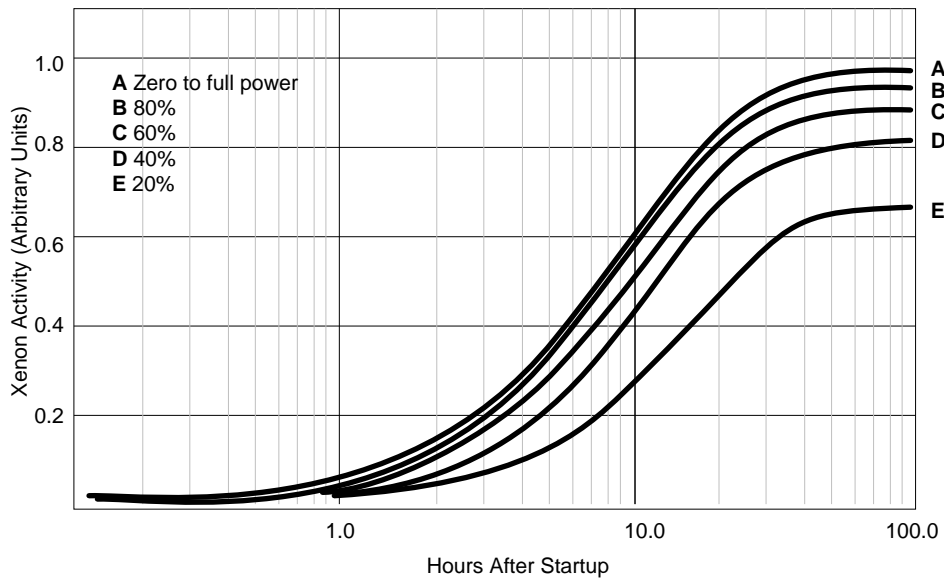
3.1.3   Steady-state xenon load

At steady state the time derivatives dI/dt and dX/dt are zero. The above equations can then be solved to give the steady state concentrations of I-135 and ^{135}Xe (I_{ss} and X_{ss}):

$$I_{ss} = \frac{\gamma_i \, \hat{\Sigma}_f \, \hat{\phi}_F}{\lambda_i}$$

$$X_{ss} = \frac{\left(\gamma_i + \gamma_x\right) \hat{\Sigma}_f \, \hat{\phi}_F}{\lambda_x + \hat{\sigma}_x \, \hat{\phi}_F}$$

It is obvious from these equations that, as a function of an increasing flux $\hat{\phi}_F$, the steady-state ^{135}I concentration increases indefinitely, while in contrast the steady-state ^{135}Xe concentration tends to an asymptotic value which will be denoted $X_{ss,\infty}$:

$$X_{ss,\infty} = \frac{\left(\gamma_i + \gamma_x\right) \hat{\Sigma}_f}{\hat{\sigma}_x}$$

This asymptotic nature of the variation of X_{ss} with $\hat{\phi}_F$, is the reason why ^{135}Xe is termed a "saturating" fission product. (Other saturating fission products are ^{105}Rh, ^{149}Sm, ^{151}Sm)

The limiting ^{135}Xe absorption rate at very high flux levels leads to a maximum reactivity of ~ -30 mk. In CANDU the equilibrium Xe load is ~ -28 mk.

3.1.4 Effect of power changes on xenon concentration

Due to the presence of the term $\sigma_x X \hat{\phi}_F$ the dX/dt equation, the variation of ^{135}Xe- with flux is non-linear. The ^{135}Xe reactivity following power (flux) changes will depend on the starting power level, the time at that level, the new power level, and the time spent at the new power level.

When the power is reduced from a steady level, the ^{135}Xe concentration increases at first. This is due to the fact that ^{135}Xe is still being produced by the decay of ^{135}I, but its burnout rate (by neutron absorption) is decreased because of the reduced neutron flux (reduced power). However, after a certain period (whose length depends on the initial and final powers and the rate of power reduction) the ^{135}I decay rate will have reduced sufficiently that the rate of ^{135}Xe production will have dropped below the rate of ^{135}Xe decay (and burnout), i.e., the ^{135}Xe concentration will have begun to decrease towards a new (lower) steady-state level (after having gone through a peak value).

Conversely, when the power is increased from a steady level, the ^{135}Xe concentration will first decrease and then go through a minimum and start increasing again to a higher steady-state level.

Some typical reactivity variations due to ^{135}Xe following step changes in power are shown in Figure 3.3. It should also be appreciated that ^{135}Xe is spatially distributed. The absorption effects will therefore be different at different points in the core. For these effects a point kinetics treatment is often inadequate.

Fig. 3.3
Xe reactivity transients following stepbacks

Hours after power setback
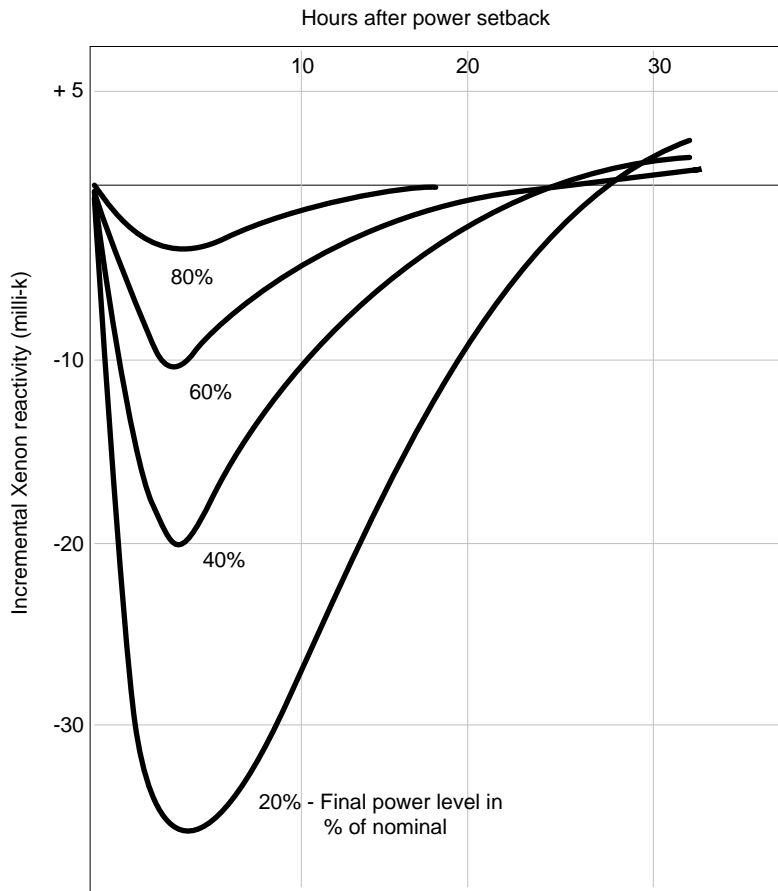
3.1.5   Xenon transient following a shutdown

Following a shutdown, the burnout of ^{135}Xe stops, whereas the production from ^{135}I decay continues for several hours. The net result is that there is an initial increase in ^{135}Xe concentration and a decrease in core reactivity. If it is required to start up shortly after shutdown, extra positive reactivity must be supplied. The ^{135}Xe growth and decay following a shutdown for a typical CANDU is shown in Figure 3.4.

Fig. 3.4
Xe reactivity transient following shutdown
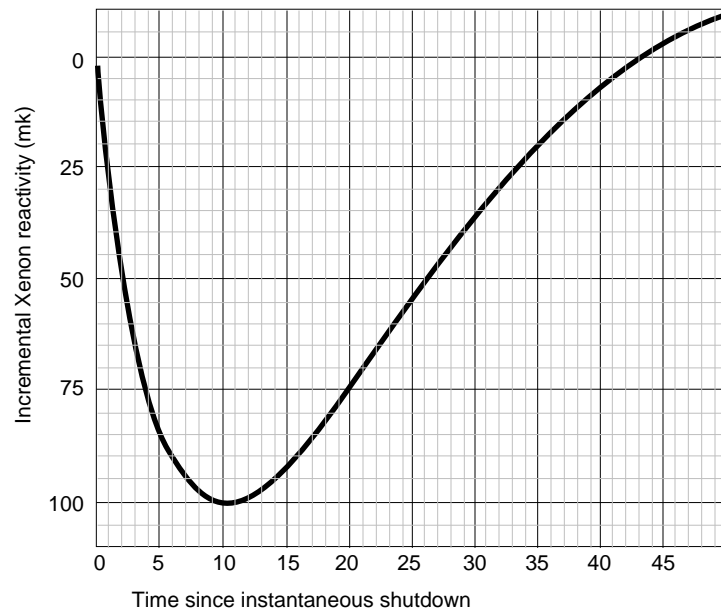
It can be seen from this figure that the reactivity worth of [135]Xe increases to several times its equilibrium value at about 10 hours after shutdown. At ~ 35-40 hours the [135]Xe has decayed back to its pre-shutdown level. If it were not possible to add positive reactivity during this period, every shutdown would necessarily last ~ 35-40 hours, before the reactor reaches criticality again.

To achieve Xenon "override" and permit power recovery following a shutdown (or reduction in reactor power), some CANDUs have a set of adjuster rods which are in core during normal operation and which can be withdrawn to provide positive reactivity. It is not possible to provide "complete" Xenon override capability as this requires more than 100 mk of positive reactivity. The CANDU 600 adjuster rods provide approximately 15 mk of reactivity, which is sufficient for about 30 minutes of xenon override following a shutdown to zero power.

3.2 Power transients and xenon oscillations

As indicated previously, the steady-state [135]Xe concentration in a bundle depends on the steady-state bundle power, and changes in this power cause a transient change in the [135]Xe concentration.

3.2.1 Xenon-135 feedback

Xenon transients can be initiated by global or local changes in power distribution. The former case consists, for example, of an overall change in reactor power level, such as a reactor shutdown or power reduction, perhaps

followed by a power recovery. Localized changes in power distribution can be caused by reactivity-device movements or channel refuelling.

Following any of these scenarios, there are changes in ^{135}Xe concentration. These can be large or small, depending on the magnitude of the power change and the degree of spatial distortion introduced in the power distribution. The change in ^{135}Xe concentration will, in general, be non-uniform through the core, and will itself create a further distortion in the flux and power distributions. This is what is called ^{135}Xe feedback. The feedback is positive, as can be seen from the following analysis. If the local power increases, the local ^{135}Xe concentration decreases, which will decrease the amount of neutron absorption, increase local reactivity, and promote a locally higher flux level (and therefore a locally higher power). Similarly, if the local power decreases, the change in ^{135}Xe will promote a lower power. Thus ^{135}Xe effects tend to reinforce local power changes. This reinforcement lasts for several hours, because of the time scale of Xe-I dynamics.

In large CANDU reactors the neutron flux distribution may vary significantly between different core configurations. Due to xenon feedback, such reactors may be azimuthally and in some cases axially unstable. For these reasons a spatial control is required. The spatial control is performed by the zone control system which is designed to provide stable symmetrical flux shapes.

3.2.2   Spatial xenon oscillations
The above analysis implies that localized changes in power distribution, such as those associated with device movements or channel refuelling, may initiate spatial xenon oscillations.

If, for instance, a withdrawal of a reactivity device induces a side-to-side tilt in the power distribution, with, say, the left side of the core increasing in power, the changes in ^{135}Xe will, at first, increase the tilt. After several hours, the ^{135}Xe concentration will go through a minimum on the left (high-power) side and through a peak on the right (low-power) side. The changes in ^{135}Xe, and therefore in power, will then start a swing in the opposite direction.

If left unchecked, xenon oscillations of the type described here can proceed, causing spatial swings in power with a period of about 24 hours. Any large reactor operating at a high power level can exhibit such spatial instability. The spatial-control system (light water zone control compartments system) in CANDU is designed to counteract xenon oscillations and remove the spatial instability, by introducing positive or negative reactivity differentially in the various core regions to maintain the power distribution close to a reference distribution.

3.3 Power recovery following a short shutdown

As seen in the previous section, a power reduction or reactor shutdown causes a transient increase in the ^{135}Xe concentration. The increased absorption by the xenon constitutes an insertion of negative reactivity. If the xenon is allowed to increase sufficiently, the reactor regulating system (RRS) will no longer be able to introduce sufficient positive reactivity to maintain (or regain) criticality. This results in a "poison-out". If a poison-out occurs, the reactor can be restarted only about 40 hours later, when the ^{135}Xe has disappeared. Thus, in order to return quickly to full power after a substantial power reduction (including a shutdown), sufficient positive reactivity must be inserted, and power must be increased quickly, so that the xenon growth is arrested and reversed.

Within a few minutes of the shutdown, the reactor operator must begin to decide whether the event initiating the reactor "trip" was spurious or serious, and whether it is desired and safe to avoid the poison-out. At about 30 minutes after a shutdown from full power, the ^{135}Xe negative reactivity has increased to about 15 mk. Since the positive reactivity available to the CANDU 600 reactor regulating system (RRS) from adjuster withdrawal is about 15 mk, it is clear that poison-out can be avoided only if the xenon growth has begun to be reversed by this "xenon-override" time.

Before power can be increased to reverse the xenon growth, however, several things must be done, so that the decision-and-action (D&A) time available to the reactor operator is significantly shorter than the xenon override time.
a   All the shutoff rods (inserted during the shutdown) must be withdrawn from the core. This takes about 2.5 minutes.
b   The mechanical control absorbers must be withdrawn from the core. This takes about 2.5 minutes.
c   The adjusters must be withdrawn from the core to regain criticality. The adjusters are withdrawn in banks. The time of withdrawal of all adjusters is about 4 minutes.
d   After criticality is regained, the power must be raised to a sufficient level (about 60% full power) to ensure that ^{135}Xe begins to be burned out again. This takes about 3 minutes.

The decision and action time is thus reduced, relatively to the xenon override time, by a total of approximately 12 minutes, i.e., the D&A time is approximately 18 minutes in the CANDU 600.

Once the power has been raised to about 60% FP, and the ^{135}Xe has begun to burn out, the power recovery can continue. It is, however, not possible to increase power to full level immediately; with the adjusters withdrawn from core, the power shape is peaked radially. At full power, this radial peaking would lead to channel powers higher than the licensed limits.

Thus the power can be raised only when the radial peaking has been reduced, i.e., at least some adjusters have been re-inserted in the core. The procedure to recover from 60% FP to 100% FP thus takes many hours and is the following:

a   Once the ^{135}Xe concentration has burned out sufficiently that the average zone-compartment is about 70% full, insert a single bank of adjusters to reduce the radial peaking. The zone fills will drop because of the bank insertion.

b   With the reduced peaking, the power can be raised a certain amount, accelerating the xenon burnout.

c   Once the average zone fill has again reached 70%, a second bank of adjusters can be re-inserted into the core, leading to less peaking, and the power can be increased by an additional amount.

The above steps can be repeated with the remaining five banks of adjusters (there are seven banks in the CANDU 600), raising power in steps and ensuring that channel and bundle powers are always at acceptable levels, until all banks are back in the core and the latter is in its nominal configuration.

4 Simulations of the Overall Nuclear Plant Behaviour

This section presents two examples of thermalhydraulic simulation of the overall nuclear plant behaviour. Such simulations can be produced for CANDU power plants with the use of thermalhydraulic codes which are able to represent adequately, as needed, some or all of the following items:

• the reactor core including the reactor regulating system (RRS) and shutdown systems (SDS1 and SDS2) with the associated core parameters (detection systems);

• thermal cycle of the primary heat transport (PHT) system with the associated process parameters (detection systems);

• the emergency core cooling (ECC) special safety system;

• the auxiliary circuits (AUX: D$_2$O inventory, feed and bleed systems, etc.);

• the thermal cycle of the secondary heat transport circuit (SEC) starting from the steam generator down to the turbine and the condenser.

The standard thermalhydraulic approaches use at least a one-dimensional homogeneous detailed representation of the various hydraulic components present in the different circuits. Figure 4.1 illustrates the typical modular representation of a CANDU 600 reactor. Special attention is paid when required for the modelisation of two-phase flow (for instance in the steam generator) and of large fraction of coolant void at the reactor channel exit at high reactor power.

Fig. 4.1

Typical modular representation used for thermalhydraulic simulation of CANDU 600 overall plant behaviour
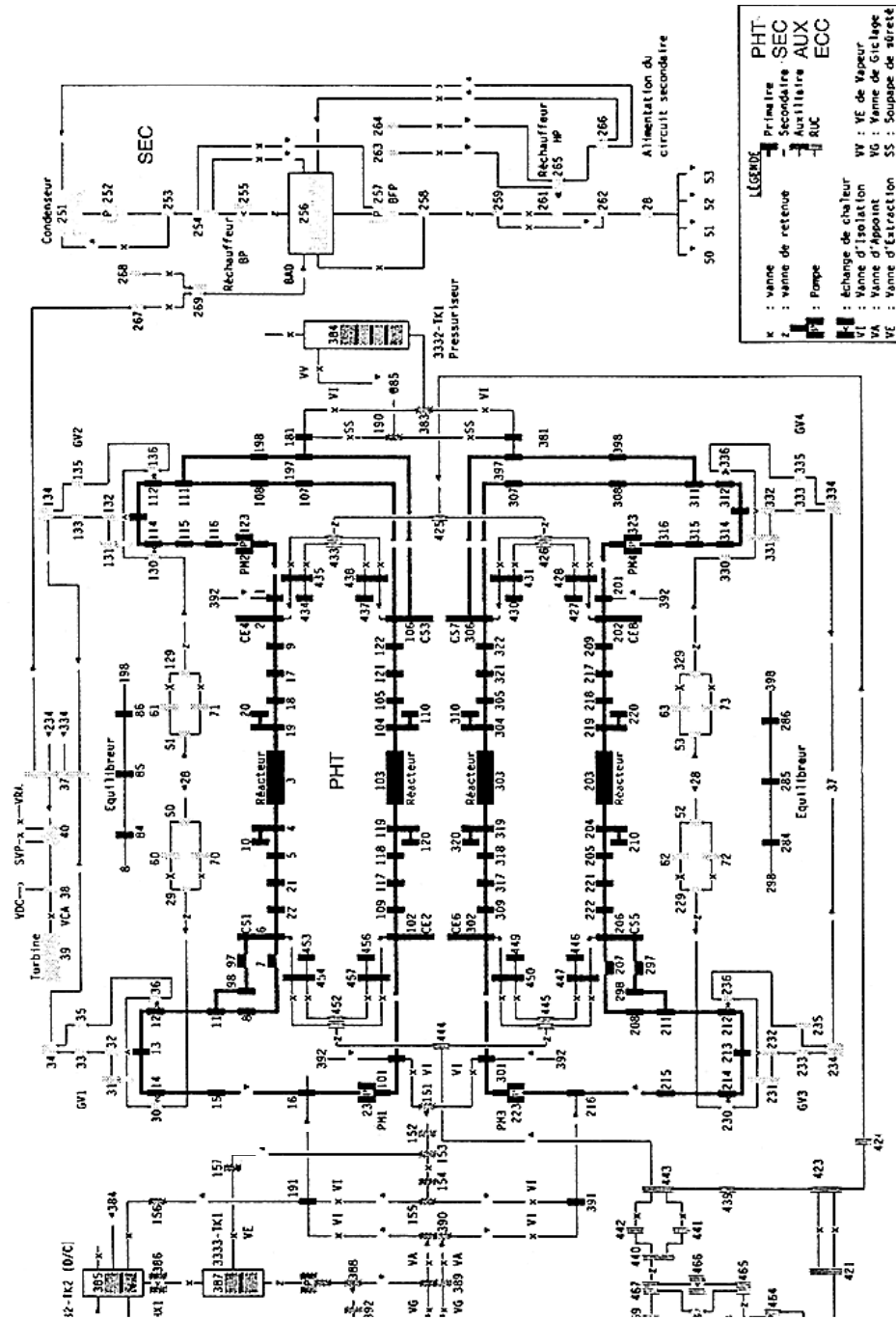
The overall plant transients presented in the next sections require a full representation of the primary and secondary heat transport circuits together with the response of the reactor regulation and shutdown systems.

4.1   Loss of Class IV

The station power systems have been classified into four specific classes: Classes I, II, III and IV. The classification relates to interruptions of power. Specific safety considerations, equipment protection and process considerations create different requirements with respect to permissible and acceptable interruptions in power supply, ranging from no interruption for Classes I and II through long duration (hours) interruption for Class IV. The availability of various classes arises from the fact that Classes I and II derive their power from Class III and /or batteries, Class III derives its power supply from the 230 kV grid and/or standby generators, and Class IV is supplied from the 230 kV grid and/or the turbine generator.

The Class IV groups the interruptible (long term duration) AC power supplies. Being at high voltage and/or requiring high electrical power, the plant equipments which require the Class IV are the turbine, the four HT pumps, the vacum pump of the condenser, etc.

The loss of Class IV is a generic class of scenarios where the Class IV power is interrupted and becomes unavailable for some period of time. The overall plant behaviour including the respective performances of the reactor regulating system and the special safety systems shall be such that the reactor power can be decreased down to zero in a safe manner and without risk of fuel overheating.

From the simulation we obtain the evolution in time of the following parameters: neutron and thermal powers (Fig. 4.2 and 4.3), inlet header pressure (Fig. 4.4), outlet header pressure (Fig. 4.5), pressurizer level (Fig. 4.6), steam generator pressure (Fig. 4.7), steam generator level (Fig. 4.8), steam flow (Fig. 4.9), reactor pressure differential (Fig. 4.10) and in core heat transport flow (Fig. 4.11).

Fig. 4.2
CANDU 600 power plant, loss of Class IV transients
Neutron Power
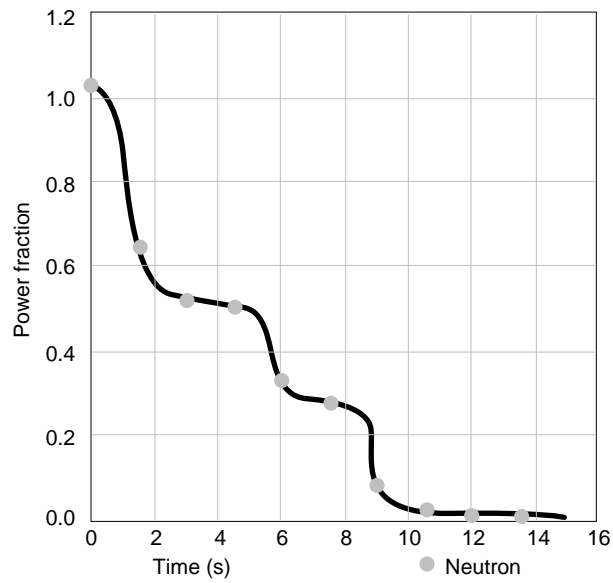
Fig. 4.3
CANDU 600 power plant, loss of Class IV transients
Neutron and Thermal Power
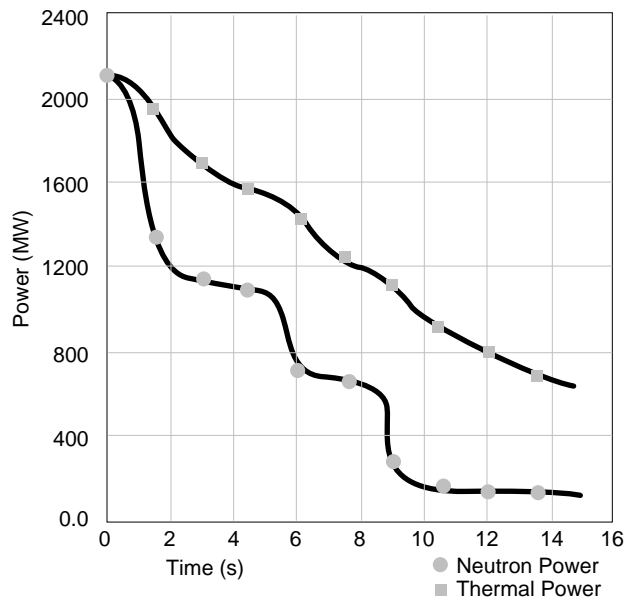
Fig. 4.4
CANDU 600 power plant, loss of Class IV transients
Reactor Inlet Header (RIH) Pressure
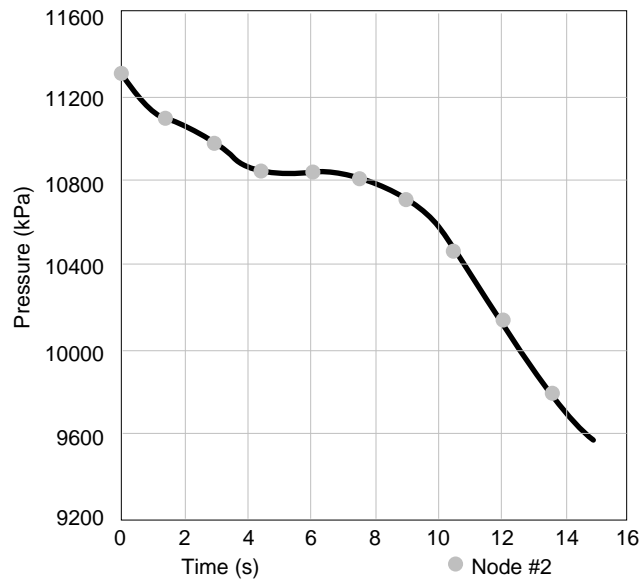
Fig. 4.5
CANDU 600 power plant, loss of Class IV transients
*Reactor Outlet Header (ROH) Pressure*
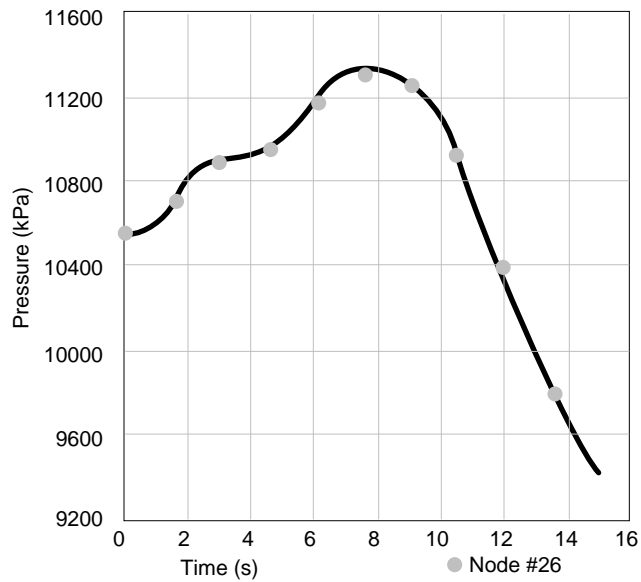
Fig. 4.6
CANDU 600 power plant, loss of Class IV transients
Pressurizer Level
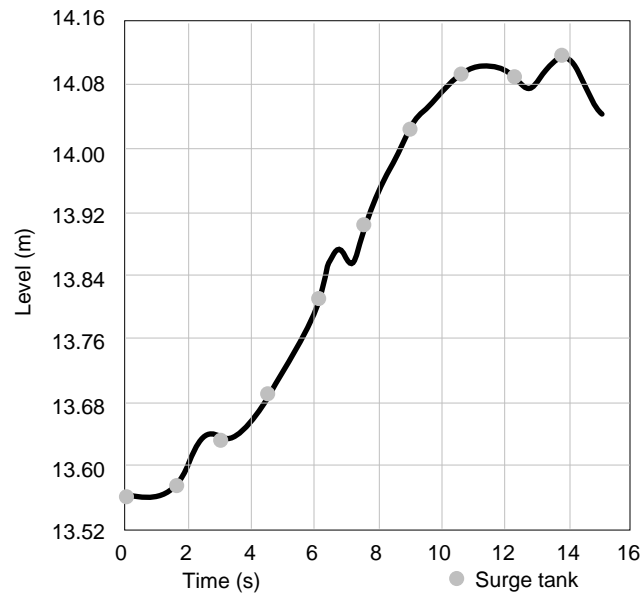
Fig. 4.7
CANDU 600 power plant, loss of Class IV transients
Steam Generator Pressure
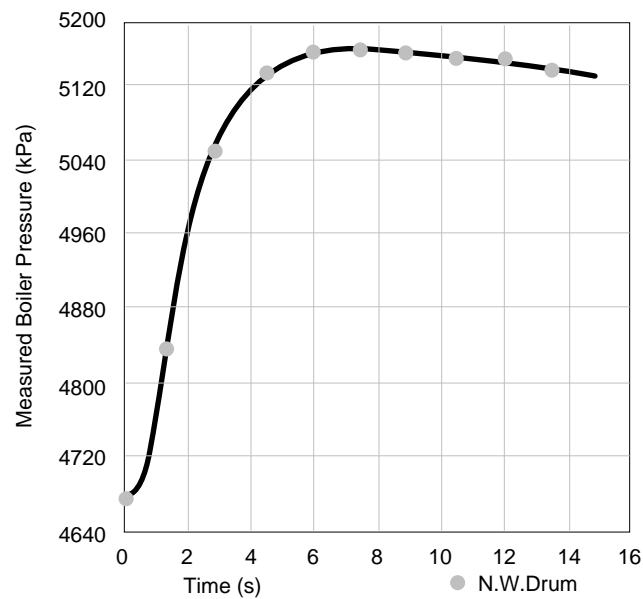
Fig. 4.8
CANDU 600 power plant, loss of Class IV transients
Steam Generator Level
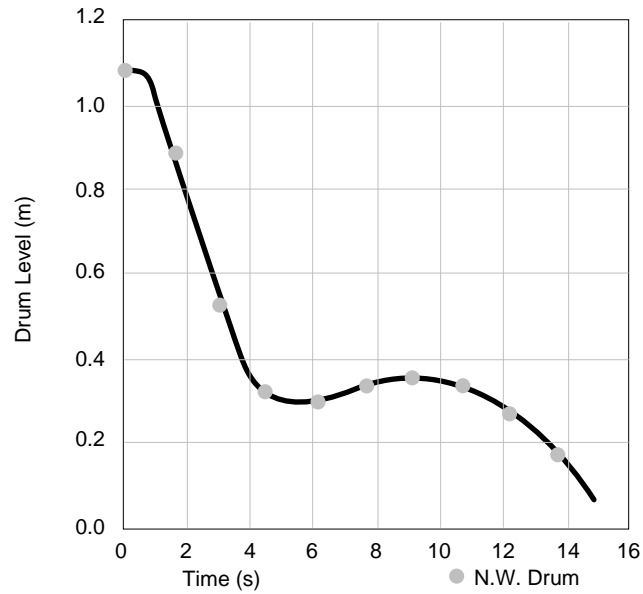
Fig. 4.9
CANDU 600 power plant, loss of Class IV transients
Steam Flow

December 1995
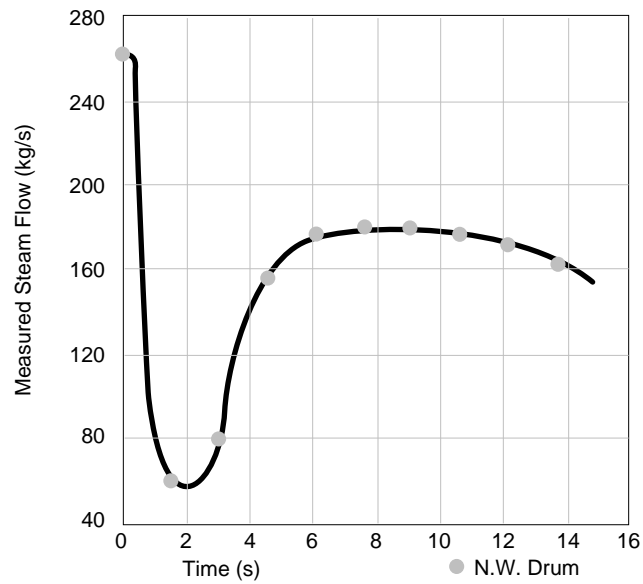
Fig. 4.10
CANDU 600 power plant, loss of Class IV transients
Reactor Pressure Differential
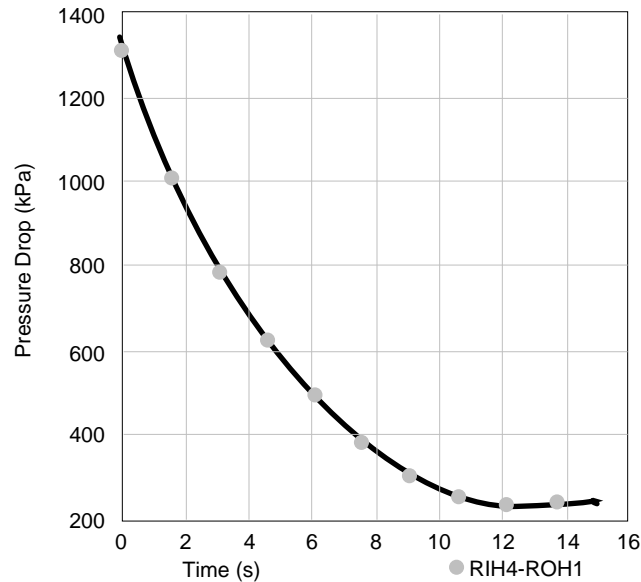
Fig. 4.11
CANDU 600 power plant, loss of Class IV transients
In Core Heat Transport Flow
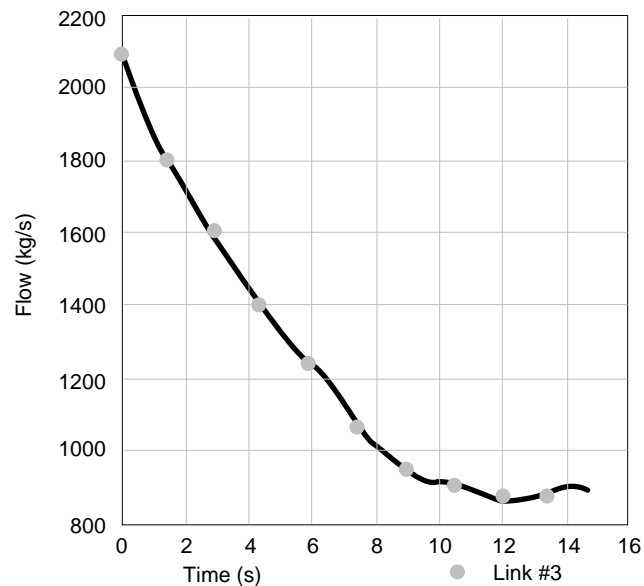
The differences between the neutron power and the thermal power are clearly illustrated in Figure 4.3. First, a time lag of about 3 to 5 s appears between the respective decreasing trends. Second, we can see that the thermal power shows a time averaging and smoothing effect and does not vary as sharply as the neutron power. The plant behaviour can be assessed by the following events

indicated in the simulation (see for instance the power evolution in Fig. 4.2):

- at t = 0 s, the loss of Class IV power forces the four HT pumps and the turbine to trip. With the turbine trip a power stepback is initiated to decrease the power down to 60 %FP and the atmospheric steam discharge valves start to open;
- at t = 1.8 s the stepback condition is cleared since the reactor power setpoint of 60 %FP is reached;
- at t = 5.0 s a new power stepback is initiated on high outlet header pressure and clears with the pressure decrease;
- at t = 8.36 s the reactor is shutdown by SDS2 (poison injection) due the detection of a low differential pressure.

The reactor core transient is then safely monitored and the neutron power comes down in a safe manner. This thermalhydraulic transient is fast and the action of the shutdown system is required if the turbine is tripped initially. In a different scenario, the turbine generator may supply its own station services by islanding just after the loss of the external 230 kV grid. In this case the loss of Class IV does not require a reactor shutdown.

4.2 Loss of one HT pump

Another interesting scenario is the failure of one HT pump which presents slower thermalhydraulic transients.

From the simulation we obtain the evolution in time of the following parameters: neutron and thermal powers (Fig. 4.12 and 4.13), inlet header pressure (Fig. 4.14), outlet header pressure (Fig. 4.15), pressurizer level (Fig. 4.16), steam generator pressure (Fig. 4.17), steam generator level (Fig. 4.18), steam flow (Fig. 4.19), reactor pressure differential (Fig. 4.20) and in core heat transport flow (Fig. 4.21).

Fig. 4.12
*CANDU 600 power plant, loss of one pump transients*
Neutron Power
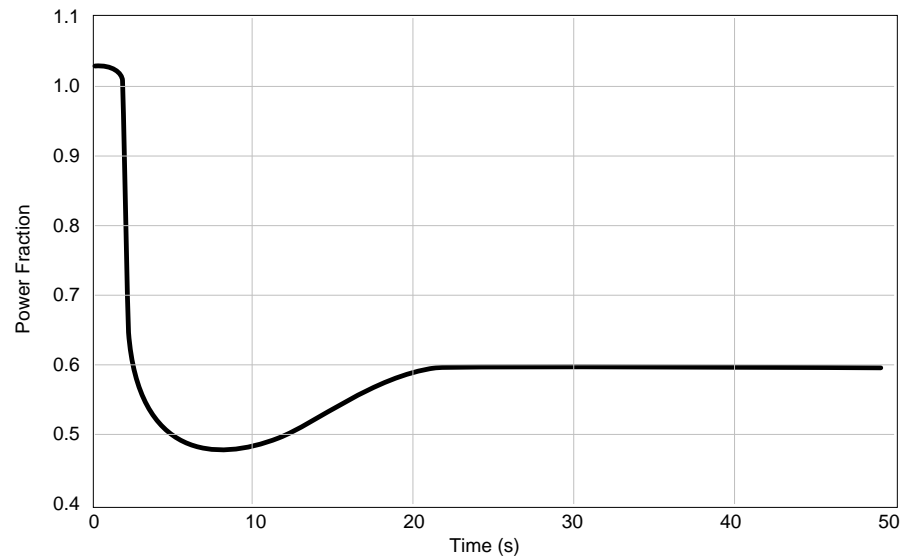
Fig. 4.13
CANDU 600 power plant, loss of one pump transients
*Neutron and Thermal Power*
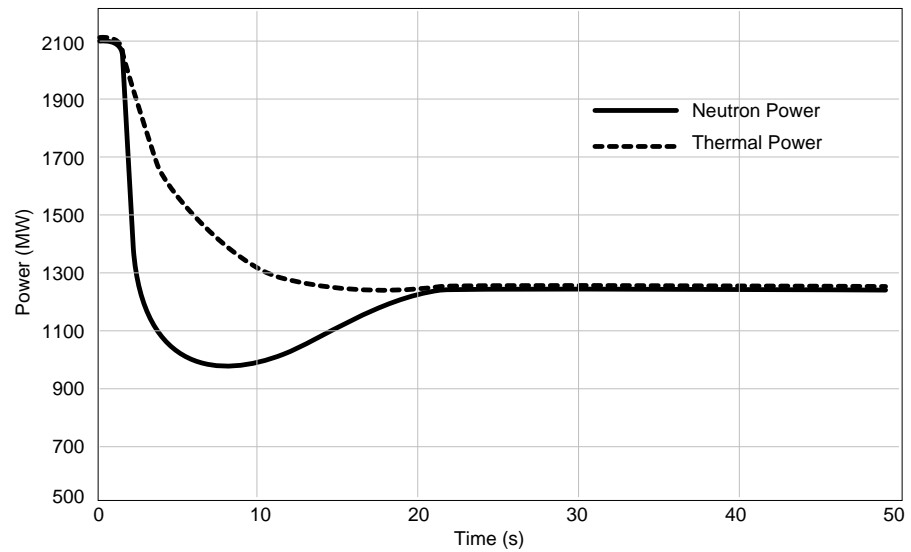
Fig. 4.14
CANDU 600 power plant, loss of one pump transients
*Reactor Outlet Header (ROH) Pressure*
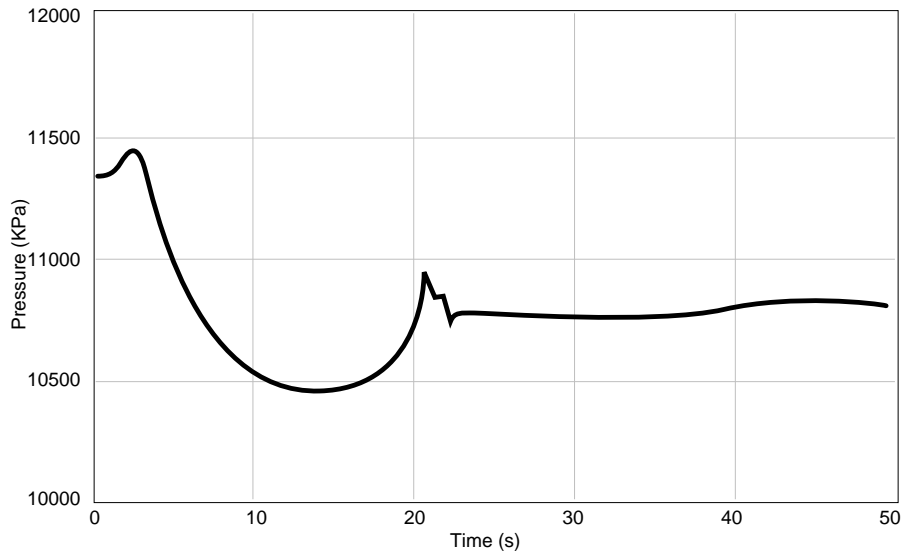
Fig. 4.15
*CANDU 600 power plant, loss of one pump transients*
Pressurizer Level

December 1995
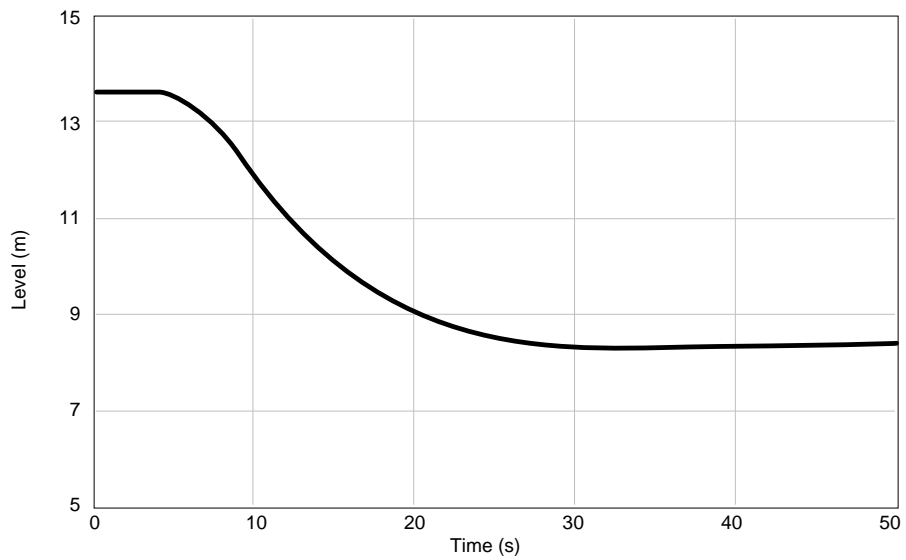
*Fig. 4.16 CANDU 600 power plant, loss of one pump transients*
Steam Generator
Pressure
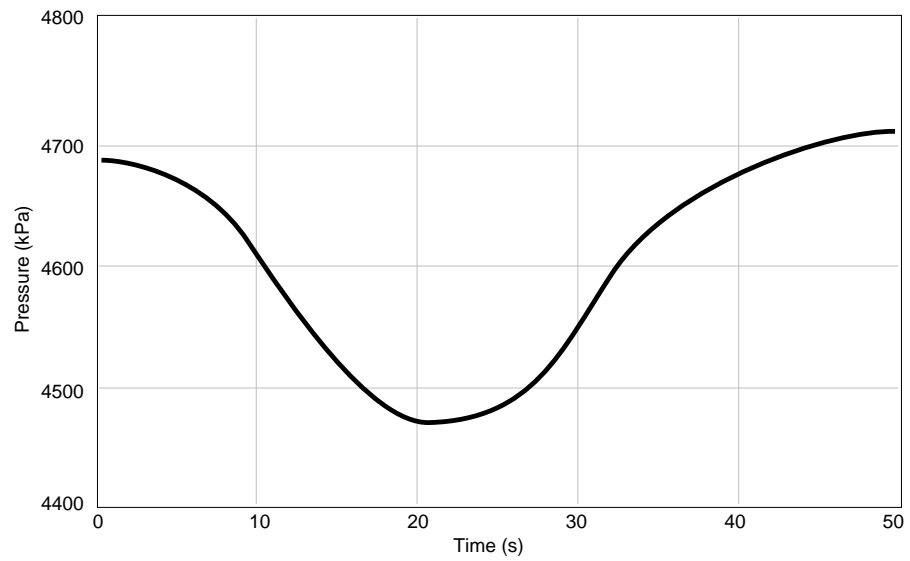
Fig. 4.17
*CANDU 600 power plant, loss of one pump transients*
Steam Generator Level
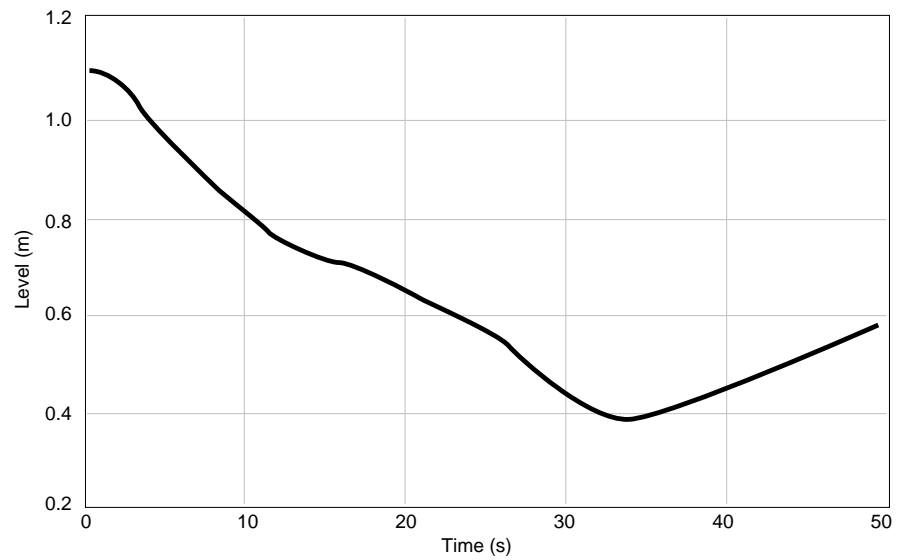
Fig. 4.18
*CANDU 600 power plant, loss of one pump transients*
Steam Flow
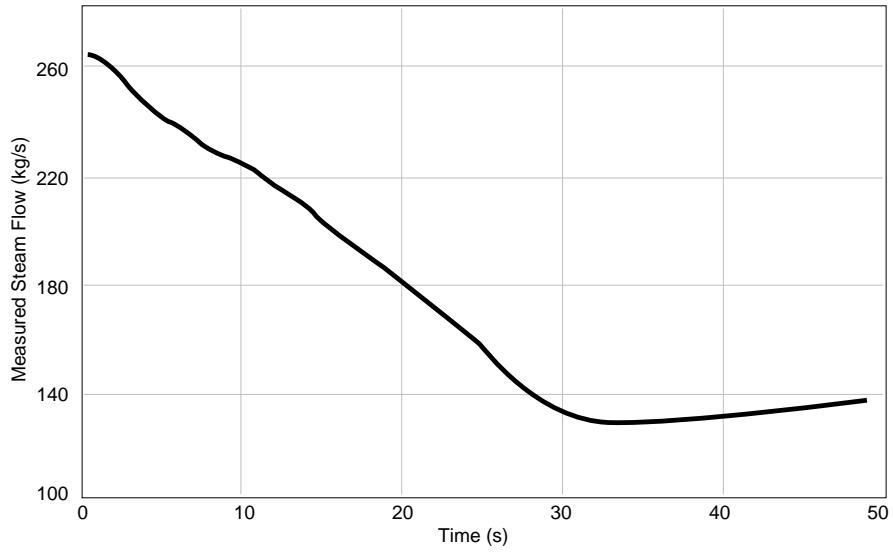
Fig. 4.19
CANDU 600 power plant, loss of one pump transients
Reactor Pressure Differential

December 1995
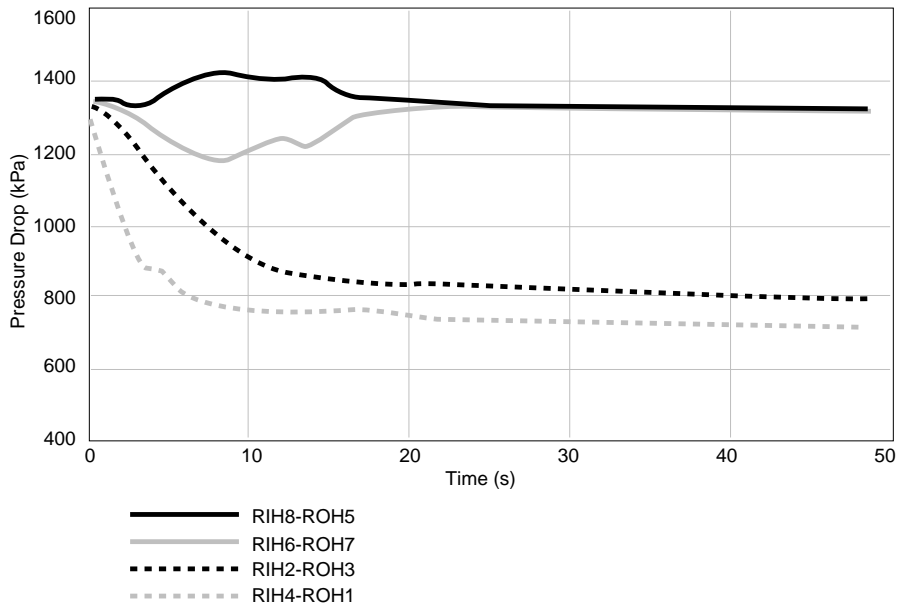
Fig. 4.20

CANDU 600 power plant, loss of one pump transients

In Core Heat Transport Flow
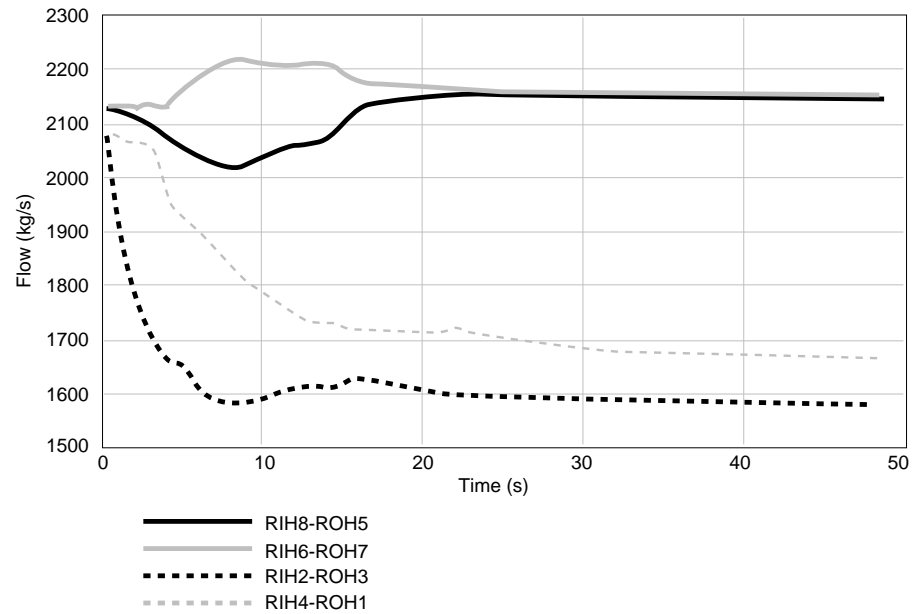
The plant behaviour can be assessed by the following events indicated in the simulation (see for instance the power evolution in Fig. 4.12):

- at t = 0 s, the loss of one HT pump occurs;
- at t = 0.9 s a stepback is initiated after the detection of the pump trip to decrease the power down to 60 %FP;
- at t = 3.5 s the stepback condition is cleared since the reactor power setpoint of 60% FP is reached;

The reactor core transient is then safely monitored and the neutron power remains stable with the required action of the regulating system, This situation cannot last since the core power is greatly unbalanced and operator action will become necessary.

December 1995